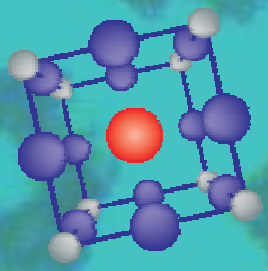

MaNEP
SWITZERLAND

FNSNF
FONDS NATIONAL SUISSE
SCHWEIZERISCHER NATIONALFONDS
FONDO NAZIONALE SVIZZERO
SWISS NATIONAL SCIENCE FOUNDATION

MaNEP

Materials with Novel Electronic Properties

Activity Report

2001 - 2004

Die Nationalen Forschungsschwerpunkte (NFS) sind ein Förderinstrument des Schweizerischen Nationalfonds.
Les Pôles de recherche nationaux (PRN) sont un instrument d'encouragement du Fonds national suisse.
The National Centres of Competence in Research (NCCR) are a research instrument of the Swiss National Science Foundation.

MaNEP – Materials with Novel Electronic Properties – is a **National Centre of Competence in Research*** (NCCR) based at the University of Geneva (home institution). It comprises a network involving ETHZ, EPFL, the universities of Fribourg, Neuchâtel and Zurich, the Paul Scherrer Institute and two major Swiss Industries.
MaNEP started its activities on July 1st, 2001. This report covers the period from July 1st, 2001 to March 31st, 2004.

MaNEP – Matériaux aux Propriétés Électroniques Exceptionnelles – est un **Pôle de Recherche National**** (PNR) basé à l'Université de Genève (institution hôte). Il se compose d'un réseau comprenant l'ETHZ, l'EPFL, les universités de Fribourg, Neuchâtel et Zurich, l'Institut Paul Scherrer et deux grandes industries suisses.
MaNEP a débuté ses activités le 1er juillet 2001. Ce rapport couvre la période du 1er juillet 2001 au 31 mars 2004.

Content

MaNEP
Department of Condensed Matter Physics
University of Geneva
24 quai Ernest-Ansermet
CH-1211 Geneva 4
Switzerland

Phone: +41-22-379.6218
Fax: +41-22-379.6869
Home page: www.manep.ch
E-mail: manep@physics.unige.ch

Prof. Ø. Fischer, *Director*
Phone: +41-22-379.6270
E-mail: oystein.fischer@physics.unige.ch

Prof. Jean-Marc Triscone, *Deputy director*
Phone: +41-22-379.6827
E-mail: jean-marc.triscone@physics.unige.ch

Mrs. Isabelle Bretton, *Administrative manager*
Phone: +41-22-379.6218
E-mail: isabelle.bretton@physics.unige.ch

Cover: The magnified cross-section of a multifilament superconducting wire.
From D. Eckert, Bruker-Biospin.

* The NCCR depend on and are supervised by the Swiss National Science Foundation
** Les PNR dépendent et sont supervisés par le Fonds National Suisse

1. Introduction: The activities of MaNEP

The scientific activities of MaNEP develop in five programmes which organize the research along complementary themes. Each programme is supervised by a coordinator who helps the director to promote an effective collaboration among the 18 groups constituting the MaNEP network.

Les activités de MaNEP se développent autour de cinq programmes de recherches aux thèmes complémentaires. Chaque programme est dirigé par un coordinateur qui assiste le directeur du pôle en vue de développer une collaboration effective entre les 18 groupes de recherche qui constituent le réseau MaNEP.

Programme A **Complex oxides and other emerging materials for future electronic technologies**

Programme coordinator: J.-M. Triscone, Université de Genève.

In a technological environment interested in new sensors and devices whose dimensions decrease continuously and approach the nanometer scale, the programme *"Complex oxides and other emerging materials for future electronic technologies"* aims at the preparation, the characterisation and a better understanding of several materials with a potential for applications in this field, namely the dielectric and ferroelectric oxides, carbon nanotubes and other nanomaterials.

From L. Schlapbach, University of Fribourg and EMPA

Oxydes complexes et matériaux émergeants pour les technologies électroniques du futur

Dans un environnement technologique où les nouveaux senseurs et les dispositifs de dimensions toujours plus petites prennent une place sans cesse croissante, ce programme vise à la préparation, à la caractérisation et à la meilleure compréhension de matériaux novateurs. Il s'agit des oxydes diélectriques et ferroélectriques, ainsi que des nanotubes de carbone et d'autres nanomatériaux.

Programme B Strongly interacting and low dimensional electron systems

Programme coordinator: H.R. Ott, ETHZ.

Many of the new physical phenomena discovered or observed in the recent years find their origin in unusual interactions, phase transitions or low dimensionality of the materials. The programme *"Strongly interacting and low-dimensional electron systems"* aims at an understanding of the possible ground states of condensed matter in these strongly interacting electronic systems. The programme develops a strong theoretical activity in close symbiosis with key experiments. The efforts concentrate mainly on organic conductors and superconductors, on other quasi-1D and quasi-2D materials, as well as on magnetic compounds.

From G. Margaritondo, EPFL

Systèmes électroniques fortement corrélés et de basse dimensionnalité

Parmi les nouveaux phénomènes physiques découverts ou observés ces dernières années dans les matériaux, certains trouvent leur origine dans des interactions électroniques peu communes, des transitions de phase ou la basse dimensionnalité des matériaux. Ce programme tend à une meilleure compréhension des états fondamentaux de la matière dans les systèmes électroniques fortement corrélés. On y mène une activité théorique en symbiose étroite avec les expériences de pointe qui sont effectuées. Les efforts se concentrent principalement sur les conducteurs et supraconducteurs organiques, sur certains matériaux quasi-1D ou 2D ainsi que sur des composés magnétiques particuliers.

Programme C Electronic properties of high temperature superconductors

Programme coordinator: T.M. Rice, ETHZ.

Superconductivity at temperatures above 30 *K, first observed by K. Alex Muller and J. Georg Bednorz in 1986,* is one of the most extraordinary discovery of the last two decades. The programme *"Electronic properties of high temperature superconductors"* contributes to the ongoing quest for an understanding of the microscopic nature of this phenomenon. The activities develop along different complementary lines and include MgB_2, a non-oxide materials recently found to be superconducting at 39 *K*, an unusual temperature for metals. The superconductivity of this material has probably a BCS origin but displays a striking two band behaviour.

From H.-R. Ott, ETHZ

Propriétés électroniques des supra-conducteurs à haute température critique

La supraconductivité à des températures supérieures à 30 *K*, observée pour la première fois en 1986 par K. Alex Muller et J. Georg Bednorz, est une des découvertes les plus extraordinaires des deux dernières décennies. Ce programme contribue à la recherche d'une compréhension précise de la nature microscopique de ce phénomène. Ses activités se développent le long de différentes lignes complémentaires qui incluent le MgB_2, un matériau non-oxyde dont la supraconductivité à 39 K a récemment été découverte, une température peu commune pour ce métal. Sa supraconductivité a probablement une origine BCS mais manifeste un comportement surprenant, reflétant l'existence de deux bandes de conduction.

Programme D **Vortices, mesoscopics, and nanostructures**

Programme coordinator: P. Martinoli, Université de Neuchâtel.

The strong spatial variations of some physical parameters and the small size of the objects considered both for practical large scale applications as well as future nano-sized devices are important aspects of the programme "*Vortices, mesoscopics and nanostructures*". It sheds light on the understanding of phenomena whose meso- and nanoscopic effects influence the properties of novel electronic materials.

From A. Furrer, ETHZ and PSI

Vortexes, structures méso- et nanoscopiques

Les fortes variations spatiales de certains paramètres physiques et la petite taille des objets considérés, à la fois pour les futures applications à grande échelle et pour les dispositifs nanoscopiques, sont les aspects importants de ce programme. Il éclaire des phénomènes dont les effets de taille (méso- et nanoscopiques) influencent les propriétés des matériaux électroniques nouveaux.

Programme E **Superconducting materials for industrial applications**

Programme coordinators: W. Paul, ABB, Baden (2001-2003) and Ø Fischer., Geneva

A major challenge for future innovations is the integration of superconducting materials in energy storage, transport, and high-tech electronic devices. The programme "*Superconducting materials for industrial applications*" aims to develop materials for high magnetic fields and high power applications, as well as for other potential applications of the high temperature superconductors.

From D. Eckert, Bruker-Biospin

Matériaux supraconducteurs pour les applications industrielles

L'intégration de matériaux supraconducteurs dans les innovations technologiques lance plusieurs défis, que ce soit dans le domaine du stockage d'énergie, du transport, ou des dispositifs électroniques de pointe. Ce programme vise principalement au développement de matériaux restant supraconducteurs en présence de champs magnétiques élevés, ainsi qu'à certaines applications dans le domaine de l'électronique de grande puissance.

2 The Five Research programmes

This chapter provides an overview of the research performed in the 18 groups of MaNEP. The most significant activities developed within the five research programmes are presented, covering three years of operation. Special emphasis is placed on recent developments, thus avoiding too much redundancy with the two previous editions of the Progress Reports.

Programme A Complex oxides and other emerging materials for future electronic technologies

Programme coordinator: J.-M. Triscone, University of Geneva.

Programme A investigates the characterization and physical properties of compounds which are interesting for future electronic applications. The development of advanced preparation techniques is also an aim of this programme focusing on dielectric and ferroelectric materials, magnetic compounds (manganites, hexaborides), carbon fullerenes, nanotubes and metallic based nanotubes.

I. Ferroelectric oxides

How thin can a ferroelectric be? This question is today central in the field of ferroelectricity and generates worldwide activities. To address this problem, high quality films with the polarization parallel to the growth direction are necessary as well as a technique sensitive enough to detect ferroelectricity in an ultrathin layer. In MaNEP, this problem was experimentally studied by growing atomically flat c-axis films of ferroelectric $PbTiO_3$ with thicknesses ranging from 500 Å down to 20 Å. Structural analyses of the film tetragonality coupled to first principles calculations allow us to demonstrate that the polarization is progressively reduced in thin films, in agreement with the depolarizing field model of Junquera and Ghosez. In addition, X-ray Photoelectron Diffraction (XPD) measurements on these films were performed with a resolution sufficient to detect atomic displacements, within the $PbTiO_3$ unit cell, caused by the reversal of the ferroelectric polarization (see Fig. A-1). Results obtained on a series of thin films suggest ferroelectricity down to 20 Å, a very striking result. Accomplishment and control of ferroelectricity in these thin ferroelectric films open promising avenues for highly integrated devices combining ferroelectrics and other electronic materials. – Collaboration between project 5 (J.-M. Triscone, UniGE) and project 14 (Ph. Aebi, UniNE).

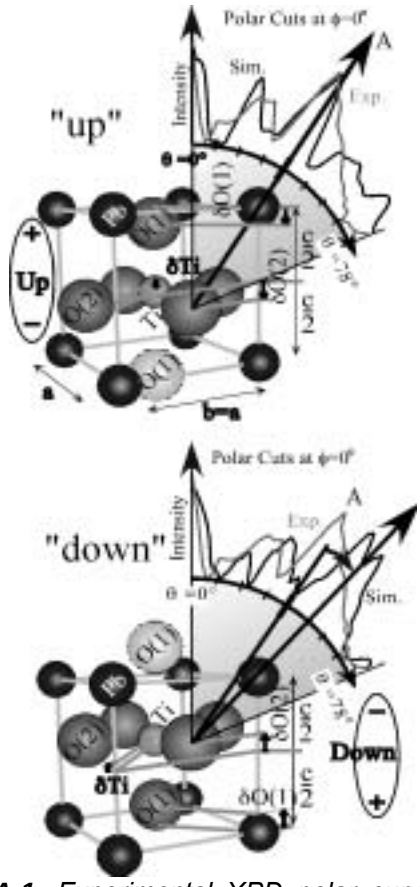

***Fig. A-1**. Experimental XPD polar curves for the "up" and "down" polarized states of $PbTiO_3$ as well as simulations superposed to the unit cells showing the atomic displacements (Ph. Aebi, UniNE, project 14).*

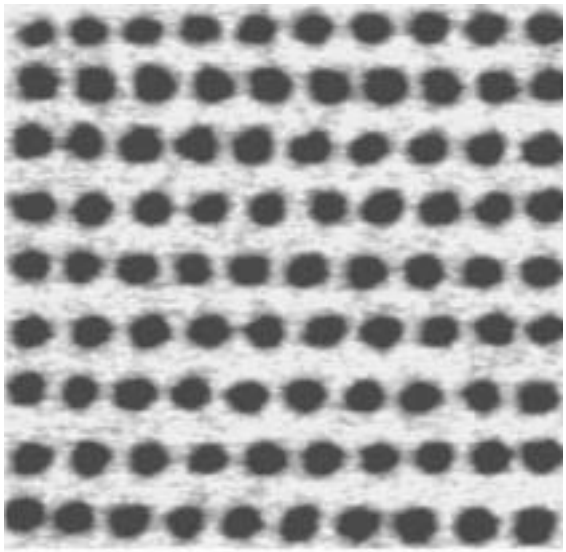

Fig. A-2 *Piezoelectric image of 90 ferroelectric domains with a pitch of 65 nm written on a 400 Å thick film of $Pb(Zr_{0.2}Ti_{0.8})O_3$. Image size: 580 x 580 nm. (J.-M. Triscone, UniGE, project 5).*

Another very active research area in the field of ferroelectricity is the use of local probes to study and modify the ferroelectric domain structure. In this programme atomic force microscopy (AFM) was used to "write", on single crystal $Pb(Zr_{0.2}Ti_{0.8})O_3$ films, arrays of ferroelectric domains such as the one shown in Fig. A-2. The relation between the domain size and the writing parameters was investigated and the relevant key parameters for obtaining nanoscale domains identified. Optimized parameters permitted the realization of high density arrays of ferroelectric domains reaching 30 Gbit/cm^2, a non-fundamental limit mostly controlled by the tip size. It was also shown that domain wall motion in epitaxial 2-D films is a disorder controlled creep process, an observation with important consequences for the understanding of domain stability in these materials. This subject has generated a strong collaboration between experimentalists and theorists and further theoretical and experimental investigations of the creep mechanism in ferroelectrics are in progress. Application of high density arrays of ferroelectric domains in the area of storage and electronic systems is today very seriously studied and is one of the motivation for this research. Collaboration between project 5 (J.-M. Triscone, UniGE) and project 18 (T. Giamarchi, UniGE).

High frequency surface acoustic wave filters (SAW) is another area where the high quality ferroelectric oxide films and the local probe manipulations of ferroelectric domains described above could find an application in

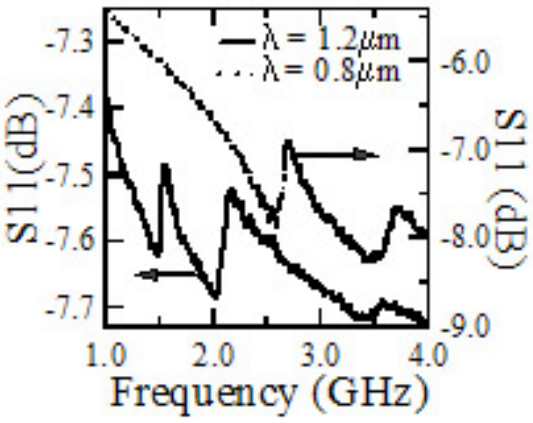

Fig A-3*. S11 reflection measurements on two different SAW devices with 0.8 and 1.3 μm wavelengths (J.-M. Triscone, UniGE, project 5).*

the nearer future. SAW devices are today used in many areas and in particular in communication technologies. The standard method of designing a SAW filter is based on metallic interdigital transducers (ITDs) deposited on a piezoelectric material. In this programme, a new type of SAW filters in which the conventional metallic ITD's are replaced by piezoelectric IDT's (produced by writing line-shaped domains) has been proposed. This should allow the realization of SAW filters operating at much higher frequencies, the wavelength of the ITD being much smaller than in traditional devices. Figure A-3 shows characteristic measurements of the S11 reflection on two piezoelectric SAWs. (Project 5, J.-M. Triscone, UniGE).

II. Magnetic materials

Compounds with colossal magnetoresistance retain considerable interest because of their exceptional transport properties, promising for technological applications. These properties, however, are far from being understood. One important issue addressed in this programme is the question of a possible electronic phase separation involving the coexistence of metallic and insulating microscopic regions in hole-doped manganites. One key question is whether the colossal magnetoresistance is related to this microscopic phase separation or is an intrinsic property of the material. Several compounds were analyzed by scanning tunneling potentiometry (STP), a technique allowing a direct local mapping of the potential drop in the material. The first measurements on $La_{0.7}Sr_{0.3}MnO_3$ did not reveal any evidence of electronic or chemical mesoscopic phase separation below T_c. In a new study, epitaxial thick films of $La_{0.7}Ca_{0.3}MnO_3$ were investigated. No evidence for phase separation, both above

and at T_c, was found. Although phase separation may occur at lower temperature, these results clearly question the universality of the phase separation hypothesis. (Project 2, Ø. Fischer UniGE).

The magnetotransport properties of the pure and doped hexaboride EuB_6 were extensively investigated and lead to important results. First, a giant magnetooptical Kerr effect was discovered in EuB_6, triggering the modeling of the magnetoresistance of pure EuB_6. The successful two band model proposed utilizes parameters which are consistent with data obtained at high temperature. Secondly, a giant magnetoresistive effect in doped $(Eu,Ca)B_6$ was discovered at low temperatures. Near a critical concentration, the electrical resistivity can be described as a percolation phenomenon using a random-resistor network, which can also account for the observed colossal magnetoresistive effects. In addition to these two discoveries, very large thermopowers in $M^{2+}B_6$ (M = Ca, Sr) were observed at room temperature. (Project 8, H.R. Ott, ETHZ).

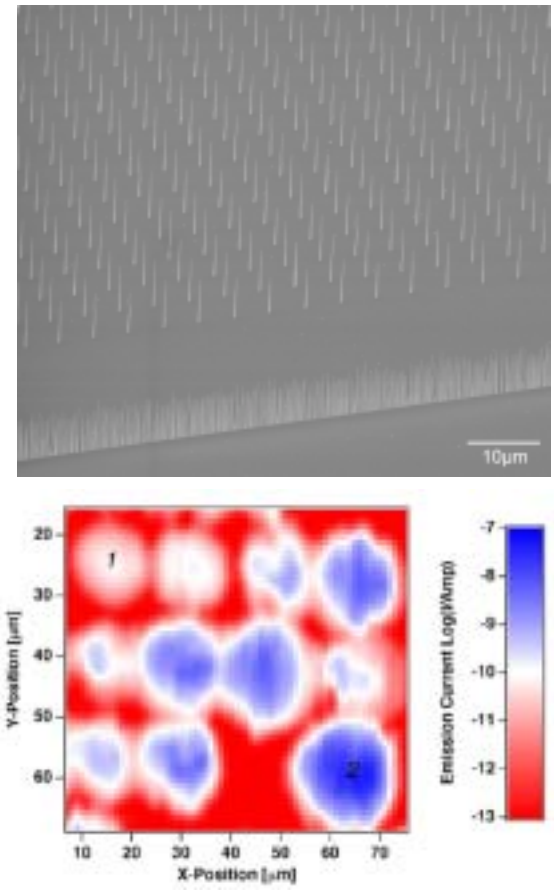

***Fig. A-4**. Upper panel: a regular array of carbon nanotubes imaged by scanning electronic microscopy. Lower panel: the emission current map at 15 V/µm. (L. Schlapbach, UniFR and EMPA, project 15).*

III. Carbon-based and other nanoscopic materials

The investigation of the field emission from planar carbon nanotube cathodes was pursued using scanning anode field emission microscopy (SAFEM). This nanoprobe provides access to relevant emission parameters such as emission homogeneity, emission site density (see Fig. A-4, lower panel), single emitter characteristics and single or collective emitter degradation. A highlight of this study was the planning, construction and implementation of a new generation of SAFEM for the Sony Display Laboratories, Atsugi, Japan. The system is used for the characterization of carbon nanotube cathodes developed for flat panel displays (see Fig. A-4, upper panel). (Project 15, L. Schlapbach, UniFR and EMPA).

In addition to carbon nanotubes, electron-doped Na_2C_{60} fullerenes were investigated. Measurements of transport properties, magnetic susceptibility and electron spin resonance (ESR) (see Fig. A-5) as a function of pressure showed that hydrostatic pressure gradually suppresses the insulating state. This observation supports the Mott-Jahn-Teller description recently proposed for these strongly correlated electron systems which are on the edge of a metal-insulator transition. (Project 11, L. Forró, EPFL).

Beyond carbon-based nano-materials, a large number of nanoscopic fibers and tubes are of potential interest. The formation, morphology and the chemical and physical properties of vanadium oxides (VO_x) nanotubes and

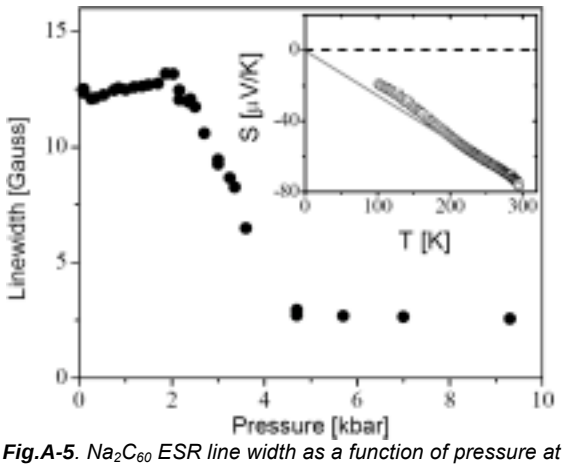

***Fig.A-5**. Na_2C_{60} ESR line width as a function of pressure at room temperature. Inset: the thermoelectric power in a pressed pellet shows that the sample is metallic at 9 kbar (L. Forró, EPFL, project 11).*

nanofibers were investigated. The route of synthesis which was adopted allows mixed material nano fibers and tubes like VO_x/SiO_2, VO_x/TiO_2, $VO_x/SiO_2/Fe$ and $VO_x/SiO_2/C$ to be produced. Also, techniques were developed to produce wires of arbitrary shapes of the novel superconductor MgB_2, nanoscopic Fe-oxides and Fe-Co oxides and, finally, nanofibers of transition metal oxides like TiO_2, MoO_3, WO_3, V_2O_5, SiO_2, Fe_2O_3 and Nb_2O_5. (Project 7, R. Nesper, ETHZ).

IV. Low energy muons: a new tool to study electronic materials

A unique low energy muon beam facility has been developed at PSI. Muon spin relaxation allows the local magnetic environment to be probed and the low energy muon beam will make possible such studies at surfaces and in thin films. As an example, low-energy muon spin relaxation (LEμSR) experiments were performed in semi-insulating silicon to investigate the formation of muonium at different temperatures. LEμSR provides a unique opportunity to study single isolated H (μ) atoms near the surface of a semiconductor. (Project 13, H. Keller, UniZH).

Programme B Strongly interacting and low dimensional electron systems

Programme coordinator: H.R. Ott, ETHZ

Strong interactions play an important role in the interpretation of the physical properties of many materials investigated in MaNEP. Most significant are these effects in substances with quasi-1D and quasi-2D structural elements, as well as in metallic substances where correlations and strong interactions affect the itinerant-electron system. Of particular interest are materials which are close to a metal-insulator transition and quantum magnets. This programme aims at understanding the various possible groundstates that may be adopted in these materials.

I. Quantum magnetism

Two different materials containing a lattice of dimers of spin carrying ions attracted recent enhanced interest. These are $TlCuCl_3$ and $SrCu_2(BO_3)_2$. In $TlCuCl_3$, the Cu^{2+} ions form dimers in an antiferromagnetically ordered singlet groundstate. Above a critical external magnetic field H_c, the lowest triplet state energy is lower than the singlet state energy. Since the triplet components may be regarded as diluted bosons, this crossing of energy levels may be regarded as a Bose-Einstein condensation (BEC) at the quantum critical point defined by H_c. Inelastic neutron scattering experiments clearly indicated the coexistence of two modes at higher energies with a low lying mode in the excitation spectrum of the magnetic field-induced ordered phase. The low energy mode is gapless and linear, providing an unambiguous demonstration of the gapless Goldstone mode characteristic for the BEC of the triplet states as shown in Fig. B-1 (Project 16, A. Furrer, ETHZ and PSI).

The magnetic excitation spectrum associated with the condensate was theoretically predicted to exhibit a gapless Goldstone mode. The field induced ordering in $MCuCl_3$ (M= Tl and K) was modeled in the dimer singlet and triplet state representation (Project 9, T.M. Rice, ETHZ). The calculated spin spectrum agrees quantitatively very well with the inelastic neutron diffraction results. The theoretical study was extended to the pressure induced quantum phase transition which is also observed experimentally in $TlCuCl_3$. The complete zero temperature [Hp] phase diagram was established, elucidating the influence of spin lattice coupling.

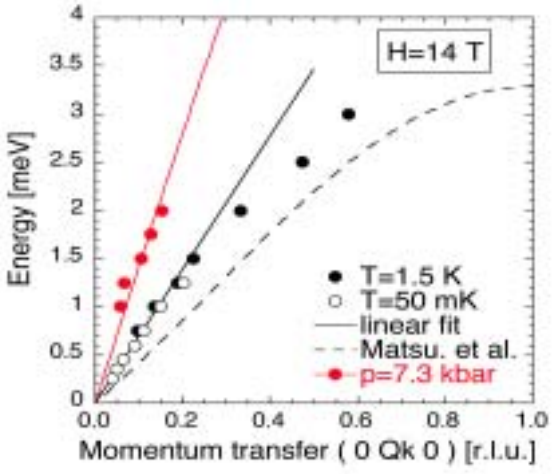

Fig. B-1 *Energy dispersion of the low-lying magnetic excitations in $TlCuCl_3$. These results from inelastic neutron scattering establish unambiguously the existence of a BEC in the Cu2+ spin system (A. Furrer, ETHZ and PSI, project 16). The dashed line is the theoretical expectation calculated within the project 9: (T.M. Rice, ETHZ, project 9).*

In the second system, $SrCu_2(BO_3)_2$, intriguing plateaus observed in the magnetization curves attracted considerable interest during the recent years. Theoretical efforts in this programme have now provided an interpretation. This system has a structure where stacking layers of $CuBO_3$ are intercalated by magnetically inert layers of Sr. A spin 1/2 resides on each Cu^{2+} ion forming a 2D orthogonal dimer lattice, a strongly frustrated system whose groundstate consists of decoupled spin-singlet dimers with a spin excitation gap. In a moderate magnetic field, the excitation gap closes and weakly itinerant magnons appear. At higher fields a plateau in the magnetization is observed where the triplet magnons form superlattices constituting a Mott-localized phase. The plateaus can be explained by including the spin lattice effects in the theoretical model of this system, hence

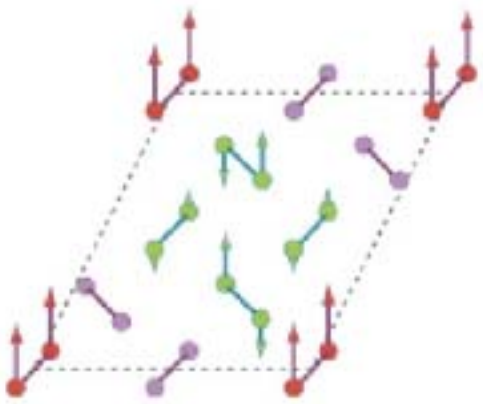

Fig. B-2 *Magnetization profile of the dimers in the extended unit layer of Sr atoms in $SrCu_2(BO_3)_2$ (F. Mila, EPFL, project 9).*

providing an explanation for this intriguing experimental result. Figure B-2 shows the crystallization of the triplets for a particular commensurate value of the magnetization (F. Mila, EPFL, associated with project 9).

A number of other quantum phase transitions and frustrated magnetic systems were investigated theoretically. In this regard we mention NH_4CuCl_3, a compound similar to $TlCuCl_3$. A microscopic model based on three inequivalent dimer sublattices was suggested to interpret the plateaus observed in the magnetization (project 9, T.M. Rice ETHZ). These results were recently confirmed experimentally by neutron scattering (project 16, A. Furrer, ETHZ and PSI).

Infrared optical properties of the S=1/2 quantum magnet system TiOCl were measured. The Fano shape of some infrared active phonon modes suggests an interaction between lattice vibrations and la continuum of low frequency spin excitations. Apart from the direct indication for the presence of the charge gap, part of the results were interpreted as also revealing a high energy scale in connection with the formation of the spin gap (Project 8, H.R. Ott, ETHZ).

An extensive investigation of $Na_2V_3O_7$ which, by considering its structural properties, may be classified as a low-dimensional S=1/2 spin system, was carried out. The temperature dependence of the magnetic susceptibility suggests that at low temperatures, only one out of 9 spin moments of the V ions is still active. A phase transition or spin-freezing phenomenon was discovered by NMR and specific heat measurements in varying external magnetic fields. The transition or freezing temperature decreases with increasing magnetic field and thus, from these studies, it is concluded that $Na_2V_3O_7$ is close to or at a quantum critical point in zero magnetic field. This is an appealing challenge for theorists as a realistic microscopic description of $Na_2V_3O_7$ is presently not available (Project 8, H.R. Ott, ETHZ; in collaboration with F. Mila, EPFL, Project 9).

II. Properties of low dimensional materials

The deconfinement transition between a one-dimensional Mott insulator and a three-dimensional metal or superconductor / superfluid was studied. A mean field approach was developed to tackle this question, replacing the coupled chains by a single chain coupled to an effective bath. The method

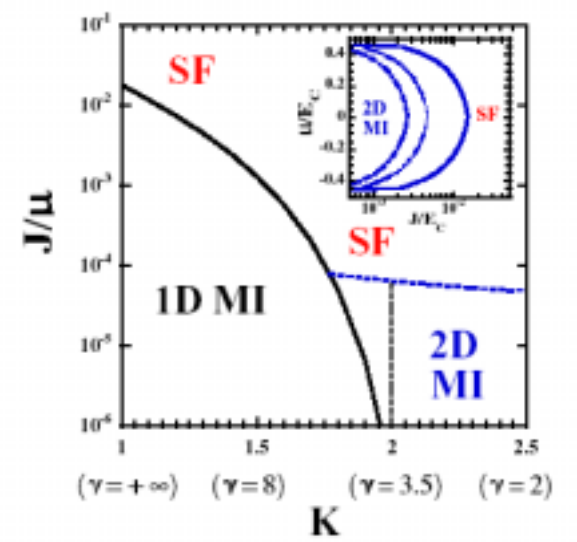

Fig. B-3 *Zero temperature phase diagram of a 2D lattice of coupled 1D boson systems. K is the Luttinger parameter, J the interchain tunneling for the bosons and μ the chemical potential (T. Giamarchi, UniGE, project 18).*

allows to describe the deconfinement of coupled Hubbard chains and to study the physical properties of the resulting low temperature Fermi liquid phase. It also permits to analyze the lifetime and excitations of the system. Deconfinement in bosonic systems was also considered in the case of a two dimensional lattice of long one-dimensional tubes, as shown in Fig. B-3. The method is also useful to treat ultracold atoms trapped in optical lattices (Project 18, T. Giamarchi, UniGE).

A bandwidth-controlled Mott transition at the surface of the quasi two-dimensional system *1T*-$TaSe_2$ was discovered by ARPES

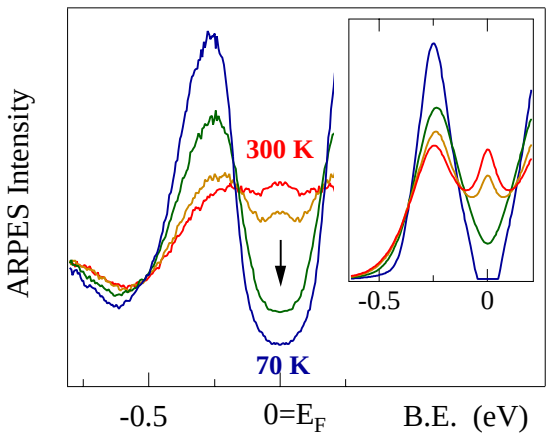

Fig. B-4*. ARPES spectra of 1T-TaSe2 measured across a surface Mott transition. Sharp Hubbard subbands emerge at low temperatures while the quasiparticle peak at E_F is suppressed and a correlation gap opens. The inset shows the results of a DMFT calculation (G. Margaritondo, EPFL, project 12).*

measurements. This result shed light on the fact that, in this system, the conduction bandwidth is controlled by the charge-density waves (CDW) which determine the atomic distances. ARPES provided great detail of the electronic structure across the metal-insulator Mott transition. As shown in Fig. B-4, the evolution of the ARPES spectra is in remarkable agreement with a state-of-the-art calculation performed within a Dynamical Mean-Field Theory (DMFT), providing the first direct experimental confirmation of an important theoretical paradigm for strongly correlated systems (Project 12 G. Margaritondo, EPFL).

The low-dimensional "conventional" transition-metal chalcogenides exhibiting CDW were also investigated but for another reason. The aim was a comparison with the "unconventional" high-T_c superconductors since chalcogenides such as *1T*-TaS_2 and *1T*-$TaSe_2$ exhibit a pseudogap which is most likely due to a CDW formation. These materials arouse interest as the origin of the CDW is still unclear; the much-claimed Fermi surface nesting does not appear to be the dominant mechanism (Project 14, Ph. Aebi, UniNE).

A low temperature investigation of *1T*-$TaSe_2$ was also performed by scanning tunneling microscopy. This study revealed the coexistence of domains with different electronic behaviour on the same cleavage plane. Imaging across the domain boundaries display a phase shift of 2 a_0, (a_0 being the lattice constant of the undisturbed lattice) in the CDW superstructure (Project 15, L. Schlapbach, UniFR and EMPA).

D. van der Marel (UniGE, project 17) recently joined MaNEP. The contribution of the new group to programme B consisted in an investigation probing the optical conductivity of MnSi, which is believed to exhibit non-Fermi liquid behaviour at high pressures. The results of these experiments suggest screening properties intermediate between those of a metal and a superconductor. These complex optical features are significantly different from conventional Drude behaviour. They can be attributed to a strong coupling of the itinerant charge carriers to spin-fluctuations or other collective modes.

In order to test theoretical predictions for the energy transport in S=1/2 and S=1 spin-chain systems, an extensive experimental investigation probing this property was made using suitable real materials, including copper oxides and quaternary chalcogenides, which may be considered as good physical realizations of the model assumptions. The results indicate that the energy transport in S=1/2 chains is quasi ballistic, reflecting the theoretically predicted infinite thermal conductivity due to itinerant spin excitations in these systems. Analogous experiments on S=1 type material indicate that the energy transport by magnetic excitations in these systems is diffusive. The characteristic difference of the energy transport in these two types of low dimensional spin systems is emphasized in Fig.B-5, displaying the temperature dependences of the respective mean free paths (Project 8, H.R. Ott, ETHZ).

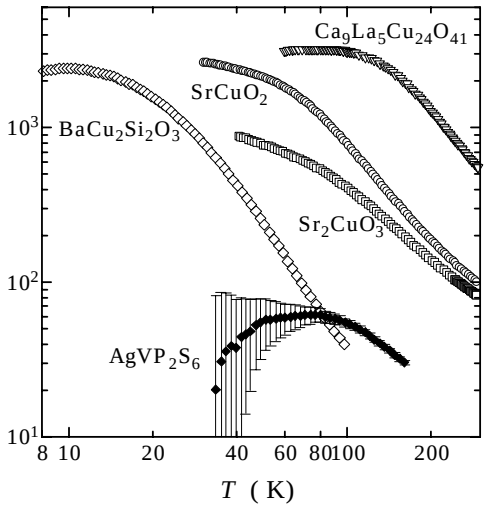

***Fig. B-5**. Mean free path of spin excitations in the S=1/2 spin-chain compounds $BaCu_2Si_2O_7$ Sr_2CuO_3 and $SrCuO_2$, and the S=1 spin-chain compound $AgVP_2S_6$. The corresponding data for the two-leg S=1/2 spin-ladder material $Ca_9La_5Cu_{24}O_{41}$ by other authors are shown for comparison (H.R. Ott, ETHZ, project 8).*

Recently introduced new materials which are considered as good physical realizations of one dimensional Heisenberg type spin systems include alkali Si and Ge oxides. The S=1 magnetic moments are provided by the V ions. A series of NMR experiments probing the alkali element nuclear spin revealed that the expected low temperature Haldane phase does not form. Instead, antiferromagnetic ordering with the formation of spin excitation gaps is observed. In combination with results of the temperature dependence of the magnetic susceptibility, the values of relevant exchange energy parameters were established. Although the interchain interactions turn out to be weak, they are, nevertheless, strong enough to quench the Haldane phase (Project 8, H.R. Ott, ETHZ; in collaboration with F. Mila, EPFL, Project 9).

Programme C Electronic properties of high-T_c superconductors

Programme coordinator: T.M. Rice, ETHZ.

Superconductivity at temperatures above 30 *K* is one of the most spectacular discoveries of the last two decades. The goals of this programme are the understanding of the microscopic nature and the fundamental mechanisms of this superconductivity.

I. The surprising discovery of MgB_2

The surprising discovery of superconductivity at 39 K in MgB_2 came just when MaNEP started its activities. Soon the unusual properties of this superconductor attracted strong interest within MaNEP and the research plans of many projects were adapted accordingly.

A prominent characteristic of MgB_2 is the two band nature of its superconductivity, in some respect similar to the situation met earlier in the p-wave superconductor, Sr_2RuO_4.

Specific heat studies were the first to show anomalous behaviour at low temperature leading to the proposal that two distinct energy gaps appear in the superconducting state. Detailed specific heat measurements were performed as a function of temperature, magnetic field and irradiation, showing that MgB_2 is a bulk two band superconductor requiring new temperature and field scales to understand its unusual properties. Figure C-1 shows that specific heat measurements cannot be explained by an isotropic single band BCS model. Recently, a search for other superconductors in which two gaps might also appear was begun. It comes out to be the case in Nb_3Sn, a compound with the A15 structure whose superconductivity has been known for about four decades. Specific heat measurements revealed a low-temperature anomaly which disappears with magnetic field, similar to MgB_2 (Project 4, A. Junod ,UniGE).

Additional unambiguous evidence for the multigap features of superconductivity in MgB_2 was provided by measurements of the thermal conductivity in single crystals, which allow the bulk upper critical field Hc_2 to be measured (Project 8, H.R. Ott, ETHZ).

An analysis of the effect of the multi-gap structure on the quasiparticle heat transport showed that the quasiparticle states of the band with the smaller gap can be delocalized at low magnetic field in impure materials, in contrast to the usual localization in the vortex cores (Project 9, T. M. Rice and M. Sigrist, ETHZ).

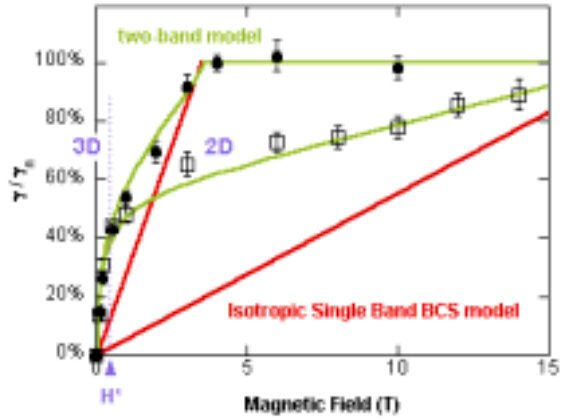

***Fig. C-1**. Normalized electronic specific heat of MgB_2 at $T \rightarrow 0$ versus H for the field applied perpendicular (●, H_{c2} = 3.5 T) or parallel (γ, H_{c2} = 18 T) to the boron planes. The single band model (red lines) does not fit. Results become isotropic below H* or for $\gamma/\gamma_n < 0.5$. (A. Junod, UniGE, project 4)*

Two gap superconductivity was also investigated by scanning tunneling spectroscopy (STM) on pure and doped single crystals of MgB_2 grown within MaNEP. Early measurements with the tunneling parallel to the c axis revealed a π-band gap of 2.2 meV. Shoulders visible around 6 meV were assigned to the σ-band. Tunneling perpendicular to the c-axis showed clearly the two gaps and allowed the σ-band gap to be measured precisely (Collaboration between project 2, Ø Fischer, UniGE and project 8, J. Karpinski, associate, ETHZ).

Electron spin resonance measurements on MgB_2 showed that the two band model seems inadequate at high fields, although it fits the experiment at low magnetic field. This discrepancy can be resolved by considering different electron-phonon couplings in the two bands (Project 11, L. Forró, EPFL).

Most of the detailed studies of MgB_2 presented in this section were made possible thanks to the preparation of single crystals grown by J. Karpinski (ETHZ, associated with project 8) and by A. Berger (EPFL, associated with project 12) and their respective collaborators. The high quality of the material required a detailed investigation of the pressure-temperature phase diagram of MgB_2. Doped single crystals were also grown to assess the

effects of aluminium and carbon substitutions in MgB_2.

II. Cuprates

Discovered by J. G. Bednorz and K. A. Muller in 1986, the high temperature superconducting cuprates have been the subject of a remarkable effort worldwide. Nowadays, we know more about these materials than almost any other class of superconductors. Despite experimental techniques being pushed to extremes, these complex materials persist in guarding their ultimate secrets. Over the years, MaNEP members have contributed strongly to this research effort.

Significant progress in photoemission studies of oxide thin films have resulted from the design and commissioning of a unique laser ablation facility for growth and in-situ spectroscopic analyses. Since this first demonstration of successful direct photoemission spectroscopy on thin cuprate films, this approach has been taken up by leading groups worldwide. Systematic measurements on superconducting thin films of $La_{2-x}Sr_xCuO_4$ revealed unexpected consequences of strain on the band structure of this material, as shown in Fig. C-2. (Project 12 G. Margaritondo, EPFL).

Another major progress in thin films was the development of a novel almost-homoepitaxial buffer technique allowing the growth of single-unit-cell films of cuprates with remarkable superconducting properties. Ultrathin

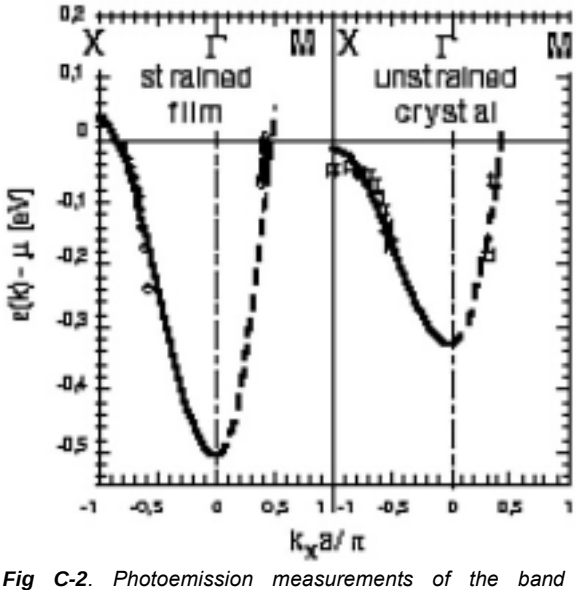

***Fig C-2**. Photoemission measurements of the band dispersion for a strained film of $La_{2-x}Sr_xCuO_4$ (left) and for an unstrained single crystal (right, data from Fujimori's group) along Γ-X and Γ-M. Fits with a tight binding dispersion are shown. (G. Margaritondo, EPFL, project 12).*

$YBa_2Cu_3O_{7-\delta}$ films were deposited to demonstrate glass-like features in the dynamic response of a 2D superconductor, under certain conditions. In a later phase of this project, a collaboration with IBM Research Laboratory explored the preparation of $La_{2-x}Sr_xCuO_4$ films. The high quality ultrathin films obtained allowed special features related to the d-wave symmetry of the order parameter in cuprates to be studied. The buffer deposition technique was also used to prepare $La_{2-x}Sr_xCuO_4$-based heterostructures with an Hf oxide layer as a gate insulator for studies of the electric-field tuned superconducting-insulating transition (Project 10, P. Martinoli, UniNE).

Ferroelectric $Pb(Zr_{0.2}Ti_{0.8})O_3$ / superconducting $NdBa_2Cu_3O_{7-d}$ heterostructures have been grown to investigate the electrostatic tuning of the electronic properties of cuprates. This new field effect device, whose gate insulator is a $SrTiO_3$ single crystal, allows the critical temperature of the superconducting film to be modulated by at least 3 K, one of the largest shifts in the critical temperature obtained by field effect in oxide superconductors (Project 5, J.-M. Triscone, UniGE).

The "dip-hump" structure observed next to the coherence peak in the low energy part of scanning tunneling spectra is a striking feature of $Bi_2Sr_2CaCu_2O_8$. High precision numerical simulations including tunneling matrix elements and band structure effects were carried out (see Fig. C-3). The conclusion of these simulations is that the van Hove singularities contribute considerably to the asymmetry of the spectra and the height of the coherence peaks. The dip-hump can be explained by an interaction with a collective mode next to the coherence peaks and the short lifetime of high-energy quasiparticles. In addition, these simulations provide evidence that the so-called 41 meV resonance seen by neutron scattering corresponds to the local mode observed by

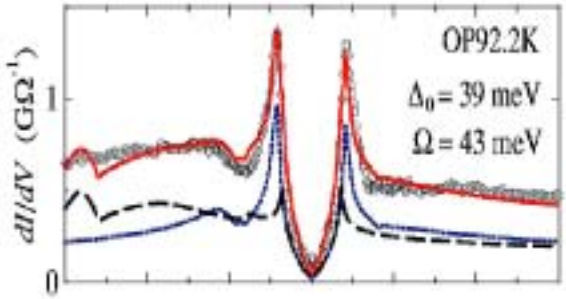

***Fig. C-3**. Experimental and calculated tunneling spectra of $Bi_2Sr_2CaCu_2O_8$. Calculation for two bands and their sum are shown. (Ø Fischer, UniGE, project 2)*

tunneling. (Project 2, Ø Fischer, UniGE).

The oxygen isotope effect (OIE) was studied on thick epitaxial films of $YBa_2Cu_3O_{7-\delta}$ and $Y_{1-x}Pr_xBa_2Cu_3O_{7-\delta}$ by low-energy muon spin rotation (LEμSR). A significant $^{16}O/^{18}O$ isotope effect was observed: 2.8(1.0)% on the in-plane magnetic field penetration depth λ_{ab} and –6.2(1.0)% on the temperature dependence of the depolarization rate of the muons (see Fig. C-4). These results show unambiguously that the OIE originates from the oxygen of the superconducting CuO_2 planes and not from the apical and chain oxygen. This suggests a strong coupling of the electronic subsystem to phonon modes involving movements of the oxygen atoms in the CuO_2 plane. (Project 13, H. Keller, UniZH). In addition, the oxygen isotope effect on the pseudogap is currently investigated using the bulk-sensitive technique of neutron crystal-field spectroscopy. (Project 16, A. Furrer, ETHZ and PSI).

The origin of the pseudogap and its relation to superconductivity is another open issue. A linear scaling between the pseudogap and the superconducting gap in $Bi_2Sr_2CaCu_2O_8$ was established by scanning tunneling spectroscopy. The same trend was obtained for the single layer $Bi_2Sr_2CuO_6$, suggesting a common origin of both gaps. Studies on $Bi_2Sr_2Ca_2Cu_3O_{10}$ are underway (Project 2, Ø. Fischer, UniGE).

Break-junction tunneling was used to assess the effect of disorder in high-T_c superconductors. The disorder was controlled by electron irradiation of optimally doped $Bi_2Sr_2CaCu_2O_8$. It was observed that point defects decrease T_c significantly, although the superconducting gap does not change measurably (Project 11, L. Forró, EPFL).

In addition, the same team investigated by electron spin resonance the hole-induced changes in the antiferromagnetic structure of a lightly doped Gd:(Y,Ca)BCO copper oxide. The results suggest a gradual ordering of the holes in so-called diagonal charged stripes. This observation seems in good correspondence with the observed gradual freezing of the stripes at low doping $YBa_2Cu_3O_{7-\delta}$ and $La_{2-x}Sr_xCuO_4$.

Optical evidence of an anomalous change of kinetic energy was found when the cuprates become superconducting. It was also demonstrated that optical spectra in the ab-plane exhibit a frequency and temperature-dependence characteristic of the behaviour expected near a quantum phase transition. (Project 17, D. van der Marel, UniGE).

The microscopic theory of high temperature superconductivity continues to be a central focus. Large efforts were devoted to this issue within MaNEP, as reported below.

A Renormalization Group analysis of the 2D Hubbard model gave new insights into the RVB phase which is the key of these materials. The results show that T* and T_c are, in underdoped cuprates, related to different parts of the Fermi surface. While the crossover at the high temperature T* signals the formation of a RVB condensate which truncates the Fermi surface near the saddle points, the transition to superconductivity at T_c is driven by a coupling in the Cooper channel between the remaining Fermi surface arcs and the truncated saddle point regions (Project 9, T. M. Rice and M. Sigrist, ETHZ).

Motivated by experimental data showing charge inhomogeneities in strongly correlated 2D electron systems (cuprates, nickelates and manganites), the issue of stripes in doped Mott

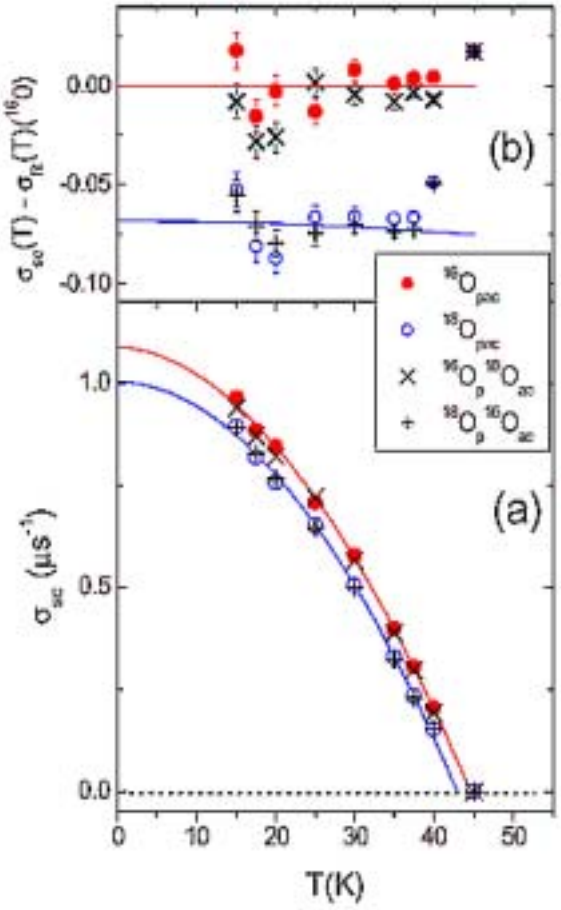

***Fig. C-4**. (a) Temperature dependence of the muon depolarization rate in $Y_{0.6}Pr_{0.4}Ba_2Cu_3O_{7-\delta}$. Red: ^{16}O; blue: ^{18}O. (b) Relative temperature dependence. (for details see project 13, H. Keller, UniZH).*

insulators was addressed. The results shed light on the connection between the formation of a low temperature tetragonal phase and the subsequent appearance of charge order in high-T_c cuprates and manganites, which is not currently understood (Project 9, D. Baeriswyl, associate, UniFR together with C. Morais Smith).

Pairing fluctuations in the pseudogap phase were investigated for their influence on specific heat and magnetic susceptibility and as a possible cause of the electronic pseudogap. This issue is related to the structure of the Cooper pairs in the pseudogap. The Bethe-Salpeter equation for the two-electron propagator was solved to investigate this phenomena. It was found that while the size of the pairs in the condensate is finite for $T > 0$, it diverges for $T \rightarrow 0$ in the case of a d-wave pairing (Project 10, H. Beck, associate, UniNE).

The same team investigated the crossover from BCS superconductivity to Bose-Einstein condensation in the framework of the attractive Hubbard model, providing a prescription for mapping fermionic onto bosonic theories in the broken-symmetry phase.

Finally, the optical properties of layered copper-oxide superconductors were investigated. It was found that spatial dispersion in the material can significantly affect the spectral properties of optically active modes of the dielectric function. Usually, the optical dielectric constant ε depends only on the frequency ω, since the wavevector q of light is very small compared to typical k-vectors in solids. Including spatial dispersion allows to account for an additional q-dependence in $\varepsilon(q, \omega)$ which can become relevant in some cases, particularly in connection with a Josephson plasma resonance in layered superconductors. The results were recently generalized to include also optical phonons. (Project 6, G. Blatter, ETHZ).

Programme D Vortices, mesoscopics, and nanostructures

Programme coordinator: P. Martinoli, University of Neuchâtel.

This programme addresses questions related to the strong spatial variations of some physical parameters. It sheds light on the understanding of phenomena whose meso- and nanoscopic effects influence the properties of novel electronic materials.

I. Vortex matter in novel superconductors

Theoretical efforts were carried out towards a better understanding of various aspects of vortex matter.

A previous theoretical treatment of vortex lattice melting in layered superconductors was extended by investigating the effect of adding a weak Josephson coupling between the layers. A dramatic effect is obtained: a large relative shift of the melting line at low magnetic fields, which brings the theoretical prediction closer to experimental results on $Bi_2Sr_2CaCu_2O_8$ single crystals. In addition, the effect of pinning by disorder was studied with numerical simulations in tilted magnetic fields where lattices of Abrikosov and Josephson vortices may cross (see Fig. D-1). (Project 10, P. Martinoli, UniNE).

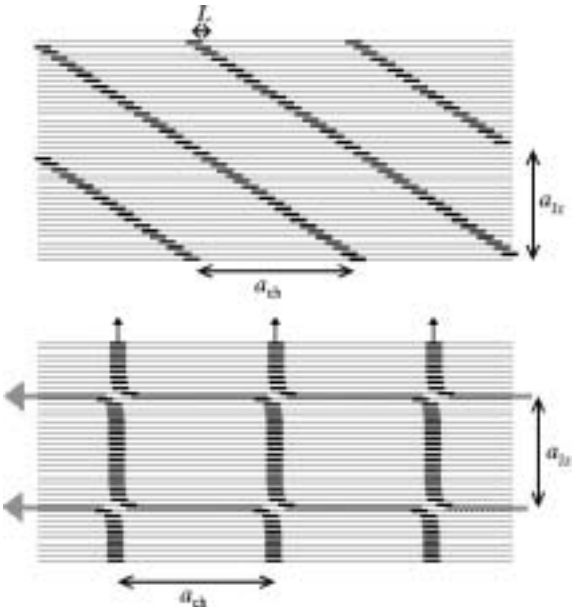

***Fig. D-1**. The tilted chain and the chain of crossing Abrikosov and Josephson vortices. (P. Martinoli, UniNE, project 10).*

The surface-induced melting of the pancake vortex system in a semi-infinite layered superconductor was investigated by implementing a substrate model, in which the three-dimensional problem is reduced to the analysis of a two-dimensional lattice interacting with a self-consistent substrate potential, within a density-functional-theory scheme. It is found that the presence of the surface acts as a nucleus for the liquid vortex phase: at the transition the liquid nucleus at the surface expands into the bulk, thereby suppressing the overheating of the solid vortex phase (Project 6, G. Blatter, ETHZ).

In the same project, the competition between various topological transitions (unbinding of pancake vortex-antivortex pairs versus evaporation of pancake vortex stacks) in layered superconductors of finite width was also investigated and an experiment allowing for the identification of the evaporation transition was proposed. In addition, an educational text on the physics of vortex matter was completed.

The mechanism responsible for the suppression of superconducting phase coherence in Josephson junction arrays on a dice lattice at full frustration was identified in the high accidental degeneracy associated with the formation of zero-energy domain walls in the ground state of the system. As a consequence, ordering becomes quite vulnerable to thermal fluctuations, which explains the unusual behavior observed in measurements of the array's magneto-inductance (Project 10, P. Martinoli, UniNE).

On the experimental side, the spin and vortex dynamics in $La_{2-x}Sr_xCuO_4$ single crystals were investigated using small-angle neutron scattering (SANS) at the Swiss spallation neutron source SINQ. A well defined vortex lattice could be observed for the first time at all doping levels. The data indicate that the results obtained in the overdoped (x = 0.2) and the slightly overdoped (x = 0.17) regimes do not change significantly, thus ruling out the stripe scenario as being responsible for the square coordination of the vortex lattice. In the underdoped (x = 0.1) region, a totally different behaviour is observed, the vortex lattice being well defined only at low magnetic fields. This strong variation of the vortex lattice structure with hole doping reflects the subtle interplay between the magnetic and electronic degrees of freedom in high-T_c superconducting cuprates (Project 16, A. Furrer, ETHZ and PSI).

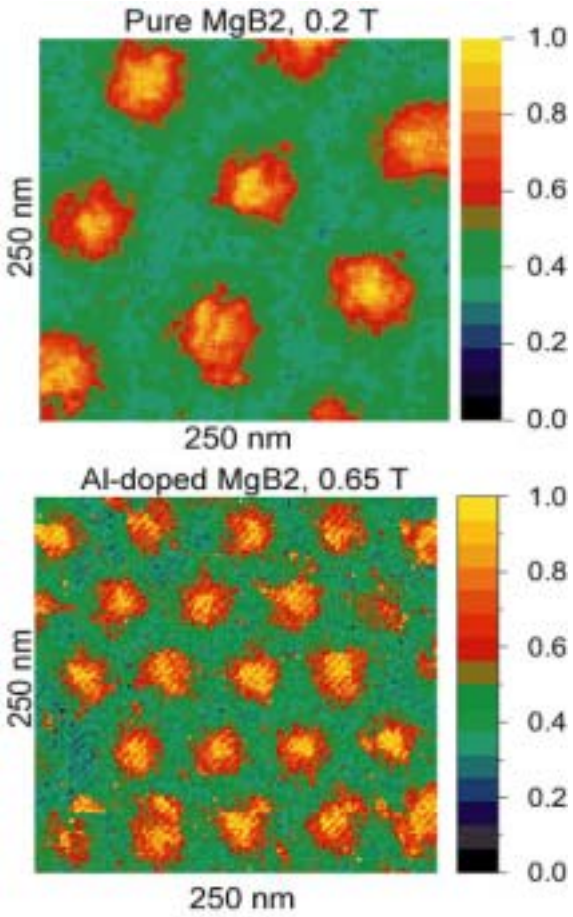

Fig D-2. *Vortex lattice in pure (T_c=39K) and Al-doped (T_c=25K) MgB_2 measured by scanning tunneling spectroscopy parallel to the c-axis. Measurements are by Ø. Fischer and collaborators (UniGE, project 2) on single crystals grown by J. Karpinski (ETHZ, associated with project 8) and co-workers.*

Another experimental study of vortex lattices was performed by scanning tunneling spectroscopy on single crystals of magnesium diboride (MgB_2). The measurements provided a surprising result: tunneling parallel to the c-axis (sampling the π-band superconducting gap) revealed vortices with a core much larger (see Fig. D-2, upper panel) than expected from the value of the coherence length extracted from Hc_2. This was an early example of how macroscopic parameters, such as T_c and Hc_2, are set by the σ-band, whereas other parameters, such as the vortex core size, are set by the π-band. Another surprising result was the absence of any localized states at the center of the vortex core, an observation which might be related to the interplay of the two bands (Project 2, Ø Fischer, UniGE, in collaboration with J. Karpinski, ETHZ, associated with Project 8).

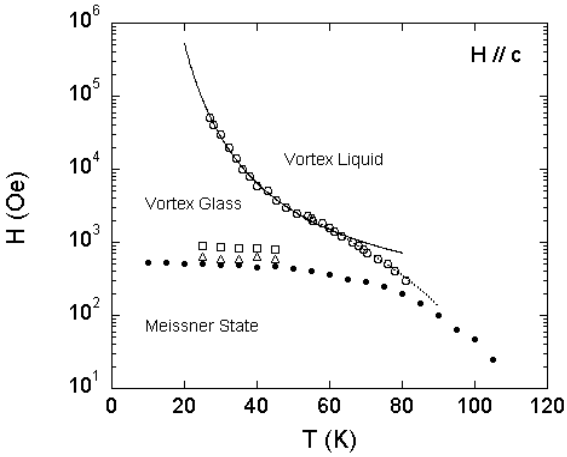

Fig. D-3*. Vortex phase diagram of $Bi_2Sr_2Ca_2Cu_3O_{10}$ single crystal. The irreversibility line (open circles) is fitted by a Lindemann-type melting criterion. Triangles and squares are the onset of the second magnetization peak. (R. Flükiger, UniGE, project 3).*

Scanning tunneling spectroscopy was also performed perpendicular to the c-axis. The vortex imaging allowed the determination of the anisotropy of the vortex lattice yielding γ = 1.2, a value much lower than the upper-critical-field anisotropy, but in good agreement with theoretical calculations of the penetration depth anisotropy (ibid).

Recently, the Geneva group focused on the effects of doping MgB_2 with aluminium (see lower part of Fig. D-2). The π-band gap is found to increase in spite of a strong reduction of T_c. Furthermore, the Al-doped samples have, surprisingly, a coherence length twice as small as the pure one, suggesting that interband scattering is enhanced by Al-doping. Scanning tunneling spectroscopy is being currently performed on C-doped MgB_2 single crystals, which were grown, like the pure and Al-doped ones, by J. Karpinski, ETHZ, associated to Project 8.

The study of the vortex phase diagram of $Bi_2Sr_2Ca_2Cu_3O_{10}$ was made possible thanks to the growth of high quality single crystals of this compound. Using a SQUID magnetometer, the vortex phase diagram was mapped out (see Fig. D-3). It was found that the irreversibility line of $Bi_2Sr_2Ca_2Cu_3O_{10}$ occurs at higher fields than $Bi_2Sr_2CaCu_2O_8$ (Project 3, R. Flükiger, UniGE).

Finally, additional progress was reported by H.R. Ott (ETHZ, Project 8) and collaborators who found a new phase transition in the mixed state of superconducting $NbSe_2$.

II. Mesoscopic physics, quantum computing and related fields

When normal conductors are connected to a superconductor, the Andreev reflection mechanism at the normal-superconductor interface introduces correlations between electrons and holes whose statistical properties were investigated. Motivated by the expanding and successful field of spintronics, the same group has also carried out the first detailed study of the interplay of the Kondo effect and ferromagnetism in quantum dots (Project 1, M. Buttiker's, UniGE).

Generation, control and manipulation of quasiparticle entanglement are a prerequisite for the implementation of quantum information and quantum computation relying on solid-state systems. New experimentally accessible schemes for orbital (instead of spin) entanglement in mesoscopic conductors, implemented in semiconductor-superconductor heterostructures and in a semiconductor in the quantum Hall regime, were proposed. (ibid).

Decoherence is the main problem one faces in the implementation of hardware for a future quantum information technology. In this connection, the first scheme for the implementation of a topologically protected quantum bit based on Josephson junction arrays was proposed. By exploiting the geometric frustration occurring in an array of superconducting islands with tetrahedral symmetry, the same group has proposed a novel qubit design in which the effect of quantum fluctuations is enhanced, thereby resulting in a reduced sensitivity to flux noise. More recently, the fundamental limitation for the coherent operation of superconducting quantum bits due to piezoelectric generation of phonon radiation in Josephson junctions was also studied (Project 6, G. Blatter, ETHZ).

Programme E Superconducting materials for industrial applications

Programme coordinator: Ø. Fischer,UniGE,
in replacement of W. Paul, ABB, Baden.

The main goals of this programme are to develop superconducting wires and tapes for high field applications and to develop thin films for power applications. The activities of this programme are strongly linked with the interests of MaNEP industrials partners, in particular ABB and Bruker BioSpin.

I. Superconducting wires and tapes for high field applications

The preparation of square Bi,Pb(2223) superconducting cables as long as 5 m sustaining currents of 200 A at a temperature of 77 K in the absence of magnetic field was achieved. Combining high filling factors and small anisotropy, these conductors allow twist pitches as short as 4 mm while maintaining more than 90 % of the critical current. A remarkable property of these square wires is the reduction by a factor of ~10 of the AC losses compared to those of a tape in a magnetic field applied perpendicular to the surface. The square cables were optimized for double pancake coils prepared for a prototype transformer in the frame of a European Growth project. Figure E-1 shows one of the final coils (Project 3, R. Flükiger, UniGE).

The Geneva group has also developed the deposition by r.f. spray pyrolysis of $YBa_2Cu_3O_7$ layers on textured substrates reaching 1 x 10^5 A/cm^2 at 77 K and 0 T and fabricated monofilamentary Fe sheathed MgB_2 tapes by an ex-situ technique allowing a critical current of 1 x 10^4 A/cm^2 at 4.2 K under a magnetic field of 8 T to be reached.

Fig. E-1. *Double pancake coils made of Bi,Pb(2223)/Ag. (R. Flükiger, UniGE, project 3).*

In addition, Nb_3Sn conductors with a Ti additive were fabricated using the bronze route, in collaboration with Bruker BioSpin. The critical currents obtained are equal to the best values of bronze wires published so far for conductors synthesized by the filament doping method.

The Geneva group has designed and constructed a unique spiral strain ring (Walter spiral – WASP) allowing the critical current of 80 cm long wires and cables to be measured under stress (see Fig. E-2). This facility allows a current of up to 1 kA in magnetic fields up to 17 T. It was used so far to measure the Nb_3Sn wires, the MgB_2 and Bi,Pb(2223) tapes as well as the $YBa_2Cu_3O_{7-\delta}$ coated conductors described above.

Most of these results benefited from 3D modeling, in particular the design of multilayer cables made of high-T_c superconductors. The modeling has proved to be of special benefit in minimizing AC losses. (M. Hasler and collaborators, EPFL, associated with project 3).

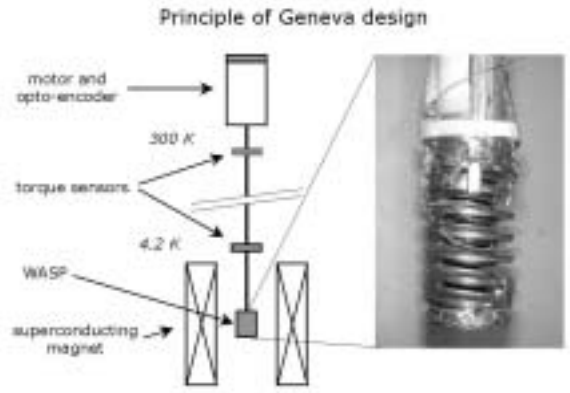

Fig. E-2*. Left: setup of the WASP device for measuring critical current as function of strain up to 1 kA and 17 T. Right: the spiral with a superconducting wire mounted for the measurements (R. Flükiger, UniGE, project 3).*

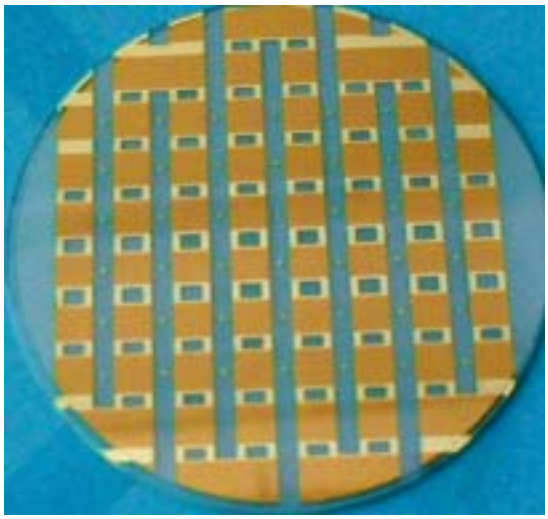

Fig. E-3. *New design for the meander of a 5kW (300V-16A) fault current limiter.*

II. Superconducting thin films for power applications

A fault current limiter (FCL) based on superconducting thin film heterostructures of Au / $YBa_2Cu_3O_{7-\delta}$ / CeO is presently developed. One issue which influences the performance of the FCL is the localization of all the dissipated power in one part of the device when the short circuit occurs. To overcome this difficulty and uniformly distribute the dissipated power over the surface of the device, a special pattern was developed and tested. The superconducting film is arranged in a meander on the substrate, as shown in Fig. E-3. The meander is designed in such a way that only the constricted parts are switching to the normal state during the first few microseconds

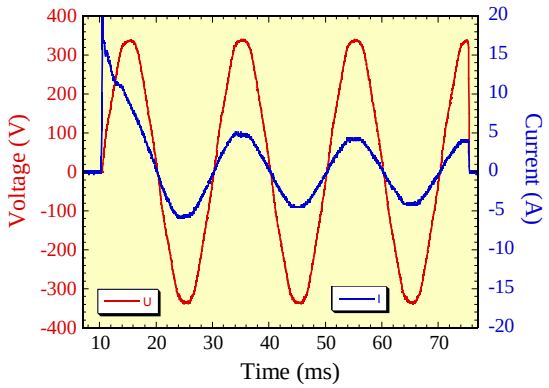

Fig. E-4*. Voltage and current in the FCL during a short circuit starting at U=0 (U_{rms}=240V). The FCL is switching after only a few μs.*

of the short circuit and that, for the maximum applied voltage, the total length of the constrictions switches. A patent has been filed for this new design (Project 2, Ø. Fischer, UniGE, in collaboration with ABB, Baden).

Prototypes, deposited on 2 inch sapphire wafers, were tested successfully at 5 kW (300 V, 16 A). For these tests, a new electronic set-up was built allowing precise control of the parameters of the short circuit. Fig. E-4 displays the voltage and the current in the superconducting FCL during a short circuit. It shows first that the FCL switches and limits the current in a few μs and secondly that the FCL can sustain the short circuit for a period of 65 ms. After this period, the current is reduced to 25% of the nominal 16 A current.

3 The Eighteen MaNEP projects

MaNEP includes presently eighteen research projects. Sixteen are active from July 1st 2001 One (project 18), started on January 2003 and another (project 17) started on January 2004

1. Nanoscale Dielectrics and Mesoscopic Properties of Superconductors

Project leader: Markus. Büttiker, University of Geneva

Research summary: Generation, control and manipulation of quasiparticle entanglement is a prerequisite for a large scale implementation of quantum information and quantum computation schemes in solid state systems. We have proposed experimentally realizable schemes for orbital (instead of the usual) spin entanglement in mesoscopic conductors, implemented in semiconductor-superconducting heterostructures and in a semiconductor two-dimensional electron gas in the quantum Hall regime, using edge channels and quantum point contacts. The entanglement is detected via violation of a Bell inequality, expressed in terms of zero frequency noise correlators. We have also investigated the statistical properties of current fluctuations in mesoscopic conductors, with the focus on normal-superconductor heterostructures. Spin injection and transport are of much current interest. We have investigated spin transport and noise in a ferromagnetic-superconducting hybrid structure. An important spin dependent phenomena in interacting low-dimensional systems, which has recently received a lot of attention, is the Kondo effect. The interplay of the Kondo effect and ferromagnetism has been investigated as well as the nonequilibrium properties of the spin transport.

Quasiparticle entanglement

Entanglement is one of the most intriguing features predicted by quantum theory. It leads to correlation between distant particles, which can not be described by any local, realistic theory. This non-local property of entanglement has been demonstrated convincingly in optics, where entangled pairs of photons have been studied over several decades. Apart from the fundamental aspects, there is a growing interest in using the properties of entangled particles for quantum cryptography and quantum computation.

Recently, much interest has been shown for entanglement of electrons in solid state systems. A controlled generation and manipulation of electronic entanglement is of importance for a large scale implementation of quantum information and computation schemes. Electrons are however, in contrast to photons, massive and electrically charged particles, which raises new fundamental questions and new experimental challenges. Existing suggestions are based on creating, manipulating and detecting spin-entangled pairs of electrons. This requires experimental control of individual spins via spin filters or locally directed magnetic fields on a mesoscopic scale.

We have proposed two spin-independent schemes for creating and detecting entanglement in mesoscopic conductors. In [1] we show that a superconductor, weakly coupled to a normal conductor, shown in Fig. 1, creates an orbitally entangled state by emitting a coherent superposition of pairs of electrons into different leads of the normal conductor.

In the *tunneling* limit, the zero-frequency correlation between currents flowing into different normal reservoirs is shown to be equivalent to a pair coincidence measurement: only correlations between the electrons from the same entangled pair contribute.

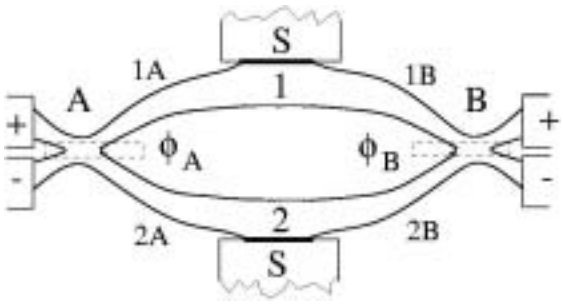

Fig.1. The normal-superconducting orbital entangler: A single superconductor (S) is connected to four normal arms via two tunnel barriers 1 and 2 (thick black lines). The arms are joined pairwise in beam splitters A and B and end in normal reservoirs + and -. See Ref [1].

As a consequence, a standard Bell Inequality (BI) can be directly formulated in terms of the zero-frequency current correlators. We find that a violation of the BI, demonstrating the entanglement of the pair state, can be obtained for arbitrary dephasing in the normal conductor.

The second proposal concerns entanglement in the electronic Hanbury Brown Twiss set-up. Hanbury Brown and Twiss (HBT) developed an interferometer which permitted them to determine the angular diameter of visual stars. The HBT effect contains two important distinct but fundamentally interrelated effects: First, light from different, completely uncorrelated, portions of the star gives rise to an interference effect which is visible in intensity correlations but not in the intensities themselves. This is a property of two particle exchange amplitudes. Exchange amplitudes are a quantum mechanical consequence of the indistinguishability of identical particles. Second, there is a direct statistical effect since photons bunch whereas fermions anti-bunch.

Fundamentally both of these effects are related to the symmetry of the multiparticle wave function under exchange of two particles. For photons emitted by a thermal source a classical wave field explanation of the HBT-effect is possible. A quantum theory was put forth by Purcell. For fermions, no classical wave theory is possible.

It has long been a dream to realize the electronic equivalent of the optical HBT experiment. This is difficult to achieve with field emission of electrons into vacuum because the effect is quadratic in the occupation numbers. This difficulty is absent in electrical conductors where at low temperatures a Fermi gas is completely degenerate. Experiments demonstrating fermionic anti-bunching in electrical conductors were reported by Oliver et al, Henny et al. and Oberholzer et al. Only very recently was a first experiment with a field emission source successful. In contrast, to date, there is no experimental demonstration of two-electron interference.

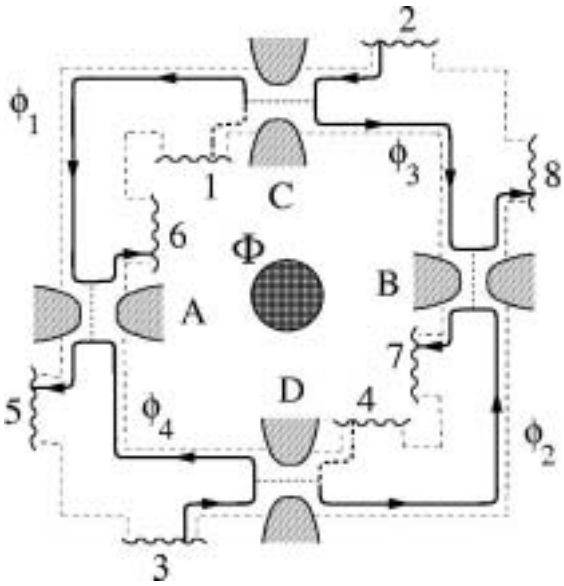

Fig.2. Two-source, four detector electrical Hanbury Brown Twiss geometry: a rectangular Hall bar with inner and outer edges (thin dashed lines) and four quantum point contacts (grey shaded). Contacts 2 and 3 are sources of electrons (a voltage eV is applied against all other contacts which are at ground). Electrons follow edge states (thick black lines) in the direction indicated by the arrows. An Aharanov-Bohm flux penetrates the center of the sample (shaded) but has no influence on the single particle properties. However, the current correlations are essentially dependent on the Aharonov-Bohm flux. See Ref [2].

In electrical conductors "beams" can be realized in high-magnetic fields in the form of edge states. Edge channels permit the transport of electrons over (electronically) large distances. In the quantized Hall state scattering out of an edge state is suppressed.

The second element needed to mimic optical geometries, the half-silvered mirror, is similarly available in the form of quantum point contacts (QPC). Indeed in high magnetic fields a QPC permits the separate measurement of transmitted and reflected carriers. A Mach-Zehnder interferometer with edge states was recently realized. This shows that it is possible to implement arrangements of linear optics in electrical conductors.

In Ref. [2] we proposed an implementation of the HBT-experiment in an electrical conductor in the quantum Hall regime. A schematic picture of the system is shown in Fig. 2. In the set-up, there is no single particle interference, however, two-particle interference is manifested as a magnetic flux dependence of the current correlators, a two-particle Aharanov-Bohm effect. We show that this two-particle effect is closely related to orbital entanglement of electron-hole pairs, recently proposed by Beenakker et al. as well as of pairs of electrons. The entanglement is detected via a violation of a Bell Inequality. Only normal electronic reservoirs, adiabatic QPC's and zero-frequency correlators are employed, greatly simplifying an experimental realization.

In addition to the two proposals for quasiparticle entanglement, we have also investigated the effect of dephasing on the entanglement [3], presented a detailed discussion on the analogy between transport in optical system and in Quantum Hall systems [4] and recently investigated the detection of spin entanglement via current correlations in a beam-splitter geometry [5].

Statistics of current fluctuations

In quantum theory, identical particles are indistinguishable. Under exchange of any pair of particles, the many-body wavefunction remains invariant up to a sign, positive for bosons and negative for fermions. It has been shown that the fermionic statistics of electrons leads to negative correlations between currents flowing in different terminals.

When normal conductors are connected to a superconductor, correlations are introduced between electrons and holes due to Andreev reflections at the normal-superconductor interface, a phenomenon known as the proximity effect. The influence of the proximity effect on the current auto-correlations, i.e. the shotnoise, in a two-terminal diffusive normal-superconductor junction was recently studied.

In multiterminal conductors, Andreev reflection can lead to positive cross correlations between currents flowing in the contacts to the normal reservoirs. So far, positive correlations have been predicted only for single mode junctions. Moreover, in multiterminal diffusive junctions it was found that cross correlations are negative in the absence of the proximity effect.

This raises two important questions: i) are the positive correlations in normal-superconducting junctions a large effect, of the order of the number of modes in multimode junctions, and if this is the case
ii) is the proximity effect necessary to obtain these positive correlations? In Ref. [6] we gave an answer to these two questions. The positive correlations are large, and surprisingly, get enhanced by normal backscattering at the normal-superconducting interface. Moreover, positive correlations can exist even in the absence of the proximity effect, if the normal-superconductor interface is nonideal.

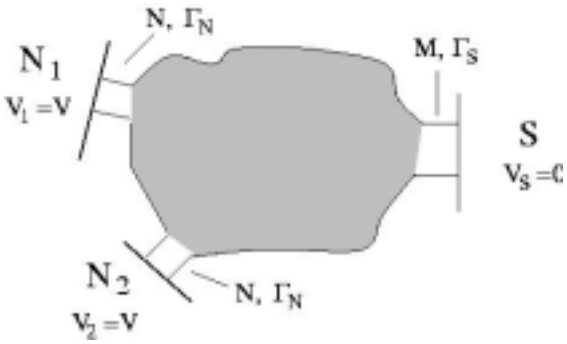

Fig.3. A chaotic quantum dot (grey shaded), acting as a beam-splitter, is connected to two normal reservoirs (N) and one superconducting reservoir S via quantum point contacts. See Ref. [6]

We have studied the current correlations in a system, shown in Fig. 3, consisting of a chaotic quantum dot connected via point contacts to one superconducting and two normal reservoirs. Systems consisting of chaotic dots coupled to superconductors have recently attracted a lot of interest. The generic properties of the model make our result qualitatively relevant for multiterminal normal-superconducting structures with random scattering.

In addition, we presented in [7] a completely semiclassical model of the current correlations in the system in Fig. 3, providing a simple explanation for the positive correlations. We have also investigated the full statistics of the charge fluctuations in normal-superconducting tunnel-barrier systems [8] as well as in incoherent multiterminal normal-superconducting systems [9]. The charge transfer statistics in a voltage biased Josephson junction was investigated in Ref. [10]. It was found that the statistics in the regime of Multiple Andreev Reflections describe charge transported in quanta of multiple electron charges. Recently, we have studied the coherent charge transport in ballistic Josephson junctions [11] and the density of Andreev reflection eigenvalues in normal-superconducting proximity systems [12].

Andreev drag effect

As we point out above, at a normal-superconducting interface, Andreev reflection causes a conversion of the quasiparticle charge *and* a flipping of its spin. The structure of interest consists of two ferromagnetic contacts connected to a normal conductor which is in turn connected to a superconductor (see Fig. 4). Of particular interest is the case of crossed Andreev reflection between ferromagnetic leads with antiparallel polarization dominating over crossed normal reflection. In such geometry, with a voltage applied to one of the leads while the other lead and the superconductor are grounded, the injected current from the biased ferromagnetic lead effectively *drags* along a current from the grounded lead. Much of the recent theoretical discussion has focused on a geometry where two needle-shaped ferromagnetic leads with antiparallel polarization are directly coupled to a superconductor at two spatially separated points. In this case, even in the case of 100% spin polarization, the crossed Andreev reflection probability is strongly suppressed.

In our research we have proposed a new geometry which overcomes the above difficulties by inserting a normal multichannel mesoscopic conductor with generic elastic scattering between the ferromagnetic electrodes and the superconductor [13]. We have included arbitrary interface conductances and spin-flip relaxation. We have found that the Andreev drag effect is observable when the conductance of the normal-superconducting interface dominates over the ferromagnetic-normal contact conductances. Furthermore, we have demonstrated that the crossed Andreev reflections have a profound influence on the zero-frequency current-current cross correlations. We have observed that both the thermal noise and the shot noise power measured between the two ferromagnetic leads yield *positive* values.

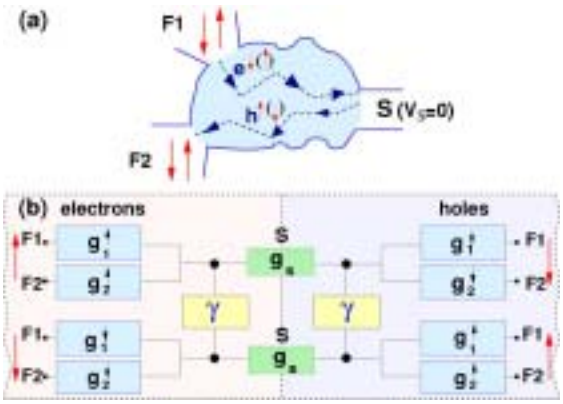

Fig. 4. (a) Generic ferromagnetic-normal-superconducting structure: the process that gives rise to the Andreev drag effect is indicated. (b) Sketch of the equivalent circuit model Ref.[13].

Kondo effect in quantum dots

Magnetic impurities embedded in metallic hosts cause anomalous resonant scattering of conduction band electrons. At the same time, the localized magnetic moments are screened at low temperature by the itinerant electron spins. This is the celebrated Kondo effect, which has been recently revived in mesoscopic physics. A flood of very recent works has introduced another interesting issue, namely how the Kondo physics is affected when the continuum electrons themselves are allowed to form *spin-dependent* bands [14]. The motivation for this research stems from the successful field of spintronics. In particular, a change has been detected in the resistivity of a Kondo alloy due to spin-polarized currents.

In our investigation we have presented a work which provides precise theoretical predictions in a wider region of the parameter space [15]. To the best of our knowledge, this is the first study of the model that sweeps across the different regimes (i.e., Kondo, mixed-valence, and empty orbital), thoroughly analyzed with the assessment of local DOS, linear conductance, and tunneling magneto-resistance (TMR). Second, we have resolved a controversy lately raised in the literature with regard to whether a spin-dependent renormalization of the impurity level induced by the spin-polarized leads will split the Kondo peak when the magnetic moments of both leads are aligned.

Double quantum dots (DQD's), also termed artificial molecules, have received a great deal of attention in different contexts, the most relevant one being possibly their application as solid-state quantum bits, by using either spin or charge degrees of freedom. Here, we have focused on the shot noise properties of DQD's at low temperatures, where strong correlations become relevant. If only spin fluctuations are important, this system can be regarded as an artificial version of the two-impurity Kondo problem [16] [two Kondo impurities coupled to conduction electrons and coupled to each other through an antiferromagnetic (AF) exchange coupling]. Indeed, we have found an abundance of regimes in the Fano factor directly reflecting the physics of the two-impurity Kondo problem in an out-of-equilibrium situation [17].

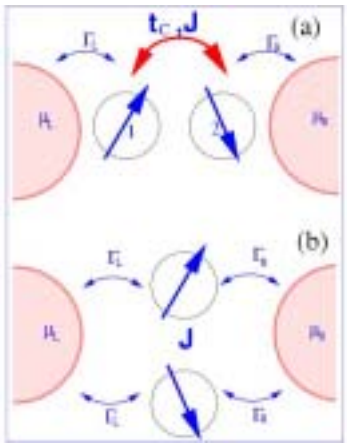

Fig. 5: (a) Double quantum dot connected in a serial configuration including an interdot tunneling coupling and the exchange interaction between the spin of the dots. (b) Double quantum dot in a parallel configuration. Ref. [17]

References:

[1] P. Samuelsson, E.V. Sukhorukov, M. Büttiker, Phys. Rev. Lett. **91**, 157002 (2003).
[2] P. Samuelsson, E.V. Sukhorukov, M. Büttiker, Phys. Rev. Lett. **92**, 026805 (2004).
[3] P. Samuelsson, E.V. Sukhorukov, M. Büttiker, Turk. J. Phys. **27**, 481 (2003) .
[4] M. Büttiker, P. Samuelsson, E.V. Sukhorukov, Physica E **20**, 33 (2003).
[5] P. Samuelsson, E.V. Sukhorukov, M. Büttiker, (to be submitted).
[6] P. Samuelsson, M. Büttiker, Phys. Rev. Lett. **89**, 046601 (2002).
[7] P. Samuelsson, M. Büttiker, Phys. Rev. B. **66**, 201306 (2002).
[8] P. Samuelsson, Phys. Rev. B. **67**, 054508 (2003).
[9] W. Belzig, P. Samuelsson, Europhys. Lett. **64**, 253 (2003).
[10] G. Johansson, P. Samuelsson, and Å. Ingerman, Phys. Rev. Lett. **91**, 187002 (2003).
[11] P. Samuelsson et al, cond-mat/0311344.
[12] P. Samuelsson, W. Belzig, Yu. V. Nazarov, cond-mat/0312133.
[13] David Sánchez, Rosa López, Peter Samuelsson, and Markus Büttiker, Phys. Rev. B 68**,** 214501 (2003)
[14] Rosa López and David Sánchez **,** Phys. Rev. Lett. **90**,116602 (2003).
[15] Mahn-Soo Choi, David Sánchez, and Rosa López, Phys. Rev. Lett. **92**, 056601 (2004).
[16] Rosa López, Ramón Aguado, and Gloria Platero Phys. Rev. Lett. **89** , 136802 (2002).
[17] Rosa López, Ramón Aguado, and Gloria Platero, submitted to Phys. Rev. B (2004).

.

2. Superconducting and Magnetic Properties of Complex Oxides

Project leader: Øystein Fischer, University of Geneva

Research summary: This project focuses on 3 main topics. In the first, we use scanning tunneling spectroscopy to investigate the local density of states of unconventional superconductors. We studied the localized vortex core states on Bi2212 and found that their energy scales linearly with the gap. To understand the detailed shape of the tunneling spectra in the superconducting state of Bi2212, we performed numerical simulations which showed that the asymmetries observed in the experimental data can be related to van Hove singularities, and that tunneling matrix elements are not anisotropic. Finally, we showed spectral traces along typically 80nm on Bi2212 surfaces that demonstrate extremely high homogeneity, ruling out that HTS are intrinsically inhomogeneous. In parallel, we investigated MgB_2 by performing detailed vortex imaging and spectroscopy by tunneling along both, the c-axis and the ab-plane. We firmly demonstrated its two band superconductivity and analyzed its anisotropy. In the second topic, we applied scanning tunneling potentiometry to study local transport in the colossal magneto-resistance materials $La_{0.7}Sr_{0.3}MnO_3$ and $La_{0.7}Ca_{0.3}MnO_3$, which are thought to exhibit an electronic phase separation. At room and low temperatures, down to a 100 nm scale, no signature of any metallic-insulating domains has been found in the local transport. In an extension of this work we investigated an electric field doped ultra-thin oxide film in contact with a ferromagnetic film and could show the existence of a field induced surface conducting state. The third topic focuses on thin film growth and heterostructure design. We are developing a fault current limiter device that is based on meander shaped $YBa_2Cu_3O_{7-\delta}$ thin films. We have developed a new design which allows to minimize and to homogeneously distribute the power along the meander. Using this design we have successfully tested a 5kW FCL submitted to an AC voltage of $240V_{rms}$ for 65ms. We also studied the effects of strain in superconducting $NdBa_2Cu_3O_7$ thin films by varying the film thickness and the substrates. We observed that the strain significantly affects the superconducting properties of the $NdBa_2Cu_3O_7$ films.

1. Scanning tunneling spectroscopy on unconventional superconductors.

We use scanning tunneling spectroscopy to investigate the local density of states (LDOS) of unconventional superconductors at variable temperatures, under vacuum and with an applied magnetic field. We focused our research on $Bi_2Sr_2Ca_{n-1}Cu_nO_{2n+4}$ with n=1,2,3 and on the recently discovered non-cuprate superconductor MgB_2.

$Bi_2Sr_2Ca_nCu_{2n+1}O_{2n+6}$

(a) To better understand the nature of the experimental tunneling spectra obtained on $Bi_2Sr_2CaCu_2O_8$, we performed numerical simulations considering the influence of tunneling matrix elements, of band structure features and of electronic effects directly related to high-T_c superconductivity (fig. 1). We concluded that van Hove singularities

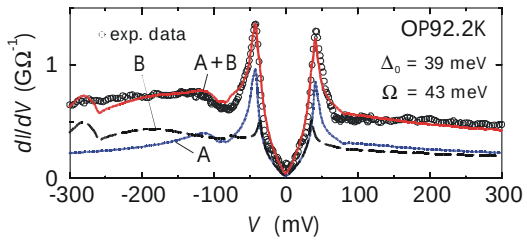

Fig. 1: Experimental and calculated tunneling spectra of Bi2212, with the data for both bands at E_F, and their sum.

contribute considerably to the asymmetry in the spectra and to the height of the coherence peaks. Interaction with a collective mode (Ω) can explain the "dip-hump" next to the coherence peaks, and the short lifetime of high-energy quasiparticles. Finally, the tunneling matrix elements do not show high anisotropy.

(b) The origin of the pseudogap and its relation to superconductivity is still not understood. Previously we showed on $Bi_2Sr_2CaCu_2O_8$ that the pseudogap scales with the super-conducting gap and that it is also present on the overdoped side of the doping phase diagram. To test the generality of these observations, we investigated the single-layer material $Bi_2Sr_2CuO_6$ and observed the same scaling behaviour, suggesting a common origin of both gaps. The extension of this study to $Bi_2Sr_2Cu_2Ca_3O_{10}$ is under way. First results have been obtained at low temperatures. The pseudogap has also been observed in vortex cores, but in addition we see low energy features in the LDOS, so-called core states. We found that their energy also scales with the superconducting gap. This is in striking contrast to the quadratic dependence expected for classical s-wave superconductors (fig. 2).

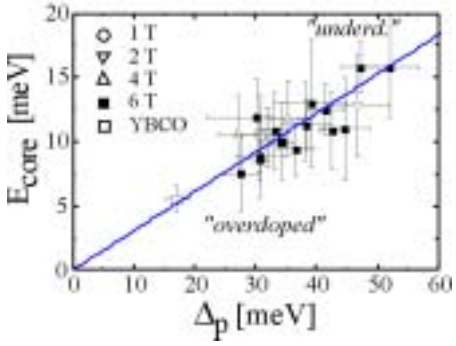

Fig. 2: Core state energy versus superconducting gap. The straight line is a fit through the Bi2212 data (1-6T). Strikingly, YBCO follows the same energy scaling.

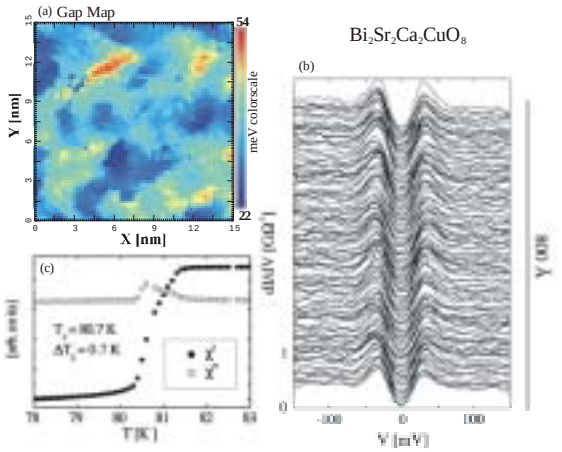

*Fig. 3: (a) Gap map of a typical **inhomogeneous** Bi2212 sample. (b) LDOS along a 80nm line on **homogeneous** sample annealed @ 15 bar O_2, 500°C, 7 days. (c) Superconducting transition $\Delta T < 1\% Tc$ of sample (b).*

(c) Investigating the LDOS at the atomic scale often reveals superconducting gap features (peak position and height, gap shape) that vary in space over distances of a few nanometres, due to impurities, defects or oxygen inhomogeneities, thus making the study of intrinsic properties more difficult. To obtain truly homogeneous samples, we concentrated on the synthesis and annealing conditions of $Bi_2Sr_2CuCa_2O_8$. The fact that the gap varies with doping indicates that the often observed inhomogeneous LDOS, is due to an inhomogeneous oxygen distribution (fig. 3a). A specific annealing yielded a very homogeneous LDOS (fig. 3b), indicating that inhomogeneity is not intrinsic to high-T_c superconductivity, at least not to overdoped samples. Our study also suggests that a prerequisite for long-range homogeneity is a superconducting transition width of less than 1% of T_c (fig. 3c).

Magnesium diboride MgB_2

MgB_2 is a recently discovered superconductor that has undergone wide study over the past few years mostly because of its interesting two-band nature: The isotropic π-band can be seen via tunneling measurements in any direction, while the highly anisotropic σ-band contributes very little to tunneling measurements parallel to the crystalline c axis.

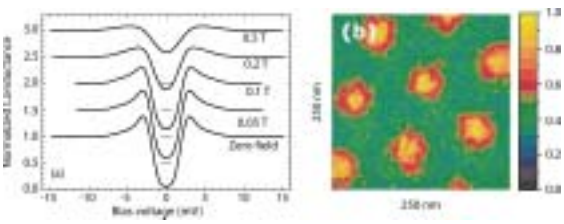

Fig. 4: (a) spectra versus field in between cores. Tunneling direction and field are parallel to c axis. The zero field data shows the smaller π-band and weak shoulders due to the larger σ-band. (b) vortex lattice at 0.2 T.

Early measurements in this group tunneling **parallel** to the c axis revealed a π-band superconducting gap of $\Delta_\pi \sim 2.2$ meV (fig. 4), with shoulders visible around +- 6 meV due to the sigma-band. Furthermore, vortex imaging in this direction provided a surprising result. The coherence length determined from Hc_2 = 3.1 T in this direction is $\xi_{Hc2} \sim 10$ nm, while the size of the vortices is much larger, giving a coherence length of ~ 50 nm, in line with an estimate based on the size of Δ_π. This was an early example of how macroscopic parameters, such as Tc and Hc_2, are set by the σ-band, whereas other parameters, such as the size of the vortices, are set by the π-band. Another surprising result is the absence of any signature of localized states at the center of the vortex core, which cannot be explained by the vicinity of the dirty limit for MgB_2. More likely, this observation might be related with the interplay between the two bands with different energies and spatial distribution of the localized states expected for each band individually.

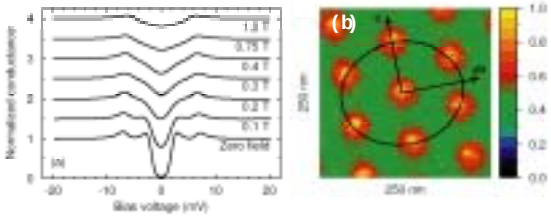

Fig. 5: (a) spectra versus field in between cores. Tunneling direction and field are perpendicular to c axis. π and σ-band gaps are clearly visible at zero field. The field quickly suppresses the π-band. (b) vortex lattice at 0.3T.

Motivated by the success of these experiments and the desire to investigate properties of both bands simultaneously, measurements were carried out in 2003 using scanning tunneling spectroscopy with the tunnel direction **perpendicular** to the c axis. These experiments allowed us to measure a σ-band superconducting gap of $\Delta_\sigma \sim 7$ meV. Furthermore, vortex imaging allowed us to determine the anisotropy of the vortex flux line lattice yielding $\gamma = 1.2$ (fig. 5). This value is much lower than the upper-critical-field anisotropy, $\gamma_H = 6$, but in good agreement with theoretical calculations for the penetration depth anisotropy.

2. Local transport in magnetic films and ferroelectric field effect

The remarkable electronic properties of a large number of novel materials are often due to a very peculiar distribution of the charge carriers throughout the compound, or to structural

features associated with non-standard electronic transport. In this part of the project, we concentrate on local transport studies using an STM with the technique of Scanning Tunneling Potentiometry (STP). The general idea is to measure locally the electrical potential while a current flows through a thin film. This allows to map the distribution of the electrical potential induced by the current, and to probe the local electronic transport with nanometer spatial resolution.

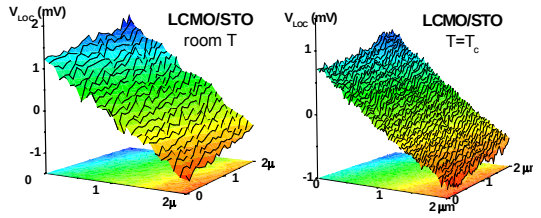

Fig. 6: Local potential drop for a $La_{0.7}Ca_{0.3}MnO_3$ thin film at room temperature (a) and at T_c (b).

Colossal magnetoresistance compounds still retain considerable interest because of their promising technological applications, but the microscopic mechanisms responsible for their exceptional transport properties are far from being completely understood. The inter-grain magnetoresistance MR is one of the properties which can be directly probed with STP. Our first studies showed that important potential drops can be observed at the grain boundaries in textured samples, at room temperature and zero magnetic field. The question whether these drops will be strongly reduced under field at low temperature (the so called low field MR) could be solved when the experimental setup necessary to carry out such measurements will be fully operational.

Another open question is the predicted electronic phase separation (PS), involving the coexistence of metallic and insulating microscopic phases in hole-doped compounds. The question whether the colossal magnetoresistance is related to such a mesoscopic phase separation and whether it is of intrinsic character is being addressed in several groups by local probe techniques, showing inhomogeneities from nm to μm scale depending on the technique and the sample. We have first shown the absence of electronic or chemical mesoscopic PS in $La_{0.7}Sr_{0.3}MnO_3$ at 300K (below Tc). We then started a study on the $La_{0.7}Ca_{0.3}MnO_3$ (LCMO) compound in order to probe a possible PS. An epitaxial 53 nm thick LCMO film annealed in situ shows a highly linear potential drop at room temperature (well above T_c), excluding any PS down to the experimental resolution. STP measurements have also been performed at $T=T_c$ on the same compound, showing also highly homogeneous potential drops (fig. 6).
This throws a doubt on the universality of the phase separation hypothesis. Experimental difficulties encountered at low temperatures have encouraged the construction of a new 4-300K controllable temperature STM/STP probe suited for studies on manganites.

A further development based on the STP technique is the study of the switching between an insulating and a conducting state in an ultrathin film placed on top of a ferroelectric thin film. The switching is obtained by commuting the ferroelectric state which affects the carrier densities by field effect. The STM is used to probe the two different electronic states induced at the top of the ultrathin film. This can be done either by sending a current through the sample and probed by STP, or by measuring the differential conductance in the two states. We have observed that the surface in an ultrathin $SrTi_{1-x}Ru_xO_3$ film switches between an insulator and a conductor upon switching the orientation of the ferroelectric polarization. Using the STM tip to polarize ferroelectric domains, one can thus write metallic nano-domains into the ultrathin film. Using the spectroscopic signal one can also observe these domains.

3. Epitaxial thin films and multi-layers

Fault Current Limiter (in collaboration with ABB)

The fault current limiters (FCL) are devices that limit the current, in an electrical network, during a short circuit. We are currently working on superconducting thin film based FCL's made of Au/YBCO/CeO heterostructures (meanders) grown onto 2 inch sapphire wafers.
One of the problems which influences the performance of FCL is the localization of all the dissipated power in one part of the meander (or wafer). This can limit the maximal power sustained by one wafer and also the possibility of having a FCL based on several wafers in series or parallel. In the first part of this project we have developed and tested a particular design of the meander which solves this problem. This design is based on our investigations of the behavior of YBCO lines submitted to voltage pulses which show that the initial length (after ~25μs) of the dissipative region varies linearly with the applied voltage. The idea is then to split this initial dissipative length into many separated small regions uniformly distributed along the meander.

This is done by locally decreasing the width of the line (and therefore the critical current); i.e. by including constrictions along the meander as shown in figure 7. The meander is designed in such a way that only the constricted parts are switching during the first microseconds of a short circuit and that, for the maximum applied voltage, the total length of the constrictions switches.

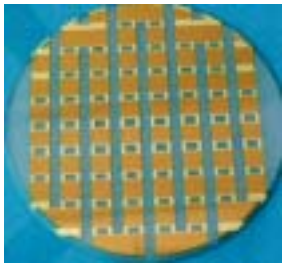

Fig. 7: New design for the meander of a 5kW (300V-16A) fault current limiter.

During the second part of this project we have developed and tested an improved design with the aim to reduce the power dissipation in the wafer. The new design took into account the observed behavior of a meander during a short circuit: after the usual initial peak current (at $3J_c$), the line is acting as a current source during the first 20-40 μs (i.e. the current is constant and independent of the applied voltage) and as a voltage source at longer time, where the current decreases due to the propagation of the dissipative region and the increase of its temperature. Thanks to the constrictions in the meander we have proposed an efficient way to minimize the dissipation during both short and long time intervals. Since only the constrictions are switching during the first μs, the dissipated power can be decreased by decreasing their resistivity. This is done by increasing the thickness of the gold layer on top of the constrictions, which requires an additional step in the lithographic process. On the other hand a thinner gold layer is grown on the connecting paths which increases their resistivity and then decreases the power density at longer times. A 5kW (300 V-16 A) FCL, using this final design is shown in figure 7. has been successfully tested, during a DC short circuit, for a periods as long as 100 ms. In collaboration with ABB we have patented this new design (patent N° EP 1 383 178 A1).

We have also focused our studies on the behavior of our FCL submitted to an AC short circuit. A new electronic set-up has been built which allows us to precisely choose the phase angle at which the short circuit starts and ends. We have measured, in the ABB laboratory in Dättwil the complete behavior of several 5 kW wafers by recording the voltage on each line of the meander.

Figure 8 presents the voltage and the current in the FCL during a short circuit started at a phase angle close to zero, which is one of the most constraining condition since only a small fraction of the constrictions is switching at the

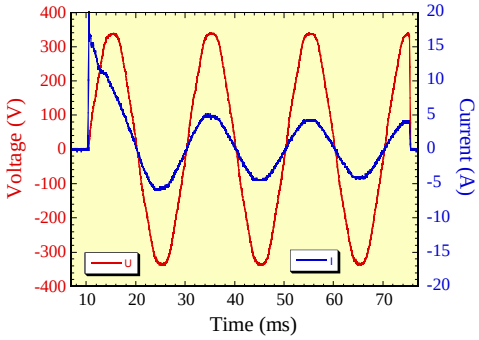

Fig. 8: Voltage and current in the FCL during a short circuit starting at U=0 (U_{rms}=240V). The FCL is switching after only few μs.

beginning of the short circuit. This result shows that our FCL is switching and limiting the current in a few μs and can sustain such a short circuit, under an AC voltage of 240 Vrms (340V peak), for a period of 65 ms. After this period, the current is as low as 25% of the nominal current or I_c (16 A).

Effects of strain on superconducting thin films

Superconducting films of $Nd_{1+x}Ba_{2-x}Cu_3O_{7+\delta}$ (NBCO) show a decrease of T_c with reduced thickness. This T_c loss depends on the substrate used, as was seen using $SrTiO_3$ and $LaAlO_3$. In order to know if this effect is due to strain induced variations of the oxygen doping, we have studied two batches of samples on $SrTiO_3$: one with varying thickness (from 3.6 nm to 100 nm), and one with reduced oxygen proportion at fixed thickness (100 nm). X-ray diffraction allowed us to measure very precisely the c-axis parameter of our samples. These measurements combined with resistivity and Hall effect measurements show that the Tc variations are not due to oxygen variations and that the strain has a direct influence on T_c.

References:

1. B. W. Hoogenboom et al., PRB. **67**, 224502 (2003).
2. M. Kugler, et al., Phys. Rev. Lett. **86**, 4911 (2001).
3. B. W. Hoogenboom et al., PRL. **87**, 267001 (2001).
4. B. W. Hoogenboom et al., Physica C **391**, 376 (2003).
5. M. R. Eskildsen et al., Phys. Rev. B **68**, 100508 (2003).
6. M. R. Eskildsen et al., Physica C **385**, 169-176 (2003).
7. M. R. Eskildsen et al., PRL. **89**, 187003 (2002).
8. B. Grévin et al., Appl. Phys. Lett. **80**, 3979 (2002).
9. S. Reymond *et al.*, Supercond. Sci. and Technol. **17**, (2004) 522
10. M. Decroux *et al.*, IEEE Trans. on Applied Superconductivity **13**, (2003) 1988.
11. L. Antognazza *et al.*, Physica C **372-376**, (2002) 1684.
12. S. Reymond *et al.*, Phys. Rev. B. **66**, (2002) 14522.
13. M. Decroux *et al.*, IEEE Trans. on Applied Superconductivity **11**, (2001) 2046.

3. Thermodynamics and Critical Currents in Superconducting Tapes and Wires for Industrial Applications

Project leader: René Flükiger, University of Geneva

Research summary: a) Square Bi,Pb(2223) wires with low AC losses: Square Bi,Pb(2223)/Ag wires with almost isotropic behaviour have been produced, with J_c = 20 kA/cm^2 at 77K,0T and considerably reduced AC losses; fabrication of a 5 m long, 200 A cable based on square Bi,Pb(2223) wires), **b**) **Y(123) by spray pyrolysis:** using a 2.5 MHz ultrasonic generator and r. f. heating, Y(123) films have been deposited, with T_c = 91 K and J_c up to 1x 10^5 A/cm^2, **c) J_c vs. strain rig at high fields:** A new spiral strain rig (WASP) for measuring J_c vs. ε on 80 cm long conductors (0.1 μV/cm criterion) up to 17 T and 1 kA has been developed. Measurements of J_c vs. B performed on Nb_3Sn, Nb_3Al wires, Bi,Pb(2223) and MgB_2 tapes, **d) MgB_2 tapes**: J_c of Fe sheathed MgB_2 tapes and wires with high j_c values have been prepared by "ex situ" technique, **e) Crystal growth**: Growth of large Bi(2223) single crystals (3 mm); new crystal structure in Bi,Pb(2212), with lower anisotropy and enhanced flux pinning; determination of vortex phase diagram in Bi(2223) and Bi,Pb(2212) single crystals**, f) AC loss characterization:** Novel 2D and 3D models for simulation of Bi,Pb(2223) tape conductors have been developed and implemented in finite element method software (3D formulation: also applicable for simulation of thin $YBa_2Cu_3O_7$ films), **g) Hall probe mapping**: A new Hall probe magnetic field mapping system has been designed. An improved electric model for optimization of HTS cable geometry has been proposed.

Bi,Pb(2223) wires for industrial application

New Bi,Pb(2223) conductors were developed with square cross-sections, smaller twist pitch than in tapes and reduced anisotropy (Fig. 1).

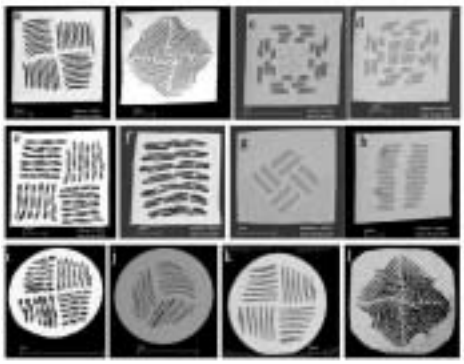

Fig.1 : Wire cross-sections and filaments arrangement for Bi,Pb(2223) conductors.

Fig. 1a combines a high filling factor and a small anisotropy. J_c(77K,0 T) values as high as 20 kA/cm^2 were reached, which is the highest value ever reported for "isotropic" Bi,Pb(2223) wires. Twist pitches as short as 4 mm were found to exhibit more than 90% of J_c for untwisted wires. In square wires, the AC losses are reduced by a factor ~10 when compared to those of a tape in a magnetic field applied ⊥ to its surface (Fig. 2).

AC losses in square wires are smaller than in tapes, in cases where the field orientation with respect to the conductor surface cannot be accurately controlled. Our study shows that AC losses can be further reduced, either by reducing the wire diameters, by introducing barriers between the filaments, or using alloyed sheath.

Etching away Ag at the surface of the tapes showed that it has a significant influence on the level of AC losses and could be envisaged to reduce the losses in square wires.

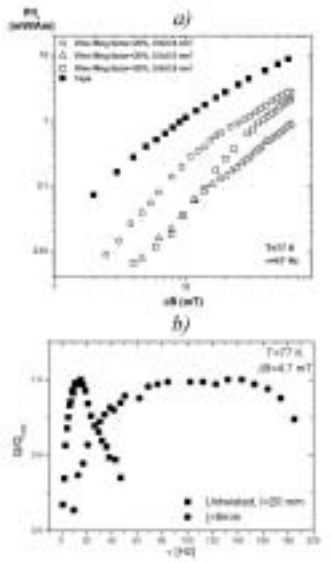

Fig.2. AC losses for different wire geometries a) and variation of losses with frequency b).

Coils made with square wires were prepared for a prototype transformer in the frame of an European GROWTH project (Fig. 3). The coils

Fig. 3: A schematic view of the coil fabrication and of the final coil.

were then sent to Skoda which used them to replace coils at the extremities of a secondary

winding. The “isotropic” conductor cable shown in Fig. 3 carried 200 A at 77K and 0.1 T.

Development of coated $YBa_2Cu_3O_{7-x}$ by spray pyrolysis

We have constructed a new spray pyrolysis device with a r.f. heating system. $YBa_2Cu_3O_{7-x}$ films have been deposited on (100) $SrTiO_3$ single crystal substrates starting from highly concentrated nitrates solutions (from dissolving Y_2O_3, $BaCO_3$ and CuO in nitric acid). It was found that composition, carrying gas flow, deposition temperature, and annealing time as well as oxygen partial pressure strongly affect the morphology and orientation of the $YBa_2Cu_3O_7$ films.
After deposition of films of 1-3 microns, we obtained J_c values of 10^4 A/cm^2 in the film even without annealing, suggesting that the key point of film formation occurs during deposition. After a heat treatment for 2 hours, the film exhibited T_c onset = 91 K and the highest inductive J_c value at 77K, 0T was 1×10^5A/cm^2 (8×10^4 in Fig. 4).

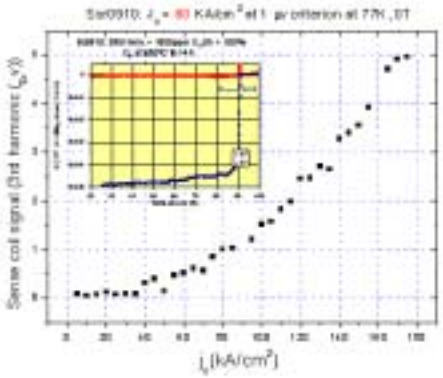

Fig. 4: J_c of a Y123 film (insert: T_c transition) obtained by spray pyrolysis at 890°C on a $SrTiO_3$ substrate.

The J_c values are an order of magnitude lower than those of the thin film grown by physical methods, this is due to a poor texturing degree and to defects and impurities at the grain boundaries. The weak point of this otherwise fast and economical method is the lack of control of the droplets at the very last stage prior to deposition.

Nb_3Sn bronze route wire development

We fabricated several conductors of 1.25 mm diameter, with the Ti additive either in composite filaments (NbTa/NbTi) or in Ti alloyed Osprey bronze (CuSnTi).
We obtained J_c,non-Cu = 285 A/mm^2 and *n* = 50 at 17 T and 4.2 K, which is equal to the best values on bronze wires published so far (Fig. 5). While these results of J_c and n clearly reveal the Ti doping by the bronze as more performing, the analysis of the residual niobium ratio of the filaments and residual Sn content in the bronze does not show a significant difference compared to the filament doping method.

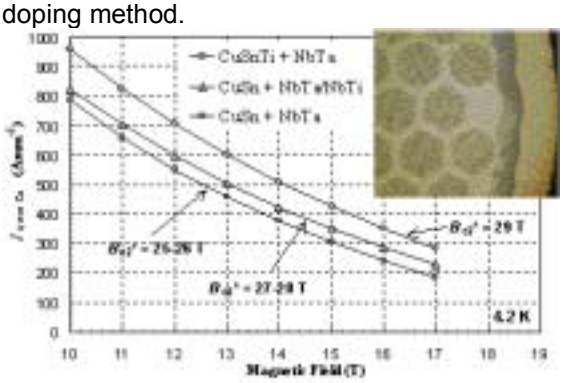

Fig. 5: Non-Cu J_c(B) for Ti and/or Ta alloyed bronze wires.

Further high resolution analysis is under work for the nanostructure analysis of the A15 phase (grains, grain boundaries) [1].

Critical current vs strain measurements of long length industrial Nb_3Sn wires using a modified Walters spring

We have developed a spiral device for the characterization of the critical current of long length high current technical superconducting wires under strain at fields up to 17 T [2]. Our device is based on the concept of the Walters spring (WASP) (see Fig. 6); the voltage taps are separated about 50 cm.

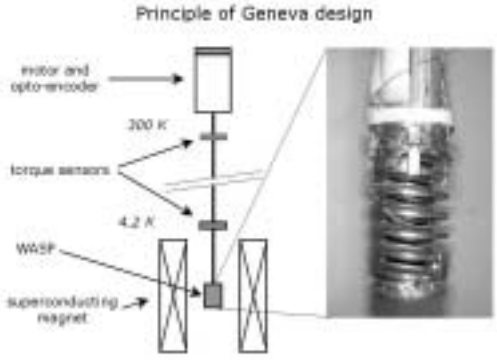

Fig. 6: Setup of the device for measuring critical current as a function of strain up to 1000 A and 17T.

High sensitivity measurements (down to 0.01μV/cm) have been performed on Nb_3Sn wires to investigate the relation between the irreversible behaviour and the shape of the V-I curve (see Fig. 7). An upward curvature and a smaller slope at $\varepsilon > 0.7$ % (lower *n* value) are the footprints of filament breakage. As shown in Fig. 7, this irreversible effect is not revealed when using the usual criterion of 1 μV/cm.
We have successfully measured Bi2223 3-ply tapes manufactured by AMSC (Fig. 8) and MgB_2 tapes manufactured at GAP (see Fig. 10 next section) [3].

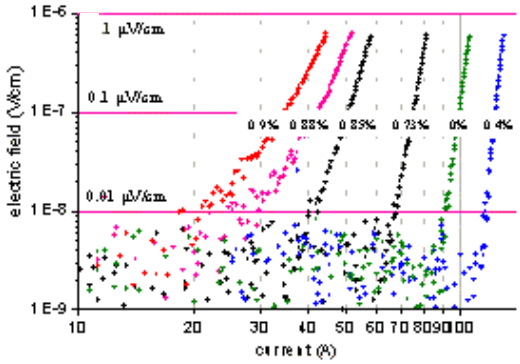

Fig. 7: V-I curves for a Nb_3Sn wire at 13T from 0% up to 0.9% of tensile strain.

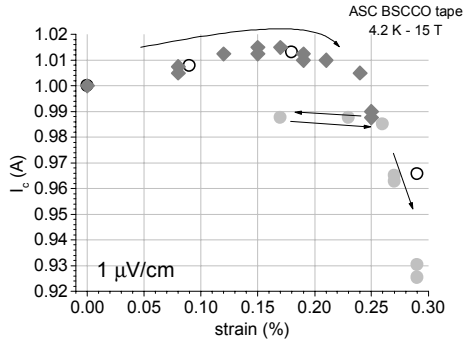

Fig. 8: Behaviour of critical current vs strain in Bi2223 3-ply tapes measured in two different samples.

MgB_2/Fe sheathed conductor development

Fe sheathed MgB_2 tapes have been produced by Powder In Tube (PIT) "ex-situ" technique [4]. It has been found that the state of the initial MgB_2 powders strongly influences the J_c values as well as the homogeneity of the produced tapes. The best performance has been achieved for powders after different dry grinding in inert atmosphere [5] (see Fig. 9).

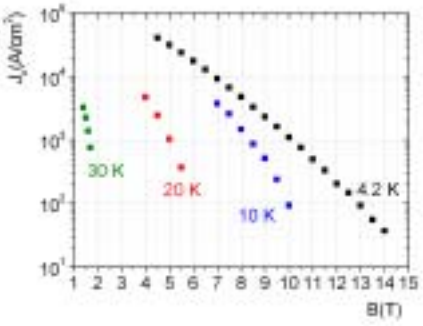

Fig. 9: J_c vs applied magnetic field at different temperatures.

The variation of the critical current under tensile strain (Fig. 10) was measured on long samples by means of the modified Walters Spiral (Fig. 6). Exceeding 0.31 % leads to filament breakage. This behaviour is explained by the differential thermal expansion between Fe and MgB_2 [5].

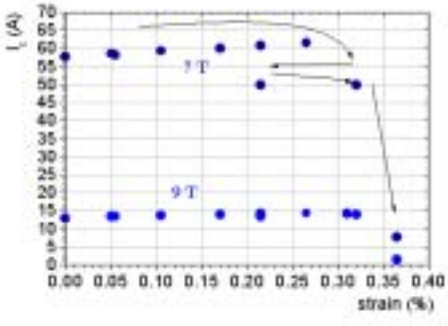

Fig. 10: Critical current vs. applied tensile strain for 0.80 m long MgB_2/Fe tape at different applied magnetic fields.

The critical current density in "ex situ" MgB_2 tapes was found to undergo a marked anisotropy, the ration between parallel and perpendicular applied field exceeding 10 under certain circumstances. This ratio may be correlated to partial texturing of MgB_2. This texturing is a consequence of the deformation process, initial powder size and HIP pressure; and is the object of further investigation.

Vortex Phase Diagram of Bi-2223 Single Crystal

The recent growth of Bi(2223) crystals in our group has enabled us to study the magnetic properties and vortex phase diagram of this material. The superconducting anisotropy is a key parameter: a value of $\gamma = 50$ is found for our Bi(2223) crystals, i.e. significantly smaller than the value for Bi(2212) single crystals, where $\gamma = 165$. Using a SQUID magnetometer, we have mapped out the vortex phase diagram of Bi(2223), shown in Fig 11. In this figure, the

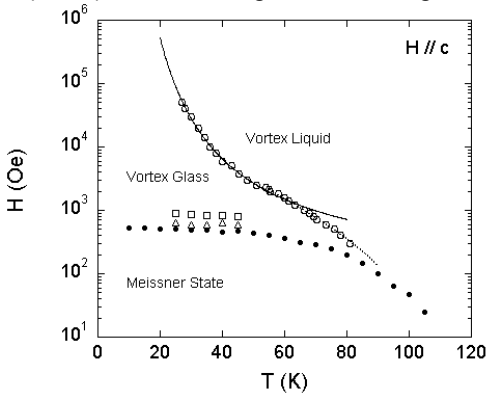

Fig. 11: Vortex phase diagram of Bi-2223 single crystal. The irreversibility line (open circles) is fitted by a Lindemann-type melting criterion.

open circles represent the irreversibility line, and the triangles (squares) are the onset of the second magnetization peak. We find that the irreversibility line of Bi(2223) occurs at higher fields than Bi(2212), being comparable to that of heavily Pb-doped Bi(2212).

2D and 3D modelling of HTS conductors

Advanced 2D anisotropic models have been developed, allowing precise numerical calculations and current density, magnetic field and AC losses of Bi(2223) conductors with various cross-sections under several operating conditions [6]. A new 3D model for simulations of HTS materials has been developed and implemented in finite element method software [7], which has been used for studying the coupling between superconducting filaments in Bi(2223) tapes (Fig. 12). The latter was also used for studying the behaviour of strip lines of a $YBa_2Cu_3O_7$ / Au Fault Current Limiters in an AC nominal use.

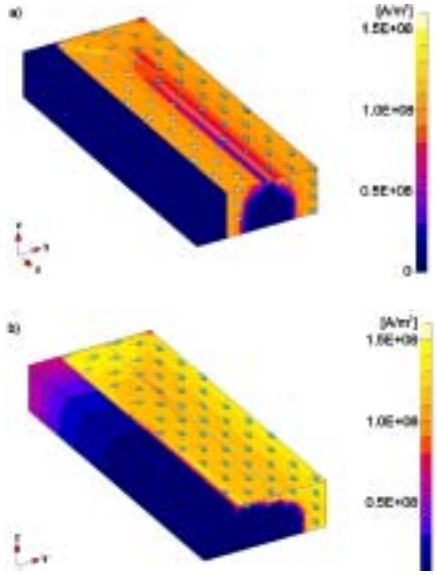

Fig.12: Current density distribution in uncoupled (a) and coupled filaments (b) in magnetic field of 5 mT at 100 Hz (a) and 10 kHz (b).

Equivalent circuit modelling

An equivalent circuit model for HTS superconductors has been developed. The model is based on Maxwell's equations, measurement results, as well on the physical structure of the superconducting wires: the circuit elements are formally a nonlinear resistance and a nonlinear inductance (superconducting core) in parallel with a linear resistance and two linear inductances (silver sheath/matrix). A new, modified power-law was used for describing the voltage-current relation of the superconducting material for currents above I_c. The outputs of the model are the instantaneous current, voltage and power loss waveforms [8].

HTS cable modelling

EPFL developed a 3D electrical model for multi-layer HTS cables, which can be used for finding the optimal geometrical configurations leading to an uniform repartition of the current among the layers and giving the lowest AC losses [9]. EPFL also used FEM software for computing in detail the current and magnetic field distribution inside the tapes composing the cable, in order to precisely evaluate the AC losses, which are strongly influenced by the geometry of the tapes and their arrangement in the cable structure.

Dynamic Hall-probe Field Mapping

A high-speed field-mapping system with 15 Hall probes at 50 Hz has been implemented using a 16-channel ultra fast digital lock-in. The system has been upgraded to perform measurements at higher sampling rate. An example of the measured field profiles is shown in Fig. 13.

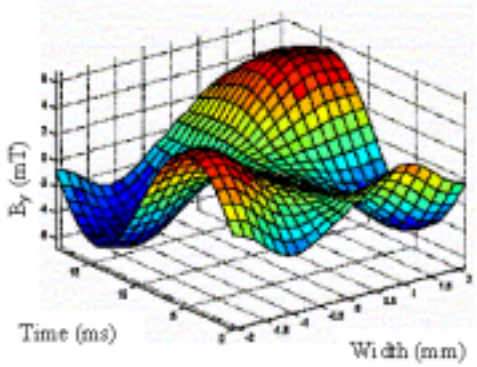

Fig.13: Magnetic field profile along the width of the sample for one cycle at 50 Hz. I_{max} = 70 A.

The data for the measured dynamic field on the surface was then used in a specially developed inverse problem algorithm for finding the corresponding current distribution in the superconductor. It was demonstrated that the current reconstruction method gives a sufficiently accurate description of the current distribution in the superconductor.

References:

[1] V. Abächerli, D. Uglietti, B. Seeber and R.Flükiger, Physica C, 372-376 (2002) 1325-1328.
[2] B. Seeber et al. – to be published.
[3] D. Uglietti – presented at "2nd Workshop on Mechano-Electromagnetic Property of Composite Super-conductors", Kyoto, May 2003, to published in proceedings.
[4] R. Flükiger et al. – Superconducting Properties of MgB2 tapes and wires – Physica C 385 (2003) 286-305.
[5] P. Lezza et al. – Transport Properites and exponential *n* values of Fe/MgB2 tapes with various MgB2 particle size – Physica C 401 (2004) 305-309.
[6] S. Stavrev al., IEEE Trans. Applied Supercond. 12 (2002) 1857.
[7] F. Grilli al., Supercond. Sci. Tech. 16 (2003).
[8] M. Sjöström al., IEEE Trans. Applied Supercond. 13 (2003) 1890.
[9] F. Grilli al., to be published in IEEE Trans. Applied Supercond., March 2004.

4. Specific Heat and Thermal Conductivity of Novel Materials in Thin Films and Crystalline Form, in High Magnetic Fields and at High Pressures

Project leader: Alain Junod, University of Geneva

Research summary: our group specializes in thermodynamic studies of superconductors and new materials. Initial research plans, focused on high pressure and thin-film calorimetry, were revised to concentrate on the new 40K-superconductor MgB_2. As a volume-sensitive probe, specific heat complemented research based on surface-sensitive spectroscopy at the DPMC. The variation of the specific heat of MgB_2 with temperature established its two-gap structure in the bulk; that along with the magnetic field gave a tool to study two-gap vortices; finally irradiation was used to study changes in the anisotropy. Other investigations based on specific-heat and/or magnetocaloric experiments encompassed the multiple magnetic phases of UAs, giant diamagnetism in Cr_2FeSe_4, antiferromagnetism in the heavy-fermion $CePd_2Si_2$, a possible condensed excitonic state in intermediate valent $TmSe_xTe_{1-x}$, type-I to type-II crossover in the superconducting boride ZrB_{12}, two-gap superconductivity in Nb_3Sn, and specific problems related to high-temperature superconductivity such as d-wave symmetry of the order parameter ($Bi_2Sr_2Ca_2Cu_3O_{10}$), melting of the vortex lattice ($NdBa_2Cu_3O_7$, $YBa_2Cu_3O_7$), and the possible opening of a pseudogap in four isotopes of $HoBa_2Cu_4O_8$. Two results are potentially interesting for applications: we obtained a large increase of the upper critical field of MgB_2 after irradiation, and we showed how the true bulk distribution of critical temperatures can be obtained inside multifilamentary Nb_3Sn superconductors. Initial goals were reactivated; first experiments in thin-film and high pressure calorimetry were successful.

Two-gap superconductors (MgB_2, Nb_3Sn)

The discovery of superconductivity near 40 K in MgB_2 arose intense interest. This compound presents an intermediate case between high-temperature superconductors, for which the coupling mechanism leading to super-conductivity remains unclear, and classical superconductors, mediated by electron-phonon coupling. We identified early large anomalies in the low-temperature specific heat of MgB_2 as a function of the temperature, and were able to explain them in the framework of a phenomenological model of two-gap superconductivity that we built on the basis of the "α-model".[1] It allowed us to measure the gap widths Δ_π and Δ_σ, and their weights, i.e. the density of states on the π and σ electron bands on which these gaps open. This unconventional gap structure immediately raised questions about the nature of vortices, and about the evolution of the gaps with increasing interband scattering.

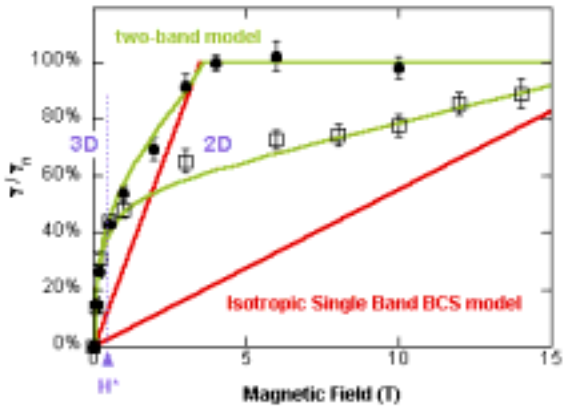

Fig.1. Normalized electronic specific heat at $T \to 0$ versus H for the field applied perpendicular (●, H_{c2} = 3.5 T) or parallel (▽, H_{c2} = 18 T) to the boron planes. The single band model (red lines) does not fit. Results become isotropic below H^* or for $\gamma/\gamma_n < 0.5$.

The specific heat of a single crystal versus the magnetic field was measured for two principal orientations of the field with respect to the crystallographic axes (Fig. 1). This uncovered the presence of a third critical field H^* (in fact, a crossover field) associated with the smaller gap Δ_π, below which the critical field becomes isotropic. This experiment also shows why the anisotropy at low temperature depends on the value of the applied field. The observed evolution with the field was entirely consistent with the presence of two superconducting gaps having different anisotropy, and was quantitatively explained by the observation of giant vortex cores by means of scanning tunneling spectroscopy in the group of Ø. Fischer.

In order to address the effect of disorder, we measured again the gap characteristics after several irradiation steps by fast neutrons, using specific heat. These experiments give an information which is valid for the entire volume of the sample. We found that the gap anisotropy remained unexpectedly large, even when the critical temperature was reduced to 2/3 of its initial value.

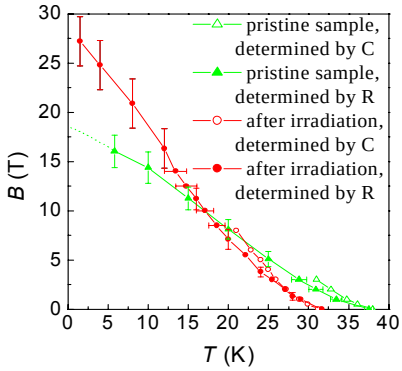

Fig. 2. Upper critical field $H_{c2}(T)$, before (green) and after (red) irradiation, as determined by specific-heat (C) and resistance (R) measurements.

In view of applications, it is interesting to note that the upper critical field increased considerably (from ~18 to ~28 T) after the first irradiation step (Fig. 2).
We looked for other superconductors in which a two-gap situation might also arise. It appears to be the case for Nb_3Sn. In this compound, we identified a low-temperature specific-heat anomaly that vanishes at high fields, similar to MgB_2 (Fig. 3) [2]. Both the width and the weight of the second gap are much smaller than for MgB_2. Features were found in point-contact spectroscopy experiments, which appear to be consistent with the presence of a second gap. Additional experiments are under way. Other classical superconductors will be investigated.

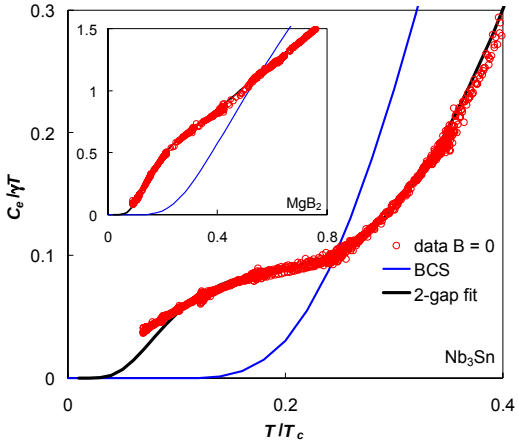

Fig.3. Specific heat of Nb_3Sn below T_c (main panel) compared to that of the two-gap superconductor MgB_2 (inset). The excess at low temperature with respect to the BCS curve, which is shown in blue, is characteristic of a second gap smaller than the main one.

Another superconducting boride (ZrB_{12})

The cubic compound ZrB_{12} has the second highest superconducting critical temperature of all borides (~6 K). We performed specific-heat, magnetisation, and thermal expansion measurements on a single crystal in order to determine the peculiarities of the phonon spectrum, measure microscopic parameters, and investigate a possible T_c enhancement by pressure. The results could be interpreted in terms of single-band, medium-coupling superconductivity in a structure having nearly optimal cell volume. We found that ZrB_{12} appears to be one of the few superconductors that changes from type I to type II as the temperature is lowered, developing 1st order transitions with a latent heat at low fields, and 2nd order transitions in higher fields (and of course also at exactly zero field, Fig. 4). Magnetization curves could also be interpreted along the same lines.

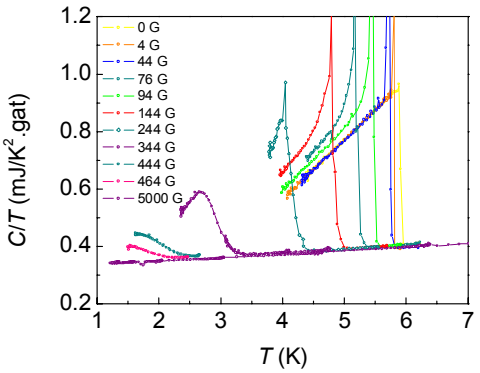

Fig.4. Specific heat of ZrB_{12} in different magnetic fields.

Magnetocaloric effect (UAs, Nd123, Y123)

We developed a sensitive heat-flow device, allowing the specific heat $(\delta Q/\delta T)_H$ and the magnetocaloric effect $(\delta Q/\delta H)_T$. to be measured in the same cell. We found that the systematic characterization of superconductors by the magnetocaloric effect, a new technique, usefully complements specific heat and magnetization. For demonstration purpose, we investigated the *H-T* phase diagram of the compound UAs, which is characterized by multiple magnetic phases.[3] Very sharp transitions were resolved. As an example, we plot the singular part of the entropy in the *H-T* plane (Fig. 5), showing how positive, zero, or negative latent heats occur along paths at $H \neq$ constant. Other tests included Tb, $NbH_{0.84}$, $SrRuO_3$, and $SrTiO_3$.

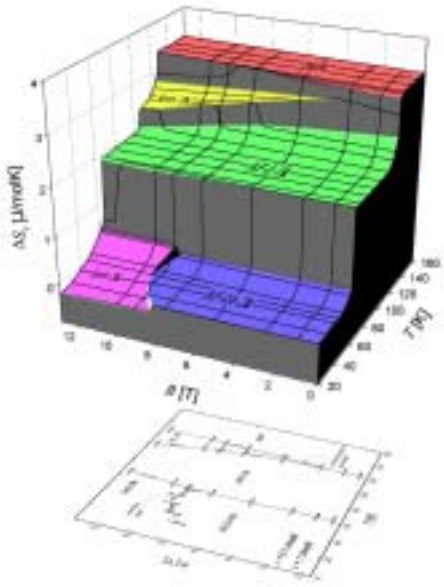

Fig.5. Singular part of the magnetic entropy, $\Delta S_s = S_s(T, H) - S_s(20\ K, 0)$, for single-crystal UAs. The steps on the surface show the latent heat at the magnetic transitions. Each line along the T (or H) direction is a specific heat (or magnetocaloric) run. Note the inversion point at 46 K and 9.3 T. The phase diagram is shown below.

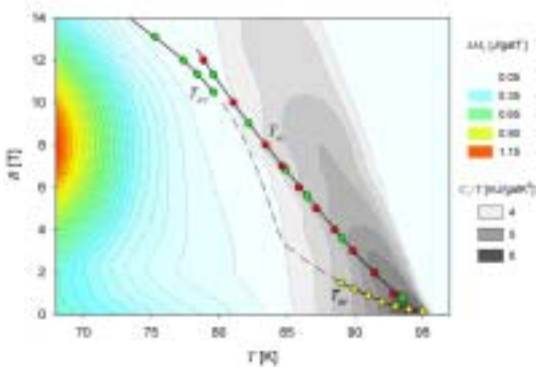

Fig. 6. Phase diagram of $NdBa_2Cu_3O_7$ in the H-T plane. The irreversibility line (T_{irr}) is determined by magnetization loops (yellow diamonds) and magnetocaloric effect (green diamonds); the dash-dotted line shows a hypothetical line connecting both parts. The melting line of vortex matter (T_m) is determined either by specific heat (red circles) or by magnetocaloric effect (green circles). The color-scale contour plot based on the magnetocaloric hysteresis $\Delta M_T = M_T^+ - M_T^-$ represents the distribution of critical current density; the red island on the left indicates a "fishtail" effect. The gray-scale contour plot shows the electronic contribution C_e/T to the specific heat. It describes the progressive evolution from the sharp second-order superconducting phase transition in zero field toward a wide crossover at higher magnetic fields.

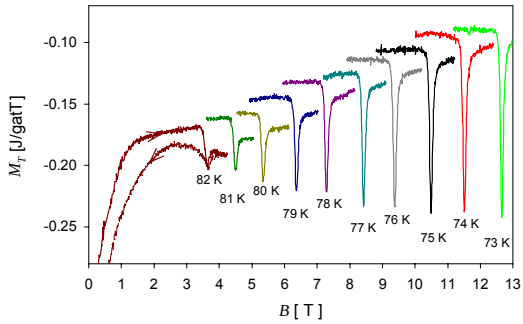

Fig.7 Isothermal magnetocaloric effect (M_T) versus magnetic field at selected temperatures, showing the melting transition of the vortex lattice in $YBa_2Cu_3O_7$. A negative peak is endothermic. Traces below 81 K are reversible both above and below the transition, whereas those above 82 K show hysteresis on the low field side; in the latter regime the transitions are marked by a step (2^{nd} order transition) rather than a peak (1^{st} order).

The next step was high-temperature superconductors. The magnetocaloric effect is closely related to the magnetization in the reversible regime through $M_T \equiv (\delta Q/\delta H)_T = -T(\partial M/\partial T)_H$. It can also measure irreversible heat transfers, e.g. the so-called "fishtail" effect that occurs in superconductors with strong pinning, and determine the irreversibility line. Finally the sensitivity is high enough to detect subtle phase transitions such as vortex melting. Therefore the magnetocaloric effect was used to study two high temperature superconductors, a single crystal of $NdBa_2Cu_3O_7$ (Fig. 6) and a detwinned crystal of $YBa_2Cu_3O_7$ (Fig. 7). The detection of the melting of the vortex lattice and its interplay with irreversibility come out very clearly using this technique. The magnetocaloric effect appears to be less sensitive to shielding effects than magnetization experiments performed in a SQUID susceptometer.

d-wave symmetry of the order parameter (Y123, Bi2223)

In principle, bulk evidence for the presence of line nodes in the gap of HTS should be given by the observation of a $\pi/2$ angular periodicity of the mixed-state specific heat at $T << T_c$ when the magnetic field is rotated in the basal plane. Theoretically, the relative change in the amplitude might be as large as ~30%. The specific heat of a 52 mg detwinned crystal of $YBa_2Cu_3O_7$ of high quality (as shown by the very small contribution of paramagnetic centers and the sharpness of the superconducting transition at 88 K), was measured for H // [100], [110], and [010]. We found a π periodicity, 6% peak-to-peak, without any extremum on the nodal direction. It clearly reflects the angular dependence of H_{c2} in the basal plane due to the presence of CuO chains, rather than the effect of nodes. This result calls into question conventional *d*-wave scenarios.

The field dependence of the low temperature specific heat of a 300 μg single crystal of the high temperature superconductor $Bi_2Sr_2Ca_2Cu_3O_{10}$ (T_c = 111 K), which is another candidate for *d*-wave superconductivity, was investigated in magnetic fields up to 14 T. The results are barely consistent with the presence of the characteristic contribution $C \propto TH^{1/2}$ of line nodes, with an amplitude representing ≈¾ of that found earlier in Y123.[4] However, this term tends to be masked in Bi2223 by the large lattice and magnetic contributions.

Pseudogap (Ho124)

Is the opening of a pseudogap at $T^* > T_c$ a true phase transition in high-temperature superconductors? Sharp features at T^* and a large isotope effect were reported for $HoBa_2Cu_4O_8$ in the literature, based on the relaxation rate of crystal-field excitations. We searched for anomalies at T^* in the specific heat of the same samples, using different isotopes (^{16}O, ^{18}O, ^{63}Cu, ^{65}Cu) to subtract off the lattice contribution in quasi-differential measurements. Our results exclude any sharp static signature in the thermodynamics to within the resolution of the experiment (≈0.02%).

Strongly correlated materials ($CePd_2Si_2$, $TmSe_xTe_{1-x}$)

We measured the specific heat of a single crystal of the heavy fermion compound $CePd_2Si_2$ in magnetic fields up to 16 T parallel to the crystallographic *a*-axis. This material orders antiferromagnetically at T_N ~ 9 K. An analysis of the field dependence of T_N pointed to the existence of a magnetic quantum critical point at ~40 T where T_N is suppressed to 0 K.[5]

The specific heat of $TmSe_xTe_{1-x}$, which has been reported to be an intermediate valence compound in which exciton condensation into a superfluid state occurs, was measured from 1 to 300 K in order to calibrate measurements performed under pressure (<20 kbar) at the ETHZ.

Giant diamagnetism (Cr_2FeSe_4)

An anomalous large diamagnetic signal was observed up to nearly room temperature in AC and DC magnetization of Cr_2FeSe_4 powder samples in small fields of several Gauss, somewhat reminiscent of superconductivity at high temperature. Based on magnetic relaxation experiments and the analysis of the slightly hysteretic behaviour, we showed that the signal may be assigned to a metastable inversed weakly ferromagnetic state, in analogy to a phenomenon known in the literature as the 'inverse Wohlleben effect'. This effect is known to appear in some small ferromagnetic samples with a surface having a slightly higher transition temperature than the bulk, so that the surface magnetization polarizes the bulk antiparallel ('diamagnetic') to the applied field.

Specific heat of multifilamentary wires

Multifilamentary $Nb_{1-x}Sn_x$ wires are the most widely used superconductors for high-field applications from ~9 to ~21 T. Further improvement requires a knowledge of the distribution of tin concentration, which may vary between x = 0.18 and x = 0.25, or correspondingly the distribution of *bulk* critical temperature, which varies between T_c = 6 K and T_c = 18 K. With the help of specific heat measurements both in zero field and high field, using about 30 mg of material with its bronze matrix, and by carefully characterising a reference Nb_3Sn sample, we devised a method that can answer this question (Fig. 8). This new characterisation is important as it can guide and quantitatively assess metallurgical improvements.

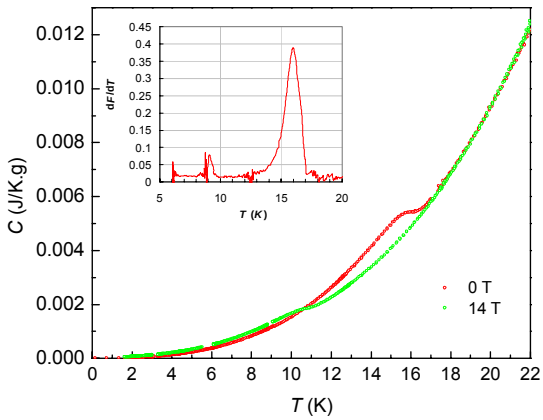

Fig.8. Specific heat of a bronze-coated multifilamentary Nb_3Sn wire containing Ti and Ta additions, and obtained by the bronze technique at H = 0 (red) and 14 T (green). Inset: distribution of T_c obtained from these curves. The small peak at 9 K is due to unreacted Nb.

Experimental equipment

A 6 T split-coil magnet was successfully commissioned, allowing field-dependent effects in anisotropic materials to be studied at low temperature. It will be fitted with a variable temperature insert in 2004.

A pressure cell for pressures up to ~20 GPa, using liquid and solid pressure transmitting media, and especially designed for the use in high magnetic fields, was successfully tested. It was possible to compensate for the thermal expansion of the cell over the temperature range from 1 to 300 K. First calorimetric experiments on high-temperature superconductors are currently under way.

Tests of calorimetry based on the "3ω" technique have been conducted in view of applications to thin films.

Concluding remarks

This work would not have been possible without collaborations in the DPMC, in Switzerland (in particular with MaNEP partners), and abroad; persons and institutions could not be cited here but appear elsewhere in this report.

References:
[1] F. Bouquet *et al.*, Physica C **385** (2003) 192.
[2] F. Bouquet *et al.*, Proceedings of the 7th Int. Conf. M^2S-HTSC, Rio de Janeiro, Brazil, 25-30 May 2003, to appear in Physica C.
[3] T. Plackowski *et al.*, Phys. Rev. B **67** (2003) 184406.
[4] Y. Wang *et al.*, Phys. Rev. B **63** (2001) 094508.
[5] I. Sheikin *et al.*, J. Phys.: Condensed Matter **14** (2002) L543.

5. Ferroelectric Based Superlattices and Nanoscale Dielectrics

Project leader: Jean-Marc Triscone, University of Geneva

Research summary: This project is studying epitaxial films and novel structures based on dielectric and ferroelectric materials. Ultrathin atomically flat films allow ferroelectricity to be investigated in layers a few unit cell thick. Atomic force microscopy is used to locally modify the ferroelectric domain structure and to study domain dynamics at nanoscale. Combining different ferroelectric and dielectric materials allows the realization of artificial structures, which can be prepared with a high degree of precision and with high surface and crystalline quality. These high quality ferroelectric films can also lead to novel devices such as a new type of surface acoustic wave filters and fast optical switches that are currently being investigated. Combining ferroelectrics with high T_c superconductors allows us to perform ferroelectric field effect experiments. This approach leads to non-volatile and reversible T_c modulation in ultrathin superconducting films.

Ferroelectricity in ultrathin films

Many experimental and theoretical studies have suggested for many years that, as the physical dimensions of a ferroelectric are made smaller, the stability of the ferroelectric phase is altered, leading to a relatively large critical thickness required for ferroelectricity. More recent studies on advanced materials and first principles calculations however suggest a much smaller critical thickness. Very recent ab-initio calculations found a critical thickness of only around 26 Å (≈6 unit cells) for the canonical ferroelectric $BaTiO_3$ [1]. Experimentally, current techniques based on a local probe approach have allowed the detection of ferroelectricity in perovskite films down to a thickness of 40 Å (10 unit cells). In our MaNEP project we actively study this important issue on one hand with Ph. Aebi in Neuchâtel (see report on project 14) using X-ray Photoelectron Diffraction (XPD). This surface technique yields information on the atomic structure of the surface layer, and its resolution is sufficient to detect the atomic displacement related to polarization reversal.

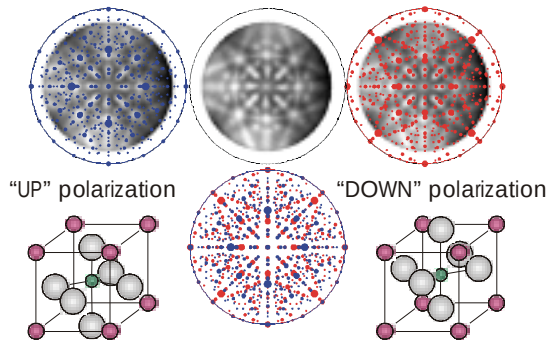

Figure 1. Angular distribution of Pb 4f photoelectrons due to forward scattering of the electrons by neighboring atoms along the crystal directions for an epitaxial thin film of $PbTiO_3$.

Fig. 1 shows XPD images obtained on a 132 Å $PbTiO_3$ film. Results on very thin films, 20 Å, have recently been obtained and suggest ferroelectricity at this scale.

On the other hand, we have studied with the theoretical support from P. Ghosez (Univ. of Liège) the evolution of tetragonality with thickness in epitaxial c-axis oriented $PbTiO_3$ (PTO) films with thicknesses ranging from 500Å down to 24Å. High resolution x-ray analyses showed a systematic decrease of the c-axis lattice parameter with decreasing film thickness below 200Å as illustrated in Fig. 2.

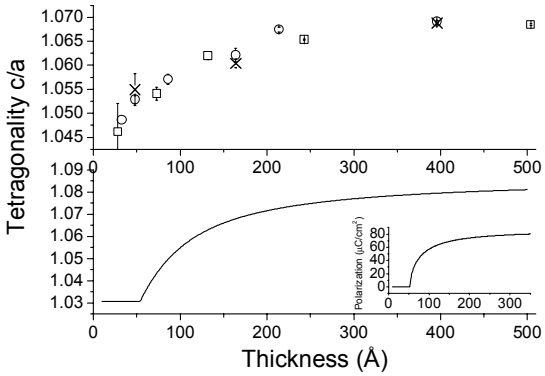

Figure 2. Evolution of the c/a ratio with the film thickness. Top: experimental results, samples with different growth rates (circles and squares) and samples with a gold top electrode (crosses). Bottom: theoretical prediction from the model Hamiltonian calculations. Inset: thickness dependence of the corresponding spontaneous polarization from the model Hamiltonian.

Using a first-principles model Hamiltonian approach, the decrease in tetragonality can be related to the reduction of polarization in thin films. The experimentally observed continuous decrease of c/a confirms that the films remain ferroelectric down to a thickness much smaller than 100 Å but also indicates a significant reduction of the polarization at small thicknesses. The data also suggest that the reduction of ferroelectricity occurs throughout the film and is not merely a surface effect. This is confirmed theoretically. Both the range of

thicknesses over which the c/a ratio is observed to decrease substantially and the shape of the c/a versus thickness curve suggest that the depolarizing field is the main driving force for the global reduction of the polarization in perovskite ultrathin films (as predicted in Ref.1). For films thinner than about 100 Å, however, the theoretical model predicts a decrease of tetragonality larger than the one observed experimentally. This suggests that films thinner than the 50 Å predicted critical thickness might be ferroelectric in agreement with our recent XPD results on a 20 Å film.

[1] J. Junquera and P. Ghosez, Nature **422**, 506 (2003).

Domain wall creep in ferroelectric films

Ferroelectric switching and domain dynamics were investigated by atomic force microscopy (AFM) in c-axis $Pb(Zr_{0.2}Ti_{0.8})O_3$ single crystal thin films, grown by RF magnetron sputtering on (001) Nb-doped $SrTiO_3$ substrates. Domain arrays were written in uniformly prepolarized regions by applying voltage pulses across the ferroelectric, between the conducting substrate and the metallic AFM tip, and imaged using their local piezoresponse. Measurements of domain size versus writing parameters showed a linear size dependence on writing voltage, and a logarithmic size dependence on writing times longer than ~20 µs [1]. For shorter writing times, the domain size saturated at ~40nm, a non-fundamental limit governed by the AFM tip size. These data, shown on Figure 3, reveal a two-step growth mechanism, in which initial nucleation is followed by radial domain wall motion perpendicular to the polarization direction. As shown on Figure 4, the electric field dependence of the domain wall velocity fits well to:

$$v \sim e^{-\frac{W_0}{k_B T}\left(\frac{E_0}{E}\right)^{\mu}}$$

The characteristic dynamical exponent µ, related to the dimensionality of the film and the nature of the disorder potential, was found to be between 0.7 and 1. This characteristic dependence of the velocity on an external driving force, which in our case is the electric field, demonstrates that ferroelectric domain wall motion is a creep process. The key parameters controlling domain size are the confinement, strength and duration of the electric field pulses. With optimized writing parameters, we realized high density arrays of ferroelectric domains reaching 30 Gbit/cm^2.

To probe the role of disorder in this domain wall motion, we introduced defects in the pure

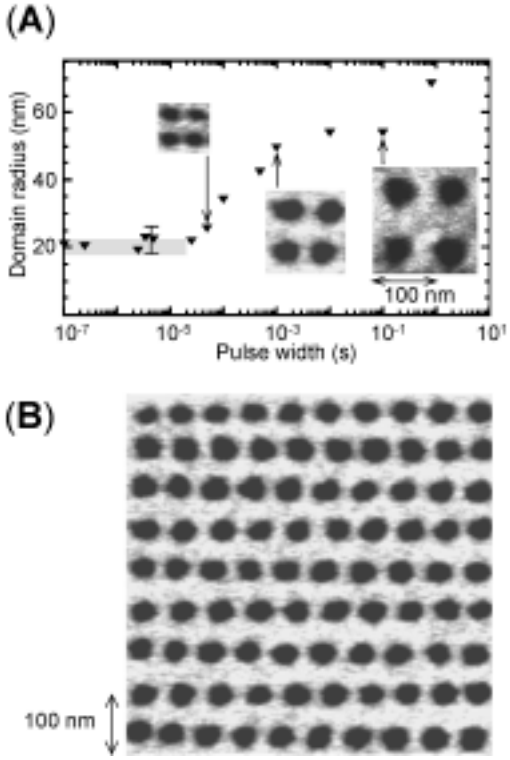

Figure 3 Influence of pulse width on domain size. Figure 3a shows the domain radius as a function of pulse width, and three piezoelectric images of AFM written ferroelectric domain arrays on a 400 Å thick film, the scale is the same in all the images. The pulse widths used were: 50µs, 1 ms, and 100ms. In 3b, a piezoelectric image of 90 ferroelectric domains is shown. A topographic image of the same area is featureless with a RMS roughness of ~0.2nm.

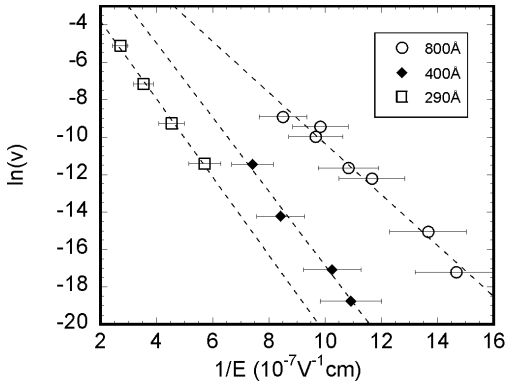

Figure 4 Logarithm of the domain wall velocity as a function of the inverse electric field for three samples.

c-axis films. Heavy ion irradiation over half of the film surface was used, allowing domain dynamics in the irradiated and as-grown regions to be directly compared. Thick films, containing a-axis inclusions, were also investigated. In all cases, 25-domain arrays were written in uniformly pre-polarized areas by applying voltage pulses via the AFM tip, and imaged using their local piezoresponse. The writing time dependence of the average domain radius was measured, allowing the

field dependence of the radial domain wall velocity to be extracted [1]. We find that the presence of defects decreases the value of μ to 0.3-0.4 in the case of the columnar irradiation defects, and even more significantly to 0.1-0.2 in the presence of the planar a-axis inclusions [2]. The variation does not appear to be thickness dependent. Since μ controls the divergence of the energetic barriers to domain wall motion as the applied field goes to zero, this decrease may have an effect on the stability of domain structures in low electric fields.

[1] Tybell et al., Phys. Rev. Lett. **89**, 097601 (2002)
[2] Paruch et al., Ann. der Phys. **13**, 95 (2004)

A high frequency surface acoustic wave filter based on ferroelectric domain manipulation

Surface acoustic wave (SAW) devices are used as filters in mobile communication networks and tiny signal processing devices such as delay lines, and resonators. In classical SAW devices, two metallic interdigital transducers (IDTs) deposited on a uniformly polarized piezoelectric material, crystal or film, act as electric input and output ports. Application of an appropriate RF voltage to the input IDT results in the launching of SAW which travel along the piezoelectric surface and are detected by the receiving IDT and converted back to an electric signal. These surface waves travel with the sound velocity of the material. The centre frequency (f_C) of the SAW device is determined by the wavelength (λ), which is the distance between the IDT fingers of the same electrode, and the sound velocity (v_S) of the material, $f_C = v_S/\lambda$. Using nanoscale domain inversion to write piezoelectric IDTs on ferroelectric materials by atomic force microscopy, we have developed a novel type of SAW filters. The novelty in the approach is to replace the conventional metallic IDTs by piezoelectric ones. The piezoelectric input and output IDTs were realized by writing line shaped domains with alternating polarization on $Pb(Zr_{0.2}Ti_{0.8})O_3$ films as shown schematically on Fig. 5. The distance between the IDTs of the same polarization defines the wavelength of the device which can be very short.

Figure 6 shows S11 reflection measurements on two devices with different wavelengths displaying clear minima related to the launching of the SAW at frequencies (2 and 3.4 GHz), in good agreement with theoretical analysis. These results are very encouraging and transmission measurements will be carried out soon on a suitable device.

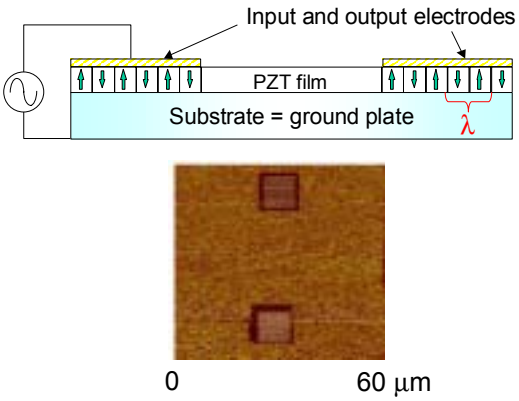

Figure 5. top. Schematic drawing of the high frequency surface acoustic wave device. Bottom. Piezoelectric image of the IDTs of device. The wavelength of the structure corresponds to a 5GHz frequency.

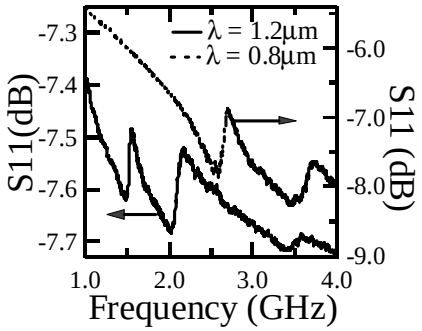

Figure 6. S11 reflection measurements on two different devices with 0.8 and 1.3 μm wavelengths

$PbTiO_3/SrTiO_3$ superlattices grown by off axis RF sputtering

Artificially modulated superlattices of ferroelectric materials present enormous opportunities both in terms of tailoring material properties to applications and also in exploring fundamental properties, particularly those related to size effects. We have grown a series of $PbTiO_3/SrTiO_3$ superlattices using off axis RF sputtering. Computer controlled shutters and gun powers allow for the growth to be carried out completely in situ.

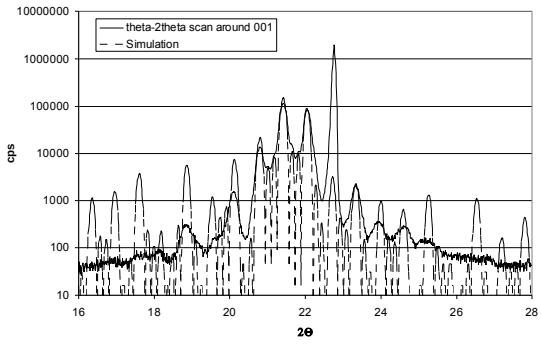

Figure 7. θ–2θ scan for a $PbTiO_3/SrTiO_3$ superlattice with 4 bilayers consisting of 20 unit cells $PbTiO_3$ and 15 unit cells $SrTiO_3$ along with an x-ray simulation.

X-Ray diffraction (see Fig. 7) shows high quality superlattices and simulations allow the

determination of the lattice parameters and superlattice wavelength. Using such structural measurements and AFM techniques we will investigate the interactions between the different layers in the superlattice.

Electrostatic tuning of the electronic properties in cuprates

(project partly financed by SNSF division II)

In this section, we very briefly discuss our results on the electrostatic modulation of superconductivity. For more details, see some of the references mentioned at the end of this section.

In epitaxially grown ferroelectric $Pb(Zr_{0.2}Ti_{0.8})O_3$ / $NdBa_2Cu_3O_{7-d}$ hetero-structures, we have used the reversible ferroelectric polarization field to electrostatically modulate the properties of thin $NdBa_2Cu_3O_7$ films. Reversing the ferroelectric polarization induces large changes in the superconducting transition temperatures and, in the normal state, in the resistivity and Hall response.

We have realized a new field effect device whose gate insulator is a $SrTiO_3$ single crystal. This device allows a modulation of the critical temperature of a thin $NdBa_2Cu_3O_x$ (NBCO) layer, epitaxially deposited on the top of the $SrTiO_3$ crystal, of at least 3 Kelvin. To realize the field effect device, we reduced the thickness of the commercial $SrTiO_3$ dielectric single crystal substrate down to about 100 microns and deposited a gold contact on the back side allowing the application of a field across the $SrTiO_3$. Fig. 8 shows the resistance as a function of temperature in the region of the critical temperature T_c of a NBCO layer for voltages between - 200 V and 250 V applied across the $SrTiO_3$ dielectric layer. We also characterized the dielectric properties of the gate insulator to be able to quantify the field effect. A shift of 2.8 Kelvin is obtained for an applied field of -1.8 10^6 V/m corresponding to a polarization of -4 $\mu C/cm^2$.This device allows us to obtain one of the largest shift in the critical temperature obtained by field effect in oxide superconductors.

The electrostatic modulation of activation energies for vortex motion was also studied using this device and we found a change in the activation energies $\Delta U/U$ almost constant as a function of the applied magnetic field of about 7%.

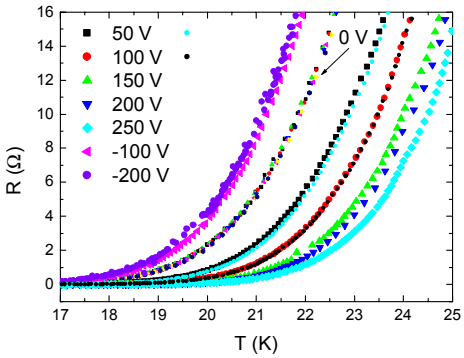

Figure 8. Resistance versus temperature of a thin NBCO layer for different voltages applied across the $SrTiO_3$ gate insulator. A shift of 2.8 Kelvin in the critical temperature is obtained between 0V and -200V corresponding to a field of -1.8 10^6 (V/m) and a polarization of -4 ($\mu C/cm^2$).

We have also performed ferroelectric field effect experiments using epitaxial heterostructures composed of ferroelectric $Pb(Zr_{0.2}Ti_{0.8})O_3$ and superconducting Nb-doped $SrTiO_3$ (Nb-STO). In the whole temperature range investigated, large differences in the resistivities (≈30 %) between the P+ and P- states were observed. The P+ state corresponds to the polarization direction which removes electrons from the Nb-STO layer. The change in T_c is about 20%. This model system may allow us to realize nanoscale superconducting switches, artificial Josephson junctions arrays, or re-writable pinning sites.

Selected references:

Nanoscale control of the ferroelectric polarization and domain size in epitaxial $Pb(Zr_{0.2}Ti_{0.8})O_3$ thin films.
P. Paruch, T. Tybell, and J.-M. Triscone.
Applied Physics Letters **79**, 530 (2001).

Electrostatic tuning of the hole density in $NdBa_2Cu_3O_{7-\square}$ films and its effect on the Hall response.
S. Gariglio, C.H. Ahn, D. Matthey, and J.-M. Triscone.
Physical Review Letters **88**, 67002 (2002).

Domain wall creep in epitaxial $Pb(Zr_{0.2}Ti_{0.8})O_3$ thin films.
T. Tybell, P. Paruch, T. Giamarchi, and J.-M. Triscone.
Physical Review Letters **89**, 097601 (2002).

Field effect in correlated oxides.
C.H. Ahn, J.-M. Triscone, and J. Mannhart.
Nature **424**, 1015 (2003).

Field effect experiments in $NdBa_2Cu_3O_{7-\delta}$ ultrathin films using a $SrTiO_3$ single crystal gate insulator.
D. Matthey, S. Gariglio, and J.-M. Triscone.
Applied Physics Letters **83,** 3758 (2003).

Ferroelectricity at the nanoscale: Local polarization in thin films and heterostructures.
C.H. Ahn, K. Rabe, and J.-M. Triscone.
Science **303**, 488 (2004).

6. Superconductivity on the Micro-, Meso, and Macroscopic Scales

Project leader: Gianni Blatter, ETH Zurich

Research summary: Work on the phenomenology of strongly fluctuating type II superconductors (e.g., layered copper oxide high-T_c superconductors) concentrated on the statistical physics of (disordered) vortex matter. Specific problems we have analyzed and solved are the implications of long-range vortex-vortex interactions on weak collective pinning, the crossover from weak to strong pinning, and the dissipative properties of vortices in moderately clean superconductors. Quantum atom optics provides new opportunities for the implementation and testing of ideas and concepts derived from condensed matter physics. In our work, we have studied the Mott-Hubbard transition in 1D bosonic atom gases subject to an optical lattice and the instabilities towards density wave formation and phase separation in 2D fermion/boson mixtures subject to an optical lattice. Mesoscopic superconducting structures exhibit interesting quantum properties and may serve for the future implementation of quantum computing via the solid-state route. We have studied quantum phase slips in thin superconducting wires, the implementation of topological quantum computing in quantum Josephson junction arrays, and have proposed a novel qubit design exploiting geometric frustration in an array of superconducting islands with tetrahedral symmetry. We have studied the decoherence in superconducting quantum bits due to the piezo-electric generation of phonon radiation in Josephson junctions and have analyzed the wave function collapse and the origin/generation of entanglement in mesoscopic solid state structures. Main achievements during the last years specifically financed via MaNEP include (1) the modification of vortex-vortex interaction due to size-dependent transverse screening in layered superconductors of finite width (stray fields in finite systems), (2) the competition between various topological transitions in layered superconductors of finite width (vortex pair-unbinding versus vortex stack evaporation), (3) the impact of surface effects on the melting transition of weakly coupled layered superconductors using density functional theory, (4) the analysis of optical properties of layered high-T_c superconductors and Josephson Plasma Resonance, (5) the theoretical interpretation of optical and transport experiments in high temperature superconductors allowing for the determination of basic material parameters such as the electronic compressibility of the CuO_2-layers or the charge imbalance relaxation rate, (6) the decoherence in superconducting quantum bits via phonon radiation.

Optics with spatial dispersion

The analysis of optical and transport properties of intrinsic Josephson junctions in high-T_c superconductors allows for the determination of key microscopic parameters of the CuO_2-layers, such as the electronic compressibility and the charge imbalance relaxation rate, parameters which are hard to obtain otherwise. In the novel material $SmLa_{1-x}Sr_xCuO_4$ with alternating junctions two peaks are observed in transmission, which are identified with the Josephson Plasma resonances due to oscillating Cooper pairs in the respective junctions. The high ratio of their relative amplitude can only be explained, if the spatial dispersion of the Josephson Plasma Resonance in the *c*-direction is taken into account [1], see Fig. 1. This dispersion is due to charge fluctuations in the superconducting layers; proper analysis of experiments demonstrates that the electronic compressibility of the layers is consistent with a free electron value. This result is further confirmed by the magnetic field dependence of the plasma peaks based on the field dependence of the critical current density, which is well known in the vortex liquid state and has been newly derived for the vortex solid [3]. Furthermore the *c*-axis quasi-particle conductivity and the London penetration depth parallel to the layers can be accurately determined. These parameters are not only relevant to understand the coupled dynamics of stacks of intrinsic Josephson junctions, e.g. for THz-applications such as coherent microwave sources, but might also provide an important input for microscopic theories of high-T_c-superconductivity.

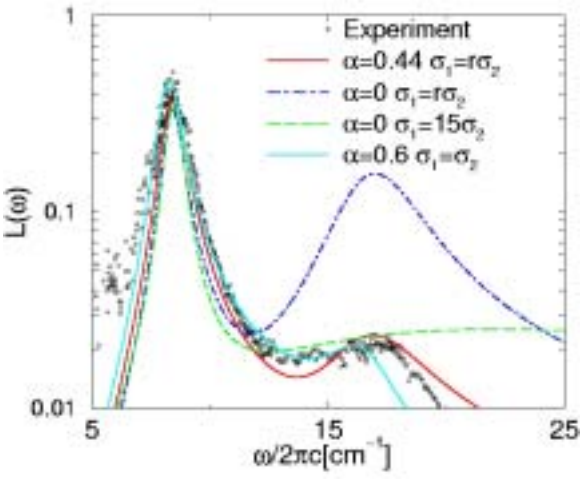

Fig.1 Experimental data together with calculated loss function L(ω), from [2]. The parameter α characterizes the c-axis dispersion and the blue line corresponds to the conventional Fresnel theory (σ_i dimensionless conductivity)

From a theoretical point of view the inclusion of the wave vector dependence of the dielectric function poses a nontrivial problem and requires one to go beyond the conventional Fresnel theory. For example, multiple eigenmodes with different group velocities are excited in the crystal and at certain frequencies

the group velocity vanishes and light can be stopped. At these extremal points the atomic structure of the crystal enters explicitly in optical properties [3,4]. We find that spatial dispersion can significantly affect the spectral properties of optically active modes near poles of the dielectric function, where the wave vector $k^2 = \omega^2\varepsilon(\omega)/c^2$ is large and short length scales become important. More specifically, we generalized our results to optical phonons [5].

Charge imbalance relaxation in high-T_c superconductors

Two different transport experiments on $Bi_2Sr_2CaCu_2O_8$ mesas can be interpreted consistently based on non-equilibrium effects in the superconducting CuO_2-layers [6]: (i) in the I-V curves of double-mesa structures the voltage measured at one mesa is influenced by the current injected into the other mesa, and (ii) in two-point measurements of the I-V curves in the presence of high-frequency radiation of frequency f, a shift of the voltage of Shapiro steps from the canonical value $V_s = hf/2e$ has been observed due to the contact resistance at the NS-contact. Both effects can be explained by a charge-imbalance between the quasi-particles and the Cooper pairs on the superconducting layers joined by resistive and superconducting junctions, where the quasi-particle distribution function is shifted from the equilibrium value. With the help of a recently developed theory [7] we can extract the charge imbalance relaxation time as ~100 ps, which was so far unknown.

Decoherence in superconducting qubits due to phonon radiation

Decoherence is the main adversary of the unitary time evolution governing the quantum systems providing the hardware for a future quantum information technology. As recent experiments have demonstrated, solid state implementations based on superconducting structures have a great potential for the construction of future quantum information processors. A crucial element in this type of hardware are the Josephson junctions with their dynamics driving the quantum fluctuations in these devices. We have found a fundamental limitation for the coherent operation of superconducting quantum bits due to phonon radiation originating within the Josephson junctions themselves (cf. Fig.2). Quality factors reported in recent experiments are in agreement with our preditions. The basic mechanism producing the phonon-radiation relies on the piezo-electric effect: a qubit residing in a superposition state involving quantum states separated by the energy $h\nu$ generates an electric field $E=h\nu\varphi/2ed$ in the junction insulator and its boundary layers. This electric field couples to the underlying crystal lattice via the piezo-electric effect generating a polarization $P=pd_zu$, with p the piezo-electric constant and u the displacement field. The radiation resistance due to phonon emission resembles the well known result for the electric dipole radiation from a capacitor, but with the velocity of light (c) replaced by that of the phonons (c_s). The smallness of c_s implies a much smaller radiation resistance and hence a much larger dissipation $P=V^2/2R_s$ at fixed driving voltage as compared to the photonic channel. We find quality factors Q of order 10^4 in agreement with recent experiments and show the way to reduce the impact of this dangerous source of decoherence through the use of qubit designs producing degenerate quantum states with $h\nu = 0$ [8].

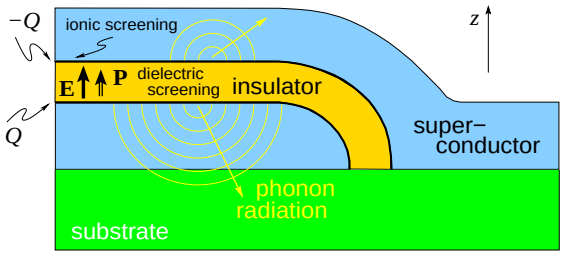

Fig.2 Schematic view of phonons emitted from superconducting Josephson junctions. The electric field E polarizes the insulator and induces displacements u via the piezoelectric effect. In addition, displaced metallic ions in the superconductor contribute to ionic screening of the surface charges Q. The oscillating displacement u produces phonon radiation into the substrate, which contributes to the energy relaxation rate and hence to the decoherence of the qubit.

Device Physics

The charge doped into a semiconductor in a field-effect transistor (FET) is generally confined to the interface of the semiconductor. A planar step at the interface causes a potential drop due to the strong electric field in the FET, which in turn is screened by the doped carriers. We analyze the dipolar electronic structure of a single step in the Thomas-Fermi approximation and find that the transmission coefficient through the step is exponentially suppressed by the electric field and the induced carrier density as well as by the step height. In addition, the field enhancement at the step edge can facilitate the electric

breakdown of the insulating layer. We suggest that these two effects may lead to severe problems when engineering FET devices with very high doping. On the other hand, steps can give rise to interesting physics in superconducting FETs by forming weak links and potentially creating atomic size Josephson junctions [9].

In ultrasmall Josephson junctions needed to observe quantum effects, such as single Cooper pair tunneling, the stray fields outside the tunneling region become important and can significantly influence the junction behaviour. In the experiments, several quantities which are usually expected to be independent of the junction width in the local theory, turn out to vary strongly when this parameter is changed. Examples for this behaviour are the voltage distance between Fiske resonances, the magnetic field periodicity of the Fraunhofer pattern, and the lower critical field. We explain these findings in a nonlocal extension of the Sine-Gordon model and discuss the implications for macroscopic quantum behaviour in small junctions [10].

Transition in bi- and multilayered superconducting systems

The superconducting phase transition in systems with reduced dimensions shows interesting and new physical properties. While an individual superconducting layer only exhibits a $T = 0$ transition, a layered (but still uncoupled) superconductor undergoes a finite T transition into the superconducting state. The origin of this different behaviour is in the transverse screening properties, as it becomes clear from the simple case of a bilayer system [11]. In this system, the low energy excitations have a topological character and correspond to a) stacks of pancake-vortices, which are the analogue of the Pearl vortices in a thin film, and b) pancake-vortex–antivortex pairs in the individual layers. Free pancake-vortex stacks are present at any temperature beyond the effective penetration length, hence the superconducting phase transition appears at $T = 0$, leaving only a sharp crossover at the temperature where the vortex-antivortex stacks unbind. Considering the individual layers, the putative Berezinskii-Kosterlitz-Thouless (BKT) transition where pancake-vortex–antivortex pairs in the individual layers unbind then describes the evaporation of the pancake-vortex stack rather than the real superconducting phase transition.

The presence of a second layer has a strong impact on the magnetic properties of pancake-vortices: the vortex superconducting current is not effectively screened, resulting in a total trapped magnetic flux $\Phi_0/2$, smaller than a flux quantum (see Fig. 3 for the dependence of the trapped flux on the total number of layers and on position). Due to the reduced trapped magnetic flux, the stack-evaporation transition appears at a temperature that is lower (by a factor one-half) than the BKT transition in bulk uncoupled layered systems. Making use of a renormalization group analysis, we have investigated the competition between the vortex-stacks and the pancake vortices residing in individual. We find that when a DC current is applied, the current induced I-V characteristic is strongly affected by the bi-layer structure: The current induced unpairing produces an algebraic voltage characteristic $V \propto I^a$, where the protective action of other layers manifests itself in a sharp change of the exponent a at large distances and small currents. We propose an experiment on a bi-layer structure in a particular connected topology which allows for the identification of the evaporation transition of pancake-vortex stacks as a new thermo-dynamic transition. We finally generalize our result to the situation with an arbitrary number of uncoupled superconducting layers.

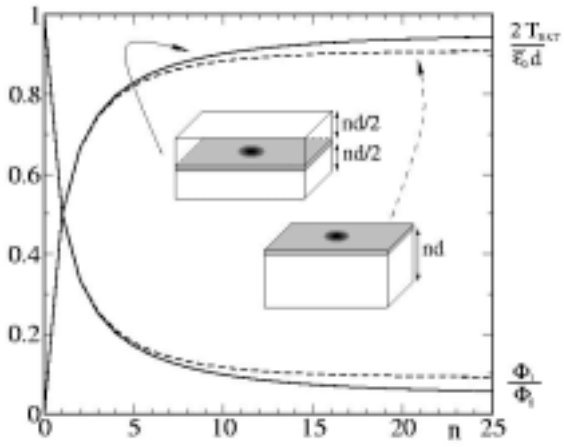

Fig.3 Dependence of the total flux and the superfluid density jump at the transition on the total number of layers for the surface (dashed line) and the bulk (solid line). A large value $\lambda/d=10$ has been chosen for illustrative reasons.

Surface induced melting of the pancake-vortex phase diagram

We consider a layered superconductor in the limit of zero Josephson coupling and discuss the effects of a surface on the vortex-solid–vortex-liquid phase transition [12]. In

general, the solid transforms into a liquid via a first-order transition exhibiting hysteretic overheating and undercooling, a consequence of the nucleation process typical of a discontinuous transition. The presence of a surface naturally assists the nucleation of the liquid phase and thus modifies or even eliminates the phenomenon of overheating. In our work, we have studied the surface-induced melting for the pancake vortex system in a semi-infinite layered superconductor. The attractive interaction between pancake vortices in neighboring layers is accounted for within a substrate model, reducing the three-dimensional problem to the analysis of a 2D lattice subject to a self-consistent substrate potential. The presence of a surface modifies the bulk scenario of [13] via the appearance of stray magnetic fields producing enhanced vortex fluctuations.

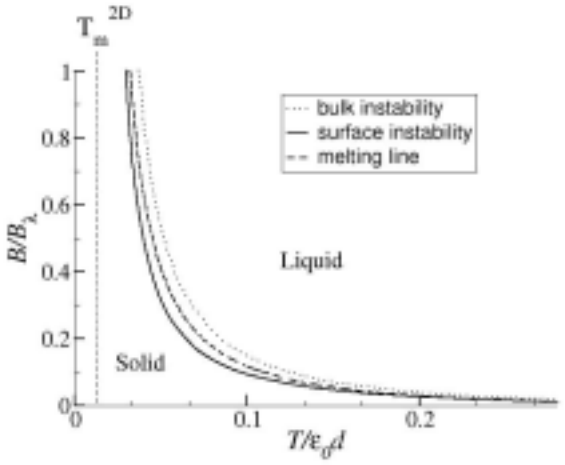

Fig.4 Results of the stability analysis for the vortex lattice on the surface and comparison with the results of [13] for bulk systems. Field and temperature scales are $B_\lambda = \Phi_0/\lambda^2$ and $\varepsilon_0 d$.

Close to the surface, the substrate potential is softened and the instability temperature of the surface layer is reduced with respect to the bulk value (Fig. 4).

A better analysis, which is not limited to the solid phase alone, is offered by an effective order parameter theory. The classic density functional theory (DFT) provides an appropriate tool as it is based on the change in the total free energy $\delta F/T$ when going from a uniform liquid with constant density ρ_0 to a modulated state (the solid) with a density function $\rho_z(\mathbf{R})$. Implementing the substrate model within the DFT scheme, we have found results superior to the previous DFT analysis of the pancake-vortex melting transition [14]. Including the surface, the translation invariance in z is broken and the order parameter becomes a function of the distance z from the surface. We find that the surface acts as a nucleus for the liquid phase and provide a quantitative description of the nucleation process. At the thermodynamic transition, the nucleus expands into the bulk and the liquid phase is established in the entire sample (see Fig. 5). This indicates that overheating of the solid is eliminated in the melting transition due to the pre-melting of the surface.

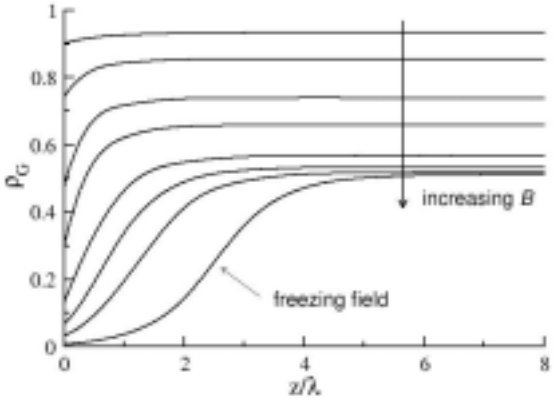

Fig.5 Profiles of the order parameter at T= 0.08 $\varepsilon_0 d$ for different values of the field. The lower line corresponds to the freezing field.

References:

[1] Ch. Helm, L.N. Bulaevskii, E.M. Chudnovsky, and M.P. Maley, Phys. Rev. Lett. **89**, 057003 (2002).
[2] Ch. Helm, L.N. Bulaevskii, Phys. Rev. B **66**, 094514 (2002).
[3] L.N. Bulaevskii, Ch. Helm, A.R. Bishop, M.P. Maley, Europhys. Lett. **58**, 415 (2002).
[4] Ch. Helm, L.N. Bulaevskii, Phys. Rev. B 66, 094514 (2002).
[5] I. Kaelin, Ch. Helm, G. Blatter, Phys. Rev. B **68**, 012302 (2003).
[6] S. Rother, Y. Koval, P. Müller, R. Kleiner, D.A. Ryndyk, J. Keller, Ch. Helm, Phys. Rev. B **67**, 024510 (2003).
[7] D. A. Ryndyk, J. Keller, C. Helm, J. Phys.: Cond. Mat. **14,** 815 (2002).
[8] L. Ioffe, D.B. Geshkenbein, C. Helm, G. Blatter, in preparation.
[9] S. Wehrli and C. Helm, submitted to J. Appl. Phys., cond-mat/0312441.
[10] A. A. Abdumalikov, Y. Koval, A. V. Ustinov, V. V. Kurin, Ch. Helm, A. De Col, Submitted to J. Appl. Phys.
[11] A. De Col, V.B. Geshkenbein, and G. Blatter, in preparation.
[12] A. De Col, V. B. Geshkenbein, G.I. Menon, and G. Blatter, Physica C, in press.
[13] M.J.W. Dodgson *et al.* Phys. Rev. Lett. **84**, 2698 (2000).
[14] G. I. Menon *et al.*, Phys. Rev. B **54**, 16192 (1996); P.S. Cornaglia and C. A. Balseiro, Phys. Rev. B **61,** 784 (2000).

.

7. Synthesis of Magnetic and Conducting Nanoscopic Particles as well as their Organization into Functional Arrays

Project leader: Reinhard Nesper, ETH Zurich

Research summary: A practical process for generating arbitrary forms, especially supported wires of the MgB_2 superconductor has been established. Heterographites which have been predicted to show HT_c superconductivity have systematically been hole-doped. Neither LiBC nor MgB_2C_2 was found to become superconducting. Structural investigation of $Na_{0.7}CoO_2$ reveal complex disorder and stacking fault sequences. Nanoscopic metal oxide particles, with focus on anisotropic transition metal oxides, have been systematically synthesized and investigated. A toolbox of different nanotube and fiber materials is available. Their growth processes have been studied and multicomponent / multilayer systems established.

MgB_2 related compounds

The discovery of superconductivity in MgB_2 at 39 K has led to a new interest in similar compounds like the closely related heterographites LiBC and MgB_2C_2 , which is a semiconductor but can be made metallic through hole doping. Recent theoretical studies predict HT superconductivity for LiBC and MgB_2C_2 [1-3]. LiBC was investigated by an extensive synthesis series. It cannot be prepared with sub-stochiometric Li content. A black material, different from the golden lustrous parent compound is found at high temperature and reduced Li pressure and its XRD pattern is significantly changed indicating the decomposition of LiBC. MgB_2C_2 exhibits an enhanced cation mobility and is much better for intercalation and de-intercalation processes.

We prepared various samples of $Mg_xB_2C_2$ with different Mg contents between 1.0>x>0.75. However, magnetic measurements did not show any Meissner effect down to 4K. The cation lattice be filled up again either by magnesium or by lithium. Maximal volume changes are in the range of 1%.

MgB_2

A procedure for developing wires and arbitrary formed shapes of the novel high-T_c superconductor MgB_2 has been developed. This starts from the synthesis of the ductile binary $LiB_{0.89}$ which can be produced in arbitrary shapes as well as in form of coating of carrier wires. Subsequently, the $LiB_{0.89}$ product is transformed into MgB_2 by treatment in an Mg-melt according to

$$2\ LiB + 9\ Mg \Rightarrow Li_2Mg_8 + MgB_2$$

A coated wire and a piece of MgB_2 coating are shown in Figure 1.

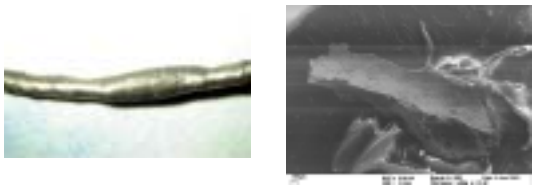

***Figure 1**: Left: a wire coated with MgB_2. Right: a piece of MgB_2 coating*

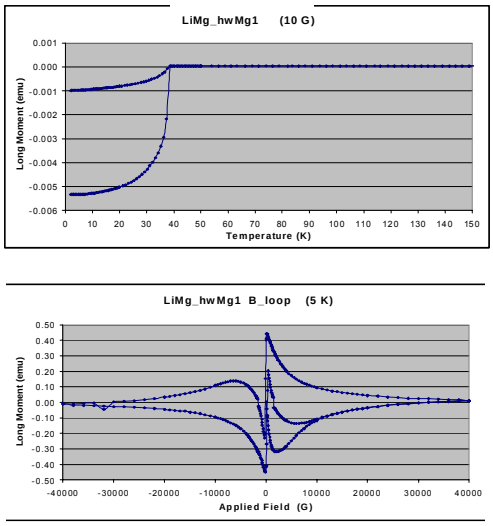

***Figure 2**: Magnetic Susceptibility of MgB2*

The final shape-preserving MgB_2 coating shows excellent bulk properties, i.e. a T_c =38K and a H_{c2} of about 30 Tesla (Fig. 2).

Nanoscopic Fe-Oxides and Fe-Co Oxides

A new synthesis route to nanoscopic Fe-Oxides and (Fe,Co) oxides (figure 3, left) with superparamagnetic behaviour and high magnetic moments (figure 3, right) has been worked out based on the complex :

$$[N(CH_3)_4]_2[OM_6(H\text{-}3Thme)_3(OCH_3)_3Cl_6].2H_2O$$
(M = Fe, Co).

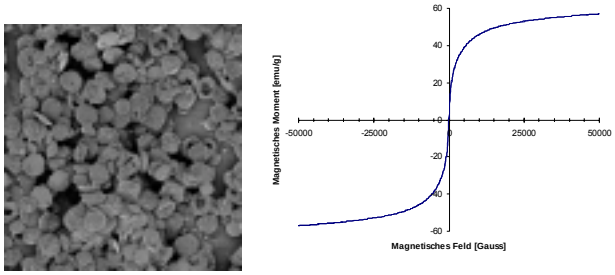

***Figure 3**: Nanoscopic (Fe, Co) oxides (left) and their magnetic moment (right).*

Vanadium Oxide Nano Fibers and Tubes

Formation, morphology, chemical composition and physical properties of VO_x nanotubes and nanofibers have extensively been investigated. The wall structure of the VO_x tubes (figure 4) was determined by joint XRD, TEM and synchrotron work.

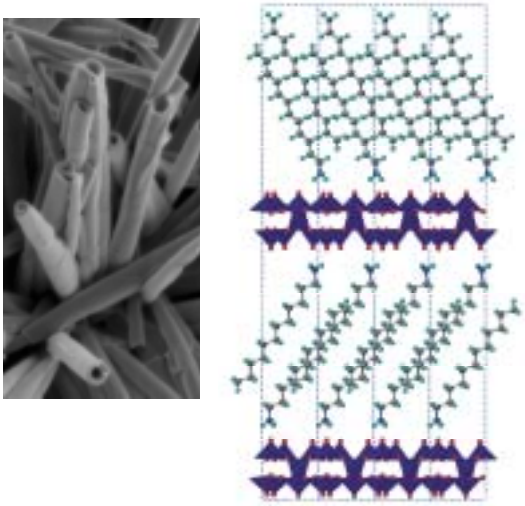

***Figure 4** VO_x tubes (left) and their wall structure (right).*

VO_x fibers were synthesized on large scale and used as base particles for building up higher functionalized multiple material fibers. This route allows us to sequentially apply a layer-by-layer design of mixed material nano fibers and tubes. In this way, VO_x/SiO_2, VO_x/TiO_2, VO_x /SiO_2/Fe, VO_x/SiO_2/C systems have already been realized.

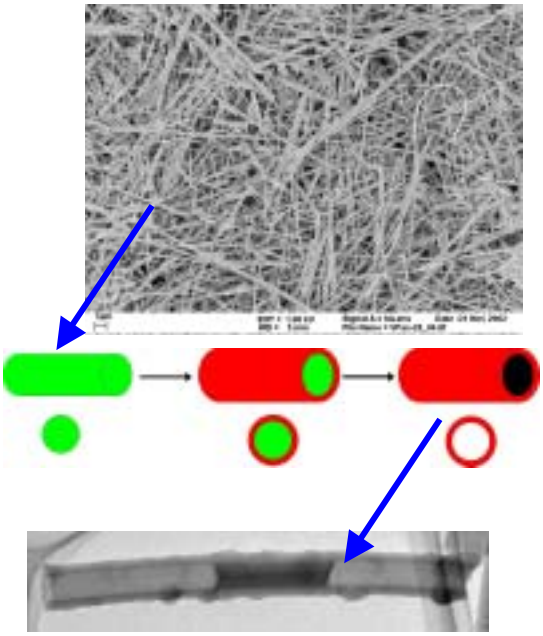

***Figure 5**: Route for the synthesis of various kind of microtubes.*

$Na_{0.7}CoO_2$

$Na_{0.7}CoO_2$ exhibits superconductivity after treatment with water [4,5]. XRD powder (Fig. 6) and single crystal investigations show that there is a phase transition between 220 and 320K. Due to stacking, diffuse scattering is observed. However the structural problem is complex because also superstructure, incommensurate partial lattices, disorder and/or/ partial occupations and also twinning problems have to be considered.

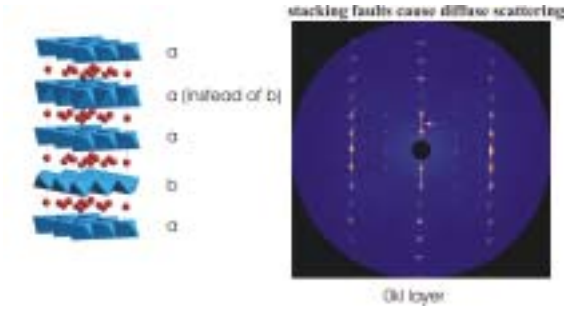

***Figure 6**: Crystal structure and X-ray diffraction pattern of $Na_{0.7}CoO_2$*

Transition Metal Oxide Nanofibers

Straightforward, one-step solvothermal syntheses were developed to prepare nanofibers of TiO_2, MoO_3, WO_3, V_2O_5, SiO_2, Fe_2O_3 and Nb_2O_5. This set of fiber materials is seen as a toolbox for further bulk powder and

single particle investigations with respect to electronic and structural phase transitions. In addition, multicomponent fibers, i.e. Mo/W double oxides and more complicated growth patterns have been investigated by systematic studies (cf. figure 7).

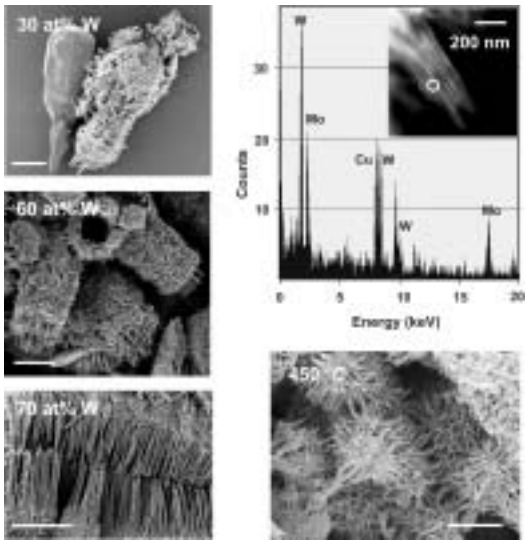

***Figure 7**: Some of the synthesized Mo/W double oxides and (upper right) the typical output of a composition analysis.*

Nanoparticular Titanates

If TiO_2 nanotubes are treated with concentrated $Sr(OH)_2$ and $Ba(OH)_2$ they transform partially into $SrTiO_3$ and $BaTiO_3$, respectively. However, because of the large volume change topochemical reaction and the formed nanocrystals of the titanates are only approximately oriented along the main axis of the supporting tubes. Figure 8 below shows $BaTiO_3$ nanocrystals of about 10-15nm on the surface of a TiO_2 nanotube. According to electron diffraction studies the $BaTiO_3$ nano-crystals exhibit an approximate common alignment.

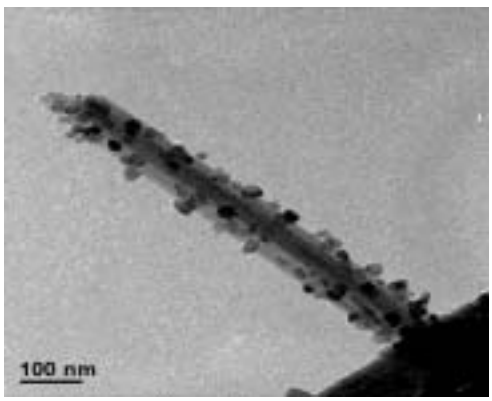

***Figure 8**: $BaTiO_3$ nanocrystals.*

Manganites

Manganites show a series of interesting interesting properties such as CMR. Suitable predursors were treated similar to the TiO_2 procedure. Depending on the reaction parameters mainly samples with isotropic morphologies have been found (Fig. 9). In some cases anisotropic rod-like form were found as well. However, no real nanotubular or nanofibrous materials have formed.

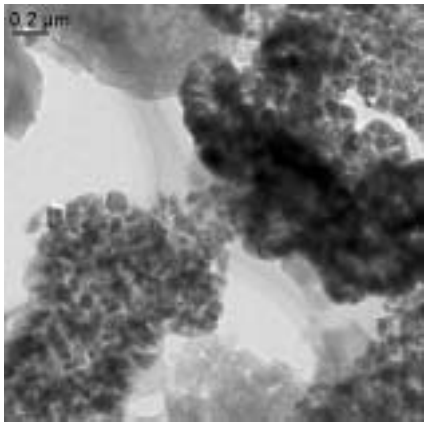

***Figure 9**: Samples of manganites synthesized by the TiO_2 procedure.*

Synthesis of Carbon Nanotubes (CNT) at low temperatures

Decomposition of solid metal carbides, metal organic compounds and acetylene in a low melting salt mixture has been investigated thoroughly as a possible way to produce low cost CNTs in large scale. The salt melts were doped by chlorides of transition metal which are known to catalyze CNT-formation.

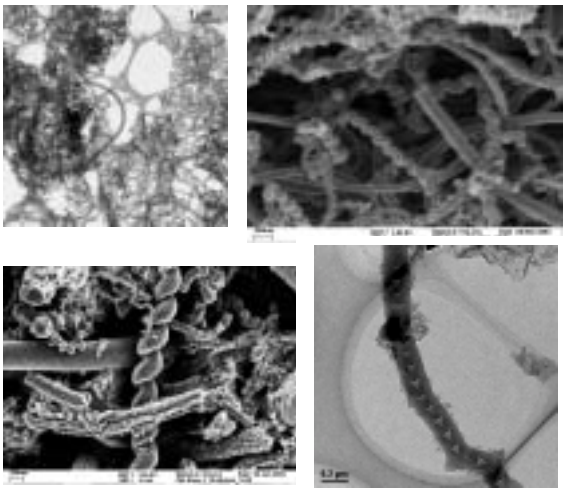

***Figure 10:** Low temperature synthesis of morphological carbonaceous nanotubes.*

A large number of different morphological carbonaceous forms have been synthesized in this way at temperatures below 1000 and even below 500 ^{o}C. Amongst linear nanotubular and fiber-like materials, helical and bamboo-type form can be generated in good yield at different conditions. However, most forms are being built from graphite platelet subunits different from classical CNTs.

References:

[1] P. Ravindran et al., *Phys. Rev.* B 2001, 64(22), 224509.
[2] M. Wörle, R. Nesper, *J. Alloys Compd.* 1994, 216(1)
[3] M. Wörle, R. Nesper, G. Mair, M. Schwarz, H. G. von Schnering, *Z. Anorg. Allg. Chem.* **1995**, *621,* 1153-1159
[4] K. Takado, H. Sakurai, E. Takayama-Muromachi, F. Izumi, R. A. Dilanian, T. Sasaki, *Nature* **422,** 53 (2003)
[5] J. L. Gavilano, D. Rau, B. Pedrini, J. Hinderer, H. R. Ott, S. M. Kazakov, J. Karpinski; submitted

8. Influence of Externally Controlled Parameters on the Properties of Metals with Strong Electron Interaction

Project leader: Hans Rudolf Ott, ETH Zurich

Research Summary: During the last 3 years we discovered and investigated remarkable magnetotransport effects in Eu-based hexaborides at low temperatures. We also contributed significantly to the growth of single crystals and to establishing the multigap features of superconducting MgB_2. Transport and NMR experiments on low-dimensional spin systems revealed new features of the physics of such systems and finally, we discovered a new type of phase transition in the mixed state of $NbSe_2$.

Magnetotransport in "pure" and doped EuB_6

We have successfully modelled the magneto-resistance of EuB_6 for temperatures between 20 and 300 K by properly accounting for the scattering of the charge carriers by impurities, phonons and the (disordered) spins of the Eu-ions, as well as for the change in carrier density with temperature and magnetic field. Our attempt to apply our formalism to the evaluation of the anomalous Hall resistivity in the compound led to values several orders of magnitude too low. The same discrepancy has been observed by other authors in Gd and Gd compounds, in which the rare-earth ion 4f shell is also half-filled, and the reason for it is still unknown. At temperatures below 10 K, both the magneto- and the Hall resistance are well reproduced by a two band model, the parameters of which are consistent with the data at high temperature. Our model also reproduces the relation between the plasma frequency and the magnetization observed in optical reflectivity experiments.

Upon replacing Eu by Ca in EuB_6, the ferromagnetic phase transition temperature decreases and finally vanishes below a critical concentration $x_p \sim 0.3$. The description of the electrical transport may be regarded as a site percolation problem with simple cubic symmetry. Transmission Electron Microscopy (TEM) reveals a phase separation between Eu- and Ca-rich domains. In Fig. 1, the Eu (Ca) map shows regions which are richer in Eu (Ca) as bright patches. Two patches, relatively rich in Ca, are marked by red rings and several patches, rich in Eu, are marked by blue circles. Near x_p the electrical resistivity can be described as a percolation phenomenon using a random-resistor network, which can also account for the colossal magnetoresistive effects.

Substituting a few cations in EuB_6 by Sm, yields additional electrons without altering the effective moment strongly, but leads to drastic effects on the physical ground state and the electrical properties. The ferromagnetism is strongly suppressed and above a concentration of only 4% of Sm, the magnetic order is of antiferromagnetic nature.

Replacing Eu by Ce also introduces an additional electron but the moment is strongly reduced. Even though the ferromagnetic interaction is strongly suppressed with increasing Ce-content, no antiferromagnetic phase is observed for $x < 0.2$ in magnetic or electrical transport measurements.

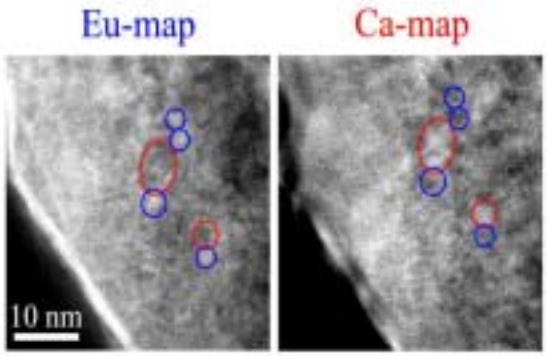

Fig. 1: TEM images for $Eu_{0.27}Ca_{0.23}B_6$. The left side shows a Eu-sensitive measurement, the right side has an energy-window on the energy of the Ca-ions.

Infrared optical properties of the spin-½ quantum magnet TiOCl

Low-dimensional quantum spin systems, based on complex transition metal oxides, recently attracted a lot of attention, particularly as a fascinating playground to study spin-charge separation, spin-gap states and quantum disorder. Proposals, that the exotic properties of low-dimensional spin-½ quantum magnets might also play a major role in shaping the mechanism for high temperature superconductivity, led to a vigorous experimental activity on materials involving Cu^{2+} ions with a $3d^9$ configuration (S=1/2). Other examples of S=1/2 are notably Ti^{3+} and V^{4+} systems in the d1 configuration (i.e., one single d-electron occupies one of the t_{2g} orbitals). In this respect, the layered TiOX (X=Cl and Br) compounds are most promising and are candidates for exotic electronic configurations. High quality single crystals of TiOCl display a kink in the spin susceptibility $\chi(T)$ below about T_{c2}=92 K, followed by a pronounced drop at T_{c1}=67 K.

We have provided a thorough analysis of the optical properties of TiOCl, emphasizing

particularly the temperature dependence of the phonon spectrum (Fig. 2). The temperature dependence of all relevant parameters, including the phonon linewidth and the spectral weight, occurs over a broad temperature interval from T_{c1} up to 200 K. This is a fingerprint for the important role played by fluctuation effects. The pronounced narrowing of the IR modes with decreasing temperature (inset of Fig. 2) coincides with the suppression of low frequency spin fluctuations, also recognized in the spin-gap phase of the NMR spectra. The behaviour of the IR spectral weight with temperature establishes the presence of a characteristic energy scale associated with the opening of a spin-gap.

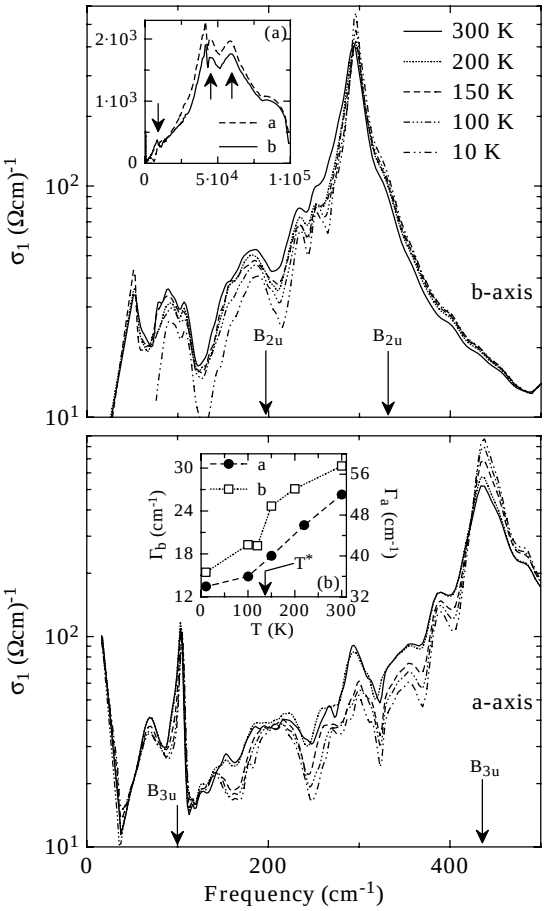

Fig. 2: Real part $\sigma_1(\omega)$ of the optical conductivity of TiOCl as a function of temperature along the b-axis and the a-axis. $\sigma_1(\omega)$ decreases with decreasing temperature in the far infrared signaling the suppression of spectral weight, which is transferred at higher energies. The inset (a) shows $\sigma_1(\omega)$ up to the ultra-violet at 300 K, where the charge gap (down arrow) and the electronic interband transitions (up arrows) are recognized. The inset (b) displays the temperature dependence of the width (Γ) of the phonon mode at 294 and 438 cm^{-1}, respectively.

Although similar findings are frequently observed in 1D systems the present case is different due to the unusually high energy scale involved.

Energy transport in S=1 and S=1/2 spin chain compounds

It has been predicted decades ago that in one-dimensional Heisenberg antiferromagnetic spin S=1/2 systems, the spin and thermal conductivities are not expected to be of diffusive character as is typical for classical systems without long-range order, but instead are based on ballistic transport of spin and energy. On theoretical grounds it was recently demonstrated that this difference is due to the conservation of spin and energy currents in integrable models which apply for 1D S=1/2 spin systems. Contrary to the half-integer spin 1D systems, theoretical discussions predict that transport in ideal 1D Heisenberg S=1 systems must be diffusive, although the situation is not clear and conflicting results have been published. The role of external perturbations, unavoidable in real spin chain compounds and leading to the destruction of integrability, thus restoring diffusive transport, is another widely discussed issue.

To address these issues experimentally, we have measured the thermal conductivity $\kappa(T)$ in several spin chain compounds, considered as good physical realizations of the 1D Heisenberg S=1/2 system (Sr_2CuO_3, $SrCuO_2$, $BaCu_2Si_2O_7$) and the 1D Heisenberg S=1 system ($AgVP_2S_6$). The measurements were done on single-crystalline samples along and perpendicular to the spin-chain directions. Assuming that the total measured thermal conductivity along the spin chains consists of a phonon contribution κ_{ph} and a magnon contribution κ_m, and that only phonons contribute to the heat transport perpendicular to the spin chains, we calculated $\kappa_m(T)$. The spin-related energy diffusion constant D_E and the mean free paths of spin excitations $l_s(T)$ were extracted from $\kappa_m(T)$. The resulting values of $l_s(T)$ are shown in Fig. 3. The similarity of the data for all S=1/2 compounds is remarkable and suggests that the relaxation processes for spin excitations are the same in all these compounds. This universal behaviour is most likely caused by the spin-lattice interaction and interaction of spin excitations with defects. In contrast, the mean free path of spin excitations in the S=1 material is small in the entire covered temperature region with absolute values consistent with predictions for diffusive transport thus supporting the previous suggestions for an intrinsic origin of the spin diffusion at high temperatures in the S=1 chains. Another important result is the observed good qualitative and quantitative agreement between our results for $D_E(T)$ and the NMR results for the spin diffusion constant $D_S(T)$, for both S=1 and S=1/2 chains.

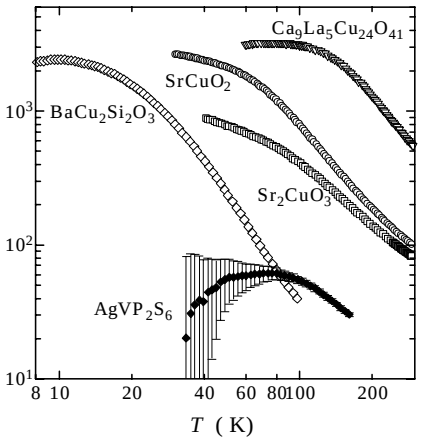

Fig. 3. Mean free path of spin excitations in the S=1/2 spin-chain compounds $BaCu_2Si_2O_7$ Sr_2CuO_3 and $SrCuO_2$, and the S=1 spin-chain compound $AgVP_2S_6$. The corresponding data for the two-leg S=1/2 spin-ladder material $Ca_9La_5Cu_{24}O_{41}$ by other authors are shown for comparison.

Multigap effects in the thermal conductivity of MgB_2

Numerous experimental results and theoretical calculations strongly suggest that the superconducting energy gap in layered MgB_2 differs substantially on parts of the Fermi surface with different dimensionality: the value of the gap of the two-dimensional (2D) parts (σ-band) is close to the value predicted by the original weak-coupling BCS theory, but the gap associated with the 3D sheets of the Fermi surface (π-band) is substantially smaller.

We have measured the thermal conductivity κ parallel to the basal plane of the hexagonal crystal lattice of MgB_2 as a function of varying magnetic fields H. For the analysis of the data, contributions to the heat transport due to both phonons (κ_{ph}) and electronic quasiparticles (κ_e) are considered. In the mixed state the quasiparticles associated with the vortices, induced in a superconductor by magnetic field, enhance the phonon scattering and reduce the phonon thermal conductivity κ_{ph}, but at the same time enhance the quasiparticle thermal conductivity κ_e. The observed κ(H) curves, as illustrated in Fig. 4 for T=0.60 K, both demonstrate a very rapid increase of κ_e at relatively low fields, unprecedented for other superconductors.

The field dependence of κ_e is explained in terms of a two-band model. The saturation of $\kappa_e(H)$ much below the upper critical field H_{c2} may be regarded as evidence for the closing of the smaller gap Δ_π. The heat transport via quasiparticles of the band associated with the larger gap Δ_σ is significant only in the vicinity of and above H_{c2}. Employing the two-band model, we separated contributions to the thermal conductivity from the σ-band ($\kappa_{e,\sigma}$) and from the π-bands ($\kappa_{e,\pi}$), as demonstrated in Fig. 4. The analysis of corresponding quasiparticle mean free paths suggests that the σ-band is in a moderately clean limit and the π-band is in the dirty limit.

Another important observation is that below 8 K, the range of possible values of κ_e in the field-induced normal state (H||c> 30 kOe) exceeds the values calculated from the experimental value of the bulk electrical resistivity using the Wiedemann-Franz law (WFL). This violation, which is expected to hold for the Fermi-liquid ground state, might be the consequence of some kind of anomalous gap formation in the electronic excitation spectrum in the normal state.

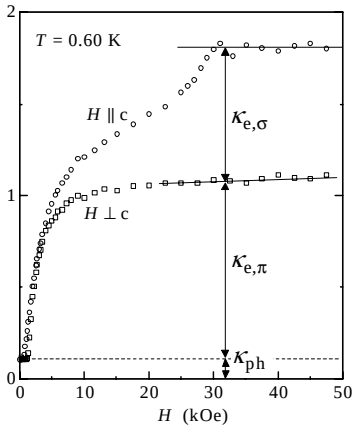

Fig. 4 : Separation of the individual contributions of the σ- and π-band quasiparticles, and the phonons to the normal state thermal conductivity of MgB_2 at T = 0.60 K.

NMR and dc-susceptibility studies of $LiVGe_2O_6$ and $NaVGe_2O_6$

$LiVGe_2O_6$ and $NaVGe_2O_6$ are new materials that, due to their structural features, are expected to be good physical realizations of quasi 1D Heisenberg systems. Our previous studies of $LiVGe_2O_6$ revealed that the V ions are trivalent (S=1), but the expected non-magnetic Haldane phase was absent. Instead we found a phase transition to an antiferromagnetic AF state at T_N = 24 K.

During the last three years we have greatly extended our previous NMR investigation of $LiVGe_2O_6$ and, in collaboration with the research group of G.W. Clark at UCLA, NMR studies in very large applied magnetic fields were produced. Unexpectedly, it was found that the onset of the AF phase is hardly affected by fields as high as 44 T.

For $NaVGe_2O_6$ we found that at high temperatures, above 100 K, the magnetic

susceptibility $\chi(T)$ also reveals an oxidation state of V^{3+} (S=1) for the V ions. $\chi(T)$ signals a magnetic phase transition at T_N = 18 K. This is reflected by a drastic change of the lineshape of ^{23}Na-NMR spectra (see Fig. 5) and an anomaly in the temperature evolution of the spin-lattice relaxation rate $T_1^{-1}(T)$. At $T << T_N$, $T_1^{-1}(T)$ decreases rapidly with decreasing temperature, indicating the existence of a gap of the order Δ/k_B = 12.5 K in the magnon excitation spectrum.

In conclusion the competition between magnetic order and the formation of the Haldane gap is resolved in favor of magnetic order for $LiVGe_2O_6$ and $NaVGe_2O_6$. This is most likely caused by the nonnegligible ratio $J_\perp/J$ between the interchain and intrachain coupling, which we found in both cases to be sufficiently large to suppress the expected Haldane phase. In particular, $J_\perp/J$ of $LiVGe_2O_6$ is 0.07, almost three times larger than the minimum value required to suppress the Haldane phase.

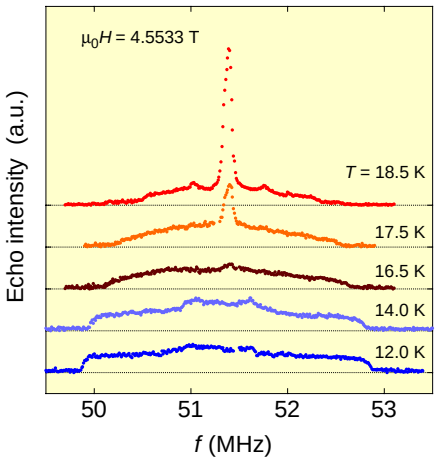

Fig. 5: ^{23}Na-NMR spectrum of $NaVGe_2O_6$ for five different temperatures. A phase transition to an antiferromagnetic state occurs at 18 K.

A low-dimensional spin S = 1/2 system at the quantum critical limit: $Na_2V_3O_7$

During the last three years we made extensive measurements of the temperature dependence of the magnetic susceptibility $\chi(T)$, the specific heat $C_p(T)$, and the ^{23}Na-NMR response of $Na_2V_3O_7$, a novel material, whose structure is built up by interconnected VO_5 square pyramids, forming nanotubes with a diameter of approximately 5 Å (see Fig. 6). $Na_2V_3O_7$ may be the first realization of a spin ½ ladder system with periodic boundary conditions in the rung direction.

From our data we infer that at high temperatures $Na_2V_3O_7$ is a paramagnetic insulator with all the V ions in the tetravalent state (S=1/2). Below 100 K, the V^{4+} moments are gradually quenched, leaving only one moment out of 9 active. The ^{23}Na-NMR response also reveals an anomaly in the same temperature range, namely, a prominent peak in the temperature dependence of the spin-lattice relaxation rate $T_1^{-1}(T)$ at 100 K. This clearly demonstrates that the quenching of the V moments is accompanied by a dramatic change in their dynamics. At much lower temperatures and in the presence of modest external magnetic fields, the $T_1^{-1}(T)$ data reveal a phase transition or spin-freezing phenomenon at a field-dependent temperature T_a. T_a shifts towards T= 0 K with decreasing external field.

The results of recent measurements of the specific heat $C_p(T)$ confirm this picture. For instance, the total magnetic entropy, per mol of V^{4+}(S = 1/2) ions, released up to 20 K, is about one order of magnitude smaller than Rln(2), supporting the claim that only a small fraction of the V ions are magnetically active at low temperatures. Furthermore below 5 K, $C_p(T)/T$ exhibits broad maxima at $T_0(H)$ which shift to higher temperatures upon increasing applied external magnetic field μ_0H. The data indicate that for H = 0 T, T_0 = 0 K. In zero magnetic field $C_p(T)/T$ diverges logarithmically towards T = 0 K. From our results we conclude that $Na_2V_3O_7$ is close to, or at a quantum critical point at μ_0H = 0 T. A realistic microscopic description of $Na_2V_3O_7$ is presently not available.

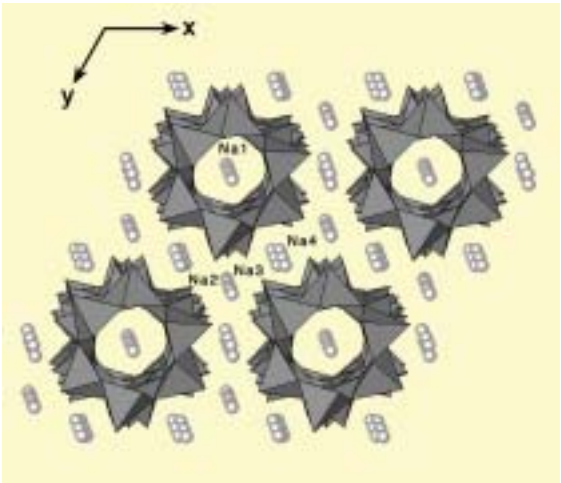

Fig. 6: Representation of the crystal structure of $Na_2V_3O_7$.

Unconventional Charge Ordering in $Na_{0.7}CoO_2$ below 300 K

The unexpected discovery of superconductivity in $Na_{0.3}CoO_2 1.3\ H_2O$ T_c = 5 K last year has triggered an enhanced interest in layered

alkali-metal cobalt oxides. Of special interest is the parent compound, $Na_{0.70}CoO_2$, whose physical properties are quite puzzling. We made measurements of the magnetic susceptibility and ^{23}Na-NMR on polycrystalline samples of $Na_{0.70}CoO_2$.

The χ(T) data suggest that for T > 75 K, the Co ions adopt an effective configuration of $Co^{3.4+}$. A static distribution of electric charge should naturally result in a distribution of different Na environments, as observed in the ^{23}Na-NMR spectra at temperatures between 200 and 230 K. However, this situation gradually changes at higher temperatures. At 300 K and above there is a single Na environment as evidenced by the characteristic shape of the ^{23}Na-NMR spectrum (see Fig. 7). The temperature evolution of the ^{23}Na-NMR linewidth of the Na central transition reveals a pronounced peak near 250 and a change of slope at 295 K, but no evidence for magnetic phase transitions is found in χ(T). Significant anomalies in the temperature dependence of the spin-lattice relaxation rate T_1^{-1} and of the spin-spin relaxation rate T_2^{-1} at or near 230 and 295 K indicate the onset of a dramatic change in the Co 3d-electron spin dynamics with an onset at 295 K. This process is completed at 230 K.

From our results we infer that below 295 K the Co 3d-electron system within the CoO layers is affected by at least one phase transition. Two scenarios seem possible: (a) a partial charge ordering phenomenon involving Co^{3+} and Co^{4+} upon decreasing temperature, completed only near 230 K; and (b) an unconventional charge density wave within the Co subsystem develops. The system remains metallic at all temperatures.

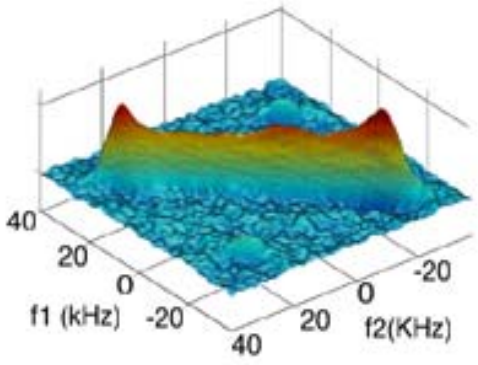

Fig. 7: 2D-NMR spectrum of $Na_{0.70}CoO_2$ at 295 K. The diagonal signal is typical of the powder pattern of a single Na environment.

9. Theoretical Modelling of Materials with Novel Electronic Properties

Project leader: T. Maurice Rice, ETH Zurich

Research summary: This report reviews the research activities of three groups at ETH Zurich (T.M. Rice, M. Sigrist), University of Fribourg (D. Baeriswyl, C. Morais Smith) and EPF Lausanne (F. Mila). The research topics cover a wide range of theoretical studies, in particular, high-temperature superconductivity, quantum phase transitions in magnetic systems, frustrated magnets and various phenomena in multi-band superconductors. Many projects have developed in close contact with experimental groups within and outside of MaNEP.

1. High-temperature superconductivity

Renormalization group studies: The microscopic theory of high temperature superconductivity continues to be a central focus. During the past 3 years a considerable effort was devoted to refining the approach to the underlying 2D Hubbard model from weak coupling although the cuprates are closer to, strong coupling. The motivation is to gain new insights into the RVB phase that is the key to these materials. Prior to the start of MANEP the functional RG method required to treat scattering processes in 2-dimensions (2D), had been developed. Attention focused on the behaviour when the hole density is such that van Hove singularities are near the Fermi energy leading to a mutual reinforcement of scattering processes in AF and d-wave pairing channels. The close similarity to the RG flow in the case of 2-leg ladders which have a RVB groundstate was noted. The above conclusions were drawn from an examination of the divergent flows as the energy (or temperature) scale was lowered. Recently Läuchli, Honerkamp and Rice developed a new method based on numerical diagonal-ization of a reduced Hamiltonian determined by the form of the divergent flow. The method was successfully tested on the short range RVB state of the 2-leg Hubbard ladder and reproduced the known results from bosonization techniques. In the 2D Hubbard model near the van Hove filling scattering processes involving the saddle point regions dominate the divergent flows. The new method shows that, although the RG equations are quite different, the resultant strong coupling phase is very similar to the RVB ladder state. This result supports the interpretation of the crossover at the high-T* temperature in the underdoped cuprates as the formation of a RVB condensate which truncates the Fermi surface near the saddle points. Supercon-ductivity appears at a lower temperature scale driven by the coupling in the Cooper channel between the remaining Fermi surface arcs and the truncated saddle point regions.

In a separate investigation, Binz together with Doucot and Baeriswyl, made a careful examination of the RG equations for densities exactly at the van Hove filling and examined the competition between a number of instabilities in the weak coupling limit, as the relative strengths of different interaction terms in a very general model Hamiltonian, were varied.

ARPES spectra electron-doped cuprates: Inspired by recent ARPES measurements on electron doped cuprates, H. Kusunose and T.M. Rice investigated the origin of states that appear in the Mott-Hubbard gap as the electron doping increases. ARPES in the case of electron doping is very interesting since it allows one to study the evolution of the Mott-Hubbard gap with doping. Good agreement was found between the calculations of the spectra based on a self-consistent coupling to spin excitations, for dopings ranging up to the critical value where the antiferromagnetic order vanishes.

Stripes: The large body of experimental data showing charge inhomogeneities in strongly correlated 2D electron systems (cuprates, nickelates and manganites) motivated the group of Morais Smith to investigate the dynamics of stripes in doped Mott insulators. These studies consider mainly the influence of lattice, disorder, and other additional dopants on the stripe dynamics. Benfatto and Morais Smith studied the response of charge stripes to an external electric field applied perpendicular to the stripe direction, accounting for both, weak and strong pinning by random impurities. The sound-like mode of the stripes moves to finite frequency due to impurity pinning. The calculation of the optical conductivity for a single and an array of stripes reveals this characteristic energy scale and explains the anomalous far-infrared peak observed recently in optical conductivity measurements on cuprates. Moreover, Hasselmann, Castro Neto and Morais Smith studied the influence of transverse stripe fluctuations on a Luttinger liquid. It was found that this coupling can lead to a $4k_F$ charge density wave instability in the longitudinal sector with a simultaneous occurrence of a zigzag order in the transverse one. This result sheds light on the as yet not understood connection between the formation of a low-

temperature-tetragonal phase and the subsequent appearance of charge order in high-T_c cuprates and manganites.

2. Quantum phase transitions

Magnetization texture with the 1/8-plateau of $SrCu_2(BO_3)_2$: This compound is the first known realization of the so-called Shastry-Sutherland system, a strongly frustrated two-dimensional spin ½ system whose groundstate consists of decoupled spin-singlet dimers with a spin excitation gap. In contrast to the previous case here the gapped spin triplet excitations (magnons) are nearly immobile making them very susceptible to localization. In a moderate magnetic field the excitation gap closes and weakly itinerant magnons appear. At higher fields a plateau in the magnetization is observed where the triplet magnons form superlattices constituting a Mott-localized phase. Miyahara and Mila have shown that the stabilization of the plateaus requires spin lattice effects. In particular for the case of the 1/8-filled, where NMR indicates the presence of 11 distinct Cu sites, they have for the first time given a unique assignment of all the lattice sites in the extended unit cell.

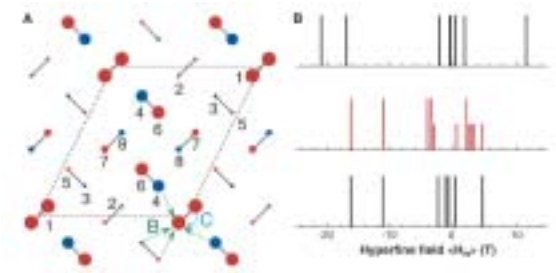

*Fig.1. (A) Magnetization profile of the dimers in the extended unit cell. (B) Histogram of the hyperfine fields. (Science **298,** 395 (2002)).*

Field- and pressure induced ordering in $MCuCl_3$: Detailed high-field neutron scattering studies of the magnon spectra of the dimer compound $MCuCl_3$ (M=Tl and K) by the group of A. Furrer (Project 16) motivated the theoretical investigation of the observed field-induced quantum phase transition. These compounds consist of quantum spin dimers which form a spin singlet groundstate and an excitation gap to strongly-dispersing dimer spin triplet magnons. Moderate magnetic fields are sufficient to close the gap yielding a quantum phase transition to a magnetically ordered phase. Matsumoto, Normand, Rice and Sigrist (MNRS) modeled this system in a dimer singlet and triplet state representation. The effect of the field is to split the degenerate triplet excitations into three, among which the lowest becomes eventually gapless. In this formulation the quantum phase transition is naturally understood a Bose-Einstein condensation (BEC) of the lowest magnons. The ordered phase is characterized by a staggered magnetic moment perpendicular to the applied field, and the excitation spectrum consists of one Goldstone mode of the condensate and two high-energy branches which show distinct renormalization features. The calculated spin spectrum agrees quantitatively very well with the experimental results. Extensive numerical simulations (stochastic series expansions) by Nohadani, Wessel, Normand and Haas examining the universal behaviour of the field-induced quantum phase transition have led to results consistent with the BEC description.
The theoretical study by MNRS has been extended to the pressure-induced quantum phase transition, as observed in $TlCuCl_3$. A complete zero-temperature phase diagram, pressure versus magnetic field, has been derived, shedding light on spin-lattice coupling effects from a macroscopic as well as microscopic point of view (exchange paths).
Finally Matsumoto has proposed a microscopic model for NH_4CuCl_3, explaining its unexpected series of plateaus in the magnetization in terms of three inequivalent dimer sublattices in this compound, which have been experimentally confirmed recently in A. Furrer's group (project 16) by neutron scattering.

Quantum phase transitions and metamagnetism in layered ruthenates: The single-layer alloy $Ca_{2-x}Sr_xRuO_4$ has a rich phase diagram reaching from an antiferromagnetic Mott insulator (x=0) to a spin triplet superconductor (x=2). The intermediate doping region shows metallic phases with distinct magnetic properties. Most characteristic is the Curie-like spin susceptibility at x=0.5 indicating the presence of one free spin ½ per Ru ion. In the region $0.2 < x < 0.5$ the alloy has an-isotropic antiferromagnetic spin fluctuations in contrast to the more ferromagnetic fluctuations for $x > 0.5$. In collaboration with the group of Anisimov, Rice and Sigrist have shown that the Curie-behaviour could result from an orbital selective Mott-transition which localizes only two of the three relevant 4d-t_{2g} orbital of the Ru ion. This aspect has been recently analyzed in detail by Koga, Kawakami, Rice and Sigrist using dynamical mean field theory to establish how a sequential Mott transition of several orbitals can take place. In this way a localized spin ½ and an isospin ½ orbital degree of freedom emerge which can be described by a

Kugel-Khomskii model. Based on this model Sigrist and Troyer have discussed the phase diagram of the doping region close to x=0.5, including spin anisotropy, metamagnetism and magneto-resistance. The overall picture is consistent with most experimental results.

Novel quantum critical behaviour in multi-layered ruthenates: The two- and three-layer ruthenates, $Sr_3Ru_2O_7$ and $Sr_4Ru_3O_{11}$, exhibit a metamagnetic transition originating likely from a quantum critical endpoint. So far this behaviour has been discussed by some groups on a phenomenological level. Binz and Sigrist gave the first microscopic derivation of the basic phase diagram using Hartree-Fock approximation for a model including van Hove singularities in the bandstructure. This leads to a first-order quantum phase transition between a paramagnetic and ferromagnetic phase which eventually terminates in quantum critical endpoint in a finite magnetic field. The meta-magnetism at low temperatures as well as the qualitative differences between two- and three-layer systems can be consistently explained.

Charge Pattern Formation: A system of electrons interacting via long-range Coulomb forces on a 1D lattice was studied by Baeriswyl Fratini and Valenzuela using a variational Ansatz, which is the strong-coupling counterpart of the Gutzwiller wave function, to describe the quantum analogue of Hubbard's classical "generalized Wigner crystal". For a system of spinless fermions, the effects of lattice commensurability generate three distinct quantum ground states: for strong interactions essentially Hubbard's classical solution, for intermediate values the Wigner crystal of the continuum model, and for weak interactions a small amplitude charge-density wave. On inclusion of the spin degrees of freedom, it was shown that in the Wigner crystal regimes these are coupled by an antiferromagnetic exchange significantly smaller than the energy scale governing the charge degrees of freedom. These results shed new light on the insulating phases of organic quasi-1D compounds where the Coulomb interaction is unscreened, and magnetic and charge orderings coexist at low temperatures. The excitations of the Wigner-crystal regime were considered as the quantum problem of kink-antikink pair generation, where the proliferation of pairs signals the onset of quantum melting of the Wigner lattice.

2. Frustrated magnetic systems

Spin tubes in $Na_2V_3O_7$: In collaboration with the group of H.R. Ott (project 8) Mila has analyzed the magnetic properties of $Na_2V_3O_7$ which forms quasi-one-dimensional spin tubes, i.e. closed spin ladders with 9 legs and one spin ½ per Vanadium. This topology constitutes for the "rungs" of the ladder in a frustrated configuration resulting in an effective spin system with one residual spin ½ per rung at low-temperature. Each of these spins should be mobile on the corresponding rung.

Phase transitions in a frustrated antiferro-magnet on the square lattice: Motivated by the first realization of the Heisenberg model on a square lattice with nearest and next-nearest neighbor exchange, Li_2VOSiO_4, Weber, Mila and collaborators have shown that the classical version of the model undergoes a finite temperature Ising transition, if the next-nearest neighbor exchange is at least half the nearest neighbor one, as seems to be the case for Li_2VOSiO_4. Becca and Mila have also shown that the appearance of the low temperature phase should induce a lattice distortion resulting in the lowering of the symmetry to orthorhombic. These predictions are largely confirmed by the NMR results obtained in the group of P. Carretta in Pavia.

Orbital degeneracy and frustration in $LiNiO_2$ and $NaNiO_2$: $LiNiO_2$ and $NaNiO_2$ are layered systems made of weakly coupled triangular lattices in which each site carries two degrees of freedom, a spin ½ because Ni^{3+} is in a low spin state, and a pseudo-spin because of the orbital degeneracy of the e_g level. Although they are isostructural, their properties are very different: $NaNiO_2$ undergoes a cooperative Jahn-Teller distortion around 400 K followed by antiferromagnetic ordering at 20 K with a symmetry that remains to be determined, while $LiNiO_2$ stays in a liquid phase down to the lowest accessible temperatures. Vernay and Mila, in collaboration with Penc and Fazekas (Budapest), have shown that orbital degeneracy can indeed lead to both types of behaviour. For reasonable values of the microscopic parameters, they have shown that two phases compete: a ferro-orbital phase with weakly antiferromagnetic chains, which could explain the properties of $NaNiO_2$, and a phase where spins are coupled into nearest-neighbor singlets, resulting into an RVB (resonating valence bond) liquid.

Topological defects in frustrated Heisenberg spin systems: Frustration can occur in a spin system also through doped holes. Hassel-mann, Castro-Neto and Morais Smith modeled the spin glass phase of $La_{2-x}Sr_xCuO_4$ assuming that the doped holes are localized near Sr in

CuO_2 plane and cause dipolar frustration for the antiferromagnetic spin background. They proposed that the incommensurate magnetic peaks observed by neutron scattering experiments in the spin glass phase of cuprates arise from a spiral distortion of the antiferromagnetic order. Renormalization group calculations show that the collinear O(3)/O(2)-symmetry is unstable towards the formation of local non-collinear correlations.
The order parameter space of frustrated Heisenberg systems is isomorphic to SO(3) and allows for topological defects. Juricic, Benfatto, Caldeira and Morais Smith proposed that the dissipative dynamics of topological defects in the spiral state is responsible for the transport properties in the spin glass phase of cuprates. Using the collective-coordinate method, they showed that the topological defects are coupled to a bath of magnetic excitations. Integrating the bath degrees of freedom out within the Feynman-Vernon path integral formalism they point out that the dynamical properties of the topological defects are dissipative. The calculated damping matrix is related to the in-plane resistivity and a good agreement is found with the available experimental data.

Ring-exchange interactions: Cyclic, four-spin exchange terms have emerged as one of the important interactions in low-dimensional cuprate materials. They have been investigated for both 1D (ladder) and 2D (planar) spin systems by Gritsev, Normand, Baeriswyl and Oles. In 1D, using quantum inverse scattering methods, an entire class of exactly soluble generalized isotropic spin ½ ladder models has been discovered. From such models on a ladder with rung, leg, diagonal, and ring-exchange interactions the exact ground states for certain parameter regimes have been obtained and perturbative techniques in the limit of strong ring-exchange coupling have been applied. The combination of these approaches with (Z_4) symmetry considerations leads to a complete phase diagram and to an elucidation of the physical properties of models with ring-exchange interactions. In 2D the relation between cyclic exchange interactions and circulating-current or “flux“ phases was investigated by means of meanfield calculations on planar clusters.

3. Multi-band superconductivity

MgB_2 is a conventional superconductor with an unprecedented high T_c. One important feature is the presence of two superconducting gaps, on the 3D σ-band and the quasi-2D π-bands, resp., as observed in tunneling spectra and in specific heat. Motivated by the thermal transport measurements in the mixed phase by the group of Ott (Project 8) Kusunose, Rice and Sigrist have analyzed the effect of the multi-band/gap structure on the quasiparticle heat transport for the mixed phase. Quasiparticles, usually localized in the vortex cores, are only released very close to H_{c2}. Thus, in the standard case the thermal conductivity κ stays low at small fields and rapidly increases just below H_{c2}. In MgB_2, however, a rapid increase of κ was observed immediately above the lower critical field and a second increase at H_{c2}. The theoretical analysis for a moderately clean two-band superconductor showed that the quasiparticle states of the band with the smaller gap can be delocalized, while those of the other band remain localized. Thus the former quasiparticles give rise to the rapid increase of κ at H_{c1} and the latter at H_{c2}. For a very clean sample all quasiparticles are localized in the vortex cores and the observation of the standard field-dependence is predicted.

There a three 4d-t_{2g} bands in *Sr_2RuO_4* which is a chiral p-wave spin triplet superconductor. A debate of multi-gap superconductivity arose in connection with apparent "powerlaws" in various thermodynamic quantities which have been interpreted in terms of line nodes in the gap using oversimplified models. While nodes are not required by symmetry in the chiral p-wave state, it still may be realized by accident. Zhitomirsky and Rice have examined the specific heat data within a two gap model assuming horizontal line nodes in one of the bands. This gave an excellent fit of the data and explained also the unnaturally wide range of powerlaw behaviour which is difficult to account for in a single-band model. A further study by Kusunose and Sigrist showed that such a model reproduces the temperature dependence of the London penetration quantitatively, if non-local corrections to the electromagnetic response are taken into account. In addition this analysis shows that the so-called γ-band is the most relevant for the superconducting phase, which has been anticipated earlier based on the discussion of spin-orbit coupling effects.

10. Study of the Superconductor-Insulator Transition of Underdoped Cuprates

Project leader: Piero Martinoli, University of Neuchâtel

Research summary: Essential for the experimental investigations carried out in this project is the preparation of high-quality ultrathin superconducting films. YBCO films deposited by laser ablation were used in the early stages of the project to study critical and dimensional crossover phenomena in relation to the vortex glass-to-vortex liquid transition. More recently, relying on an original almost-homoepitaxial buffer deposition technique, ultrathin LSCO films with remarkable superconducting properties were grown, which allowed to observe features consistent with the d-wave symmetry of the order parameter in studies of the in-plane magnetic penetration depth performed below 1K. On the theoretical side, we have studied underdoped superconductors in the framework of the attractive Hubbard model. Cooper pairing and charge density waves of d-symmetry are possible types of order resulting from the electronic interaction. Phase and amplitude fluctuations of the pairing field influence specific heat and magnetic susceptibility and produce the electronic pseudogap. D-density-waves modify the optical sum rule and can lead to a violation of the Wiedemann-Franz law. Vortex-lattice melting in strongly anisotropic superconductors has also been studied theoretically by taking into account the effect of Josephson coupling between the layers. The study of Josephson junction arrays on a dice lattice allowed to identify accidental degeneracy as the mechanism which suppresses phase coherence at full frustration.

Growth and superconducting properties of ultrathin cuprate films

A considerable fraction of our experimental activity is dedicated to the growth of ultrathin [*i.e.*, a few unit cells (UC) thick] epitaxial films. Besides their relevance to explore fundamental aspects of superconductivity in the cuprates, ultrathin layers are essential for investigations of the superconductor-insulator (SI) transition based on the electric field effect. Because of their very weak diamagnetic response, they also prove to be ideally suited for studies of the in-plane magnetic penetration depth λ_{ab} with methods developed in our laboratory.

In the first stage of this project, ultrathin YBCO films deposited by laser ablation were used [1] to demonstrate the existence, below a frequency-dependent temperature $T^*(\omega)$, of glasslike features in the dynamic response of a 2D superconductor, where, strictly speaking, a genuine vortex glass (*i.e.,* such that the linear resistance vanishes) should not occur. This observation suggests the idea of a vortex liquid which, below $T^*(\omega)$, appears to be frozen at the time scales $1/\omega$ of the experiments. Critical dynamic scaling and dimensional crossover phenomena in relation to the vortex glass-to-vortex liquid transition were also observed in angular dependent resistivity measurements.

In collaboration with J.P. Locquet and J. Fompeyrine of the IBM Research Laboratory, in the subsequent phase of the project we explored new methods to prepare MBE-grown $La_{2-x}Sr_xCuO_4$ (LSCO) films, which, in previous work [2], were shown to reach remarkably high T_c (~50K) when deposited on $SrLaAlO_4$ (SLAO) substrates. We have developed an original almost-homoepitaxial buffer deposition technique [3], which allows to grow 1UC thick LSCO films with noteworthy superconducting properties. It consists in depositing a normal (*i.e.*, x=0.4) buffer LSCO layer (n_1 UC) on top of which the relevant ultrathin (s UC) LSCO film (x=0.1) is grown. A normal (x=0.4) LSCO cap (n_2 UC) is then deposited to protect the structure. This method has the great advantage to largely eliminate structural mismatch and chemical interactions at the film-substrate interface which tend to suppress superconductivity in ultrathin films. The inverse kinetic inductance ($1/L_k$) data, shown in Fig. 1 for different $n_1/s/n_2$ structures, demonstrate the superior superconducting properties one can achieve with the buffer technique: $T_c \approx 8$ K and $\lambda_{ab}(0) = [L_k(0)d/\mu_0]^{1/2} \approx 535$ nm of a single UC LSCO film are, respectively, comparable to and much smaller than the corresponding values for thicker layers grown in a similar way on STO or directly deposited on SLAO.

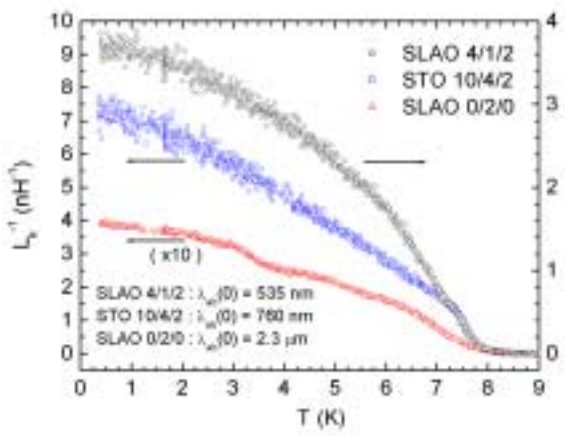

Fig.1.Temperature dependence of the inverse kinetic inductance of various LSCO-based $n_1/s/n_2$ film structures.

These high-quality ultrathin films are excellent candidates to study peculiar features related to the d-wave symmetry of the order parameter in cuprate superconductors. As predicted by theoretical models incorporating both the d-wave symmetry and impurity scattering [4], at

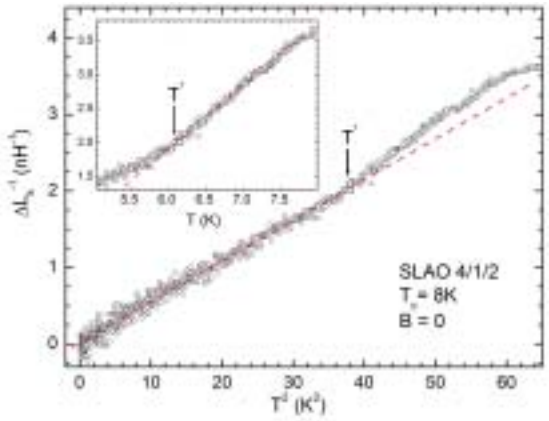

Fig.2. Inverse kinetic inductance change $\Delta L_k^{-1}(T)$ vs T^2 for a single UC LSCO film embedded in a 4/1/2 structure. T^* is the crossover temperature from the quadratic to the linear regime (shown in the insert).

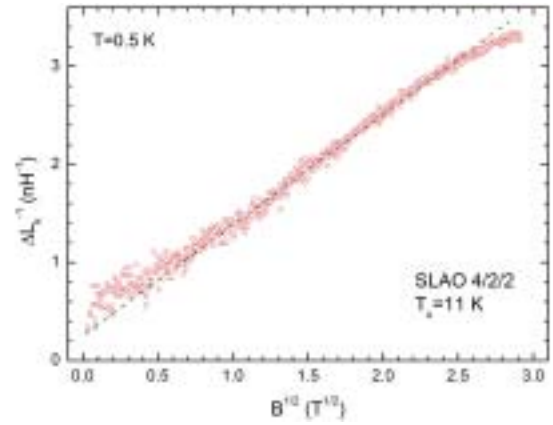

Fig.3. Low temperature magnetic-field dependence of the inverse kinetic inductance change $\Delta L_k^{-1}(B)$ for a 2 UC LSCO film embedded in a 4/2/2 structure.

low temperatures $\Delta L_k^{-1}(T) \equiv L_k^{-1}(0) - L_k^{-1}(T)$, the quantity measuring the thermal suppression of the areal superfluid density, is found to vary algebraically as T^2 (in striking contrast with the BCS exponential behaviour), while a crossover to a linear T-dependence is observed at higher temperatures (Fig. 2). The analysis of the data (slope) allows to extract $v_F/v_\Delta \approx 30$ for the ratio between the Fermi and gap velocities, a value in good agreement with that reported by other authors. With a recently installed ^{3}He cryostat, the magnetic-field dependence of ΔL_k^{-1} was also investigated in fields up to 9 T. As shown in Fig. 3, at low temperatures $\Delta L_k^{-1}(B)$ varies as $B^{1/2}$ over a broad field range, in agreement with Volovik's prediction for superconductors with a nodal gap structure in the excitation spectrum.
Using the buffer deposition technique, we have also prepared LSCO-based heterostructures with an Hf-oxide layer as a gate insulator for studies of the electric-field tuned SI transition.

Effect of Josephson coupling on vortex-lattice melting in layered superconductors

Motivated by the strongly anisotropic nature of the underdoped cuprates, we have extended our previous theoretical treatment of vortex

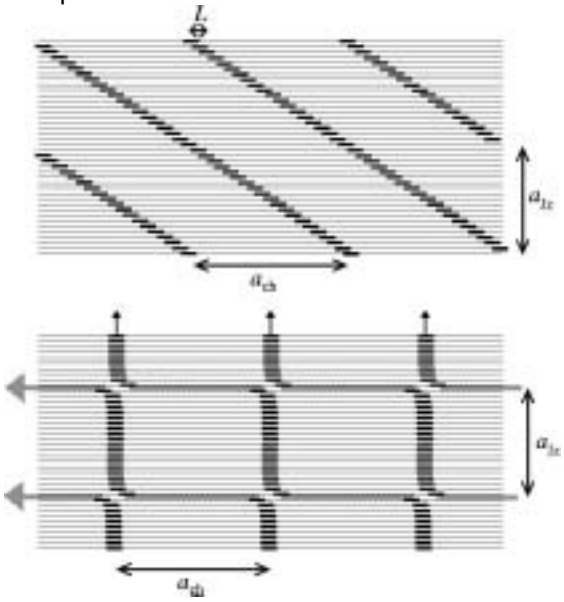

Fig.4. The tilted chain and the chain of crossing Abrikosov *and Josephson vortices. Calculations show that the energy of the crossing chain is lowest at low densities for parameters appropriate to BiSCCO. However, thermal fluctuations are greater in the tilted chain, which can lower the free energy at finite temperature, leading to a first-order phase transition from the crossing to the tilted lattice.*

lattice melting in the absence of Josephson coupling between layers, where we have found the melting temperature as a function of magnetic field, both with a semi-analytic method and a full numerical simulation [5].
We have now investigated the effect of adding weak Josephson coupling within the semi-analytic method, and shown that this has a dramatic effect on the melting line, with a large relative shift at low magnetic fields. This takes the theoretical line closer to that observed experimentally in BiSCCO single crystals. We have also considered the effect of pinning disorder with numerical simulations, which moves the melting line down to a constant field at low temperatures, consistent with the general experimental findings. The situation is complicated further at tilted fields, where there may exist crossing lattices of Abrikosov and Josephson vortices (Fig. 4). An effective attraction between these two species means that chains of Abrikosov vortices may appear "pinned" along the location of a Josephson vortex. We have found some novel features to the melting of a vortex chain. In addition we attribute the experimentally observed "reentrant melting" of an isolated vortex chain to a first-order switch to a chain of tilted vortices.

Josephson junction arrays (JJA)

In close collaboration with S.E. Korshunov (L.D. Landau Institute), we have carried out and completed a detailed study of frustration phenomena in classical JJAs on a dice lattice. A distinctive and novel aspect of this lattice geometry is the strong suppression of phase coherence one observes in the array magneto-inductance at full frustration. This unusual behaviour is shown [6] to arise from accidental degeneracy, a mechanism allowing for the formation of zero-energy domain walls in the ground state of the system, thereby making ordering quite vulnerable to fluctuations.
An new set-up designed to detect the weak diamagnetic response near the SI transition of quantum JJAs (prepared by the Chalmers group) is currently being implemented.

Low temperature superfluid stiffness of d-wave superconductors in a magnetic field

The influence of vortices on temperature and field dependence of the superfluid density ρ_s of a d-wave superconductor is calculated by using the quasi-classical approximation for the coupling of the electrons to the phase gradient of the superconducting pairing field. Below some temperature T*, proportional to the square root of the applied magnetic field, the linear T-dependence of ρ_s crosses over to a T^2- dependence.

Amplitude and phase fluctuations in underdoped high-T_c superconductors

In the attractive Hubbard model the electronic degrees of freedom are coupled to fluctuations of the complex pairing field Δ, even above the critical temperature T_c. There are two temperature windows: the phase of Δ is correlated in space between T_c and T_ϕ, whereas the mean amplitude stays finite up to much higher T. Above T_ϕ, there are no correlations between the local fluctuating pairs. Observable quantities can have contributions coming from both phase and amplitude fluctuations [7]. For the specific heat, phase fluctuations give rise to true critical behaviour at T_c, whereas amplitude fluctuations produce a broad hump way above T_c (Fig 5). The pseudogap in the electronic density of states is dominated by spatially correlated phase fluctuations near T_c. Above T_ϕ, it is maintained by the local pairing fluctuations and it is filled up at T*, where the thermal energy is of the order of the binding energy of the fluctuating local pairs. The diamagnetic susceptibility is dominated by phase (*i.e.*, supercurrent) fluctuations. It is sizeable only up to T_ϕ, as it

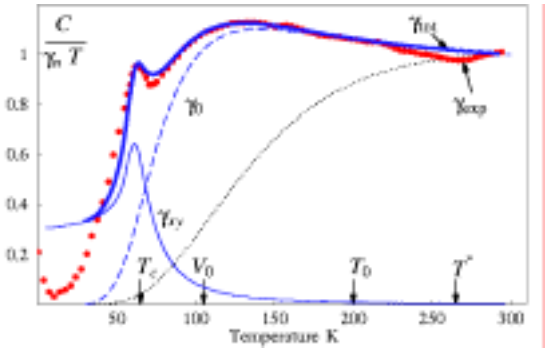

Fig.5. Normalized specific heat data for $YBa_2Cu_3O_{6.76}$. The total specific heat (thick blue) is the sum of the XY (thin blue) and the amplitude contributions (dashed blue).

has been observed in some underdoped compounds. The spin susceptibility, however, deviates from Pauli behaviour up to T*, since fluctuating (singlet) pairs do not contribute. Recent observations of the Hall constant, ultrafast relaxation times and Nernst effect seem to support the distinction between the two temperature regions, dominated, respectively, by phase correlations and by uncorrelated local pair fluctuations.

Structure of Cooper pairs in the pseudogap and in the superconducting regions

In order to obtain information about the internal structure of preformed pairs in the pseudogap region we solve the Bethe-Salpeter equation for the two-electron propagator. The typical size of a pair is on the order by the range of the attraction. Lower temperatures and higher electron densities, as well as the formation of the pseudogap enhances pair formation. Moving pairs are slightly contracted compared with pairs at rest. Below the superconducting transition temperature T_c there are fluctuating pairs and pairs in the superconducting condensate. The former have a similar internal structure as the "preformed" pairs above T_c. The size of the pairs in the condensate is finite for $T > 0$, but it diverges for $T \rightarrow 0$ in the case of d-wave pairing.

Crossover from BCS superconductivity to Bose-Einstein condensation

In the framework of the Hubbard model we identify diagrams that reduce the current correlation function to the ordinary fermionic BCS approximation in the weak-coupling limit and to the bosonic Bogoliubov approximation in the strong-coupling limit. The temperature dependence of the superfluid density (from the BCS exponential behaviour at weak coupling to a power-law behaviour at strong coupling), and the form of the Pippard-like kernel at zero temperature are explicitly obtained from weak to strong coupling. A prescription is provided

for mapping the fermionic onto the bosonic diagrammatic theories in the broken-symmetry phase.

Orbital current (d-density wave) states : optical sum-rule

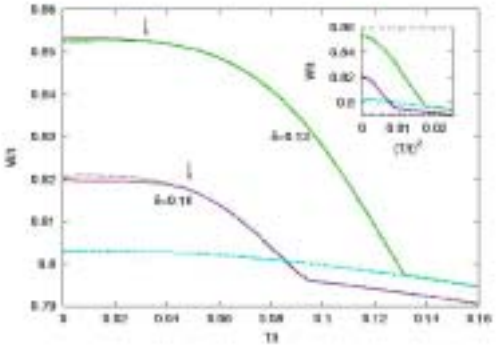

Fig.6. Integral over the real part of the optical conductivity W/t (in units of the hopping energy t) as a function of temperature T/t for different dopings δ. It increases over the normal state value (dash-dotted) when dDW-order sets in. Below the superconducting transition (arrows) the decrease is small.

Recent optical measurements on high temperature superconductors show an unexpected temperature dependence of the integrated optical conductivity. We have evaluated [8] the optical sum rule for a system of non-interacting electrons showing d-density-wave (dDW) order. In the corresponding model Hamiltonian an applied vector potential couples not only to the kinetic energy of the electrons, but also to the (momentum dependent) interaction term, producing the dDW order. This fact indeed allows to reproduce the observed T-dependence of the integrated spectral weight (Fig. 6).

Magnetic oscillations in planar systems with a Dirac-like spectrum of quasiparticle excitations

Various quasi two-dimensional physical systems show a linear quasiparticle dispersion in the vicinity of the chemical potential (d-wave superconductors, materials with alternating orbital currents, pyrolythic graphite or carbon nanotubes.) We have derived analytic expressions for the magnetic oscillations (de Haas–van Alphen effect) showing up in various observables in the presence of impurities. The detailed shape of the oscillations could be used for detecting the possible opening of a gap around the chemical potential that might be due to some other non-trivial interaction.

Electronic structure of impurities in the pseudogap regime of anisotropic superconductors

In order to find the electronic density around an isolated impurity we have calculated the electronic polarizability χ in the pseudogap phase and a possible d-density-wave (dDW) state. This study is motivated by the recent proposal that analyzing the polarization effect of an impurity might allow to distinguish between precursor pairing and dDW order as being responsible for pseudogap. For the dDW state, χ shows the fingerprints of nesting producing hole pockets that can be seen in its space and frequency dependence.

Transport properties of the d-density wave (dDW) state in an external magnetic field

We have calculated [9] electrical and thermal conductivity of the dDW state of a two-dimensional lattice in an external magnetic field B. In the zero temperature limit the Wiedemann-Franz (WF) law remains intact irrespectively of the value of the applied field and the chemical potential as soon as there is scattering from impurities. For low T a WF law violation is possible and enhanced by the external field (Fig 7). Depending on B and T electrical conduction may dominate heat conduction or vice versa. For a sufficiently high value of the chemical potential the WF is restored even in the presence of the external field.

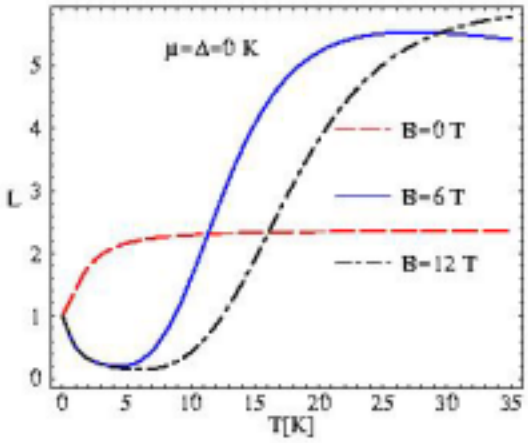

Fig.7. Normalized Lorenz number L/L_0 as a function of temperature for 3 values of the magnetic field at half-filling

References:
[1] M. Calame *et al.*, Phys. Rev. Lett. **86**, (2001) 3630.
[2] J.-P. Locquet *et al.*, Nature **394**, (1998) 453.
[3] A. Rüfenacht *et al.*, Solid-State Electr. **47**, (2003) 2167.
[4] S.G. Sharapov *et al.*, Phys. Rev. B **66**, (2002) 012515.
[5] H. Fangohr *et al.*, Phys. Rev. B **67**, (2003) 174508.
[6] M. Tesei *et al.*, in preparation.
[7] Ph. Curty and H. Beck, Phys. Rev. Lett. **91**, (2003) 257002.
[8] L. Benfatto *et al.*, submitted to Phys. Rev. B.
[9] S. G. Sharapov *et al.*, Phys. Rev. B **67**, (2003) 144509.

11. Electronic Transport in Novel Materials

Project leader: László Forró, IPMC, EPF Lausanne

Research summary: Over the past three years we investigated strongly correlated electron systems, including nanotubes, fullerides, diborides and cuprate superconductors with a large variety of experimental techniques: ESR, break-junction tunneling and transport measurements both at ambient and high pressures.

Diagonal antiferromagnetic easy axis in lightly hole doped $Y_{1-x}Ca_xBa_2Cu_3O_6$ – diagonal charge stripes?

The structure of the magnetic elementary cell is well established in $YBa_2Cu_3O_6$, the antiferromagnetic (AF) parent compound of a high temperature superconductor, but little is known about how introducing holes affects the magnetic structure. Neutron diffraction found a chessboard-like AF order in the (a,b) plane [1], which, in high purity crystals, alternates along the c direction with the periodicity of the lattice as shown in Fig. 1(a). In $YBa_2Cu_3O_{6+y}$, no hole induced change of this structure has been reported until now, while in $La_{2-x}Sr_xCuO_4$, the other well studied AF parent compound for high Tc superconductivity, hole doping changes the magnetic structure in a peculiar way [2].

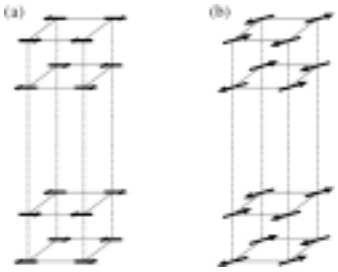

Fig.1. (a) AFI(0) is the magnetic structure of undoped $YBa_2Cu_3O_6$ at all temperatures below T_N ~ 420 K. (b) AFI(π/4) is the suggested low temperature magnetic structure of $Y_{1-x}Ca_xBa_2Cu_3O_6$.

We investigated the hole induced changes in the AF structure of a lightly Ca doped $Gd:Y_{1-x}Ca_xBa_2Cu_3O_6$ copper oxide single crystal with x~0.008 by Gd^{3+} electron spin resonance [3]. Gd replaces Y in the crystal, and it serves as a local ESR probe of the magnetic spin susceptibility and charge redistribution in the AF CuO_2 sandwich.
We were able to distinguish the ESR signal of those Gd^{3+} ions that have a first neighbor Ca^{2+} from those which are surrounded by only Y^{3+} ions as demonstrated in Fig. 2. We proved that holes do not localize to Ca^{2+} ions above 2.5 K since the charge distribution and local spin susceptibility next to the Ca^{2+} are independent of temperature. Furthermore, the local susceptibility around the Ca^{2+} ion is equal to that of the bulk AF. However, due to the extremely low doping level, this observation alone would still allow that either the holes are trapped somewhere outside the CuO_2 sandwich or that the holes are never delocalized from the Ca^{2+} ions. The magnetic behaviour of the sample implies that this is not the case.

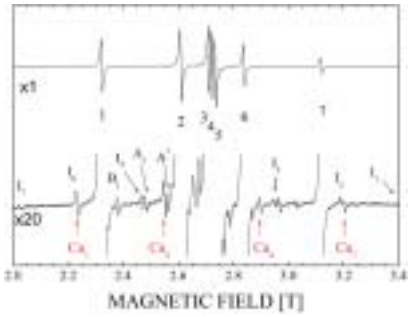

Fig.2. Assignment of lines in the ESR spectrum of $Gd:Y_{1-x}Ca_xBa_2Cu_3O_6$. "1" to "7": The main Gd^{3+} fine structure series arises from Gd^{3+} with no Ca^{2+} neighbors. "Ca1", "Ca2", "Ca6", and "Ca7" are the Ca satellite series from Gd^{3+} ions with one first neighbor Ca^{2+} ion. Other lines are independent of Ca doping. (B//c, $\omega_L/2\pi$=75 GHz and T=18 K.)

Both hole doped and pristine crystals are magnetically twinned with an external magnetic field dependent antiferromagnetic domain structure. Unlike in the undoped crystal, where the easy magnetic axis is along [100] at all temperatures, the easy direction in the hole doped crystal is along the [110] diagonal at low temperatures (Fig. 1(b)) and changes gradually to the [100] direction between 10 and 100 K.
The Ca doped crystal was prepared under the same conditions and from the same starting materials as the undoped reference sample. Point-like defects (due to Ca) cannot induce a magnetic anisotropy with such symmetry into the system. This strongly implies that the holes themselves order in such a pattern at low temperature that introduces diagonal anisotropy. The gradual appearance of the diagonal anisotropy suggests a gradual ordering of the holes, which is in good correspondence with the observed gradual freezing of the stripes at low doping in YBCO and LSCO [4].

Magnetic-field induced density of states in superconducting MgB_2 measured by CESR

The four disconnected Fermi surface sheets of MgB_2 result in unusual superconducting properties. An effective two-band model with two gaps (one for the σ-sheets and one for the π-sheets) of different magnitudes describes

well the heat capacity experiments [5, 6], as well as optical [7] and tunneling spectra [8, 9].
We used conduction electron spin resonance (CESR) spectroscopy to measure the electronic spin susceptibility, χ_s, of MgB_2 in the superconducting state as a function of magnetic field. The CESR has an advantage over measuring the NMR Knight shift: the intensity of the signal measures χ_s directly, there is no need for corrections such as the NMR chemical shift and the diamagnetic shielding of the superconductor. Also, measuring χ_s from the NMR relaxation time, T_1, is complicated by the extra relaxation caused by thermal vortex vibrations. CESR intensity is affected by the limited microwave penetration depth in a metal, and we investigate MgB_2 powders of very fine grain size (<0.5 μm) mixed with insulating SnO_2 to eliminate this effect [10].

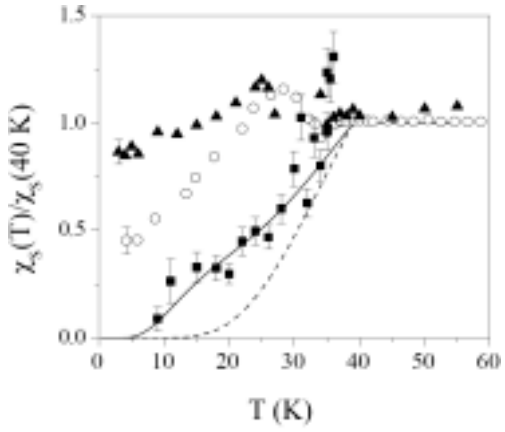

Fig.3. The temperature and magnetic field dependent spin susceptibility of MgB_2 below T_c (squares: 0.14 T, circles: 0.34 T, triangles: 1.28 T). Dashed curve: expected dependence for an isotropic s-wave BCS superconductor. Solid curve: anisotropic two-gap superconductor assuming H_{C2}^{c}=2 T and H_{C2}^{ab}=16 T.

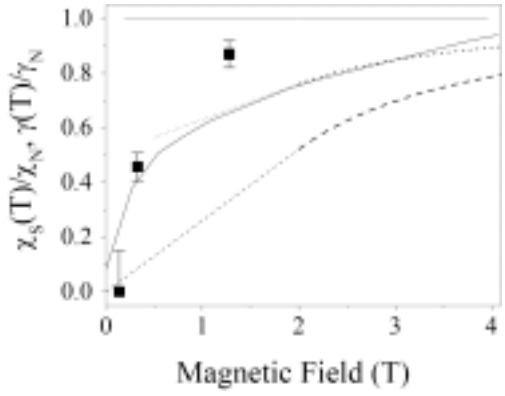

Fig.4. Comparison of the normalized χ_s/χ_N at 4 and 3 K at 0.34 and 1.28 T, respectively (squares) and the normalized specific heat coefficient γ/γ_N (solid line) at 3 K from Ref. [11]. Dashed curve: H dependent DOS for an anisotropic superconductor with H_{C2}^{c}=2 T and H_{C2}^{ab}=16 T. Dotted curve: a similar superconductor assuming that half of the DOS is restored already by applying B = 0.5 T.

The diamagnetic shift of the ESR lines below T_c confirms that we indeed observe the CESR of the superconducting MgB_2. We recorded the temperature dependence of χ_s in magnetic fields 0.14, 0.34 and 1.28 T corresponding to 3.8, 9.4 and 35 GHz ESR frequencies, respectively (Fig. 3). At the lowest field we were able to fit our data with the simple two-band model proposed by Bouquet et al. [12], while at higher fields this model was inadequate.
Ref. [8] suggests that 0.5 T already closes the gap on the π Fermi sheets. This model (dotted curve in Fig. 4) describes well the magnetic-field dependence of the electronic heat capacity, while the density of states (DOS) as measured by the CESR still varies stronger with magnetic field. This discrepancy can be resolved if we consider that the electron-phonon couplings (EPC) are different in the σ and in the π sheets: $\lambda_{\sigma\sigma}$~1 and $\lambda_{\pi\pi}$~0.45 [6]. EPC changes the effective mass of the electrons and the DOS measured by heat capacity by a factor of 1+λ. Meanwhile, the renormalization of χ_s by EPC is much weaker, since the Zeeman interaction does not influence the electronic orbitals until the LS coupling is not too strong. Since the magnetic field restores the Fermi surface at the π sheets first, where 1+λ is smaller, the electronic heat capacity is less enhanced compared to its normal state value than the spin susceptibility.

Gradual pressure-induced insulator-to-metal transition in Na_2C_{60}

Electron doped fullerenes (fullerides) are strongly correlated electron systems on the brink of a metal-insulator transition (MIT), and a fine tuning of physical parameters can push them on either side of the transition [13]. Their electronic properties are often determined by the interplay between the electron-electron and the electron-phonon interactions since the lowest unoccupied molecular orbitals of the C_{60} are threefold degenerate and they give rise to a strong Jahn-Teller (JT) effect. The on-site electron-repulsion is U = 1-1.5 eV, while the intermolecular hopping can be tuned by a hydrostatic pressure. We applied high pressure transport and high pressure electron spin resonance (ESR) measurements to investigate the nature of the metal-insulator transition in Na_2C_{60}. Na_2C_{60} is an insulator at ambient pressure with two electrons per C_{60} molecules. Its magnetism is determined mostly by the molecular singlet-triplet excitations of the C_{60}^{2-} molecule leading to a thermally activated spin susceptibility.

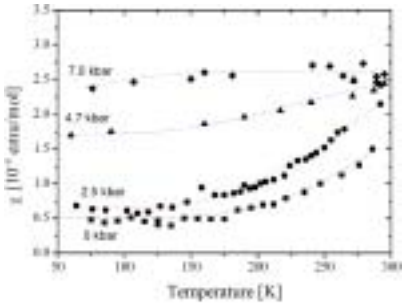

Fig.5. Spin susceptibility of Na_2C_{60} as a function of temperature, measured at various hydrostatic pressures. The pressure induces an insulator-to-metal transition. The lines are fits to equation (1).

Fig. 5 demonstrates how the pressure changes this gradually into a Pauli-like (temperature independent) behaviour by increasing the W overlap between neighboring molecules. The data can be well fit by

$$(1)\quad \chi_s(T) = N_{ST}\frac{2N_A g^2 \mu_B^{\,2}}{3k_B T}\frac{3\exp(-\Delta_{ST}/T)}{1+3\exp(-\Delta_{ST}/T)} + \chi_P$$

where N_{ST} is the proportion of the localized electrons, Δ_{ST} is the spin gap of the singlet-triplet transition, and χ_P is the Pauli contribution of the delocalized electrons, which measures the density of states at the Fermi level. (N_A is the Avogadro number, g is the electronic gyromagnetic ratio, and k_B is the Boltzmann constant.)

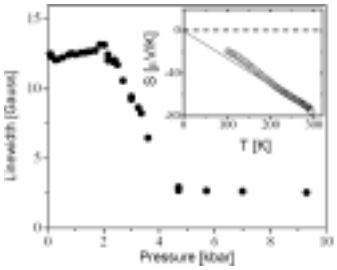

Fig.6. Na_2C_{60} ESR line width as a function of pressure at room temperature. Inset: the thermoelectric power in a pressed pellet shows that the sample is metallic at 9 kbar.

We also measured the ESR line width as a function of pressure (Fig. 6). Once the electrons delocalize, the dipolar broadening of their ESR diminishes due to motional narrowing. The inset of the figure displays the thermoelectric power at 9 kbar which also supports that the sample is metallic at high pressures. Fig. 6 demonstrates that the localization-delocalization of the electrons is gradual, contrary to the behaviour of the simple Mott-Hubbard model [14]. We believe still that the transition is of purely electronic origin, i.e. not due to a gradual structural change, e.g. polymerization: no hysteresis in the ESR was observed [15], and neutron diffraction experiments up to 4 kbar also exclude polymerization [16]. The Mott-Jahn-Teller scenario introduced by Tosatti and co-workers [17] also shares the most important features our observations.

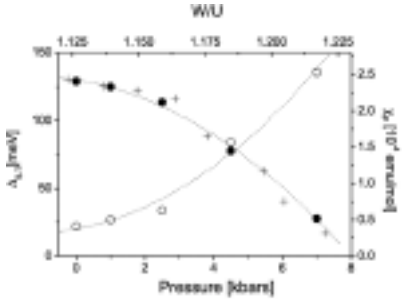

Fig.7. Pressure evolution of singlet-triplet molecular gap (closed circles, left scale) and Pauli contribution to spin susceptibility (open circles, right scale). Crosses represent the spin gap calculated by DMFT [17] with the U/W parameter mapped into pressure considering the pressure effects on the bandwidth [18]. Lines are guides for the eye.

This gives us confidence that our interpretation of the data is correct and to treat the parameters obtained by fitting Eq. (1) to the temperature dependence curves as physically meaningful. Fig. 7 shows the evolution of the singlet-triplet gap and the Pauli contribution to the susceptibility (proportional to the number of delocalized electrons) as a function of pressure. Our results are in remarkably good agreement with the Mott-Jahn-Teller model.

Effects of disorder in high T_c superconductors: break-junction tunneling study

By irradiating optimally doped BSCO 2212 with high-energy electrons we induced point defects without changing the doping. These defects reduced the T_C from the original value of 90 K to 27 K. Our finding is counterintuitive (Fig. 8): the superconducting gap did not change measurably while T_C changed by a factor of 3.

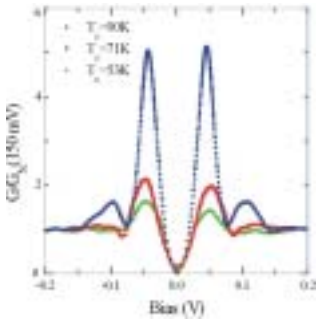

Fig.8. Normalized conductance curves of disordered but optimally doped 2212. T_C=90 K corresponds to the non-irradiated sample.

Following the theory of Emery and Kivelson [19], we interpret this as a result of fluctuations of the order parameter. Bulk superconducting transition occurs only when the order parameter has a well defined phase over the whole sample, but local and dynamic pairing

may occur already above T_C. This effect is expected to be more significant in the cuprates than in conventional superconductors because the number of overlapping Cooper pairs in the cuprates is much less due to their low charge density and short pair coherence length. Point defects seem to hinder the establishment of a global phase coherence while their pair breaking effect plays a less important role since we do not observe an appearance of a finite DOS near zero energy. [20].

Pressure dependence of the thermoelectric power of single-walled carbon nanotubes

Soon after the discovery of multi-walled carbon nanotubes and single-walled carbon nanotubes (SWNT) it was immediately realized that metallic tubes represent the ultimate one-dimensional conductor, and they generated considerable interest due to the possible realization of the Luttinger liquid (LL) behaviour in nature. Indeed, conductivity measurements performed on individual nanotubes have shown the canonical power-law behaviour of conductance as function of temperature and voltage. Thermoelectric power should also indicate whether the LL scenario is valid.

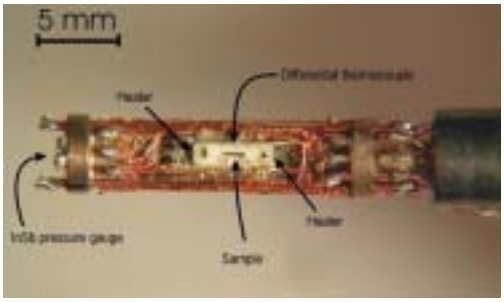

Fig.9. The sample was mounted on a home made thermopower sample holder which fits into a clamped pressure cell. The temperature gradient was generated by small metallic heaters installed at both ends of the sample, and the temperature gradient was measured with Chromel-Constantan differential thermocouple. The pressure medium used in this study was kerosene and the maximum pressure was 2.5 GPa.

In order to clarify the picture, we have made a setup (Fig. 9), which enabled us to measure thermopower and resistivity in a clamped pressure cell up to 2.5 GPa. S(T) curves at three different pressures are shown in Fig. 10. High pressure measurements helped to clarify the overall temperature dependence of S. The low temperature metallic thermopower was found to be pressure independent, the high temperature unusual TEP contribution was strongly suppressed by the application of pressure. We showed that the thermopower of our sample is due to metallic nanotubes, and we excluded non-intrinsic effects, like Kondo scattering of residual impurities or doping by adsorbed oxygen. Our results suggest that the temperature and pressure dependencies are governed by the change of population of phonons, connected with the thermal excitation of the hexagons (the building units of the SWNTs) [21].

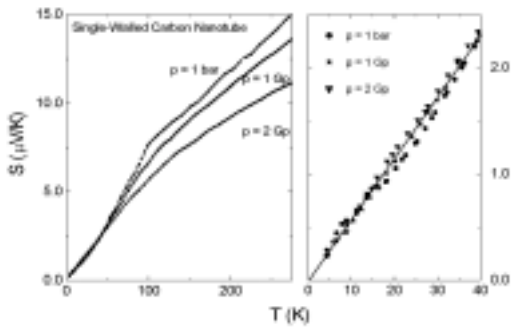

Fig.10. The thermoelectric power of SWNT at 1 bar, 10 and 20 kbar as a function of temperature. b) the low-temperature part a) enlarged.

References:

[1] J. M. Tranquada *et al.*, Phys. Rev. Lett. **60** (1988) 156.
[2] M. Matsuda *et al.*, Phys. Rev. B **62** (2000) 9148.
[3] A. Jánossy, T. Fehér and A. Erb, Phys. Rev. Lett. **91** (2003) 177001.
[4] Ch. Niedermayer *et al.*, Phys. Rev. Lett. **80** (1998) 3843.
[5] Y. Wang, T. Plackowski and A. Junod, Physica C **355** (2001) 179.
[6] A. A. Golubov *et al.*, J. Phys.: Condens. Matter **14** (2002) 1353.
[7] A. B. Kuz'menko *et al.*, Solid State Comm. **121** (2002) 479.
[8] M.R. Eskildsen *et al.*, Phys. Rev. Lett. **89** (2002) 187003.
[9] A. E. Koshelev and A. A. Golubov, Phys. Rev. Lett. **90** (2003) 177002.
[10] F. Simon *et al.*, Phys. Rev. Lett. **87** (2001) 047002.
[11] F. Bouquet *et al.*, Physica C **385** (2003) 192.
[12] F. Bouquet *et al.*, Phys. Rev. Lett. **87** (2001) 047001.
[13] L. Forró and L. Mihály, Rep. Prog. Phys. **64** (2001) 649.
[14] P. Fazekas, Lecture Notes on Electron Correlation and Magnetism (World Scientific, Singapore, 1999).
[15] S. Garaj *et al.*, Phys. Rev. B **68** (2003) 144430.
[16] T. Yildirim *et al.*, Phys. Rev. B **60** (1999) 10707.
[17] M. Capone *et al.*, Science **296** (2002) 2364.
[18] S. Satpathy *et al.*, Phys. Rev. B **46** (1992) 1773.
[19] V. J. Emery and S. A. Kivelson, Nature **374** (1995) 434.
[20] R. Gaál et al., submitted for publication.
[21] N. Barišić et al., Phys. Rev. B **65** (2002) 241403(R).

12. High-Resolution Photoemission of High-Temperature Superconductors and other Low-Dimensional Correlated Systems

Project leader: Giorgio Margaritondo, EPF Lausanne

Research summary: i) We performed milestone ARPES experiments on LSCO thin films: we find that unstrained films are identical to single crystals, but our results on strained films question common theoretical models; ii) High-resolution ARPES on the layered material *1T*-$TaSe_2$ clarifies the mechanism behind the metal-insulator Mott transition; iii) We probed the bulk electronic properties of correlated systems by resonant photon in - photon out spectroscopies; and iv) we made available new high-quality single crystal specimens to all MaNEP groups.

Thin films

We have developed a laser deposition (PLD) system at the Wisconsin Synchrotron Radiation Center (SRC), and optimized thin film growth and transfer procedures to perform *in-situ* angle-resolved photoemission (ARPES) investigations of high temperature superconductors. Such measurements not only make the study of non cleavable materials possible, but also yield new insights into the properties of the superconducting cuprates [1].

Taking advantage of the unique *in-situ* preparation facility, we set out to perform a systematic ARPES study of ultra-thin (<30nm) superconducting cuprate films. We put special emphasis on the role of strain and its influence on electronic properties. In-plane compressive strain is known to increase the critical temperature (T_c) of high temperature superconductors, and is obviously related to the mechanism of high-T_c superconductivity. The phenomenon is quite dramatic in $La_{2-x}Sr_xCuO_4$ (LSCO) thin epitaxial films: for x = 0.1, T_c doubles with respect to relaxed LSCO (and increases by a factor of five with respect to films with in-plane tensile strain). The published theoretical studies predicted the in-plane compressive strain to flatten the bands. This could provide a simple explanation for the dramatic T_c-increase, since band flattening implies an enhanced density of states (DOS) near the Fermi energy, (E_F).

However, our first direct angle-resolved photoemission spectroscopy (ARPES) study on strained LSCO films flatly contradicts [2,3] this picture by revealing a dispersing band that crosses E_F (see Figure 1). Our experimental results thus directly impact models dealing with the influence of pressure on superconducting properties. The justification of strain effects must be sought beyond the band flattening framework. Furthermore, measured T_c's of 20K (underdoped (UD); 24K in overdoped (OD)) in unstrained, and 40K in compressively strained LSCO films (OD and UD) directly scale with measured apical oxygen distances and indicate that the out-of-plane contributions play an important role.

Further studies are underway on the role of tensile strain on the electronic properties of our LSCO films. Since our demonstration of successful direct photoemission spectroscopy on thin cuprate films, this approach is now being pursued by leading groups worldwide. Our LSCO films were also successfully used in femtosecond spectroscopy studies.

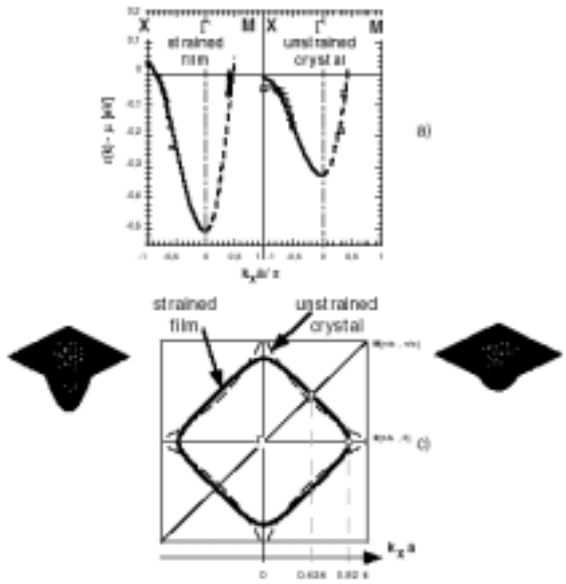

Figure 1: (a) Fits of band dispersion for a strained film (left) and for an unstrained single crystal (right), [data from Fujimori's group] along Γ-X and Γ-M. Tight binding best-fit of the dispersion are shown for an optimally doped in-plane compressed film (left) and for an unstrained optimally doped single crystal (right). (c) Schematic illustration of changes in the Fermi surface topology.

High-resolution spectroscopies

High-energy spectroscopies play an important role in the investigation of strong correlations in solids. This is true in particular for high-resolution ARPES which, thanks to its momentum selectivity, provides us with a direct image of the properties of the fundamental *quasiparticle* (QP) excitations. ARPES is also an invaluable probe of the broken-symmetry ground states which are generated by strong correlations, especially in reduced dimensions.

Quasi one-dimensional systems

Quasi-one dimensional (1D) conductors are interesting as the most likely candidates to exhibit signatures of non-Fermi liquid (Tomonaga-Luttinger or Luther-Emery or polaronic) ground states. They also exhibit a characteristic tendency to form low-temperature non-metallic ground states. We have investigated the spectral signatures of the metal-insulator Peierls transition in typical 1D materials like $(TaSe_4)_2I$ and $(NbSe_4)_3I$ [4,5]. We find that the ARPES band dispersion is generally consistent with a weak-coupling scenario of the transition, based on the concept of Fermi surface *nesting*.

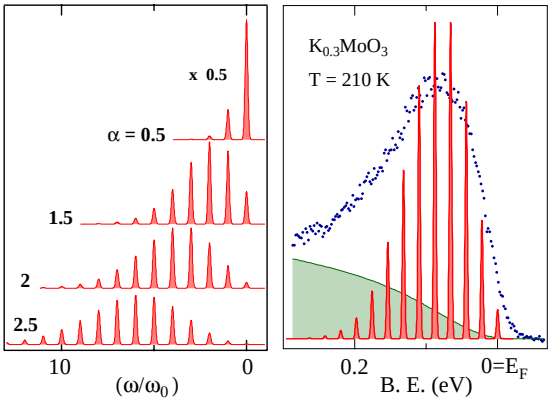

Fig. 2. The ARPES spectrum of the 1D compound $K_{0.3}MoO_3$ measured at the Fermi surface in the metallic state (right) is compared with the spectral function of a single electron coupled to a harmonic oscillator. The left panel illustrates how the lineshape evolves with the coupling strength.

However, the spectral lineshapes, both in the normal metallic or in the insulating state, are incompatible with a standard description in terms of weakly interacting quasiparticles. This is illustrated by the spectrum of $K_{0.3}MoO_3$, measured at the Fermi surface (Fig. 2). Instead of the expected sharp QP peak, one observes a broad maximum and a reduced spectral weight near E_F. We suggest that the coherent QP weight is suppressed by strong interactions between the electrons and the lattice, the same interactions that are responsible for the Peierls transition in this and similar 1D materials. Due to the strong interactions, the spectral function is essentially incoherent. In this scenario, the QPs are small polarons, i.e. electrons heavily dressed by a phonon cloud, and move coherently with the local lattice deformation. Interestingly, the large breadth of the corresponding momentum-distribution-curves suggests a short coherence length for the QPs (λ~10 Å), of the order of the charge-density-wave period. This interpretation is supported by the calculated spectral lineshapes of an electron strongly coupled to a harmonic oscillator (Fig. 2, left panel), which provides a schematic approach to the small polaron problem.

Strong correlations in two dimensions

The metal-insulator (M-I) Mott transition is one of the most typical and intensely studied manifestation of correlations. Nevertheless, fundamental questions about the changes of the electronic structure which lead to the disappearance of the Fermi surface and the opening of an energy gap, remain open. Our recent ARPES experiment on the quasi two-dimensional compound *1T*-$TaSe_2$ [3] shed new light on this important issue. In this material the conduction bandwidth (W) is controlled by a modulation of the atomic distances associated with a temperature-dependent charge-density-wave (CDW). At the surface, the ratio (W/U) between the bandwidth and the local Coulomb repulsion reaches a critical value at T_C ~260 K. Below T_C the metallic state is unstable, and a *bandwidth-controlled* (M-I) *surface* Mott transition to a correlated insulator ensues. Interestingly, the bulk remains metallic, as a result of the larger coordination and more efficient screening.

Changes of the electronic structure across the transition can be followed in great detail by high-resolution ARPES. The spectra of Fig. 2 were measured at the Fermi surface, and symmetrized around E_F in order to remove spurious temperature effects due to the Fermi-Dirac distribution. Well into the metallic phase (300 K) a weak and sharp peak at E_F identifies the QP, but a large part of the spectral weight is in the incoherent sideband at ~ -0.3 eV, consistent with the "poor metal" character of the material, and with a strong *e-ph* coupling.

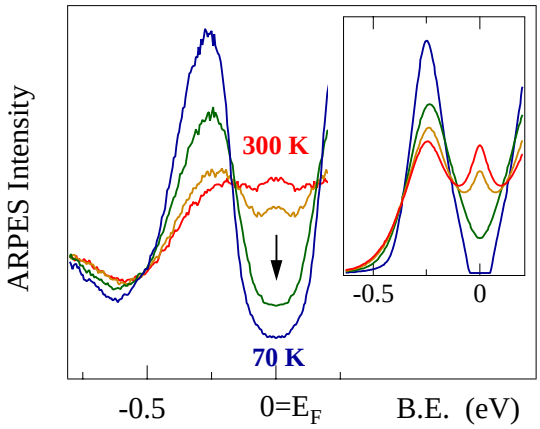

Fig. 3. Symmetrized ARPES spectra of the 2D CDW system 1T-$TaSe_2$, measured across a surface Mott transition at the Fermi surface. Sharp Hubbard subbands emerge at the lower temperatures from the broad incoherent sidebands, while the QP peak at E_F is suppressed and a correlation gap opens. The inset shows the results of a DMFT calculation.

At lower temperatures the spectra illustrate the disappearance of the QP and the opening of a correlation gap, with sharp Hubbard subbands growing out of the incoherent background which characterizes the metallic phase. The evolution of the ARPES spectra qualitatively reproduces the spectral changes predicted by a state-of-the-art calculation performed within the Dynamic Mean-Field Theory (DMFT) with appropriate parameters. This remarkable agreement provides the first *direct* experimental confirmation of an important and general theoretical paradigm for strongly correlated systems.

Novel spectroscopies

In the previous example the large surface sensitivity of ARPES represents a considerable advantage. When, on the other hand, a true bulk information is necessary, photon in - photon out techniques are more appropriate. Moreover, resonant X-ray spectroscopies provide local, orbital selective information on the electronic states. Such novel synchrotron-based techniques are now available at the ESRF (Grenoble) and will be implemented in the future at the Swiss Light Source (SLS). By Resonant Inelastic X-ray Scattering (RIXS) - the X-ray analogue of resonant electronic Raman spectroscopy - the signatures of specific electronic configurations can be selectively enhanced. This is schematically illustrated in Fig. 4 for the important case of an intermediate valence (IV) system.

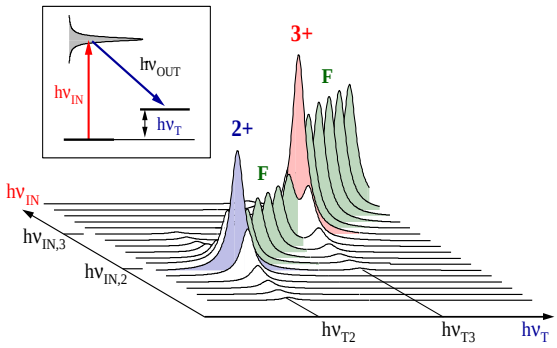

Fig 4. Schematic view of a RIXS experiment on an intermediate valence (2+, 3+) Yb system. The total-energy level scheme of the inset illustrates the resonant absorption and emission processes. In the main figure, the RIXS spectral function is shown in the two-dimensional $h\nu_{in}$ - $h\nu_{out}$ plane. Resonances are clearly identified.

The possibility of varying both the incident and emitted energies, literally adds a new dimension, from which precious information can be gained. We have exploited these features to demonstrate the existence of a spectroscopic small-energy Kondo scale in (IV) Yb compounds [6], thus solving a long-standing controversy. We also used RIXS to determine how the Yb valence changes under pressure in $YbAl_2$ [7] and in other selected IV systems. RIXS is also a powerful probe of the local *d-d* (crystal field) excitations, e.g. in the cuprates [8]. These *neutral* excitations are not accessible by photoemission, nor by optical measurements since they are forbidden by dipole selection rules. RIXS therefore opens a new window on strongly correlated materials

Crystal growth

Our laboratory produces a broad range of high-quality single crystals, grown from vapour or liquid phases. These specimens are characterized at EPFL, and made available to all member groups of MaNEP, and to collaborating groups abroad, for transport, magnetic, STM, thermodynamic, optical, and spectroscopic studies.

Fig. 5. High quality single crystals grown in the EPFL laboratory.

We mention here only a few representative materials:

- Superconducting cuprates:

- $Bi_2Sr_2CaCu_2O_{8+x}$, $Bi_2Sr_2Ca_{1-x}Pr_xCu_2O_{8+x}$, $Bi_{2-x}Pb_xSr_2CaCu_2O_{8+x}$, $Bi_{2-x}Pb_xSr_2Ca_{1-x}Y_xCu_2O_{8+x}$ (x = O.1-O-8),
- $RuSr_2GdCu_2O_{8+\delta}$, $RuSr_2GdCu_{2-x}Li_xO_{8+\delta}$;

- 1D systems:

- $TaSe_3$, $NbSe_3$, $ZrSe_3$ with dimensions compatible with ARPES and optical measurements;
- $Cu_2Te_2O_5X_2$ (X=Cl,Br) quantum spin systems;
- $BaVS_3$, and substitutional alloys, which exhibit interesting magnetic transitions and non-Fermi liquid behaviour under pressure;
- LiV_2O_4 with puzzling heavy-fermion behaviour;
- V_6O_{13} which exhibits mixed valence, M-I and magnetic transitions.

- 2D systems:

- $1T\text{-}TaS_2$, $1T\text{-}TaSe_2$, $2H\text{-}NbSe_2$ $2H\text{-}TaSe_2$ with rich CDW phase diagrams and the interplay of electronic correlations.
- Na_xCoO_2, charge-ordered, it exhibits superconductivity in two-dimensional CoO_2 layers when intercalated with H_2O.
- $KFeS_2$, $CsFeS_2$, Fe_xTaSe_2, CuV_2S_4, CoS_2 and $CoSe_2$

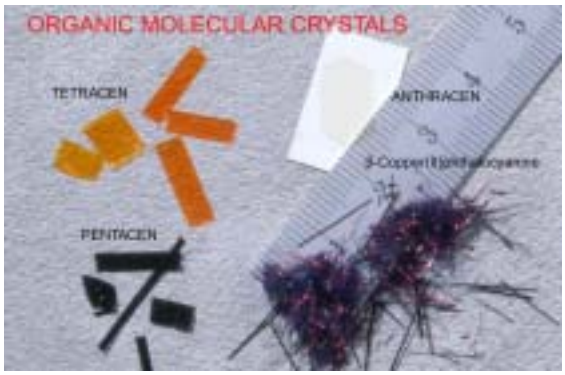

Fig. 6. Large organic single crystals grown at EPFL are also available to all MaNEP members.

- Molecular crystals:

- Pentacene, Tetracene, . β-Cu(II) phthalocyanine.

- Other strongly correlated materials:

- $CuSb_2O_6$, $CaRuO_3$, MoO_3, WO_3, $La_2Li_{0.5}Cu_{0.5}O_4$, CuO, $Na_{0.7}CoO_2$

References:

[1] M. Abrecht *et al.*, J. Appl. Phys. **91**, 1187 (2002).
[2] M. Abrecht *et al.*, Phys. Rev. Lett. **91**, 057002 (2003).
[3] M. Abrecht *et al.*, Int. J. Mod. Phys. B **17**, 3449 (2003).
[4] L. Perfetti *et al.*, Phys. Rev. Lett. **87**, 216404 (2001).
[5] L. Perfetti *et al.*, Phys. Rev. B **66**, 075107 (2002).
[6] C. Dallera *et al.*, Phys. Rev. Lett. **88**, 196403 (2002).
[7] C. Dallera *et al.*, Phys. Rev. B **68**, 245114 (2003).
[8] G. Ghiringhelli *et al.*, submitted to Phys. Rev. Lett.

13. Probing Microscopic Magnetic Properties of Materials with Novel Electronic Properties with Muons

Project leader: Hugo Keller, University of Zurich

Research summary: Detailed studies of the oxygen-isotope ($^{16}O/^{18}O$) effect (OIE) and the site-selective oxygen isotope effect (SOIE) on the in-plane penetration depth $\lambda_{ab}(0)$ in $Y_{1-x}Pr_xBa_2Cu_3O_{7-\delta}$ by means of low-energy and bulk muon-spin rotation (μSR) are presented. Substantial isotope effects are observed, indicating strong coupling of the electronic subsystem to the lattice. We also started investigations of the tri-layer structure $YBa_2Cu_3O_7/PrBa_2Cu_3O_7/YBa_2Cu_3O_7$. Preliminary results point to a possible coupling of two superconducting YBCO layers via the antiferromagnetic $PrBa_2Cu_3O_7$ layer. In order to investigate the fundamental physical properties of low-energy muons in condensed matter in more detail we performed first test measurements in high-quality semi-insulating silicon.

Direct observation of the oxygen isotope effect on the in-plane magnetic penetration depth in optimally doped $YBa_2Cu_3O_{7-\delta}$

More than 15 years after the discovery of the cuprate high-temperature superconductors (HTS), the fundamental interactions responsible for pairing are still not understood. A direct way to explore the role of the electron-phonon interaction in HTS is to investigate the isotope effect on the in-plane penetration depth λ_{ab} [1,2]. We used the advantages of the low-energy μSR (LEμSR) technique, developed recently at the Paul Scherrer Institute (PSI) [3], for the direct measurement of the oxygen isotope ($^{16}O/^{18}O$) effect (OIE) on λ_{ab} in optimally doped $YBa_2Cu_3O_{7-\delta}$ films [4].

The principle of λ determination by using LEμSR is shown schematically in Fig. 1. Low-energy muons of tuneable energy can be implanted at a different and controllable depth *z* beneath the surface of the superconductor in the Meissner state. Due to the random nature of the muon scattering process, the implantation depths are distributed over a nanometer scale, and the implantation depth profile *n(z)* depends on the muon energy [Fig. 1(a)]. Knowing the value of the mean implantation depth $\bar{z}$ the magnitude of the local field $B(\bar{z})$ is obtained from the muon spin precession frequency using μSR.

The measurements of the in-plane magnetic penetration depth λ_{ab} were performed on a 600nm thick epitaxial $YBa_2Cu_3O_{7-\delta}$ film in the Meissner state. A weak external magnetic field of 9.2mT was applied parallel to the sample surface after the sample was cooled in zero magnetic field from a temperature above T_c to 4K. In this geometry (the thickness of the sample is negligible in comparison with the width), currents flowing in the *ab*-planes determine the magnetic field profile along the crystal *c*-axis inside the film [see Fig. 1(b)]. Spin-polarized muons were implanted at a depth ranging from 20-150nm beneath the surface of the film by varying the energy of the incident muons from 3 to 30keV. The muon implantation depth profile *n(z)* for the given implantation energy was calculated using a Monte-Carlo code TRIM.SP [5]. The reliability of the calculated *n(z)* was crosschecked by previous LEμSR experiments on thin metal layers [6].

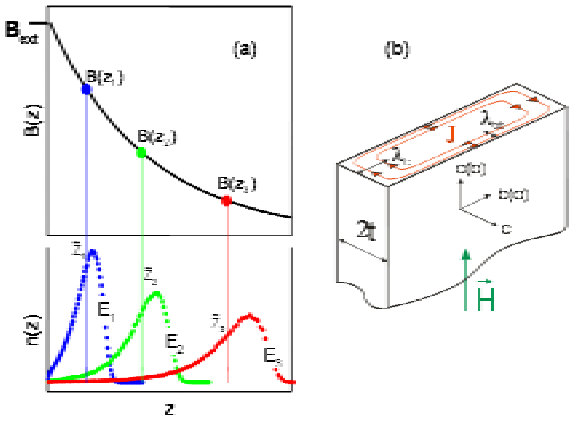

*Fig.1. (a) The principle of λ determination using LEμSR. By tuning the energy E of the incident muons they are implanted at controllable distances $\bar{z}$ beneath the surface of the superconductor in the Meissner state. The local magnetic field $B(\bar{z})$ is determined from the muon precession frequency using μSR. (b) Schematic distribution of the screening current in a thin anisotropic superconducting slab of thickness 2t in a magnetic field applied parallel to the flat surface. The screening current **J** flows preferably parallel to the ab-planes, giving rise to an exponential field decay along the crystal c-axis. Due to twinning in the ab-plane (a and b axes are not distinguishable) the so called in-plane magnetic penetration depth λ_{ab} is measured.*

For each implantation energy the average value of the magnetic field $\bar{B}$ and the corresponding average value of the stopping distance $\bar{z}$ were extracted. The value of $\bar{B}$ was taken from the fit of the μSR time spectrum assuming a Gaussian relaxation function. The value of $\bar{z}$ was taken as the first moment of the emulated *n(z)* distribution. Results of this analysis for the ^{16}O and ^{18}O substituted $YBa_2Cu_3O_{7-\delta}$ films are shown in Fig. 2. The data points for the ^{18}O film are systematically higher than those for the ^{16}O

film, showing that $^{16}\lambda_{ab} < {}^{18}\lambda_{ab}$. The solid lines represent a fit to the $B(\bar{z})$ data by the function:

$$B(z) = \cosh[(t-z)/\lambda_{ab}]/\cosh(t/\lambda_{ab}) \quad (1)$$

where $B(0)$ is the field at the surface of the superconductor, and $2t$ is a film with thickness. Fits with Eq. (1) to the extracted $^{16}B(\bar{z})$ and $^{18}B(\bar{z})$ yield $^{16}\lambda_{ab}(4K)=151.8(1.1)$nm and $^{18}\lambda_{ab}(4K)= 155.8(1.0)$nm. Taking into account a ^{18}O content of 95%, the relative shift was found to be $\Delta\lambda_{ab}/\lambda_{ab}=2.8(1.0)\%$ at 4K.

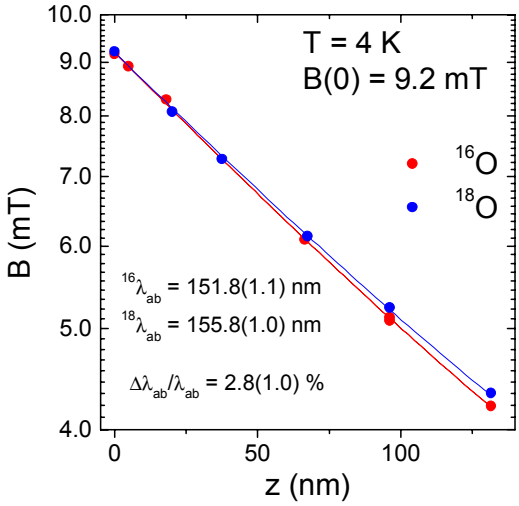

Fig.2. Magnetic field penetration profiles B(z) on a logarithmic scale for a ^{16}O substituted (red circles) and a ^{18}O substituted (blue circles) $YBa_2Cu_3O_{7-\delta}$ film measured in the Meissner state at 4K and an external field of 9.2mT, applied parallel to the surface of the film. The data are shown for implantation energies 3, 6, 10, 16, 22, and 29keV starting from the surface of the sample. Solid curves are best fits by Eq.(1).

To confirm that the observed OIE on λ_{ab} is intrinsic, additional measurements of the Meissner fraction in fine powder samples with an average grain size compatible to λ_{ab} were performed. Analyzing the data using the procedure described in Ref. [1] gives $\Delta\lambda_{ab}/\lambda_{ab}=2.7(1.0)\%$, in agreement with the LEμSR results.

It was pointed out [1,2,4,7,8] that the OIE on λ_{ab} arises mainly from the oxygen-mass dependence of the in-plane effective mass m^*_{ab}. Therefore, our finding implies that even in optimally doped HTS for which only a small isotope effect on T_c is observed, the supercarriers are strongly coupled to the lattice.

Site-selective oxygen isotope effect on the in-plane magnetic penetration depth in $Y_{0.6}Pr_{0.4}Ba_2Cu_3O_{7-\delta}$

The observation of an OIE on λ_{ab} in HTS indicates an unusual (e.g., non-adiabatic) coupling of the electrons to phonon modes involving the movement of the isotope substituted atoms. It is important to identify the relevant phonon modes responsible for this effect. This can be achieved by investigating the site-selective oxygen-isotope effect (SOIE). We used transverse-field μSR to study SOIE on T_c and λ_{ab} in underdoped $Y_{0.6}Pr_{0.4}Ba_2Cu_3O_{7-\delta}$ powder samples [9].

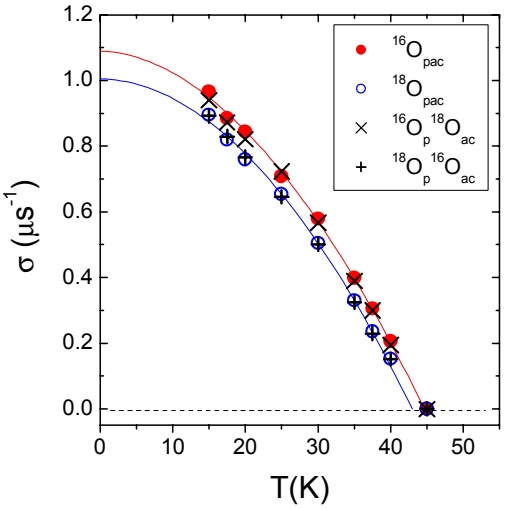

Fig.3. Temperature dependence of the depolarization rate σ in site-selective $Y_{0.6}Pr_{0.4}Ba_2Cu_3O_{7-\delta}$ samples (200mT, FC). The solid lines correspond to fits to the power law $\sigma=\sigma(0)(1-T/T_c)^n$ for the $^{16}O_{pac}$ and $^{18}O_{pac}$ samples.

In order to prepare oxygen site-selective samples a two-step exchange process was applied [9-11]. The following site-selective samples were prepared: $^{16}O_{pac}$, $^{18}O_{pac}$, $^{16}O_p{}^{18}O_{ac}$, and $^{18}O_p{}^{16}O_{ac}$ where indexes *p*, *a* and *c* denote planar (within CuO_2 planes), apical and chain oxygen, respectively. The site-selectivity of the oxygen exchange was checked by Raman spectroscopy confirming that the site-selective oxygen substitution is almost complete in all the samples.

The μSR measurements were performed at PSI using the πM3 beam line. The samples were cooled from far above T_c in a magnetic field of 200mT. In a highly anisotropic layered superconductor the in-plane penetration depth λ_{ab} can be extracted from the muon-spin depolarization rate $\sigma(T) \propto 1/\lambda_{ab}^2$ which probes the second moment of the probability distribution of the local magnetic field function $p(B)$ in the mixed state [12].

The depolarization rate σ was extracted from the μSR time spectra using a Gaussian relaxation function [12]. Figure 3 shows the temperature dependence of σ for the $Y_{0.6}Pr_{0.4}Ba_2Cu_3O_{7-\delta}$ site-selective samples. It is evident that a remarkable oxygen isotope shift of T_c as well as of σ is present. More importantly, the data points of the site-selective $^{16}O_p{}^{18}O_{ac}$ ($^{18}O_p{}^{16}O_{ac}$) samples coincide with those of the $^{16}O_{pac}$ ($^{18}O_{pac}$) samples.

Therefore, our results show unambiguously that the OIE on both the transition temperature T_c and the in-plane magnetic penetration depth λ_{ab} comes from the oxygen *within the superconducting CuO_2 planes* and not from the apical and chain oxygen. Noting that the lattice parameters remain essentially unaffected by the isotope substitution [13], our results show the existence of a strong coupling of the electronic subsystem to phonon modes involving movements of the oxygen atoms in the CuO_2 plane, while suggesting that modes involving apical and chain oxygen are less strongly coupled to the electrons.

Low energy muon study of a $YBa_2Cu_3O_7$/ $PrBa_2Cu_3O_7$/ $YBa_2Cu_3O_7$ tri-layer

There are several motivations behind the study of high-T_c multilayered structures. First, there is a technological need for heterostructures containing superconductors and insulating (or metallic) layers, for instance in the fabrication of Josephson and proximity effect junctions. Second, multilayers have in the past been demonstrated to be very powerful tools for studying the basic physics of semiconductors [14] and metals [15].

We started the project with the simplest system of a 33nm/50nm/115nm YBCO/PBCO/YBCO structure grown at the University of Geneva. Our first μSR measurements in zero magnetic field taken at 25K are presented in Fig. 4. Implantation energies of incoming muons were tuned to stop most of the muons in the appropriate layer (3keV/12.5keV/30keV). In the top YBCO layer, we observed a slow relaxing signal (due to the copper nuclear moments). Nice precession seen in the intermediate layer, corresponding to a local field B_{int} ~ 15mT at the muon site, indicates that PBCO is in a antiferromagnetic state [see Fig. 4(b)]. We see no significant change in B_{int} at 110K (which is above the superconducting transition for bulk YBCO) and at 5K (which is well below T_c). The value observed is similar to the internal magnetic field known for the bulk PBCO at 100K. A small precession signal seen in the spectrum measured at 30keV corresponds to the small part of the muons which are still stopped in the antiferromagnetic intermediate layer; most of the muons stop inside the last YBCO layer and give rise to the slow relaxing signal. The zero field measurements confirmed good quality of the tri-layer and demonstrate the capability of the LEμSR technique.

We also started measurements in a weak ($H<H_{C1}$) external field applied parallel to the surface of the tri-layer. A preliminary analysis shows that the magnetic field measured inside both of YBCO layers is screened better than if it is estimated for separated YBCO layers in the Meissner state. This finding requires further experimental study. In particular we are planning experiments in thin films of PBCO and YBCO.

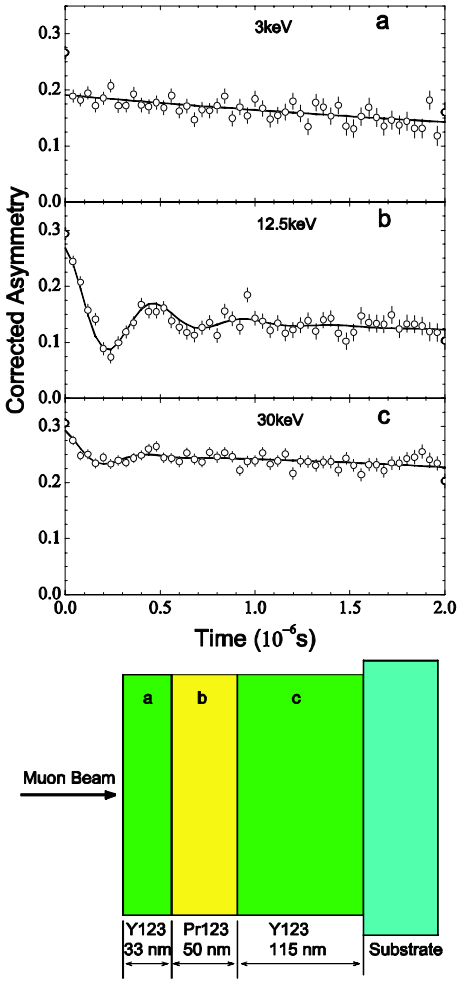

Fig. 4. Experimental μSR spectra measured at T=25K in zero magnetic field in: a) first $YBa_2Cu_3O_7$ layer; b) intermediate $PrBa_2Cu_3O_7$ layer; c) second $YBa_2Cu_3O_7$ layer.

Low energy muon study of muon/muonium states in semiconductors

Understanding the fundamental physical properties of matter at a microscopic level enables the extension of existing technologies and leads to the development of reliable new materials for tomorrow's applications. Researchers generally use the μSR technique to tackle fundamental problems in condensed matter physics that one cannot investigate by other means.

However, when employing standard μSR to study physical phenomena of the interest, one should always bear in mind that measurements start just after the injection of an energetic (several MeV) muon (μ^+) into the

sample. In early μSR experiments it was acceptable to consider the stopped muon separately from it's own track products. During the last decade, however, μSR experiments in electric fields have shown that in condensed samples the stopped muon is very close to (at distances less than 100nm) or even surrounded by its own track products. It is extremely important to check this scenario while using the LEμSR technique, which now becomes an instrument to study near-surface phenomena. Semiconductors are materials with very high electron mobility, moreover due to the technological progress they can be produced with extremely high purity (and controlled impurity content), they can be very good characterized with common techniques and are well studied by standard (high implantation energy) μSR. That is why semiconductors are the most suitable samples to test muon-track interaction in LEμSR technique.

The electronic structure and dynamics of isolated atomic hydrogen (H) in semiconductors and insulators is of fundamental interest, since it is the simplest and the lightest interstitial impurity. To obtain an atomistic picture of the isolated hydrogen centres, studies of the analogous states of muonium (Mu = μ^++e^-) are at a considerable advantage in terms of sensitivity, selectivity and timescale. The usage of LEμSR opens a unique opportunity to study *a single isolated* H (Mu) atom near the surface of a semiconductor.

On the other hand, the process of muonium formation is relevant to the process of the electron capture by an isolated trapping center. This phenomenon of delayed muonium formation is very sensitive to the electron mobility and, thus, opens the possibility to study excess electron transport to the attractive center near a semiconductor interface.

This year we performed the first test experiment in a semi-insulating Si sample. We measured weak transverse magnetic field (5mT) temperature scans with different muon implantation energies: 2keV (which corresponds to the implantation depth of 18nm), 9.4keV (66nm), 23.4keV (187nm) and 30keV (259nm). The part of the muons which does not form muonium (the so-called diamagnetic fraction) is shown in Fig. 5. For the comparison, we also plotted the diamagnetic fraction measured in a similar sample with high-energy muons. At high temperature, where there are intrinsic electrons around the muon, one can clearly see that the diamagnetic fraction is energy independent. Data start to deviate at T<225K. The low energy points are systematically higher. One can estimate the characteristic energy (penetration depth) where the high and slow energy pre-history of the incoming muon becomes indistinguishable to be ~10keV (70nm). At low temperatures, thermally activated carriers are frozen and muonium formation is possible with the muon's own track electrons only. The lack of the track electrons may result in the big free muon fraction seen at 2keV. An alternative explanation implies the track electron transport to the surface of the sample. To test this idea, LEμSR experiments with electrics fields are planned in the next beam period.

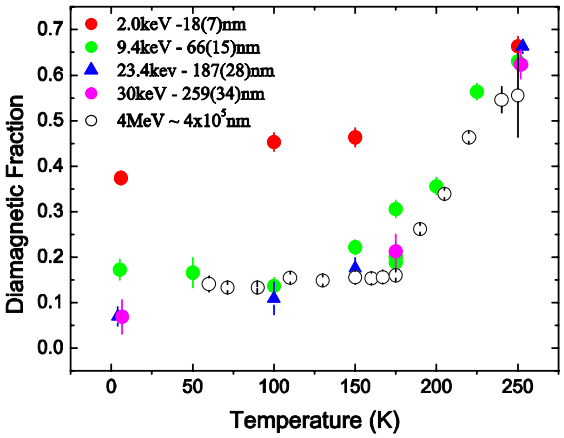

Fig.5. Temperature dependence of the diamagnetic fraction formed by muons with different implantation energies in semi-insulating Si: 2keV – red circles; 9.4keV – green circles; 23.4keV – blue triangles; 30keV – magenta circles. Open circles represent bulk μSR measurements with the energy for incoming muons of about 4MeV. Appropriate penetration depth is listed in the insert.

References:

[1] G.M. Zhao *et al*., Nature (London) **385**, (1997) 236.
[2] J. Hofer *et al*., Phys. Rev. Lett. **84**, (2000) 4192.
[3] E. Morenzoni *et al*., J. Appl. Phys. **81**, (1997) 3340.
[4] R. Khasanov *et al*., Phys. Rev. Lett. **92**, (2004) 057602.
[5] W. Eckstein, *Computer Simulations of Ion-Solid Interctions* (Springer-Verlag, Berlin, 1992).
[6] E.Morenzoni *et al.*, Nucl.Instrum.Methods B, **192**, 254 (2002).
[7] G.M.Zhao *et al*., J. Phys.: Condens Matter **10**, (1998) 9055.
[8] R. Khasanov, *et al*., J. Phys.: Condens Matter **15,** (2003) L17.
[9] R. Khasanov *et al*., Phys. Rev. B **68**, (2003) 220506.
[10] D. Zech, *et al*., Nature (London) **371**, (1994) 681.
[11] K. Conder, Mater. Sci. Eng. **R32**, (2001) 41.
[12] P. Zimmermann, *et al*., Phys. Rev. B **52**, (1995) 541.
[13] F. Raffa, *et al*., Phys. Rev. Lett. **81**, (1998) 5912.
[14] L. Esaki in *Synthetic Modulated Structures*, ed. by L.L. Chang and B.C. Giessen (Academic Press, New York, 1985), ch. 1.
[15] C.M. Falco and I.K. Schuller in *Synthetic Modulated Structures*, ed. by L.L. Chang and B.C. Giessen (Academic Press, New York, 1985), ch. 9,10.

14. Geometrical and Electronic Structure at and Near Surfaces of Materials with Novel Electronic Properties

Project leader: Philipp Aebi, University of Neuchâtel

Research summary: Two material systems have been studied with angle-resolved photoemission: (1) Ultra-thin ferroelectric films on the atomic scale. Using X-ray photoelectron diffraction we have made it possible to access films that are too thin to be identified for their ferroelectric polarization by other methods so far. Indeed we find films of 60Å to be polarized, representing a film thickness close to the theoretical limit for ferroelectricity to persist. (2) The low-dimensional, layered transition-metal chalcogenides (TMCs) with charge density waves (CDWs). These "conventional" materials are interesting to compare with "unconventional" high temperature superconductors (HT_c's). For instance, the TMC 1*T*-TaS_2, as the HT_c's, also exhibits a pseudogap which could be identified as due to the CDW. Furthermore, these quasi two-dimensional materials are interesting since it is still unclear what is at the origin of the CDW. The much-claimed "Fermi surface nesting" does not appear as the dominant mechanism.

Thin perovskite films

From a fundamental point of view, ferroelectricity has long been seen as a *collective* phenomenon suggesting that a relatively large critical volume of aligned dipoles is necessary to stabilize the ferroelectric phase. As a consequence, it has been predicted that the stability of the ferroelectric phase should be altered in small particles and very thin films. Recent *ab-initio* calculations performed on $BaTiO_3$ perovskite thin films predict the loss of ferroelectric properties below a critical thickness of 24 Å [1]. For advanced memories and integration of ferroelectrics in microelectronic devices as well as from a fundamental point of view, this question of finite size effect in ferroelectrics is an important issue. At the same time probing ferroelectricity in very thin films is challenging since a technique sensitive to a few unit cells is required.

In this project we have shown that X-ray photoelectron diffraction (XPD), already known as an important tool for surface structure analysis, is useful to address the problem of ferroelectricity in ultra-thin films. [2] In particular, we have studied ultra-thin epitaxial *c*-oriented $PbTiO_3$ (PTO) films grown in Geneva (J.-M. Triscone). The two "up" and "down" equivalent and electrically switchable states are characterized by the corresponding displacements of the Ti and O atoms in the unit cell delimited with Pb atoms (Fig. 1). For the data analysis and simulation of the experiment we have used multiple scattering calculations.

During transfer from the growth chamber to the XPD experiment the samples were exposed to air. Nevertheless, no surface cleaning procedure was applied before the measurements. Despite the presence of surface contamination, we obtain well-defined diffraction patterns.

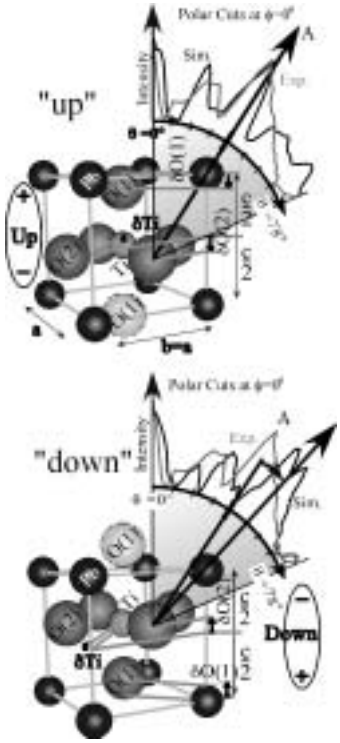

Fig.1. Structures for PTO corresponding to the "up" and "down" states. Cell parameters are a=3.902 Å and c=4.156 Å. The displacements, in fractional units, from cubic phase sites are, δTi=0.0377 for titanium, δO(1)=0.1118 for the first oxygen type (alternating along the c axis with the titanium) and δO(2)=0.1174 for the second oxygen type (in the vertical Pb plane), according to literature. The polarization is induced by electric dipoles originating from the different shifts of the titanium and the oxygen atoms. A sketch of polar cuts extracted from Fig.2 is included.

A 2π emission-angle intensity scan of a given X-ray photoemission line permits the determination of the local geometry around the selected atom. The angular dependence of the collected electron intensity originates from the interference of the directly emitted photo-electron wave and the scattered electron waves. XPD being sensitive at an atomic scale, it can therefore be used to analyze crystal structures down to the monolayer and,

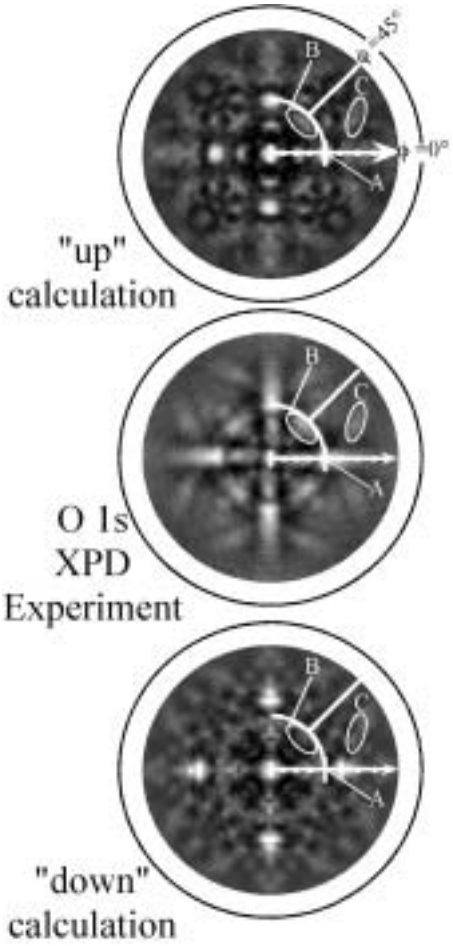

Fig.2. MgK$_\alpha$ excited O 1s photoelectrons at E$_{kin}$=724.1 eV. Simulated diffractograms for PTO "up" (top) and "down" (bottom) state plotted in stereographic projection. The corresponding structures are shown in Fig.1. Experimental result (center) for a c-axis oriented PTO 60 Å-thin film deposited on SrTiO$_3$ (Nb doped, 0.2%). Cell parameters are indicated in Fig.1.

in particular, to study thin films of PTO. The analysis of diffraction patterns is facilitated due to the so-called "forward focusing" effect occurring if the photoemitted electron has a kinetic energy above approximately 0.5 keV. Scattering calculations predict strong enhancement of the emission intensity in direction of near neighbors and more generally along densely packed rows of atoms corresponding to low-index crystallographic directions.

The diffractograms produced by the Pb 4f emission are completely dominated by the scattering of the heavy Pb atoms. This is due to the larger Pb scattering cross section compared to Ti or O. By selecting O atoms as emitters, therefore, we change the reference system from which the photoelectrons are ejected. Instead of looking at the displacement of the light-atom sublattice relative to Pb, we expect to see the corresponding shifts of Ti and Pb atoms relative to O atoms.

In Fig. 2, we display the calculated O 1s core level diffractograms for the PTO "up" and “down” states, respectively (see also Fig. 1). Figure 2 (center) shows the O 1s core level experiment at E$_{kin}$=724.1 eV for a 60 Å thin film. To bring into evidence the region of large differences between the two different structures, we present (in Fig.1) polar cuts at ϕ = 0° starting at normal emission ([001]) up to θ = 78° polar angle, plotted each time with the experimental result along the same direction.

The main difference comes from the scattering of O 1s photoelectrons on nearest Pb atoms (label A in Fig. 2). The corresponding principal "forward focusing" intensity appears to be the same in the “up” calculation and in the experiment. Secondly we observe intensity enhancements (B). Again, the length and the width of this modulation agree well between the experiment and the "up" state calculation. Similar features (C) appear, but differences between "up" and "down" in this case are not significant enough to identify the different states.

Therefore, we are able to make a distinction in the calculations between the "up" and "down" state, and subsequently we are able to observe the sample as mainly "up" polarized. We obtain this behaviour for a 60 Å thin film being close to the theoretical limit for ferroelectricity to persist. The ferroelectric behaviour of thinner films will be categorized in further measurements.

As this experimental method is sensitive at the atomic scale, we plan to investigate size effects in very thin films. Nevertheless, a problem could occur for very thin films (thinner than the mean free path of the photoelectrons), where the contribution to the measured signal of oxygen contained in the substrate (Nb-SrTiO$_3$) is not negligible. As a consequence, measurements should be done with Pb atoms as emitters. In order to decrease the "forward focusing" domination of Pb photoelectrons scattered on Pb atoms, lower photoelectron energies, accessible at the Swiss light source may have to be used.

Charge density wave compounds

Low dimensional systems have particularly attracted interest through the discovery of high temperature superconductors (HT$_c$'s). Many angle-resolved photoemission (ARPES) experiments have been conducted on such materials. With the improvement of the energy and momentum resolution on the experimental

side, the interpretation has become very sophisticated and many unusual signatures in the spectral function have been found. Among them is the signature for the opening of a pseudogap, for a sort of collective mode (of unknown origin) and, very recently, for a spontaneous symmetry breaking of time reversal symmetry. Also, stripes, i.e., doped holes that are self-organized, a sort of density waves, appear to play an important role. Nevertheless, the final word about the mechanism behind HT_c is not spoken. It is therefore important to relate these findings and apply the same sophistication in the analysis to other layered materials.

Layered transition-metal dichalcogenides are a class of quasi two-dimensional (2D) materials. Many exhibit charge density waves (CDW's) and even become superconducting at low temperatures. Indeed there is renewed and growing activity on these materials. 1*T*-TaS_2 is such a material exhibiting CDW's and a quite complex phase diagram as a function of temperature. The studies on such materials serve a better understanding of the mechanisms at work in low dimensional electron systems in general.

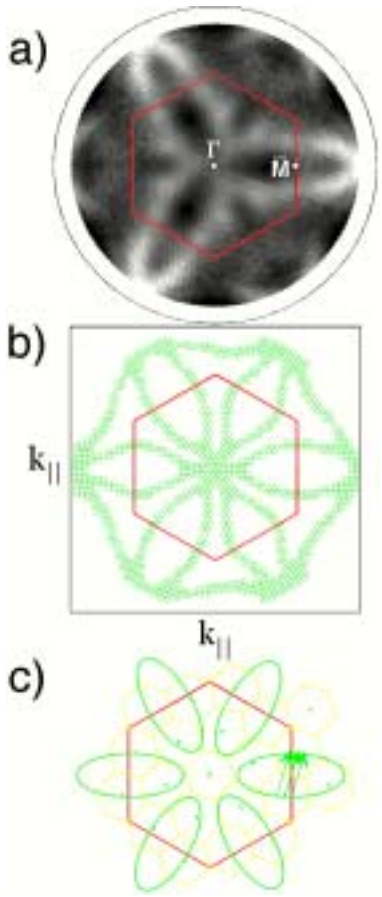

Fig.3. (a) Experimental Fermi energy intensity map taken with HeI radiation at room temperature, plotted linearly in k||; high intensity is in white; center and outer circle correspond to normal and 90° emission, respectively; the hexagon represents the normal state BZ. (b) Corresponding density functional theory calculated map for the normal state. (c) Superposition of normal- and CDW-state BZ's, together with a sketch of the FS contours; possible nesting vectors are plotted (see text).

Figure 3(a) displays the result of an E_F mapping experiment at room temperature (RT). At RT the CDW is well established as seen in low energy electron diffraction (not shown) and consists of commensurate CDW domains of approximately 70 Å in diameter with incommensurate regions in between. The RT phase is called the quasi-commensurate phase in contrast to the commensurate ("C") phase below 180 K where no in-commensurate regions exist anymore. The first order transition to the "C"-phase is accompanied by a jump in the resistivity of more than an order of magnitude (see e.g. Ref. [3]). 1*T*-TaS_2 in its unreconstructed or normal state consists of hexagonal Ta planes sandwiched between sulfur atoms. In the ionic picture Ta[Xe] $4f^{14}5d^{3}6s^{2}$ gives four of its five electrons to the two sulfur (S[Ne]$3s^{2}3p^{4}$) atoms creating a system with one d-electron per unit cell. Indeed, bandstructure calculations for the normal state [3] display a single Ta d-band dispersing close to E_F. The calculation for the E_F-scan (Fig.3(b)) is in good agreement with the experiment (Fig. 3(a)). The BZ of the non-reconstructed structure is also drawn in Fig. 3(a). It is important to note that despite the presence of the CDW at RT, the experiment exhibits the symmetry of the normal state BZ, as is also evident from the good agreement of experiment (Fig. 3(a)) and normal state calculation (Fig. 3(b)). This observation is a consequence of the spectral weight distribution, as measured by ARPES, remaining strongest along the bandstructure of the non-reconstructed phase. [4] The experiment only shows strong intensity for three of the six ellipses, a fact attributed to the final state scattering of the outgoing photoelectron.

Another important point to notice is that the FS appears pseudogapped [5], i.e., the E_F-map (Fig. 3(a)) does not currently represent the locations of quasiparticle peaks crossing E_F. As a matter of fact no clear crossing has been observed in ARPES data. A careful study of experimental data combined with band-structure calculations *including* the lattice distortion concluded that the pseudogap can be explained by the splitting and backfolding of bands introduced by the new BZ's.[6]

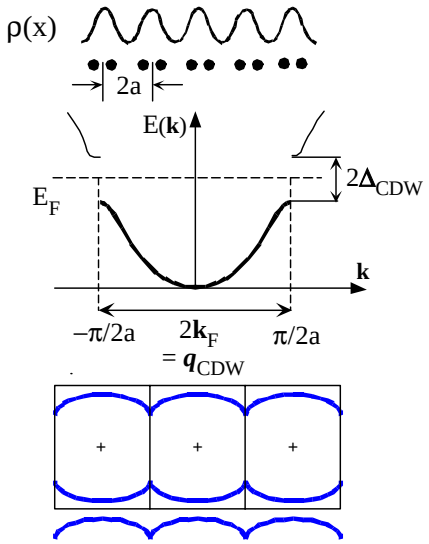

Fig.4. Sketch of the behaviour of the bandstructure and Fermi surface contours of a quasi-1D system with one electron per unit cell (see text).

Figure 3(c) displays a sketch of the situation with both, the (√13x√13)-R13.9° reconstructed (small hexagons) and the un-reconstructed BZ's plotted. We have an elliptically shaped normal state FS with evidence for nested parts along the flat parts of the ellipses (see arrows in Fig. 3(c)). The important question is what drives the CDW. Is it the classical Peierls transition as in 1D? If this is the case, what do we expect from a strongly nested quasi-1D FS?

Figure 4 sketches the situation for a strongly nested quasi-1D FS. If we consider chains of atoms with one electron per atom (and unit cell) and distance *a* ($k_F=\pi/(2a)$ with the quasi-1D band half filled). If the lattice is distorted in order to double the periodicity (Fig. 4), i.e., to introduce a CDW with wavelength 2*a*, elastic energy has to be paid. At the same time a doubling of the periodicity in real space results in reducing the dimension of the BZ by a factor of two. The consequence is that the BZ boundary is now located at $k_F=\pi/(2a)$ and the band is full (two electrons per unit cell) with the opening of a gap at the new BZ boundary at $\pi/(2a)$ and a corresponding gain of electronic energy. Therefore, what we expect from a strongly nested FS is that its nested parts disappear (due to the gap opening) with the occurrence of the CDW (Fig.4).

However, looking carefully at Fig. 3, this is not what we observe. The boundaries of the new BZ's are not along the expected nested parts of the normal state FS (indicated by arrows in Fig. 3(c)) indicating that we do not have a quasi-1D system and the classical Peierls mechanism does not appear to be dominant.

It is necessary to explore the ingredients of the energy balance of the transition. The energy balance of elastic energy paid and electronic energy gained is expressed in terms of the susceptibility (polarization function or Lindhard function), the elastic spring constant of the lattice, and the magnitude of the electron-lattice interactions. The susceptibility (appearing in the electronic energy part) basically describes the FS nesting. As seen from Fig. 3(c) it is not clear whether nesting is strong since the system has not chosen to align the new BZ's along potentially nested parts (flat parts of the ellipses) of the FS contour as expected for a quasi-1D system. However, even for a moderate susceptibility it is possible to obtain a favorable energy balance if only the electron-phonon coupling is strong enough.

The (√13x√13)-R13.9°, reconstructed (large) unit cell is 13 times larger and contains 13 Ta and 26 sulfur atoms. Star-like arrangements develop around one central Ta atom with six nearest and six next nearest neighbors. Realistic bandstructure calculations [2] including the CDW-induced star-like lattice distortion show that the single Ta d-band of the normal state is split and 7 sub-bands develop, six of them filled and the seventh crossing E_F. The reconstructed unit cell contains 13 inequivalent Ta atoms with a total of 13 electrons assuming the ionic picture. In order to place these electrons (two per band) 6 filled bands one half filled, crossing E_F are needed.

Therefore, we can identify two avenues for the system to gain electronic energy. First, the introduction of many small new BZ's results in the normal state FS contours to be cut into many pieces and many small gaps contribute to a lowering of electronic states. Second, the reconstruction (unit cell with 13 Ta atoms, 39 atoms in total) leads to a bandstructure where six of seven sub-bands are completely lowered below E_F, again indicative for a lower electronic energy in the CDW state. However, it is presently not possible to say whether these two observations represent the driving force for the CDW formation or are merely the consequence.

References:
[1] J. Junquera and P. Ghosez, Nature **422** (2003) 506.
[2] L. Despont *et al.*, Phys. Rev. B, submitted.
[3] M. Bovet *et al.*, Phys. Rev. B **67** (2003) 125105.
[4] J. Voit *et al.*, Science **290** (2000) 501.
[5] Th. Pillo *et al.*, Phys. Rev. Lett. **83** (1999) 3494.
[6] M. Bovet *et al.*, Phys. Rev. B, accepted.

15. Carbon Nanostructures and the Role of Hydrogen for Novel Electronic Materials

Project leader: Louis Schlapbach, University of Fribourg, and EMPA

Research summary: We have investigated the interaction of hydrogen with sp^2-bonded carbon by means of photoelectron spectroscopy (PS) and scanning tunneling microscopy (STM). Experiments performed with graphite, single-walled carbon nanotubes and C_{60} molecules indicate a marked lowering of the adsorption energy barrier of hydrogen for increased curvatures in the sp^2-network. Scanning tunneling microscopy of individual adsorption sites on graphite reveals the scattering of the delocalized electron states at the affected carbon site, which appears as long-range standing wave patterns in the vicinity of the defect.
The field emission of carbon nanotubes has been characterized using the scanning anode field emission microscope with regard to emission homogeneity, emitter degradation and shielding effects.
The investigation of the *1T*-$TaSe_2$ surface by means of STM and scanning tunneling spectroscopy (STS) reveals large domains with different electronic properties. The only structural difference of the domains is a characteristic phase shift of the CDW superstructure across the domain boundary, which suggests a different stacking sequence of the superstructure lattice, in neighboring domains.

Hydrogen chemisorption on sp^2-bonded carbon: local electronic effects

The adsorption of hydrogen on sp^2-bonded carbon has attracted considerable interest in the past few years. One of the main driving forces for studies in this field has been the ongoing effort to store hydrogen in carbon nanostructures, which requires a detailed knowledge of the interaction of hydrogen with the carbon network. Prominent examples belonging to the family of sp^2-bonded carbon are graphite, carbon nanotubes and C_{60} molecules (Buckminster fullerenes). Our main motivation stems from the possibility to locally modify the electronic properties of the carbon structure by chemically binding hydrogen to the sp^2-bonded carbon network. The chemisorption of hydrogen is particularly interesting since it locally changes the coordination number of the carbon atoms, which is expected to have a large influence on the charge transport properties. The influence on the electronic properties is known to be especially large on carbon structures in the nanometer range, where the introduction of individual defects completely changes their conduction behaviour.
We have investigated the interaction of atomic hydrogen and low-energy hydrogen ions with graphite, single-walled carbon nanotubes and C_{60} molecules, which allowed us to study the influence of the curvature of the carbon network on the adsorption properties of hydrogen [1,2]. These structures cover a radius of curvature in the range of $r = \infty$ (graphite) to $r = 3.55$ Å (C_{60}). Hydrogen chemisorption on sp^2-bonded carbon structures locally removes the delocalized π-states of the valence band due to the local change in hybridization from sp^2 to sp^3. This can be observed by photoelectron spectroscopy (PS) whereby the lowering of the intensity on the π-related features gives a measure for the amount of hydrogen that is chemisorbed to the carbon network. Our study shows that the energy barrier for hydrogen adsorption is lowered for increased curvatures in the sp^2-bonded carbon network. Whereas in the case of C_{60} and single-walled carbon nanotubes the hydrogen adsorption can be achieved by exposure to atomic hydrogen, on graphite it requires hydrogen ions of low kinetic energy (~1 eV). This lowering of the adsorption energy barrier is attributed to the small admixture of sp^3-bonding, which is present as soon as curvature is introduced in sp^2-bonded carbon networks and therefore has atomic configurations that are nearer to the purely sp^3-bonded structure after hydrogen adsorption.

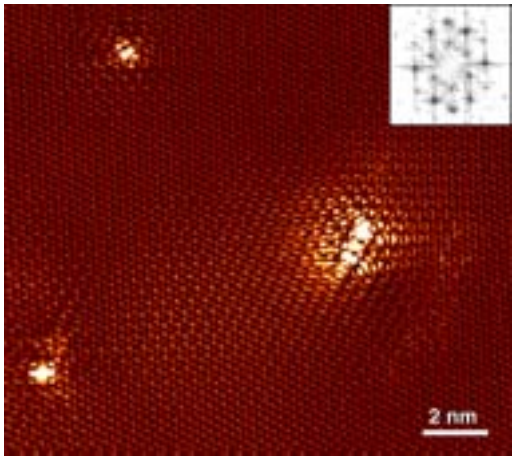

Figure 1: *Overview current image acquired in the combined AFM/STM mode showing two hydrogen adsorption sites (left) and a vacancy type defect. The inset shows the Fast Fourier Transform (FFT) of the same image. The small hexagon reflects the defect-related ($\sqrt{3} \times \sqrt{3}$)R30° superstructure.*

Furthermore, hydrogen adsorption on sp^2-bonded carbon structures leads to an important lowering of the electron work function. The lowering of the work function depends nearly linearly on the hydrogen coverage and amounts to up to 1.3 eV for C_{60}. The observed effect is attributed to a change in

the surface dipole due to the on-top adsorption of hydrogen, which is less electronegative than carbon and thus lowers the energy barrier at the surface.
The study of the local electronic modifications of single point defects such as hydrogen adsorption sites and atomic vacancies has been performed on graphite using STM and atomic force microscopy (AFM). Due to the flat and largely defect free arrangement of the sp^2-bonded carbon layers, graphite is the ideal substrate for the study of long-range modifications of the electronic structure induced by artificially introduced defects. The combination of AFM and STM using conductive AFM cantilevers has allowed the identification of two types of point defects, namely hydrogen adsorption sites and atomic vacancies (Fig. 1) [2,3]. A common feature of both defects is the long-ranged (~5 nm) redistribution of the charge density in the vicinity of the defect. This redistribution is observed as a $(\sqrt{3} \times \sqrt{3})R30°$ superstructure in the current image. It reflects the standing wave that is created by the scattering of the delocalized electrons at individual point defects. The structure of the standing wave is given by the allowed wave vectors of the incoming and the reflected electrons and thus reflects the Fermi surface of graphite, which has a point-like structure.

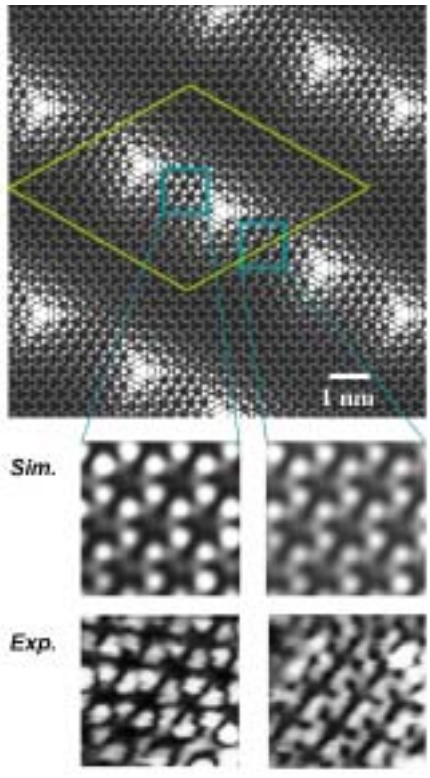

Figure 2: *Comparison of calculated local density of states (Tight Binding) with experiment (bottom details). The experimental details have been recorded between defects on a sample with high defect density.*

As soon as the defect density is increased in a way that the typical distance between individual defects is smaller than the range of the standing waves of single defects, interference gives rise to new patterns in the charge density, which are completely different from the usually imaged charge density distribution of an undisturbed graphite lattice.
Further insight on the nature of the observed charge distribution has been gained by Tight Binding simulations, which has been performed in collaboration with *M. Melle-Franco and F. Zerbetto, Universitá degli Studi di Bologna*. Simulation of different defect configurations (affected type of atom and relative position of defects) reveal sensitive changes of the observed charge distributions for different defect configurations (Fig. 2).
The observation of standing wave pattern for hydrogen adsorption sites and atomic vacancies demonstrates the strong scattering behaviour of both types of defects. The presence of such defects on carbon nanostructures (e.g. nanotubes) should, due to their low dimensionality, sensitively change their conduction behavior.

Field emission of carbon nanotubes: Oriented growth and emitter degradation

The field emission of electrons is regarded as one of the first application of carbon nanotubes (CNT) with a major economic impact. The main reason for the success of CNT field emitters can be seen in the relative ease and the low cost approaches to produce planar emission cathodes, that can deliver emission characteristics similar to those of metal micro-tip arrays. Further the CNT show such positive material properties as:

- High aspect ratio leading to strong field enhancement.
- Chemical inertness preventing oxidation of the nanometer sized structures when handled in air or operated in poor vacuum.
- Mechanical strength preventing structural modification, when exposed to strong electric fields (e.g. migration of atoms at the tip apex).
- Withstands the high current densities ($J>10^6$ Acm^{-2}) which occur in field emission.

The performance of a planar field emission cathode will be mainly determined by the following four parameters: Cathode emission current density [Acm^{-2}], Emission site density (ESD) [cm^{-2}], the applied field for operation [$V\mu m^{-1}$] and the temporal stability or life time of the cathode. These parameters are

determined by a complex relation between the geometrical structure of the field emission cathode as well as the CNT materials and electrical contact properties to the substrate.
Using the homebuilt scanning anode field emission microscope (SAFEM) we are able to investigate all the relevant emission properties down to the micrometer scale in order to gain more insight in the mechanisms determining the performance of field emission cathode, where the investigation is not limited to CNT's.
For field emission cathodes with randomly oriented CNT-films, grown by chemical vapor deposition (CVD), we have evidenced an exponential relation for the frequency distribution f(β) of emitters and the field enhancement factor β, of the following form $f(\beta) = C_1 \cdot exp(C_2 \cdot \beta)$, where C_1 and C_2 are positive constants (Fig. 3).

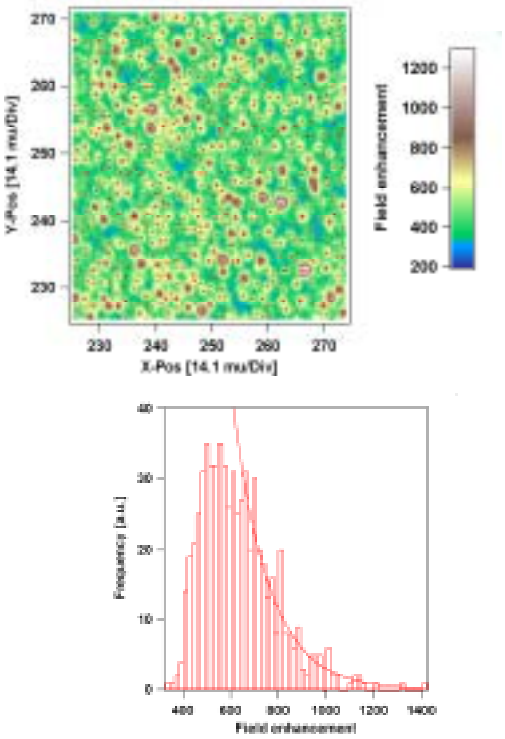

Figure 3: *Upper panel: Field enhancement map (700x700 μm^2) of a randomly oriented CNT cathode on Si (individual emitter are highlighted by red diamonds). Lower panel: The field enhancement distribution f(β) of this cathode, showing the exponential distribution on the high β side. (The deviation from the exponential law in the low β region is due to the fact that emitters with low β are over cast by emitters with a high β value.)*

From the measured field enhancement distribution we could perform simulations of the dependence of applied field and the emission site density. Although most CNT cathodes display a threshold field of the order of 1-2 $V\mu m^{-1}$ to obtain measurable emission currents, the threshold field to get homogenous emission with ESD well above 10^6 cm^{-2} is much higher than 20 $V\mu m^{-1}$. Using high resolution scanning we could experimentally demonstrate ESD above $5 \cdot 10^6$ cm^{-2} for CVD grown CNT on Si for applied electric fields of 30-40 $V\mu m^{-1}$. This value represents to the best of our knowledge the highest ever reported ESD for CNT cathodes.
The exploitation of high ESD regime is however hindered by the emitter degradation, which leaves open only a relatively small window of applied field, where an emitter is effectively contributing to the emission. This window is limited on one side by the critical emission current an emitter can deliver before it gets destroyed. The critical current is therefore one of the most important parameters limiting the performance of a field emission cathode.

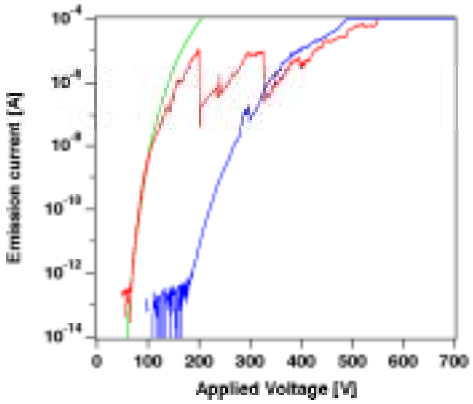

Figure 4: *I-V characteristic of a single CVD grown CNT emitter. The red curve shows the initial I-V characteristic with two abrupt irreversible degradation events at 190 V and 310 V. After this degradation the emission current is stable up to 100 μA and reversible (blue curve). It should be noted that the emitter had been current conditioned before this measurement, leading to some what higher critical current of 10 μA in the red curve.*

We have identified different degradation mechanisms attributed to current induced contact failure, field induced emitter disruption due to bad adhesion, continuous emitter degradation due to tip erosion and triggering of vacuum discharges due to desorbing gases from the emitter during emission. It has been found that initial degradation for multi-walled as well as single-walled CNT occurs at emission currents of 1-5 μA. This degradation affects the emitters with highest field enhancement values. After repeated degradation steps however the remaining active emission sites show much higher critical currents of over 100 μA, but at strongly reduced field enhancement values (Fig. 4). A direct relation between critical current and field enhancement is however difficult to establish, as, during the degradation, the cathode undergoes strong morphological modifications.

The development of an efficient CNT cathode requires ideally a maximization of the critical current as well as an optimization of the field enhancement distribution via a controlled emitter geometry [4]. In collaboration with the University of Cambridge (*W. Milne and K. Teo*) as well as Thales S.A. (*P. Legagneux*) within the European project CANVAD we could produce and measure regular, vertically aligned CNT with controlled height and diameter.

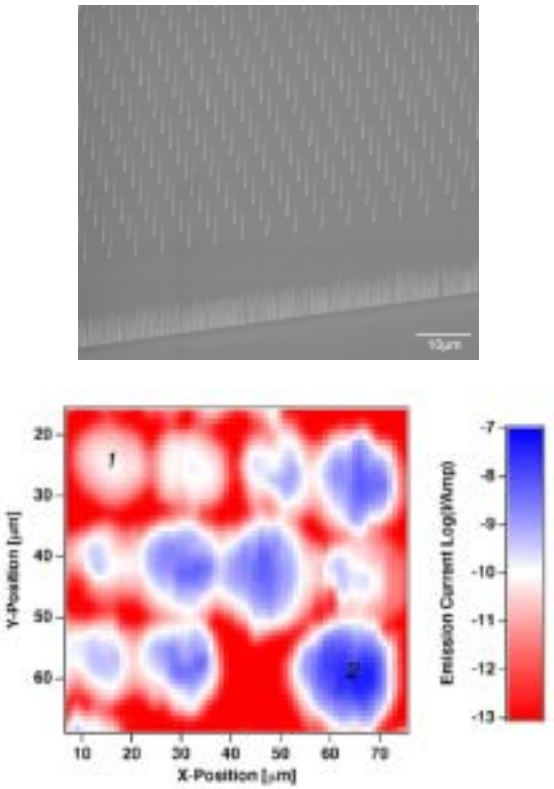

Figure 5: *SEM image of a regular array of DC PE-CVD grown CNT. Lower panel SAFEM emission current map at 15 Vμm^{-1} on a CNT array with 17 μm spacing. Emitter 2 delivers >1'000 times more current than emitter 1.*

Using emitter arrays with different spacing between the CNT we could experimentally prove the theoretically predicted ideal emitter spacing of twice the emitter height. As can be seen from Fig. 5 the degree of control on the emitter geometry is still not sufficient to guarantee homogenous emission.
During the project period we started collaborations with the following industrial partners: Thales S.A. (France), SONY Corp. (Japan), Mapper Lithography (Netherlands) and COMET AG (Switzerland).

Domains with different electronic properties at the surface of *1T*-$TaSe_2$

Charge density wave (CDW) compounds have attracted considerable interest due to their electronic properties, which are related to transitions that occur in the in-plane structure as a function of temperature.
STM of the CDW-phase reveals the well-known $\sqrt{13} \times \sqrt{13}$-superstructure at the surface layer (Fig. 6).

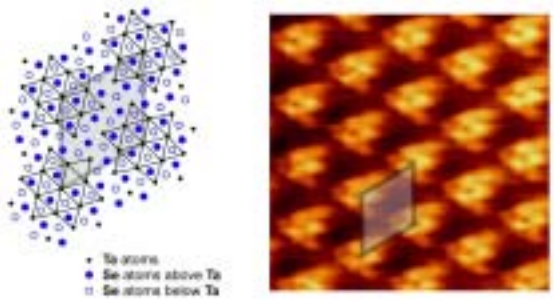

Figure 6: *Schematic structure of 1T-$TaSe_2$ in the CDW phase with the ($\sqrt{13} \times \sqrt{13}$) superstructure indicated. STM topography image recorded at 77 K (4.8 x 4.8 nm^2, U = -0.5 V).*

Further information is gained by recording scanning tunneling spectra. This investigation reveals domains of several hundred nanometers in diameter, which differ in their electronic properties. One type shows semiconducting behaviour, whereas the other shows metallic properties (Fig. 7). However, topography images of both domains show identical atomic structures.

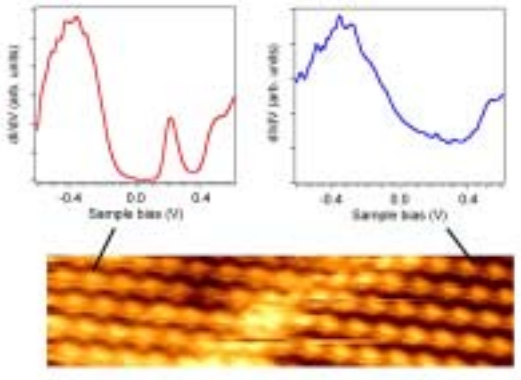

Figure 7: *Spectra recorded on two neighboring domains revealing prominent differences in the LDOS. Topography image: 19 x 4.5 nm^2; U = 0.7 V.*

The only difference is a phase shift of $2a_0$ (a_0 is the lattice constant of the undisturbed lattice) of the superstructure lattice across the domain boundary. The unchanged structure in the plane indicates that the reason for the different electronic properties originates from the interaction between subsequent layers in terms of a different stacking sequence of the superstructure lattice.

References:

[1] P. Ruffieux *et al.*, Phys. Rev. B **66** (2002) 245416
[2] P. Ruffieux *et al.*, acc. for pub. in Appl. Phys. A (2004)
[3] P. Ruffieux *et al.*, submitted to Phys. Rev. Lett. (2004)
[4] P. Gröning *et al.*, Adv. Eng. Mat., **5**, (2003) 541

16. Neutron Scattering Investigations of High-Temperature Superconductors and Quantum Phase Transitions

Project leader: Albert Furrer, ETH Zurich and PSI Villigen

Research summary: (1) Doping, pressure and oxygen isotope effects on the pseudogap temperature T* in the high-T_c superconductor (HTSC) Ho@$La_{2-x}Sr_xCuO_4$ ($0.11 \le x \le 0.25$) were investigated by neutron crystal-field spectroscopy. The observed doping dependence of T* supports the generic phase diagram of HTSC with $T^* > T_c$ even in the heavily overdoped regime. The observed opposite shifts of T* upon pressure application and oxygen isotope substitution can be qualitatively explained by a Jahn-Teller polaron-like pairing mechanism in HTSC. (2) With use of small-angle neutron scattering a well defined vortex lattice was observed for the first time in $La_{2-x}Sr_xCuO_4$ for all doping levels. Furthermore, it is found that both the structure of the vortex lattice and the spin dynamics depend strongly on the hole doping, thus reflecting the subtle interplay existing between the magnetic and electronic degrees of freedom in this material. (3) For the first time the existence of the theoretically predicted gapless Goldstone mode characteristic of the Bose-Einstein condensation of excited triplet states in the quantum spin dimer compound $TlCuCl_3$ could be unambiguously verified by inelastic neutron scattering. The quantum criticality was reached by the application of both an external magnetic field and hydrostatic pressure. The unusual three-plateau structure of the magnetization in NH_4CuCl_3 was found to be due to the existence of three different magnetic subsystems.

Doping, pressure and isotope effects on the pseudogap in Ho@$La_{2-x}Sr_xCuO_4$

Superconductivity is the result of two distinct quantum phenomena, pairing of the charge carriers at a characteristic temperature T* and long-range phase coherence at the superconducting transition temperature T_c. In conventional superconductors these two phenomena occur simultaneously, i.e., $T^* = T_c$. In contrast, for high-temperature superconductors we have $T^* > T_c$ over a large doping range, thus the so-called pseudogap region ($T_c < T < T^*$) is clearly the most challenging part of the phase diagram. The experimental discovery of the pseudogap region gave rise to an impressive number of models for the mechanism of high-temperature superconductivity. Consequently, experiments which produce changes of the pseudogap temperature T* are of crucial importance to discriminate between the different pairing scenarios developed for the cuprate superconductors.

We have applied neutron crystal-field spectroscopy as a bulk-sensitive technique to the high-T_c compounds Ho@$La_{2-x}Sr_xCuO_4$ ($0.11 \le x \le 0.25$) in order to study the doping, isotope and pressure dependence of the pseudogap temperature T*. The technique is based on the relaxation behaviour of crystal-field transitions in rare-earth containing high-T_c compounds. In the normal metallic state the linewidth of crystal-field transitions associated with the rare-earth ion increases almost linearly with increasing temperature according to the well-known Korringa law which describes the interaction of the crystal-field states with the charge carriers. In the superconducting (and in the pseudogap) state, on the other hand, the pairing of the charge carriers creates an energy gap Δ_k, so that crystal-field excitations with energy $\hbar\omega < 2\Delta_k$ do not have enough energy to span the gap. Consequently, the interaction with the charge carriers and thereby the line broadening of the crystal-field transitions is suppressed, giving rise to deviations from the Korringa law below T*. These effects were clearly observed in neutron scattering experiments carried out with use of the high-resolution time-of-flight spectrometer FOCUS installed at the spallation neutron source SINQ, PSI Villigen, Switzerland. As an example the opening of the pseudogap at $T^* >> T_c$ as well as the oxygen isotope effect on T* is visualized in Fig. 1 for the heavily overdoped compound with x=0.25.

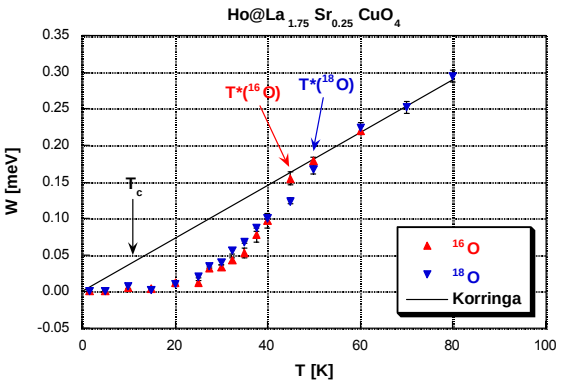

Fig.1. Temperature dependence of the intrinsic linewidth W corresponding to the lowest ground-state crystal-field transition in Ho@$La_{1.75}Sr_{0.25}CuO_4$. The line denotes the linewidth in the normal state according to the Korringa law.

Our results obtained so far can be summarized as follows: With increasing doping, T* is found to decrease from 80 K (x=0.11) to 60 K (x=0.15), 50 K (x=0.20), and 45 K (x=0.25) [1-3]. The application of hydrostatic pressure (p=0.8 GPa) results in a downward shift of T* by 5 K for the optimally doped compound (x=0.15) [2,4]. Upon oxygen isotope substitution (^{18}O vs ^{16}O), T* is shifted

upwards by 20 K (x=0.11), 10 K (x=0.15), 5 K (x=0.20), and 5 K (x=0.25) [1-3]. The opposite effect of pressure and oxygen isotope substitution on T* can be qualitatively explained by a Jahn-Teller polaron-like mechanism [5] and underlines the importance of lattice effects in models for high-T_c superconductivity.

Spin and vortex dynamics in $La_{2-x}Sr_xCuO_4$

Using small-angle neutron scattering (SANS) at the spallation neutron source SINQ, PSI Villigen, Switzerland, we have been able to observe for the first time a well ordered vortex lattice in the bulk of a $La_{2-x}Sr_xCuO_{4+\delta}$ (LSCO) single crystal (slightly overdoped, x=0.17) [6], a member of the original family of high-temperature superconducting (HTSC) cuprates discovered by Bednorz and Müller. Furthermore, our SANS investigations of the mixed phase reveal a crossover from triangular to square coordination with increasing magnetic field. The existence of an intrinsic square vortex lattice has never been observed in HTSC, and is indicative of the coupling of the vortex lattice to some source of anisotropy. Several theoretical models have been proposed to explain our observation: (a) anisotropy of the d-wave order parameter, (b) anisotropy of the Fermi velocity, (c) anisotropy due to the presence of stripes.
In order to test these various scenarios, we have decided to follow two different experimental routes:
(A) Investigation of the vortex lattice at very high fields since the scenario (b) predicts an additional phase transition above 6 Tesla. By making use of the unique high-field facility at SINQ, we have been able to explore the magnetic phase diagram of LSCO (x=0.17) for fields up to 10.5 Tesla (see Figure 2) [7]. Our data do not indicate the presence of additional phase transitions between 0.5 and 10.5 Tesla. However, we cannot rule out a phase transition at even higher fields.

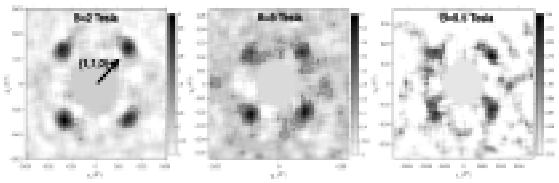

Fig. 2. SANS data obtained for LSCO with x=0.17 at various magnetic fields.

(B) Investigation of the doping dependence of the vortex lattice, since the scenarios (a-c) predict very different behaviours as a function of doping. We have succeeded to measure the vortex lattice at all doping levels of the phase diagram. Our data indicate that for the overdoped sample (x=0.20, see Fig. 3) the results do not change significantly in comparison to those obtained for the slightly overdoped ones (x=0.17, see Fig. 2), thus ruling out the stripes scenario as being responsible for the square coordination. In the underdoped region (x=0.10, see Fig. 3) we observe a totally different behaviour, since the vortex lattice is well defined only at low fields [8].

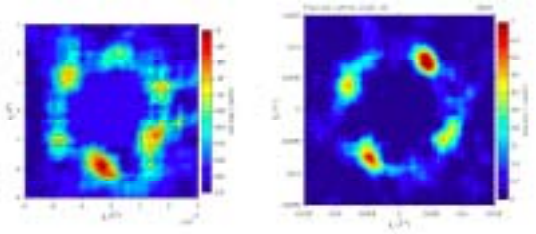

Fig. 3. Left: LSCO with x=0.10 at H=0.01 T. Right: LSCO with x=0.20 at H=0.4 T.

Our inelastic neutron scattering experiments (see Fig. 4) of the spin excitations show that while (below T_c) a well defined spin gap ($\Delta_{SG} \approx$ 6 meV) can be observed in slightly overdoped (T_c=37 K) LSCO [9], we are not able to observe a substantial temperature dependence of the spin excitations in underdoped (T_c=28 K) LSCO down to energy transfers of 2 meV. This clearly indicates that the ratio Δ_{SG}/T_c is doping dependent.

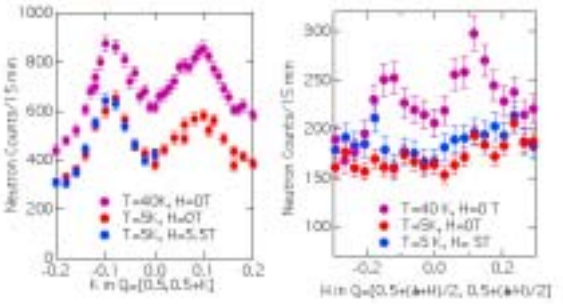

Fig. 4. Spin excitations of LSCO in the underdoped (x=0.10, left) and optimally doped (x=0.17, right) regimes at various temperatures and magnetic fields.

One might be tempted to interpret this result in terms of a stripe model. Static stripes have been observed in LSCO when superconductivity is suppressed by Nd doping. Within this interpretation the vanishing of the spin gap in the underdoped regime could be regarded as some kind of precursor of the static stripes. Here we would like to discuss an alternative hypothesis based on a Fermi liquid like scenario. In this context one would expect

that the value of the spin gap scales with the (d-wave) superconducting (SC) gap or with T_c. This is obviously not the case in LSCO, since Δ_{SG}/k_BT_c~1.9 for x=0.17 whereas Δ_{SG}/k_BT_c<0.8 for x=0.10. Notice, however, that the spin gap value is determined by the magnitude of the SC gap close to the nodes and not by the maximum SC gap value Δ_{max}. As soon as the d-wave SC gap is smoother around the nodes, the simple relation Δ_{SG}/k_BT_c~constant does not hold even in a simple Fermi liquid like picture. Indeed, our previous angle resolved photoemission spectroscopy (ARPES) measurements of the SC gap in the underdoped regime of $Bi_2Sr_2CaCu_2O_{8+y}$ indicate that the simplest d-wave gap function $\Delta\phi=\Delta_{max}\cos(2\phi)$ has to be corrected by higher order $\cos(6\phi)$ terms [10]. The $\cos(2\phi)$ and $\cos(6\phi)$ terms correspond to nearest neighbor and next-nearest neighbor interaction, respectively, therefore suggesting a more long-range pairing interaction in the underdoped regime. When higher order terms are included in the SC gap function, a strong renormalization of the spin gap occurs, which could explain the observed strong decrease of Δ_{SG} in the underdoped regime [11].

Bose-Einstein condensation of excited triplet states in $ACuCl_3$ (A=Tl, NH_4)

Up to the present, little attention has been paid to Bose-Einstein condensation (BEC) in magnetic compounds. Recently, a tremendous interest arose for the compounds $ACuCl_3$ (A=K, Tl, NH_4) in which the two Cu^{2+} ions forming a dimer in a crystalline network are antiferromagnetically coupled [12]. The dimer ground state is then a singlet with total spin S=0, separated by an energy gap from the excited triplet state with total spin S=1. At a critical external magnetic field H_c the energy of the Zeeman split triplet component S_z=+1 intersects the ground-state singlet and long-range magnetic order occurs, thus H_c is a quantum critical point separating a gapped spin-liquid state ($H<H_c$) from a field-induced magnetically ordered state ($H>H_c$). The triplet components with S_z=+1 can be regarded as diluted bosons, thus BEC is expected to occur in these dimer compounds at the quantum critical point H_c [13]. The magnetic excitation spectrum associated with the condensate has been theoretically predicted to be a gapless Goldstone mode [14].
With use of inelastic neutron scattering we explored the full energy dispersion of the magnetic fluctuation modes of $TlCuCl_3$, thus conclusively characterizing the typical time and space scale related to the excitation spectrum in the field-induced ordered phase of a quantum spin liquid. The experiment has been performed on the triple axis spectrometer FLEX at HMI Berlin. The results at fixed T=1.5K and H=14T clearly indicated the coexistence of two higher-lying modes and a low-lying mode. The higher-lying modes are gapped and retain a quadratic dispersion around the Bragg point, whereas the low-lying mode is gapless and linear, see Fig. 5 [15]. The latter result provides an unambiguous verification of the theoretically predicted gapless Goldstone mode characteristic of the BEC of the triplet states.

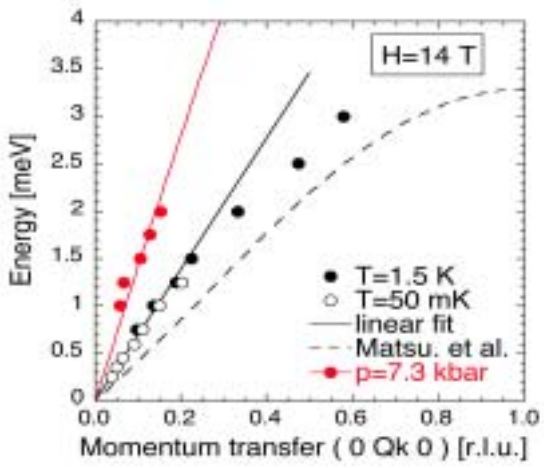

Fig. 5. Energy dispersion of the low-lying magnetic excitations in $TlCuCl_3$. The black circles correspond to the linear Goldstone mode observed in an external magnetic field of 14 T. The dashed line is a theoretical expectation with no disposable parameters [14]. The red circles show the linear Goldstone mode observed under the application of hydrostatic pressure (p=0.73 GPa) at T=1.5 K in zero field. The full lines are linear fits to the data.

The energy gap in $TlCuCl_3$ can also be closed by the application of hydrostatic pressure (p≥0.2 GPa) [16]. This offers the unique possibility to realize and explore the quantum phase transition into a magnetically ordered state by another external parameter. We performed corresponding neutron scattering experiments with use of the triple axis spectrometer TASP at SINQ under a hydrostatic pressure of p=0.73 GPa which results in a magnetically ordered state below T_N≈13 K. The resulting excitation spectrum turned out to be similar to that obtained by the field-induced experiments described above, with two gapped higher-lying modes exhibiting a quadratic dispersion and a gapless, linear low-lying mode, see Fig. 5. The stiffness of the latter, however, is about twice as large as in the field-induced case, which means that pressure has a significant effect on the exchange coupling between the Cu^{2+} ions.

The quantum criticality in $TlCuCl_3$ can eventually be realized yet by a third method. Partial substitution of Tl^+ by K^+ will change the exchange parameters and produce randomness in the exchange network between the Cu^{2+} ions. According to theories this randomness will result in the appearance of gapless and short-range spin correlations in zero field [17]. In order to study the evolution of the excitation gap as a function of K doping we performed inelastic neutron scattering experiments with use of the triple axis spectrometer TASP at SINQ on the mixed compounds $Tl_{1-x}K_xCuCl_3$ ($x \leq 0.20$). Indeed, we observed a decrease of the spin gap with increasing K content up to x=0.15, in agreement with magnetization data [18]. However, this trend is not continued for x=0.20, which possibly means that the excitation gap remains finite as the K concentration is further increased beyond x=0.20.

In contrast to $TlCuCl_3$, the related compound NH_4CuCl_3 is magnetically ordered already in zero field. NH_4CuCl_3 exhibits a highly unusual magnetization m(H) behaviour with so far unexplained low-temperature quantum plateaus corresponding to m=1/4 and m=3/4 of the saturated moment for 4T<H<13T and 18T<H<25T, respectively [19]. Matsumoto et al. explain these features by postulating a segregation of the Cu spin dimers into individual subsystems with volume fractions of 25%, 50%, and 25% [20]. However, this hypothesis only holds if the compound exhibits a phase transition from the monoclinic structure at room temperature to a structure of lower symmetry at low temperatures. Such a structural phase transition was currently suggested to occur at T=70 K by the observation of anomalies for the elastic constants c_{22} and c_{66} [21].

We performed a structural study on a deuterated ND_4CuCl_3 single crystal with use of the neutron diffractometer TriCS at SINQ in order to search for the postulated phase transition at T=70 K. A Eulerian cradle combined with three two-dimensional detectors allowed the simultaneous data collection in the whole reciprocal space. Fig. 6 displays the data of omega scans collected at T=2 K and T=87 K which exhibit significant differences. In particular, Bragg peaks at half-integer positions are observed at low temperatures, indicating the doubling of the chemical unit cell along the b-direction as a result of the structural phase transition (suggested to occur at T=70 K [21]) which is now verified by the present neutron diffraction data. This means that the proposed segregation into three different magnetic subsystems [20] is confirmed, since at least a doubling of the chemical cell along the b-direction is required for the model to be applicable.

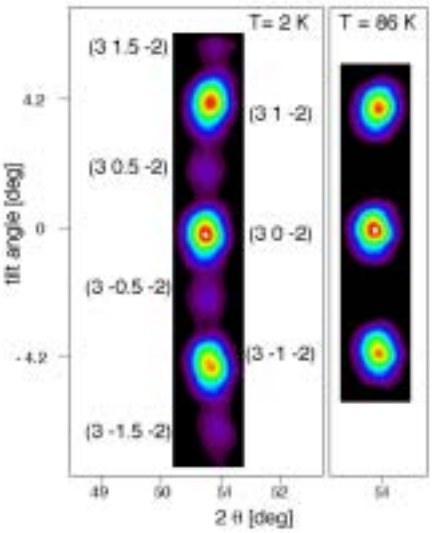

Fig.6. (3 k –2) Bragg peaks observed for ND_4CuCl_3 at T=2 K and T=87 K with λ=1.176 Å. Half-integer peaks are observed along b below T≈70 K.*

Inelastic neutron scattering experiments performed on a single crystal of ND_4CuCl_3 with use of the triple axis spectrometer FLEX at HMI Berlin confirmed the existence of three different magnetic subsystems, since the excitation spectrum was found to consist of three branches which were identified as triplet waves by their characteristic Zeeman splitting.

References:

[1] D. Rubio Temprano *et al.*, Phys. Rev. B **66** (2002) 184506.
[2] A. Furrer *et al.*, Physica C (in press).
[3] P.S. Häfliger *et al.*, Europhys. Lett. (to be submitted).
[4] P.S. Häfliger *et al.*, Phys. Rev. Lett. (submitted).
[5] L.P. Gor'kov, J. Supercond. **13** (2000) 765.
[6] R. Gilardi *et al.*, Phys. Rev. Lett. **88** (2002) 217003. Notice that Fig. 2 of this publication was displayed on the cover page of Phys. Rev. Lett., volume 88, issue 21.
[7] R. Gilardi *et al.*, Int. J. Mod. Phys. B **17** (2003) 3411.
[8] U. Divakar *et al.*, Phys. Rev. Lett. (submitted).
[9] R. Gilardi *et al.*, Europhys. Lett. (submitted).
[10] J. Mesot *et al.*, Phys. Rev. Lett., **83** (1999) 840; S.V. Borisenko *et al.*, cond-mat/0204557 (2002).
[11] A. Schnyder *et al.*, in preparation.
[12] T.M. Rice, Science **298** (2002) 760.
[13] T. Nikuni *et al.*, Phys. Rev. Lett. **84** (2000) 5868.
[14] M. Matsumoto *et al.*, Phys. Rev. Lett. **89** (2002) 077203.
[15] Ch. Rüegg *et al.*, Nature **423** (2003) 62.
[16] H. Tanaka *et al.*, Physica B **329-333** (2003) 697.
[17] R.A. Hyman *et al.*, Phys. Rev. Lett. **76** (1996) 839.
[18] A. Oosawa *et al.*, Phys. Rev. B **65** (2002) 184437.
[19] W. Shiramura *et al.*, J. Phys. Soc. Jpn. **67** (1998) 1548.
[20] M. Matsumoto *et al.*, Phys. Rev. B **68** (2003) 180403.
[21] S. Schmidt *et al.*, Europhys. Lett. **53** (2001) 591.

17. Fundamental Excitations of Correlated Matter

Project leader: Dirk van der Marel, University of Geneva

Research summary: Our group works on the properties of interacting electrons in solids. Prominent examples of unanticipated new phenomena are the fractional quantum Hall effect, high temperature superconductivity, colossal magneto resistance, and quantum phase transitions. The project focuses on physical situations where changes of state of matter take place. Invariably a transition of one state of matter to another is accompanied by a characteristic change of the kinetic energy of the electrons, which can be monitored by measuring the phase stiffness as revealed by the low energy optical spectral weight. Phase transitions are moreover often accompanied by an abrupt change of symmetry at the critical point, and this is revealed optically by the appearance or disappearance of vibrational modes in the infrared range, and by changes of the visible part of the optical spectrum. Ordering phenomena are usually accompanied by the appearance of new collective modes, which in some cases can be detected optically. With this approach we investigate the electronic structure of superconductors in the cuprate and heavy fermion families, Kondo insulators, itinerant ferromagnetic materials and (in)organic one-dimensional materials.

Temperature dependence of the low energy spectral weight

When we cool down a superconductor below the critical temperature, the material enters a qualitatively different state of matter, manifested by quantum coherence over macroscopic distances. Because the critical temperature represents a special point in the evolution of the internal energy versus temperature, the internal energy departs from the temperature dependence seen in the normal state when superconductivity occurs. Because for $T<T_c$ the superconducting state is the stable equilibrium state, the internal energy in equilibrium at T=0 is an absolute minimum. Hence cooling down from above the phase transition one would expect a drop in the internal energy when at the critical temperature. This drop of internal energy stabilizes the superconducting phase among all alternative states of matter.

Understanding the mechanism of superconductivity means to understand what stabilizes the internal energy of the superconducting state. In BCS theory superconductivity arises as a result of a net attractive interaction between the quasi-particles of the normal state. Note that, implicitly, this approach is firmly rooted in the paradigm of a Fermi-liquid type normal state. On the other hand, the school based on Anderson's original work asserts that a strong on-site *repulsive* interaction can also give rise to high T_c superconductivity. The latter models typically require that the material is not a Fermi liquid when superconductivity is muted, either by raising the temperature or by other means. In Fig. 1 we illustrate the predictions of BCS theory for the temperature dependence of the kinetic energy, and the low frequency spectral weight.

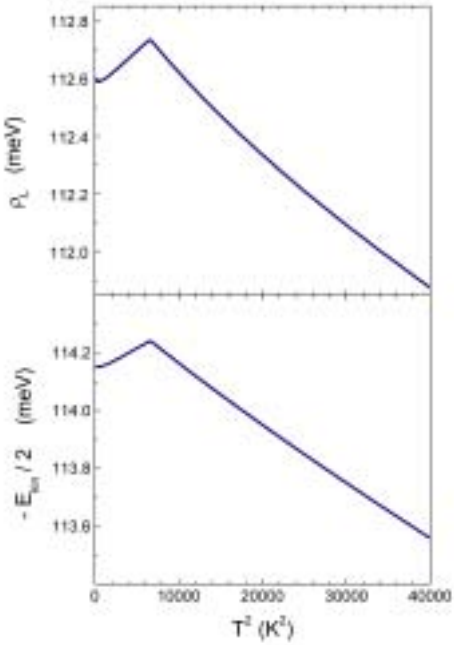

Fig.1. BCS prediction of the kinetic energy and the low phase stiffness [1].

Experimentally, we have observed the same trend in Bi-2212 for the temperature dependence of the ab-plane low frequency spectral weight as in the BCS-calculation, but the kink at T_c has the opposite sign: contrary to the BCS prediction, the kinetic energy of the superconducting state is lower than in the normal state (taking into account a correction for the temperature trends of the normal state). In Fig. 2 our experimental have been reproduced. Comparing this with the BCS prediction clearly demonstrates the large qualitative discrepancy between theory and experiment. Clearly the type of mechanism assumed in BCS theory is not at work here.

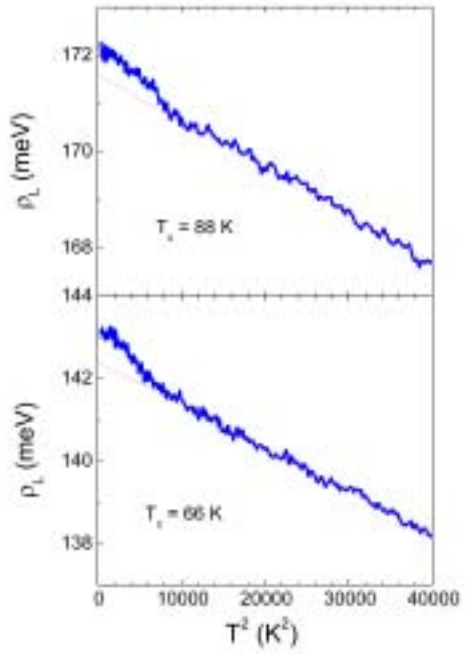

Fig.2. Experimental values of the ab-plane spectral weight function in Bi-2212 [2]. Upper panel: optimally doped. Lower panel: underdoped.

Novel collective modes in cuprate superconductors I: Bi-layer plasmons

In the bi-layer high Tc materials the coupling within the bi-layers may provide an additional source of frustrated interlayer kinetic energy, which can in principle be released when the material enters the superconducting state. This can in principle be monitored with infrared spectroscopy, because quite generally a stack of Josephson coupled layers with two different types of alternating weak links (in the present context corresponding to inter-bilayer and intra-bilayer) should exhibit three Josephson collective modes instead of one [3,4,5]: two of these modes are longitudinal ones, which show up as peaks in the energy loss function, $\mathrm{Im}(-1/\varepsilon(\omega))$. In between the two longitudinal resonances the theory predicts the presence of a transverse optical plasma resonance, which is revealed by a peak in the optical conductivity, Re $\sigma(\omega)$. In essence the extra two modes are out-of-phase oscillations of the two types of junctions. The existence of two longitudinal modes and one associated transverse plasmon mode at finite frequencies has been confirmed experimentally [6,7,8,9,10] for $SmLa_ySr_{1-y}CuO_{4-x}$ at various chemical compositions (see Fig. 3).

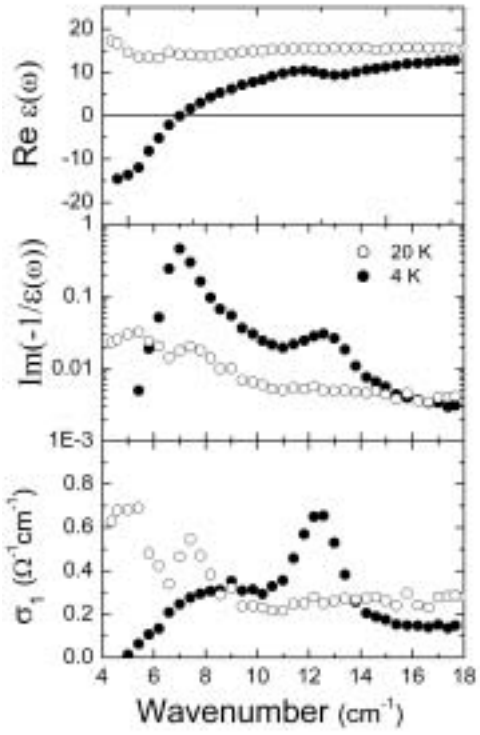

Fig.3. (a) Real part of the c-axis dielectric function of $SmLa_{0.8}Sr_{0.2}CuO_{4-x}$ for 4 K (closed symbols), and 20 K (open symbols) (b) The c-axis loss function (c) Real part of the c-axis optical conductivity.

Novel collective modes in cuprate superconductors II: 100 meV peak.

The most commonly used experimental method for studying optical properties of solids is by measuring the reflectivity spectrum, and to use Kramers-Kronig analyses to obtain the optical conductivity. This method fails if the spectrum contains large frequency regions where the conductivity is small, due to the non-local progression of experimental errors which are intrinsic to Kramers-Kronig analyses. One encounters this situation for the c-axis optical conductivity of most cuprate superconductors in the frequency range between 0.1 and 3 eV. In these cases one can try to measure both the reflectivity and transmission through a slab of suitable dimensions. Because the electric polarization of the infrared waves has to be parallel to the c-axis, it is necessary to have the c-axis parallel to the surface of the slab. The thickness of slab should be of the order of 10 to 20 micrometer, in order to have a reasonable throughput of infrared light, and the lateral dimensions should be on the order of a millimeter. The fact that most cuprates are weakly bonded along the c-direction poses a serious experimental challenge. In Figs 4 and 5 we illustrate two examples of such slabs, for

a La214 single crystal and for a Bi2212 single crystal.

In all different superconducting cuprate investigated up to date (underdoped and optimally doped La214, optimally doped and overdoped Y123, optimally doped Bi2212) we observe a weak absorption peak at approximately 0.1 eV (see Fig. 6). This peak therefore appears to be a common feature of the cuprate family. The intensity of the 0.1 eV resonance tracks the superfluid density, hence it appears to have some connection to the superconducting order.

The nature of this new resonance mode is not clear. In the case of the single layer materials La214 bi-layer plasmons do not exist, making the assignment to internal Josephson modes unlikely. Several alternatives should now be considered, for example amplitude modes of the superconducting order parameter, amplitude or phase modes of competing types of order such as charge-, spin-, or current ordering [12].

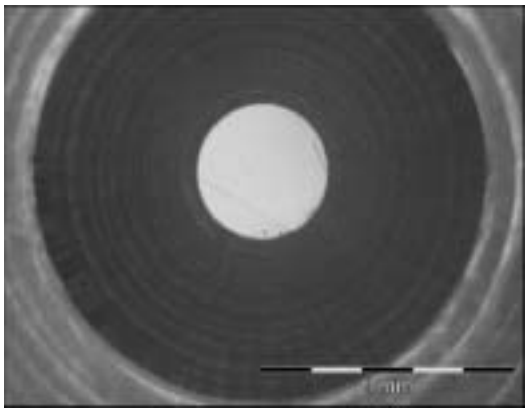

Fig.4. 20 μm thick slab $La_{1.85}Sr_{0.15}CuO_4$ which was cut perpendicular to the planes. The light gray area in the middle is the ac-face of the sample. The dark circular shape is a conical aperture placed in front of the sample. It serves both as a sample support and as an optical aperture defining the diameter of the infrared beam passing through the sample [11].

Fig.5. 20 μm thick slab of $Bi_2Sr_2Ca_{0.92}Y_{0.08}Cu_2O_8$ which was cut perpendicular to the planes. The gray area surrounding the slab is stycast, which serves to support this brittle material. The sample with stycast was mounted on a conical sample holder of the kind shown in Fig. 4.

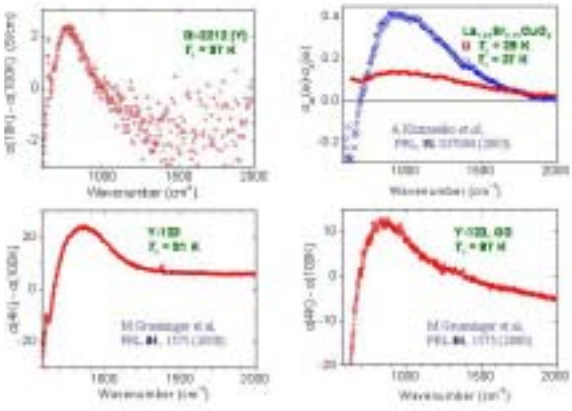

Fig. 6 Optical conductivity along the c-axis of four different high Tc superconductor measured at temperatures far below the superconducting phase transition. The optical conductivity of the normal state has been subtracted. For all four materials a weak absorption peak is observed at approximately 0.1 eV. [11]

Scale invariant optical response in optimally doped Bi2212

The possibility that a quantum critical state of matter can be realized in correlated electron systems near a quantum phase transition (QPT) occurring at zero temperature, is at the focus of current research in condensed matter physics, because the response of such a system is expected to follow universal patterns defined by the quantum mechanical nature of the fluctuations. This universality manifests itself through power-law behaviours of the response functions. Candidates are found both in heavy fermion systems and in the cuprate high Tc superconductors. Although there are indications for the occurrence of a quantum critical state in optimally doped cuprate superconductors, the reality of a QPT in these materials and the physical nature of the phases are still under debate.

The most important piece of evidence comes from the measured phase of the optical conductivity, which turns out to be independent of the wavelength and frequency of the light (see Fig. 7). We demonstrate that the experimentally measured phase angle agrees precisely with the exponent of the optical conductivity. Further proof was presented by demonstrating that temperature and (radiation-)frequency are, up to a point, interchangeable in the quantum critical region. This points towards a QPT in the cuprates close to optimal doping, although of an unconventional kind.

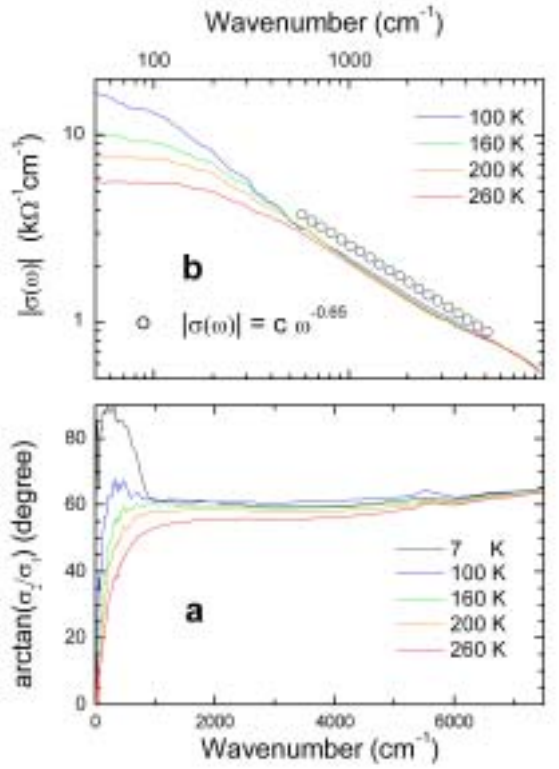

*Fig.7. Universal power law of the optical conductivity and the phase angle spectra of optimally doped $Bi_2Sr_2Ca_{0.92}Y_{0.08}Cu_2O_{8+\delta}$. In **a** the phase function of the optical conductivity, Arg(σ(ω)) is presented. In **b** the absolute value of the optical conductivity is plotted on a double logarithmic scale. The open symbols correspond to the power law $|\sigma(\omega)|=C\omega^{-0.65}$ [13].*

Heavy Carriers and Non-Drude Optical Conductivity in MnSi

Recent neutron and transport data of MnSi suggest that at pressures above 18 GPa this material has a non-Fermi liquid state, coexisting with a novel form of short range magnetic order [14,15].

Our optical conductivity experiments of this material indicate screening properties intermediate between a metal and a superconductor [16]. MnSi has anomalous optical reflectivity properties at low frequencies, which deviate considerably from the Hagen-Rubens behaviour observed in common metals. The magnetism of MnSi and Co-doped FeSi is commonly attributed to itinerant charge carriers. For MnSi this is confirmed by the observation of a narrow Drude-like peak in the optical spectra at low temperatures. Yet the spectral weight in this peak is small, indicating that the charge carriers are rather heavy. When MnSi is cooled below 100 K the effective mass develops a strong frequency dependence at low frequencies, while the scattering rate develops a sub linear frequency dependence. The complex optical conductivity is significantly different from conventional Drude behaviour, which can be attributed to a strong coupling of the itinerant charge carriers to spin-fluctuations or other collective modes.

The DC resistivity obeys the relation $\rho(T)=1/(\sigma_{IR}+\alpha T^{-1})$ with a remarkable accuracy (see Fig. 8), where σ_{IR} =3500 S/cm and α=620 kS/Kcm. This so-called parallel resistor formula has been known since 1977, in particular for the A15 compounds. MnSi presents the cleanest example of this behaviour reported in the literature, where the temperature dependent component seems to follow a perfect linear temperature dependence over the entire temperature range in the paramagnetic state (i.e. for T>30 K), with no apparent negative zero temperature offset. The formula suggests that the approach of the Ioffe-Regel limit at high temperature effectively follows a two-fluid approach.

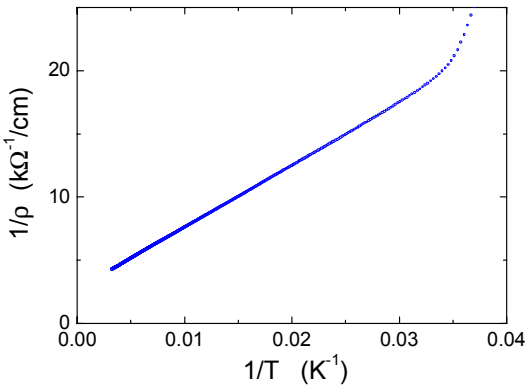

Fig.8. The temperature dependence of the DC resistivity of MnSi, plotted as 1/ ρ(T) versus 1/T [16]. The upward curvature at 1/30 K is where the phase transition into the helimagnetic phase takes place.

References:

[1] D. van der Marel *et al.*, Concepts in electron correlation, p. 7-16, A.C. Hewson and V. Zlatic (eds), Kluwer (2003).
[2] H. J. A. Molegraaf *et al.*, Science **295** (2002) 2239.
[3] J. Leggett, Prog. Theor. Phys. **36** (1966) 901.
[4] D. van der Marel and A. Tsvetkov, Czech. J. Phys. **46** (1996) 3165.
[5] D. van der Marel and A. Tsvetkov, Phys. Rev. B **64** (2001) 024530.
[6] H. Shibata and T. Yamada, Phys. Rev. Lett. **81** (1998) 3519.
[7] H. Shibata, Phys. Rev. Lett. 86 (2001) 2122.
[8] T. Kakeshita *et al.*, Phys. Rev. Lett. **86** (2001) 4140.
[9] D. Dulic *et al.*, Phys. Rev. Lett. **86** (2001) 4144.
[10] Pimenov *et al.*, Phys. Rev. Lett. 87 (2001) 177003.
[11] A.B. Kuzmenko *et al.*, Phys. Rev. Lett. 91 (2003) 037004.
[12] P.A. Lee and N. Nagaosa, Phys. Rev. B 68 (2003) 024516.
[13] D. van der Marel *et al.*, Nature 425 (2003) 271-274.
[14] N. Doiron-Leyraud *et al.*, Nature 425 (2003) 595.
[15] C. Pfleiderer *et al.*, Nature 427 (2004) 227.
[16] P. Mena *et al.*, Phys. Rev. B 67 (2003) R241101.
[17] H. Wiesmann *et al.*, Phys. Rev. Lett. 38 (1977) 782.

18. Electronic Properties of Low Dimensional Materials and Dimensional Crossover

Project leader: Thierry Giamarchi, University of Geneva

Research summary: The project which has been in the framework of MANEP since January 2003, focuses on two main directions. One concerns the effects of interactions in one and quasi-one dimensional systems. In one dimension the interactions lead to a Luttinger liquid. One of the questions is to understand how to go from this Luttinger liquid to a more conventional Fermi liquid state by coupling low dimensional systems. When a single chain is an insulator, the dimensional crossover is replaced by a deconfinement transition between a one dimensional insulator and a three dimensional metal or superconductor/superfluid. This question of dimensional crossover/deconfinement is relevant for experimental systems such as organic superconductors, spin chains and bosons in optical traps. The second part of the project concerns the transport properties in strongly correlated systems. In systems such as Wigner crystals and Luttinger liquids, disorder has drastic effects and transforms these systems into glassy insulators. The transport then becomes non-linear. Its computation is a difficult, but, experimentally, very relevant task. In addition to transport, other physical quantities, such as thermodynamic quantities, are strongly affected by the presence of disorder and need to be determined. Finally the need to be able to determine full nonlinear I-V characteristics occurs also in experiments such as tunneling between unconventional metals or superconductors

Deconfinement in coupled Luttinger liquids

One dimensional systems are very peculiar in the sense that interactions and quantum fluctuations play a crucial role. This leads to a special ground state, known as a Luttinger liquid, with very slowly decaying (power-law) correlation functions. Such a state has been observed both in spin chains and in fermionic systems (organic conductors, nanotubes etc.). However many such physical systems are made of coupled one dimensional chains. This raises the concern of a dimensional crossover between a regime where the one dimensional effects are dominant and a regime where the system behaves as a more conventional three dimensional crystal. Such an issue is of course also relevant (in higher dimensions) for many other physical systems (e.g. the layered High Tc superconductors). If the one dimensional system has a gap this crossover becomes a deconfinement transition between a one dimensional gapped state and a three dimensional gapless one. Since in one dimension a Mott insulator state is much ease to obtain than in higher dimensions, for coupled 1D chains the competition between the Mott insulating physics and interchain hopping gives a transition between a 1D insulator and a 3D metal, superfluid or superconductor.

For fermions this transition remains a theoretical challenge and has been observed in coupled chain systems such as the organic conductors (so called Bechgaard salts). Experimentally it was clearly shown that these materials are Mott insulators/Luttinger liquids at high temperature, but the dimensional crossover remained very poorly understood. We developed a mean field approach to tackle this question, by replacing the problem of coupled chains by a single chain coupled to an effective bath.

This method allows us to describe the deconfinement transition for coupled Hubbard chains and to study the physical properties of the resulting low temperature Fermi liquid phase. In Fig. 1 the variation of the Luttinger parameter K_ρ probing the deconfinement transition is shown.

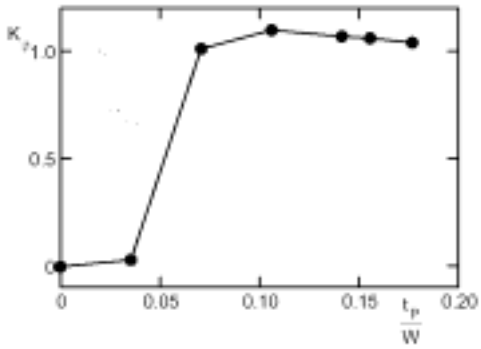

Fig.1. Solution for a system of coupled Hubbard chains. The Luttinger parameter K_ρ. goes from zero to one when the interchain hopping $t_\perp$ is increased relatively to the intrachain bandwidth W. This is the characteristic of a transition from a one dimensional Mott insulator to a three dimensional Fermi liquid.

The method also allows analysing the lifetime and excitations of the system. Fig. 2 shows the self energy at the transition. Around $k = \pm\pi/2$ points with small quasiparticle residue (hot spots) might exist. On the metallic side the quasiparticle residue is quite uniform along the Fermi surface and no sign of hot spots is found within our calculation [1].

We are now pursuing efforts to extend these calculations to quarter filled Mott insulators and to study the transport properties in the Mott insulating phase, in connection with the experiments performed in the Bechgaard salts.

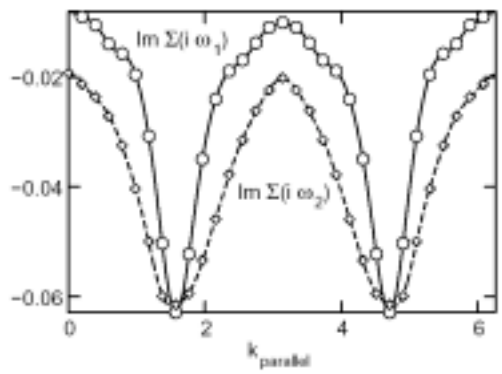

Fig.2. Imaginary part of the self-energy as a functions of the momentum k along the chains, for the two lowest Matsubara frequencies. The strong dip indicates that around k = ±π/2 metallic points with very small quasiparticle residues could exist.

The deconfinement transition is important not only for fermionic systems, but also for bosonic ones. In condensed matter, the bosonic situation applies in the context of spin chains (spins are equivalent to hard core bosons) but recently an extremely clean and tunable realization of such a system has been provided by ultracold atoms trapped in optical lattices. We thus investigated a system made of a two dimensional lattice of long one dimensional tubes. Such a system has a deconfinement transition between a Mott insulator of bosons and a three dimensional superfluid (see Fig. 3).

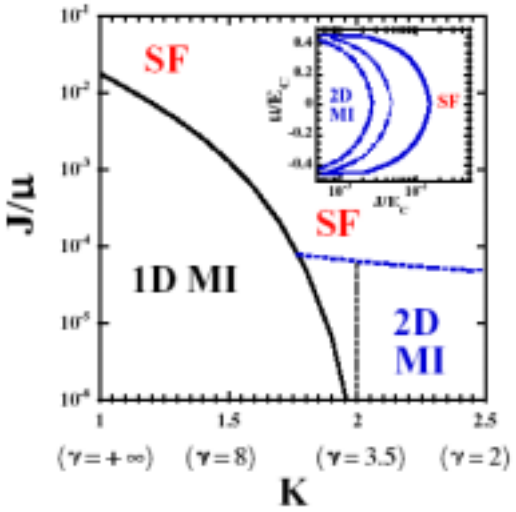

Fig.3. Zero-temperature phase diagram of a 2D lattice of coupled 1D boson systems. K is the Luttinger parameter, J the interchain tunneling for the bosons and μ the chemical potential. For infinite 1D systems only two phases exist: a 1D Mott insulator (1D MI) and a 3D (but anisotropic) superfluid (SF). For finite tubes, a 2D Mott insulator can exist below the horizontal dashed curve. The insert is the phase diagram of a 2D optical lattice of finite 1D systems.

We computed the phase diagram and the various physical quantities (condensate fraction, modes etc.). Due to the interactions there is a large depletion of the condensate which makes the physics quite different from the usual case of a simple anisotropic three dimensional Bose condensate. Recently the quasi one dimensional geometry has been realized and the phases found are in agreement with our predictions [2].

Pinning of quantum crystals

Strong enough interactions can lead to drastic effects even in higher dimensions. As predicted a long time ago by Wigner, if the density of an electronic system is low enough or if the kinetic energy can be blocked by a very strong external magnetic field, the electrons crystallize. This quantum crystal of electrons is a unique phase of matter with remarkable properties. This phase has thus been long searched for. Since no direct imaging of the Wigner crystal has been feasible so far, one can access the properties of this phase mostly through its transport properties, which makes it quite difficult to know whether this phase is indeed realized or not.

In the presence of disorder this crystal is pinned by impurities and acquires remarkable glassy properties. We investigated the physical properties of such a Wigner glass phase, using a variational approach. This approach, tailored to deal with glasses, allowed us to compute the optical longitudinal and Hall conductivities and, in particular, to obtain the density and magnetic field dependence of the pinning peak (see Fig. 4). Our calculation shows a good agreement of these dependencies with the observed ones, proving that a Wigner crystal was indeed formed. We also obtain correctly an asymmetric lineshape, in agreement with experiment, at variance with the Lorentzian broadening that was commonly used.

We have also looked at the case where Wigner crystallization occurs even in the absence of an external magnetic field.

Such a situation is relevant for the 2DEG systems exhibiting the so called Metal-Insulator transition. Besides the question of the existence of such a transition, which is still very controversial, one important issue is whether or not the insulating phase in these systems is a Wigner crystal. Optical conductivity is again a probe to decide unambiguously on this issue. As an example we show in Fig. 5 the surface acoustic wave (SAW) velocity shift predicted for such a system.

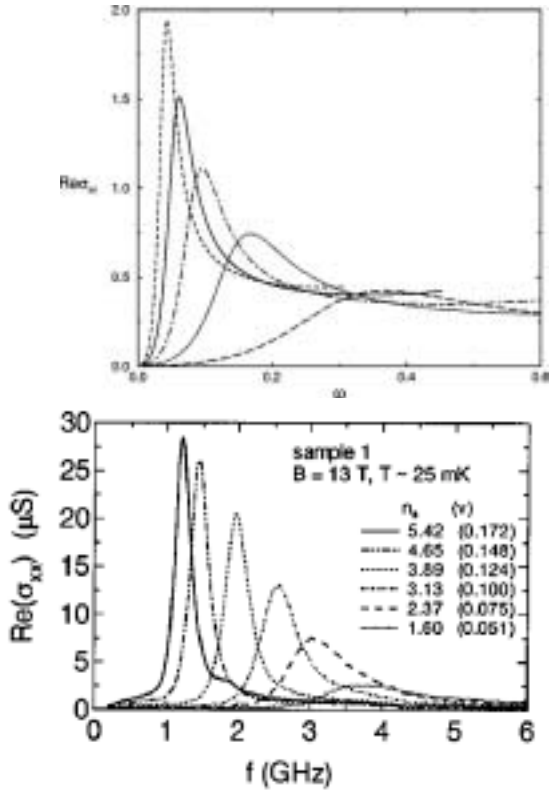

*Fig.4. Calculation of the optical conductivity of a disordered Wigner crystal (top). The maximum of absorption corresponds to the pinning frequency. The lineshape, density and magnetic field dependence are in good agreement with the observed dependence in a two dimensional electron gas under a strong magnetic field (bottom, from C. C. Li et al PRB **61** 10905 (2000)).*

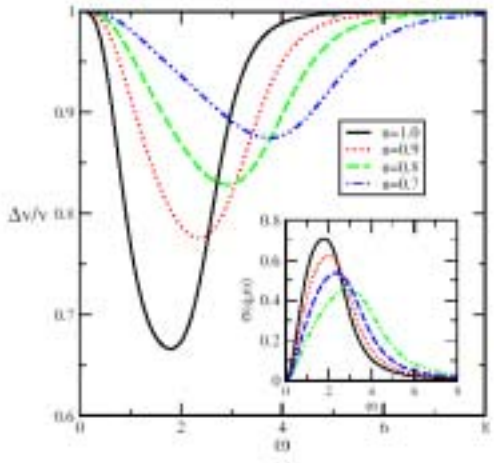

Fig.5 The SAW velocity shift (in arbitrary units) as a function of the frequency ω = vq The curves are plotted for various values of the density n. The corresponding q dependent conductivity is shown in the inset.

Using the same approach we could compute other physical quantities such as the capacitance of a Wigner crystal system (often referred in the literature as "compressibility"). We showed that this thermodynamic "compressibility" (i.e. rigorously at zero frequency) is negative and unaffected by the disorder. The negative compressibility traduces the overscreening of an external charge by the Wigner crystal. However, as a consequence of the glassy nature of the system, the same ``compressibility'' measured at a small frequency (the experimentally relevant situation) is zero. This property is reminiscent of the Coulomb gap [3].

Finally the same approach allowed us to extract the specific heat of such quantum glasses. Indeed understanding the behaviour of the specific heat in disordered and glassy systems is a long standing problem. A general, although phenomenological interpretation was proposed assuming the existence of two level systems and led to a linear specific heat at low temperatures. Despite its remarkable success for many systems, the range of applicability and microscopic justification of such a model are still open questions. Furthermore for classical system the behaviour depends on whether the variables are taken to be discrete or continuous Contrarily to the naïve expectation of a linear T dependence, we find a T^3 behaviour at low temperatures. Since then, this behaviour has also been found in other models such as quantum impurity models. The physical reason why the linear term cancels in these quantum systems is still unclear. A possibility could be the presence of an hidden symmetry [4].

Non linear transport in Mott insulators and Luttinger liquids

Many strongly interacting systems (Luttinger liquids, Mott insulators, Wigner crystals) are very sensitive to perturbations that can localize the charge. This is the case of a periodic potential (due for example to the presence of the lattice) or to impurities. The first case leads to a Mott insulating state, the second one to an Anderson insulator where the electrons are localized by the impurities. These two states are insulators, and thus their linear conductivity vanishes at zero temperature, and these systems present a non linear I-V characteristics. Despite its experimental importance it is very difficult to compute the transport in such systems, and only phenomenological models could be developed (such as the variable range hopping for disordered noninteracting electrons).

For the case of the one dimensional Luttinger liquid we computed this non linear response for the case of very small electric field E, using an instanton technique. In that case the transport is determined by tunneling events

between pinned states (either on the periodic potential or the impurities) and is of the form

$$I \propto e^{-(A/E)^{\nu}}$$

where ν=1 for the Mott insulator and ν=1/2 for the disordered case. Such a behaviour is the quantum analogue of the creep phenomenon for classical systems where the system overcomes barriers though thermal activation. Here quantum effects allow it to pass the barriers.
At finite temperature the system can overcome the pinning, thanks to thermal activation, and the response becomes linear with the current proportional to the electric field. The conductivity has the same exponential form as above but with E replaced by the temperature T. For the disordered case this is a law similar to the variable range hopping of Mott. It is interesting to note that in our result the interactions are completely taken into account. As a consequence the energy scales (the constant A) are determined by the kinetic energy and the electron-electron interaction, which considerably changes the value of this constant (simply the density of states for the standard VRH law). How such a law evolves in higher dimensions is an interesting still yet open question [5].

Tunneling between superconductors

In order to study the nonlinear transport in strongly interacting systems, such as Luttinger liquids, connected to superconducting leads, we have started to develop a formulation of this problem based on the Keldish technique, the only one at the moment able to tackle out of equilibrium situations.
As a first step to this problem we have computed the tunneling directly between the two leads. In addition to the standard singlet pairing in the leads, our technique allows us to treat the case of spin triplet paring. It thus allows for a complete calculation of the I-V tunneling characteristics, with the only approximation of a BCS-like Hamiltonian to describe the leads.
As a result of this calculation, we have shown that distinctive features are present in the I-V characteristics of different kinds of junctions, in particular when the Zeeman effect of a magnetic field is taken into account (see *Fig.6*). Thus in addition to the methodological interest itself our calculation can be used to directly probe the symmetry pairing of some triplet pairing candidates. Our analysis is particularly relevant for the case of the quasi-one dimensional organic conductors. Indeed, it was observed during recent years that, at low temperatures, certain superconducting organic compounds (like $(TMTSF)_2$ -PF_6, -ClO_4, etc.) show upper critical fields in excess of the Pauli-Clogston paramagnetic limit; usually depending on the angular orientation of the field with respect to the crystalline axes.

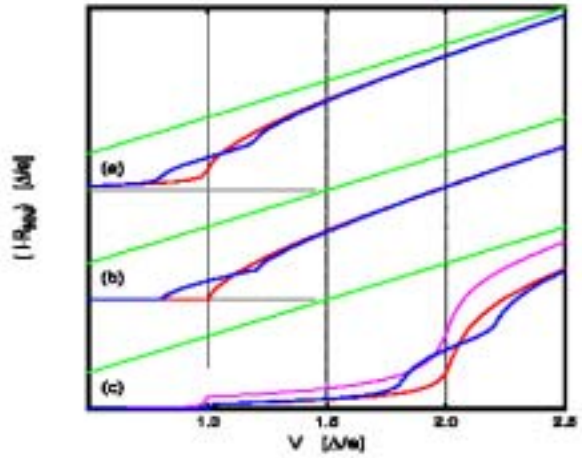

Fig.6. Three different sets of I-V characteristics vertically displaced for clarity. From top to bottom: (a) for an N-S junction, (b) N-T junction, (c) S-T junction. The red (blue) lines correspond to the characteristics in the absence (presence) of an oriented magnetic field. In all three sets, the curve for the N-N case (green) is plotted as reference and in the third one the curve for an S-S junction (purple) is also given for comparison.

High critical fields constitute an indication of possible triplet-pairing superconducting phases. An unambiguous interpretation of this effect is of course difficult and independent confirmations of the unconventional paring scenario are therefore desirable. A large number of independent experimental checks were both proposed and some carried out, but none were conclusive. The observation of the features shown in Fig. 1 would constitute a sensitive experiment that permits one to identify the type of pairing in these materials [6]

References:
For more details and further references see:

[1] T. Giamarchi, S. Biermann, A. Georges and A. Lichtenstein, cond-mat/0401268 (to be published in J. Physique IV).
[2] A.F. Ho, M. A. Cazalilla and T. Giamarchi, cond-mat/ 0310382.
[3] R. Chitra, T. Giamarchi and P. Le Doussal, PRB B **65**, 035312 (2002) ; R. Chitra and T. Giamarchi cond-mat/2004.
[4] G. Schehr, T. Giamarchi and P. Le Doussal, PRL **91** 117002 (2003); cond-mat/0301053 (to be published in Europhys. Let.).
[5] T. Nattermann, T. Giamarchi and P. Le Doussal, PRL **91**, 056603 (2003).
[6] C. Bolech and T. Giamarchi, cond-mat/ 0309195 (to be published in PRL).

4 Three years of MaNEP's life

4.1 Inauguration and Open Doors

The inauguration of MaNEP was held on September 10th 2002 at the home institution, University of Geneva. Political, scientific and academic authorities, as well as MaNEP researchers were invited to the official ceremony held in the Physics Department. A total of 250 participants attended this event. During the ceremony, a 15 minutes movie produced by MaNEP, "*Voyage en classe perovskite*", aimed at high school students, was presented for the first time.

In the days following the inauguration, Open Doors were organized for classes of high schools and the general public of Geneva. A total of about 1000 persons have attended the Open Doors, half of them were high schools students.

L'inauguration de MaNEP a eu lieu le 10 septembre 2002 à l'Université de Genève, institution hôte. Les autorités politiques, scientifiques et académiques, ainsi que les chercheurs de MaNEP, ont été invités à la cérémonie officielle qui s'est tenue à la Section de Physique. Au total, environ 250 participants ont assisté à cet événement. Pendant la cérémonie, "*Voyage en classe perovskite*", un film de 15 minutes, produit par MaNEP à l'intention des étudiants et des lycéens, a été présenté pour la première fois.

Des journées *Portes Ouvertes* ont été organisées à l'intention des écoles et du public genevois dans les jours qui ont suivi l'inauguration. Environ un millier de personnes ont participé à l'événement, la moitié formée de classes d'élèves des Collèges et des Cycles d'Orientation genevois.

Demonstrations to the public

Levitation train

Magnetic levitation

Fault current limiter

Visit of laboratories

Scanning electron microscopy

Applied superconductivity

Scanning tunneling microscopy

4.2 Newsletters and Catalogue of Facilities

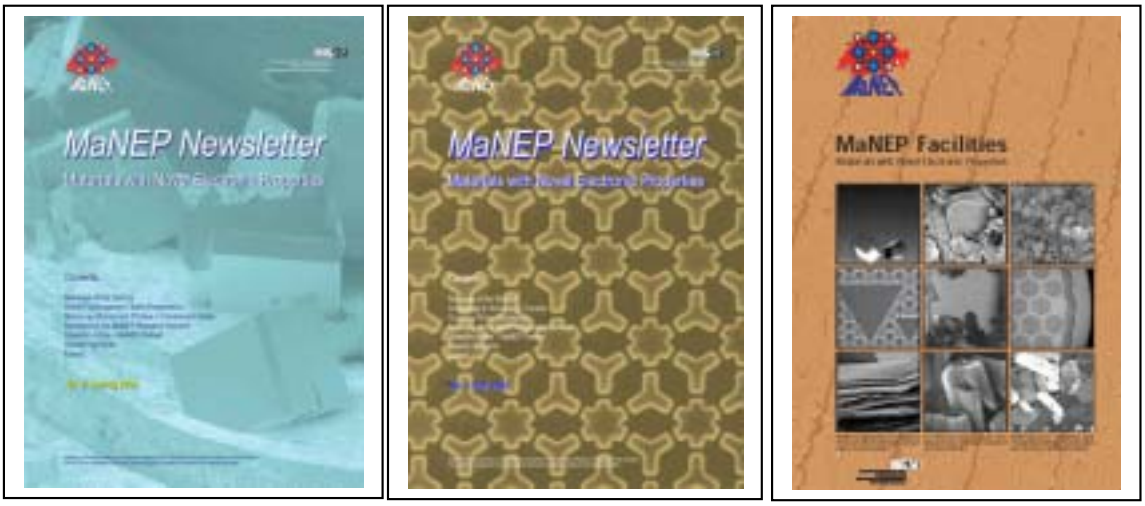

The biannual *MaNEP Newsletters* were distributed to the MaNEP's members and to the members of InduNet, the industrial Network. The Newsletter provides information on recent results obtained in the field of MaNEP.

MaNEP Facilities is a reference document containing a directory of the material synthesised within MaNEP, a description of all experimental devices and related techniques; and a summary of the theoretical competencies available within MaNEP.

4.3 Movie "*Voyage en classe perovskite*"

The scenario of this movie was written for young students and special care was taken to adap the scientific content to the level of students with few or even no knowledge of advanced physics. To reach this goal, the scenario mixes reality (present equipment with conventional materials) and virtuality (dreams concretised with these new materials with surprising properties) to suggest what may become possible if the development of such new materials can be pushed further. We hope that this movie, along with the Open Doors, will motivate students to study physics and pursue a career as a researcher in the field of material sciences.

4.4 Education and training

Since MaNEP was launched, a number of educational and training activities were organized:

Topical meetings

The topical meetings serve several purposes. One important aim is in education and training. Since students participating to these meetings come from different backgrounds, we plan to introduce each topic with an overview aimed at the younger participants. The first topical meeting was held in Neuchâtel on "*Non-Fermi Liquids and Low Dimensional Systems*", Professor Thierry Giamarchi gave a much appreciated tutorial on "*Physics of one dimensional metals*". This tutorial was a fine introduction to the 3 other sessions presented by younger speakers.

The second brought together 72 participants and was organized in Neuchâtel on June 25-26, 2003 just before the site visit of the MaNEP

Review Panel. The specific topic was: "*Materials: preparation, characterization, and specific properties*". The program of this topical meeting is given in Appendix E.

The third meeting was particular: The Swiss Physical Society (SPS) invited the three NCCR in physics (NANO, Quantum Photonics and MaNEP) to participate actively to its annual meeting. This joint-event took place in Neuchâtel on March 3-4, 2004. In parallel to the sessions of the SPS, each NCCR had its own session. The MaNEP session brought together 142 participants. At the end, everybody could participate to a half-day poster session where MaNEP presented 101 posters. The program of this meeting is also given in Appendix E.

Swiss Workshop on Materials with Novel Electronic Properties (SWM):

The SWM workshops are organized every second year. The last one took place in Les Diablerets, from September 29 to October 1, 2003. With 207 participants, we reached the maximum capacity offered by the conference room "*Centre des Congrès*". However, the workshop was, once more, a privileged occasion for the whole MaNEP scientific community to gather. The schedule of these three days was very dense, as it can be seen from the program given in Appendix E. Several invited speakers came from abroad to deliver outstanding talks which contributed to trigger fruitful discussions all along the workshop duration.

Mobile post-docs

The program for the mobility of the young advanced researchers was presented in the last report. It is now active and two post-doc positions financed by MaNEP were awarded by the Advisory Board.

Summer schools

MaNEP co-organized with PSI the 2002 Summer School on *Magnetism in Condensed Matter*. Several project leaders were actively involved in this event. A special thanks to Prof. A. Furrer and his administrative team who were deeply involved in this organisation at the great satisfaction of all the participants. 93 scientists from many European countries participated to this summer school. Among them, 50 were from Swiss institutes, indicating that the great interest of the scientific community to this subject corresponded to a demand.

The second MaNEP Summer School was actively prepared during the present term. It shall be held in Saas-Fee on September 6-11, 2004. Registration is open at the time of writing this report. The purpose of this summer school shall be to provide basic theoretical knowledge of the physics of strongly correlated electron systems. Three main courses will give an overview of the physics of materials with weak to strong electronic correlations. The lecturer will be:

- D. Khomskii, University of Cologne, Germany, on *Basic Electronic Structure*,
- T. Giamarchi, University of Geneva: *From Fermi to non-Fermi liquids,*
- and M. Sigrist, ETH-Zurich on *Conventional and Unconventional Superconductivity.*

Additional presentations will be focused on physical properties, development of applications and materials processing of these new materials with a total of ten lecturers.

5 Three Years of Publications

The most important publications are outlined by an asterisk in front of the first author.

5.1 Scientific articles in journals with peer review

Project 1, M. Büttiker, University of Geneva

W. BELZIG, P. SAMUELSSON
Full counting statistics of incoherent Andreev transport
Europhys. Lett. ***64****, 253 (2003)*

M. BÜTTIKER , P. SAMUELSSON
Hanbury Brown-Twiss effects in channel mixing normal-superconducting systems
Proceedings of the XXIII Conference on Low Temperature Physics, Hiroshima, Japan, Aug. 20 - 27, 2002. Physica E (unpublished)

M. BÜTTIKER, P. SAMUELSSON, E.V. SUKHORUKOV
Entangled Hanbury Brown Twiss effects with edge states
Physica E ***20****, 33 (2003)*

M.-S. CHOI, D. SÁNCHEZ, R. LÓPEZ
Kondo effect in a quantum dot coupled to ferromagnetic leads : A numerical renormalization group analysis
Phys. Rev. Lett. ***92****, 056601 (2004)*

G. JOHANSSON, P. SAMUELSSON, Å. INGERMAN
Full counting statistics of multiple Andreev reflection
Phys. Rev. Lett. ***91****, 187002 (2003)*

R. LÓPEZ, R. AGUADO, G. PLATERO
Shot noise in strongly correlated double quantum dots
Submitted to Phys. Rev. B (2004)

D. SANCHEZ, R. LÓPEZ, P. SAMUELSSON, M. BÜTTIKER
Andreev drag effect in ferromagnetic-normal-superconducting systems,
Phys. Rev. B ***68****, 214501 (2003)*

K.E. NAGAEV, P. SAMUELSSON , S. PILGRAM
Cascade approach to current fluctuations in a chaotic cavity
Phys. Rev. B ***66****, 195318 (2002)*

P. SAMUELSSON
Energy dependent counting statistics in superconducting tunnel junctions
Phys. Rev. B, to appear

P. SAMUELSSON, W. BELZIG, YU. V. NAZAROV
Andreev reflection eigenvalue density in mesoscopic conductors
cond-mat/0312133

***** P. SAMUELSSON, M. BÜTTIKER
Chaotic dot-superconductor analog of the Hanbury Brown-Twiss effect
Phys. Rev. Lett. ***89,*** *046601(4 pages) (2002)*

P.SAMUELSSON, M. BÜTTIKER
Semiclassical theory of current correlations in chaotic dot-superconductor systems
Phys. Rev. B ***66,*** *201306 (2002)*

P. SAMUELSSON, Å. INGERMAN, G. JOHANSSON, E.V. BEZUGLYI, V.S. SHUMEIKO, G. WENDIN, R. KÜRSTEN, A. RICHTER, T. MATSUYAMA, U. MERKT
Coherent current transport in wide ballistic Josephson junctions
cond-mat/0311344

***** P. SAMUELSSON, E.V. SUKHORUKOV, M. BÜTTIKER
Two-particle Aharonov-Bohm effect and Entanglement in the electronic Hanbury Brown - Twiss set-up
Phys. Rev. Lett ***92****, 026805 (2004)*

P. SAMUELSSON, E.V. SUKHORUKOV, M. BÜTTIKER
Orbital entanglement and violation of Bell inequalities in mesoscopic conductors
Phys. Rev. Lett. ***91****, 157002 (2003)*

P. SAMUELSSON, E.V. SUKHORUKOV, M. BÜTTIKER
Orbital entanglement and violation of Bell inequalities in the presence of dephasing
Turk. J. Phys. ***27****, 481 (2003)*

P. SAMUELSSON, E.V. SUKHORUKOV, M. BÜTTIKER
Electrical current noise of a beam-splitter as a test of spin entanglement

To be submitted

Project 2, Ø. Fischer, University of Geneva

L. ANTOGNAZZA, M. DECROUX, S. REYMOND, E. DE CHAMBRIER, W. PAUL, M. CHEN, Ø. FISCHER
Simulation of the behavior of superconducting YBCO lines at high current densities
Physica C ***372-376,*** *1684-1687(2002)*

R. CUBITT, M. R. ESKILDSEN, C. D. DEWHURST, J. JUN, S. M. KAZAKOV, J. KARPINSKI
Effects of Two-Band Superconductivity on the Flux Line Lattice in Magnesium Diboride
Phys. Rev. Letter. ***91****, 047002 (2003)*
In collaboration with project 8 H.R. Ott, ETHZ

M. DECROUX, L. ANTOGNAZZA, S. REYMOND, W. PAUL, M. CHEN, Ø. FISCHER
Studies of YBCO strip lines under voltage pulses: optimisation of the design of fault current limiters
*IEEE Trans. On Applied Superconductivity, Vol.****13****, 1988 (2003)*

M. R. ESKILDSEN, C. D. DEWHURST, B. W. HOOGENBOOM, C. PETROVIC AND P. C. CANFIELD
Hexagonal and Square Flux Line Lattices in $CeCoIn_5$
Submitted to Phys. Rev. Lett. (cond-mat/0211585)
In collaboration with project 8 H.R. Ott, ETHZ

M.R. ESKILDSEN, N. JENKINS, G. LEVY, M. KUGLER, Ø. FISCHER, J. JUN, S.M. KAZAKOV, J. KARPINSKI
Vortex Imaging in Magnesium Diboride with H_c
Physical Rev.B ***68****, 100508 (2003)*
In collaboration with project 8 H.R. Ott, ETHZ

***** M. R. ESKILDSEN, M. KUGLER, S. TANAKA, J. JUN, S. M. KAZAKOV, J. KARPINSKI, Ø. FISCHER
Vortex Imaging in the π***-Band of Magnesium Diboride***
Phys. Rev. Lett. ***89****, 187003 (4pages) (2002)*
In collaboration with project 8 H.R. Ott, ETHZ

M. R. ESKILDSEN, M. KUGLER, G. LEVY, S. TANAKA, J. JUN, S. M. KAZAKOV, J. KARPINSKI, Ø. FISCHER
Scanning Tunneling Spectroscopy on Single Crystal MgB_2
Physica C ***385****, 169-176 (2003)*
In collaboration with project 8 H.R. Ott, ETHZ

M. R. ESKILDSEN, M. KUGLER, G. LEVY, S. TANAKA, J. JUN, S. M. KAZAKOV, J. KARPINSKI, Ø. FISCHER
Vortex lattice imaging in single crystal MgB_2 ***by scanning tunneling spectroscopy***
Physica C ***388-389****, 143 (2003)*
In collaboration with project 8 H.R. Ott, ETHZ

B. GRÉVIN, I. MAGGIO-APRILE, A. BENTZEN, O. KUFFER, I. JOUMARD, Ø. FISCHER
Scanning tunneling potentiometry search for mesoscopic phase separation in $La_{0.7}Sr_{0.3}MnO_3$
Appl. Phys. Lett. ***80****, 3979 - 3981 (2002)*

B. W. HOOGENBOOM, C. BERTHOD, M. PETER, Ø. FISCHER, A. A. KORDYUK
Modeling scanning tunneling spectra of $Bi_2Sr_2CaCu_2O_{8+d}$
Phys. Rev. B ***67****, 224502 (2003)*
In collaboration with project 4 A. Junod, UniGe

B. W. HOOGENBOOM, C. BERTHOD, M. PETER, Ø. FISCHER, A. A. KORDYUK
Modeling scanning tunneling spectra of $Bi_2Sr_2CaCu_2O_{8+d}$
cond-mat/0212329
In collaboration with project 4 A. Junod, UniGe

***** B. W. HOOGENBOOM, K. KADOWAKI, B. REVAZ, M. LI, CH. RENNER, Ø. FISCHER
Linear and field-independent relation between vortex core state energy and gap in $Bi_2Sr_2CaCu_2O_{8+\delta}$
Phys. Rev. Lett. ***87****, 267001 (2001)*
In collaboration with project 3 R. Flükiger, UniGe

N. JENKINS, M.R. ESKILDSEN, M. KUGLER, Ø. FISCHER, J. JUN, S.M. KAZAKOV, J. KARPINSKI
Shrinking of the π ***band in*** MgB_2 ***by aluminium doping***
submitted to Phys. Rev. Lett.
In collaboration with project 8 H.R. Ott, ETHZ

A. JUNOD, Y. WANG, F. BOUQUET, I. SHEIKIN, P. TOULEMONDE, M. R. ESKILDSEN, M. EISTERER, H. W. WEBER, S. LEE, S. TAJIMA
Specific heat of ceramic and single crystal MgB_2
Physica C, ***388-389****, 107-108 (2003*
In collaboration with project 4 A. Junod, UniGe

J. KARPINSKI, M. ANGST, J. JUN, S. M. KAZAKOV, R. PUZNIAK, A.WISNIEWSKI, J. ROOS, H. KELLER, A. PERUCCHI, L. DEGIORGI, M. R. ESKILDSEN, P. BORDET, L. VINNIKOV, A. MIRONOV
MgB₂ single crystals: high pressure growth and physical properties
Supercond. Sci. Technol. ***16****, (2003) 221-230*
In collaboration with project 8 H.R. Ott, ETHZ and project 13 H. Keller, UniZh

S. REYMOND, L. ANTOGNAZZA, M. DECROUX, Ø. FISCHER
Simulation of the initial response of a high T_c ***superconducting film submitted to a voltage source***
Superconducting Science and Technology ***17****, 522 (2004)*

S. REYMOND, Ø. FISCHER
Low temperature scanning contact potentiometry
Review of Scientific instrument ***75****, 694 (2004)*

M. SALLUZZO, C. ARUTA, M.G. MAGLIONE, F. RICCI, F. NATALI, E. KOLLER, Ø. FISCHER, N.L. SAINI
Evidence of local structural transition during oxidation process of RBCO epitaxial films using time resolved RefleXafs measurements.
Submitted to European Physical Journal B, December 2001

S. REYMOND, L. ANTOGNAZZA, M. DECROUX, E. KOLLER, P. REINERT, Ø. FISCHER
Current-induced highly dissipative domains in high-T_c thin films
*Phys. Rev. B **66**, 14522 (7pages) (2002)*

Project 3, R. Flükiger, University of Geneva

V. ABÄCHERLI, D. UGLIETTI, B. SEEBER, R. FLÜKIGER
$(Nb,Ta,Ti)_3Sn$ multifilamentary wires using Osprey bronze with high tin content and NbTa/NbTi composite filaments
*Physica C **372-376**, 1325-1328 (2002)*

N. CLAYTON, N. MUSOLINO, E. GIANNINI, V. GARNIER, R. FLÜKIGER
Lower Critical Field and Mixed State Magnetisation of Single Crystal $Bi_2Sr_2Ca_2Cu_3O_{10}$
Submitted to Europhysics Letters, January 2004

M. COSTA, E. MARTÍNEZ, C. BEDUZ, Y. YANG, F. GRILLI, B. DUTOIT, E. VINOT, P. TIXADOR
3D modelling of coupling between superconducting filaments via resistive matrix in AC magnetic field
IEEE Trans. Appl. Supercond. (2003) to appear

J. DURON, F. GRILLI, B. DUTOIT, S. STAVREV
Modelling the E-J relation of high-T_c superconductors in an arbitrary current range
*Physica C **401**, 231-235 (2004)*

R. FLÜKIGER, P. LEZZA, C. BENEDUCE, N. MUSOLINO, H. L. SUO
Improved transport critical current and irreversibility fields in mono- and multifilamentary Fe/MgB_2 tapes and wires using fine powders
*Supercond. Sci. Technol. **16** 264-270 (2003)*

R. FLÜKIGER, H. L. SUO, N. MUSOLINO, C. BENEDUCE, P. TOULEMONDE, P. LEZZA
Superconducting properties of MgB_2 tapes and wires
*Physica C **385** (1-2) 286-305 (2003) and Physica C **387** (3-4) 419 (2003)*

V. GARNIER, R. PASSERINI, E. GIANNINI, R. FLÜKIGER
New understanding of the role of Ag at underformed Ag/Bi,Pb (2223) interface: texturing and outgrowths
*Supercond. Sci. Technol **16**, 820-826 (2003)*

E. GIANNINI, V. GARNIER, R. GLADYSHEVSKII, R. FLÜKIGER
Growth and characterization of $Bi_2Sr_2Ca_2Cu_3O_{10}$ and $(BiPb)_2Sr_2Ca_2Cu_3$ $O_{10-\delta}$ single crystals
*Supercond. Sci. Technol. **17**, 220-226 (2004)*

E. GIANNINI, V. GARNIER, I. SAVYSYUK, R. PASSERINI, G. WITZ, X.D. SU, B. SEEBER, L. HUA, R. FLÜKIGER
Partial melting and HIP processing of Bi(2223): bulk and tapes
*IEEE Transactions on Applied Superconductivity, **13** (2) 3008-3013 (2003)*

E. GIANNINI, I. SAVYSYUK, V. GARNIER, R. PASSERINI, P. TOULEMONDE, R. FLÜKIGER
Reversible melting and equilibrium phase formation of $(Bi,Pb)_2Sr_2Ca_2Cu_3O_{10+\delta}$
*Supercond. Sci. Technol. **15**, 1577-1586 (2002)*

E.GIANNINI, R. PASSERINI, P. TOULEMONDE, E. WALKER, M. LOMELLO-TAFIN, D. HEPTYAKOV, R. FLÜKIGER
Bi,Pb(2223) equilibrium and decomposition: in situ high-temperature neutron diffracion study
*Physica C **372-376,** 895-898 (2002)*

R. GLADYSHEVSKII, N. MUSOLINO, R. CERNY, E. WALKER AND R. FLÜKIGER
Crystal Structure of modulation-free Bi,Pb-2212
Submitted to Acta Cryst., January (2004)

F. GRILLI, M. COSTA BOUZO, Y. YANG, C. BEDUZ, B. DUTOIT
Finite element method analysis of the coupling effect between superconducting filaments of different aspect ratio
*Superconductor Science and Technology **16**, 1228-1234 (2003)*

F. GRILLI, M. SJÖSTRÖM
Prediction of resistive and hysteretic losses in a multi-layer high-T_c superconducting cable
*Superconductor Science and Technology **17**, 409-416 (2004)*

F. GRILLI, S. STAVREV, B. DUTOIT, Y. LE FLOCH, E. VINOT, G. MEUNIER, I. KLUTSCH, P. TIXADOR
Finite element method modelling of superconductors: from 2D to 3D
submitted to IEEE Trans. Magn.

F. GRILLI, S. STAVREV, B. DUTOIT, S. SPREAFICO
Numerical analysis of the effects of the magnetic self-field on the transport properties of a multi-layer HTS cable
*IEEE Trans. Applied Superconductivity **14** (2004) to be published*

F. GRILLI, S. STAVREV, B. DUTOIT, S. SPREAFICO
Numerical Modelling of a HTS Cable
*IEEE Trans. Applied Superconductivity **13**, 1886-1889 (2003)*

F. GRILLI, S. STAVREV, B. DUTOIT, S. SPREAFICO, R. TEBANO, G. COLETTA, F. GÖMÖRY, J. ŠOUC
Numerical modelling of a HTS cable in AC regime
*Physica C **401**, 176-181 (2004)*

B. W. HOOGENBOOM, K. KADOWAKI, B. REVAZ, Ø. FISCHER
Homogeneous samples of $Bi_2Sr_2CaCu_2O_{8+d}$
Physica C **391,** 376 (2003)
In collaboration with project 2 Ø. Fischer, UniGe

***** B. W. HOOGENBOOM, K. KADOWAKI, B. REVAZ, M. LI, CH. RENNER, Ø. FISCHER
Linear and field-independent relation between vortex core state energy and gap in $Bi_2Sr_2CaCu_2O_{8+\delta}$
*Phys. Rev. Lett. **87**, 267001 (2001)*
In collaboration with project 2 Ø. Fischer, UniGe

P. LEZZA, V. ABÄCHERLI, N. CLAYTON, C. SENATORE, D. UGLIETTI, H.L. SUO, R. FLÜKIGER
Transport properties and exponential n-values of Fe/MgB_2 tapes with various MgB_2 particle sizes
*Physica C **401**, 305-309 (2004)*

N. MUSOLINO, S. BALS, G. VAN TENDELOO, N. CLAYTON, E. WALKER AND R. FLÜKIGER
Modulation-free phase in heavily Pb-doped (Bi,Pb) 2212 crystals
*Physica C **399**, 1-7 (2003)*

N. MUSOLINO, S. BALS, G. VAN TENDELOO, N. CLAYTON, E. WALKER, R. FLÜKIGER
Investigation of (Bi,Pb) 2212 crystals: observation of modulation-free phase
*Physica C **401,** 270-272 (2004)*

N. NIBBIO, S. STAVREV, B. DUTOIT
Finite element method simulation of ac loss in HTS tapes with B-dependent E-J power law
*IEEE Transactions on Applied Superconductivity, Vol. **11**, Nr. 1, 2631-2634 (2001)*

N. NIBBIO, S. STAVREV
Effect of the geometry of HTS on AC loss by using finite element method simulation with B-dependent E-J power law
*IEEE Transactions on Applied Superconductivity, Vol. **11**, Nr. 1, 2627-2630 (2001)*

R. PASSERINI, M. DHALLÉ, E. GIANNINI, R. FLÜKIGER
SEM investigation of outgrowths formation mechanism in Ag-sheathed Bi,Pb(2223) tapes
*Supercond. Sci. Technol. **15**, 1203-1212 (2002)*

R. PASSERINI, M. DHALLÉ, B. SEEBER, AND R. FLÜKIGER
Mechanical properties of Bi,Pb(2223) single filaments and $I_c(\varepsilon)$ behaviour in longitudinally strained tapes
*Supercond. Sci. Technol. **15**, 1507-1511(2002)*

B. SEEBER, D. UGLIETTI, V. ABÄCHERLI, D. ECKERT, P. LEZZA, A. POLLINI, R. FLÜKIGER
Critical current vs. Strain measurement up to 1000 A of long length superconducting wires and tapes
submitted to Supercond. Sci. Technol., October 2003

C. SENATORE, M. POLICHETTI, N. CLAYTON, R. FLÜKIGER, S. PACE
Non-linear magnetic response of MgB_2 bulk superconductors
Physica C **401**, 182-186 (2004)

M. SJÖSTRÖM, B. DUTOIT, J. DURON
Equivalent Circuit Model for Superconductors
IEEE Trans. Applied Superconductivity **13**, 1890-1893 (2003)

S. STAVREV, B. DUTOIT
Geometry considerations for transport current applications of Bi-2223 conductors with anisotropic $J_c(B)$ in external magnetic field
EUCAS 2001, 26-30 August, Copenhagen, Submitted to Physica C

S. STAVREV, B. DUTOIT, F. GRILLI
Self-field and geometry effects in transport current applications of multifilamentary Bi-2223/Ag conductors
*IEEE Trans. Applied Suuperconductivity **13**, 3807 – 3813 (2003)*

S. STAVREV, B. DUTOIT, P. LOMBARD
Numerical modelling and AC losses in multifilamentary Bi-2223/Ag conductors with various geometry and filament arrangement
*Physica C **384**, 19-31 (2003)*

S. STAVREV, B. DUTOIT, P. LOMBARD
AC Losses of Multifilamentary Bi-2223/Ag Conductors with Different Geometry and Filament Arrangement
*IEEE Trans. Applied Superconductivity **13**, 3561-3665 (2003)*

S. STAVREV, B. DUTOIT, N. NIBBIO
Geometry considerations for use of Bi-2223/Ag tapes and wires with different models of $J_c(B)$
*IEEE Trans. Appl. Supercond., vol. **12**, no. 3 1857-1865 (2002)*

S. STAVREV, Y. YANG, B. DUTOIT
Modelling and AC losses of BSCCO conductors with anisotropic and position-dependent J_c
*Physica C **378-381**, 1091-1096 (2002)*

S. STAVREV, I. KLUTSCH, P. SKOV-HANSEN, F. GRILLI, E. VINOT, J. B. HANSEN, B. DUTOIT, P. TIXADOR, G. MEUNIER
Numerical modelling of Bi-2223 multifilamentary tapes with position- dependent J_c
*Physica C **372-376**, 1800-1805 (2002)*

S. STAVREV, E. VINOT, Y. YANG, F. GRILLI, I. KLUTSCH, E. MARTINEZ, B. DUTOIT, G. MEUNIER, N. NIBBIO, P. TIXADOR
Comparison of numerical methods for modelling of superconductors
IEEE Trans. Magn. Vol. ***38,*** *no. 2 849-852 (2002)*

X.D. SU, G. WITZ, K. KWASNITZA, R. FLÜKIGER
Fabrication of square and round Ag/Bi(2223) wires and their ac loss behaviour
Supercond. Sci. Technol. ***15****, 1184-1189 (2002)*

H.L. SUO, C. BENEDUCE, M. DHALLÉ , N. MUSOLINO, X.D. SU, R. FLÜKIGER
High transport and inductive critical currents in dense Fe- and Ni-Clad MgB_2 tapes using fine powder
Advances in Cryogenic Engineering Materials, volume ***488****, 872-879*

***** H.L. SUO, C. BENEDUCE, M. DHALLÉ, N. MUSOLINO, J-Y. GENOUD, R. FLÜKIGER
Large transport critical currents in dense Fe- and Ni-clad MgB_2
Applied Physics Letters ***79****, 3116, (2001)*

H.L. SUO, C. BENEDUCE, X.D. SU, R. FLÜKIGER
Fabrication and transport critical currents of multifilamentary MgB_2/Fe wires and tapes
Supercond. Sci. Technol. ***15****, 1058 (10 pages) (2002)*

H.L. SUO, J.-Y. GENOUD, P. CARACINO, S. SPREAFICO, M. SCHINDL, E. WALKER, R. FLÜKIGER
Mechanically reinforced {110}<110> textured Ag/Ni-alloys composite substrates for low-cost coated conductors
Physica C ***372-376****, 835-838 (2002)*

H.L. SUO, P. LEZZA, D. UGLIETTI, C. BENEDUCE, V. ABÄCHERLI, R. FLÜKIGER
High transport critical current densities and n factors in mono and multi-filamentary MgB_2/Fe tapes and wires using fine powder
I*EEE Transactions on Applied Superconductivity* ***13*** *(2). 3265-3268 (2003)*

D. UGLIETTI, B. SEEBER, V. ABÄCHERLI, A. POLLINI, D.ECKERT, R. FLÜKIGER
A device for critical current versus strain measurements up to 1000 A and 17 T on 80 cm long HTS and LTS technical superconductors
Supercond. Sci. Technol. ***16****, 1000-1004 (2003)*

D. UGLIETTI, B. SEEBER, V. ABÄCHERLI, A. POLLINI, D. ECKERT, R. FLÜKIGER
A device for critical current vs strain measurements up to 1000 A and 17 T on 80 cm long HTS and LTS technical superconductors
Supercond. Sci. Technol. ***16****, 1000–1004 (2003)*

F. VENTURINI, M. OPEL, H. BERGER, L. FORRÓ, B. REVAZ
Doping dependence of the electronic Raman spectra in cuprates
J. Phys. Chem. Solids ***63****, 2345 (2002)*

In collaboration with project 11 L. Forró, EPFL and project 12 G. Margaritondo, EPFL

F. VENTURINI, M. OPEL, T. P. DEVEREAUX, J. K. FREERICKS, I. TÜTTO, B. REVAZ, E. WALKER, H. BERGER, L. FORRÓ, R. HACKL
Observation of an unconventional metal-insulator transition in overdoped CuO_2 compounds
Phys. Rev. Lett. ***89****, 107003 (2002)*
In collaboration with project 11 L. Forró, EPFL and project 12 G. Margaritondo, EPFL

Y. WANG, F. BOUQUET, I. SHEIKIN, P. TOULEMONDE, B. REVAZ, M. EISTERER, H.W. WEBER, J. HINDERER, A. JUNOD
Specific heat of MgB_2 after irradiation
J. Phys.: Cond. Matter ***15****, 883-893 (2003)*
In collaboration with project 4 A. Junod, UniGe and project 8 H.R. Ott, ETHZ

G. WITZ, X.-D. SU, K. KWASNITZA, M. DHALLÉ, C. BENEDUCE, R. PASSERINI, E. GIANNINI, R. FLÜKIGER
Reduction of AC losses in Bi-Pb(2223) tapes by the introduction of barriers and the use of new wire configurations
Physica C ***372-376****, 1814-1817 (2002)*

X.D. SU, G. WITZ, K. KWASNITZA, R. FLÜKIGER
Fabrication of square and round Ag/Bi(2223) wires and their ac loss behaviour
Supercond. Sci. Technol. ***15****, 1184-1189 (2002)*

X.D. SU, G. WITZ, R. PASSERINI, K. KWASNITZA, R. FLÜKIGER
Square and round Bi(2223) wire configurations and their AC losses
Physica C ***372-376****, 942-944 (2002)*

Project 4, A. Junod, University of Geneva

***** F. BOUQUET, Y. WANG, R.A. FISHER., D.G. HINKS, J.D. JORGENSEN, A. JUNOD, N.E. PHILLIPS
Phenomenological two-gap model for the specific heat of MgB_2
Europhys. Lett. ***56****, 856-862 (2001)*

***** F. BOUQUET, Y. WANG, I. SHEIKIN, T. PLACKOWSKI, A. JUNOD, S. LEE, S. TAJIMA
Specific heat of single crystal MgB_2: a two-band superconductor with two different anisotropies
Phys. Rev. Lett. ***89****, 257001 (4 pages) (2002)*

***** F. BOUQUET, Y. WANG, I. SHEIKIN, P. TOULEMONDE, M. EISTERER, H.W. WEBER, S. LEE, S. TAJIMA, A. JUNOD
Unusual effects of anisotropy on the specific heat of ceramic and single crystal MgB_2
Physica C ***385,*** *192-204 (2003)*

F. BOUQUET, Y. WANG, P. TOULEMONDE, V. GURITANU, A. JUNOD, M. EISTERER, H.W. WEBER, S. LEE, S. TAJIMA
Using Specific Heat to Scan Gaps and Anisotropy of MgB_2
In Proceedings of the 7th International Conference on Materials and Mechanisms of Superconductivity and High Temperature Superconductors (M2S-RIO), Rio de Janeiro, Brazil, 25-30 May 2003, to be published in Physica C

B. W. HOOGENBOOM, C. BERTHOD, M. PETER, Ø. FISCHER, A. A. KORDYUK
Modeling scanning tunneling spectra of $Bi_2Sr_2CaCu_2O_{8+d}$
Phys. Rev. B ***67****, 224502 (2003)*
In collaboration with project 2 Ø. Fischer, UniGe

***** A. JUNOD, Y. WANG, F. BOUQUET, I. SHEIKIN, P. TOULEMONDE, M.R. ESKILDSEN, M. EISTERER, H. W. WEBER, S. LEE, S. TAJIMA
Specific heat of ceramic and single crystal MgB_2
Physica C, ***388-389****, 107-108 (2003)*
In collaboration with project 2 Ø. Fischer, UniGe

T. PLACKOWSKI, Y. WANG, A. JUNOD
Specific heat and magnetocaloric effect measurements using commercial heat-flow sensors
Rev. Sci. Instrum. ***73****, 2755-2765 (2002)*

T. PLACKOWSKI, A. JUNOD, F. BOUQUET, I. SHEIKIN, Y. WANG, A. JEŻOWSKI, K. MATTENBERGER
Specific heat and isothermal magnetocaloric effect for single crystal UAs
Phys. Rev. B ***67,*** *184406 1-13 (2003)*

T. PLACKOWSKI, C. SULKOWSKI, J. KARPINSKI, J. JUN, S.M. KAZAKOV
Magneto-thermopower for single-crystal MgB_2: An evidence for strong electron-phonon coupling anisotropy
Phys. Rev. B in print
In collaboration with project 8 H.R. Ott, ETHZ

I. SHEIKIN, Y. WANG, F. BOUQUET, P. LEJAY, A. JUNOD
Specific heat of heavy-fermion $CePd_2Si_2$ in high magnetic fields
J. Phys.: Cond. Matter ***14****, L543-L549 (2002)*

Y. WANG, T. PLACKOWSKI, A. JUNOD
Specific heat in the superconducting and normal state (2-300 K, 0-16 T), and magnetic susceptibility of the 38-K superconductor MgB_2: evidence for a multicomponent gap.
Physica C ***355****, 179-193 (2001)*

Y. WANG, F. BOUQUET, I. SHEIKIN, P. TOULEMONDE, B. REVAZ, M. EISTERER, H.W. WEBER, J. HINDERER, A. JUNOD
Specific heat of MgB_2 after irradiation
J. Phys.: Cond. Matter ***15****, 883-893 (2003)*
In collaboration with project 3 R. Flükiger, UniGe and project 8 H.R. Ott, ETHZ

Project 5, J.-M. Triscone, University of Geneva

***** C.H. AHN, K. RABE, J.-M. TRISCONE
Ferroelectricity at the nanoscale: Local polarization in thin films and heterostructures
Science ***303****, 488 (2004)*

***** C.H. AHN, K. RABE, J.-M. TRISCONE
Field effect in correlated oxides
Nature ***424****, 1015 (2003)*

A. DEMUER, D. JACCARD, J. REINER, C.H. AHN, J.-M. TRISCONE
Magnetism of $SrRuO_3$ thin films under high hydrostatic pressures
Annalen der Physik ***13****, 72 (2004)*

L. DESPONT, C. LICHTENSTEIGER, F. CLERC, C. KOITZSCH, D. NAUMOVIC, M.G. GARNIER, F.J. GARCIA DE ABAJO, M.A. VAN HOVE, J.-M. TRISCONE, P. AEBI
Study of the ferroelectric polarization of ultra-thin films of $PbTiO_3$ by X-ray photoelectron diffractio,
Phys. Rev. B, submitted
In collaboration with project 14 P. Aebi, UniNe

***** S. GARIGLIO, C.H. AHN, D. MATTHEY, J.-M. TRISCONE
Electrostatic tuning of the hole density in $NdBa_2Cu_3O_{7-\delta}$ films and its effect on the Hall response
Phys. Rev. Lett. ***88****, 67002 (4 pages) (2002)*

***** F. LE MARREC, A. DEMUER, D. JACCARD, M.K. LEE, C.B. EOM, J.-M. TRISCONE
Magnetic behavior of epitaxial $SrRuO_3$ thin films under pressure up to 23 GPa
Appl. Phys. Lett. ***80****, 2338 (2002)*

C. LICHTENSTEIGER, J.-M. TRISCONE
Investigation of ferroelectricity in ultrathin $PbTiO_3$ films
To appear in Ferroelectrics, Proceedings of the 2003 conference EMF, Cambridge.

D. MATTHEY, S. GARIGLIO, C.H. AHN, J.-M. TRISCONE
Electrostatic modulation of the superconducting transition in thin $NdBa_2Cu_3O_{7-\delta}$ films: the role of classical fluctuations.
Physica C ***372-376****, 583-586 (2002)*

D. MATTHEY, S. GARIGLIO, C.H. AHN, J.-M. TRISCONE
Field effect and ferroelectric field effect in correlated oxide films
In "Superconducting and related Oxides: Physics and Nanoengineering V", Proceedings of SPIE, volume ***4811****, 236 (2002)*

* D. MATTHEY, S. GARIGLIO, J.-M. TRISCONE
Field effect experiments in $NdBa_2Cu_3O_{7-\delta}$ ultrathin films using a $SrTiO_3$ single crystal gate insulator
*Applied Physics Letters **83**, 3758 (2003)*

P. PARUCH, T. TYBELL, J.-M. TRISCONE
Nanoscale control and domain wall dynamics in epitaxial ferroelectric $Pb(Zr_{0.2}Ti_{0.8})O_3$ thin films
*Advances in Science and Technology, **33**, 675 (2002)Proceedings of the 10th international Ceramics Congress, part of CIMTEC 2002 - 10th International Ceramics Congress and 3rd Forum on New Materials, Florence, Italy July 14-18,2002. Ed. P. Vincenzini, Part D, Section K, **675** (2002)*

P. PARUCH, T. GIAMARCHI, J.-M. TRISCONE
Domain wall creep in mixed c-a axis $Pb(Zr0_{.2}Ti0_{.8})O_3$ thin films
*Annalen der Physik **13**, 95 (2004)*
In collaboration with project 18 T. Giamarchi, UniGe

A. RÜFENACHT, P. CHAPPATTE, S. GARIGLIO, C. LEEMANN, J. FOMPEYRINE, J.-P. LOCQUET, P. MARTINOLI
Growth of single unit-cell superconducting $La_{2-x}Sr_xCuO_4$ films
*Solid State Electronics **47**, 2167 (2003)*
In collaboration with project 10 P. Martinoli, UniNe

A.K. SARIN KUMAR, P. PARUCH, D. MARRÉ, L. PELLEGRINO, T. TYBELL, S. BALLANDRAS, J.-M. TRISCONE
A novel high frequency surface acoustic wave device based on piezoelectric interdigital transducers
To appear in Ferroelectrics, Proceedings of the 2003 conference EMF, Cambridge

* K. TAKAHASHI, D. MATTHEY, D. JACCARD, J.-M. TRISCONE
Electrostatic modulation of the electronic properties of Nb-doped $SrTiO_3$ superconducting film.
To appear in Applied Physics Letters

K. TAKAHASHI, D. MATTHEY, D. JACCARD, J.-M. TRISCONE
Transport properties of reduced $SrTiO_3$ single crystal "thin films"
*Annalen der Physik **13**, 68 (2004)*

* T. TYBELL, P. PARUCH, T. GIAMARCHI, J.-M. TRISCONE
Domain wall creep in epitaxial ferroelectric $Pb(Zr0_{.2}Ti_{0.8})O_3$ thin films
*Phys. Rev. Lett. **89**, 097601 (4 pages) (2002)*
In collaboration with project 18 T. Giamarchi, UniGe

T. TYBELL, P. PARUCH, J.-M. TRISCONE, C.H. AHN
Nanoscale study of polarization phenomena in $Pb(Zr_{0.2}Ti_{0.8})O_3$ thin films
*In "Superconducting and related Oxides: Physics and Nanoengineering V", Proceedings of SPIE, **4811**, 256 (10 pages) (2002)*

Project 5 J.M. Triscone, UniGe

Project 6, G. Blatter, ETH Zurich

A. A. ABDUMALIKOV, Y. KOVAL, A. V. USTINOV, V. V. KURIN, CH. HELM, A. DE COL
Nonlocal electrodynamics of long ultra-narrow Josephson junctions: Experiment and theory
J. Appl. Phys. Submitted (2004)

G. BLATTER
The qubit duet, News and Views
*Nature **421**, 796 (2003)*

G. BLATTER, V.B. GESHKENBEIN, J.A.G. KOOPMANN
Weak- to Strong Pinning Crossover
*Phys. Rev. Lett. **92**, 067009 (4 pages) (2004)*

H.P. BUCHLER, G. BLATTER
Signature of Quantum Depletion in the Dynamic Structure Factor of Atomic Gase,
Phys. Rev. Lett. submitted, cond-mat/0312526 (2003)

H.P. BUCHLER, G. BLATTER
Phase separation of atomic Bose-Fermi mixtures in an optical lattice
In preparation

H.P. BUCHLER, G. BLATTER
Supersolids in atomic Bose-Fermi mixtures
*Phys. Rev. Lett. **91**, 067007 (4 pages) (2004)*

H.P. BUCHLER, G. BLATTER, W. ZWERGER
Commensurate-incommensurate transition of cold atoms in an optical lattice
*Phys. Rev. Lett. **90**, 130401 (4pages) (2003)*

H.P. BUCHLER, V.B. GESHKENBEIN, G. BLATTER
Quantum fluctuations in thin superconducting wires of finite length
*Phys. Rev. Lett. **92**, 130404 (4 pages) (2003)*

L.N. BULAEVSKII, CH. HELM, A.R. BISHOP, M.P. MALEY
Optical properties of crystals with spatial dispersion: Josephson plasma resonance in layered superconductors
*Europhys. Lett. **58**, 415-421 (2002)*

L.N. BULAEVSKII, CH. HELM
Field dependence of the Josephson plasma resonance in layered superconductors with alternating junctions
*Phys. Rev. B **66**, 174505 (5 pages) (2002)*

N.M. CHTCHELKATCHEV, G. BLATTER, G.B. LESOVIK, T. MARTIN
Bell inequalities and entanglement in solid state devices
*Phys. Rev. B **66**, 161320 (4 pages) (2002)*

A. DE COL, G. BLATTER

Surface and screening effects in weakly coupled layered superconductors
in preparation

A. DE COL, V.B. GESHKENBEIN, G. BLATTER
Berezinskii-Kosterlitz-Thouless transition in bi- and multi-layer superconducting systems
in preparation

A. DE COL, V.B. GESHKENBEIN, G.I. MENON, G. BLATTER
Surface effects on the pancake vortex phase diagram
Physica C (2004) in press

A. DE COL,T.B. LIVERPOOL
Statistical mechanics of double helical polymers
Submitted to Phys. Rev. E

M.V. FEIGEL'MAN, L.B. IOFFE, V.B. GESHKENBEIN, P. DAYAL, G. BLATTER
Superconducting Tetrahedral Qubits
*Phys. Rev. Lett. B **92**, 098301 (4 pages) (2004)*

A. FRANZ, Y. KOVAL, D. VASYUKOV, P. MÜLLER, H. SCHNEIDEWIND, D.A. RYNDYK, J. KELLER, C. HELM
Thermal fluctuations in ultrasmall intrinsic Josephson junction,
*Phys. Rev. B **69**, 014506 (2004)*

D.A. GOROKHOV, D.S. FISHER, G. BLATTER
Quantum collective creep: A quasiclassical Langevin equation approach
*Phys. Rev. B **66**, 214203 (23 pages) (2002)*

CH. HELM, L.N. BULAEVSKII
Optical properties of layered superconductors near the Josephson plasma resonance
*Phys. Rev. B **66**, 094514 (23 pages)* (2002)

CH. HELM, L.N. BULAEVSKII, E.M. CHUDNOVSKY, M.P. MALEY
Reflectivity and Microwave Absorption in Crystals with Alternating Intrinsic Josephson Junctions
*Phys. Rev. Lett. **89**, 057003 (4 pages) (2002)*

CH. HELM, L.N. BULAEVSKII, D. RYNDYK, J. KELLER, S. ROTHER, Y. KOVAL, P. MÜLLER, R. KLEINER
Electronic compressibility and charge imbalance relaxation in cuprate superconductors
Physica C, in press, cond-mat/0304167

***** L.B. IOFFE, M.V. FEIGEL'MAN, A. IOSELEVICH, D. IVANOV, M. TROYER, G. BLATTER
Topologically protected quantum bits from Josephson junction arrays
*Nature **415**, 503 (2002)*

L. IOFFE, V.B. GESHKENBEIN, C. HELM, G. BLATTER
Decoherence of Josephson junction qubits due to phonons
In preparation

D.A. IVANOV, L.B. IOFFE, V.B. GESHKENBEIN, G. BLATTER
Interference effects in isolated Josephson junction arrays with geometric symmetries
*Phys. Rev. B **65**, 024509 (8 pages) (2002)*

D.A. IVANOV, R. VON ROTEN, G. BLATTER
Minigap in a long disordered SNS junction: analytical results
Phys. Rev. B **66,** 052507 (4 pages) (2002)

KAELIN, CH. HELM, G. BLATTER
Optical Resonances in Reflectivity due to Crystal Modes with Spatial Dispersion
*Phys. Rev. B **68**, 012302 (4 pages) (2003)*

H.G. KATZGRABER
On the existence of a finite-temperature transition in the two-dimensional gauge glass
*Phys. Rev. B **67**, 180402 (4 pages) (2003)*

H.G. KATZGRABER
Numerical studies of the two- and three-dimensional gauge glass at low temperature
*J. App. Phys. **93**, 7661-7663 (2003)*

H.G. KATZGRABER, I.A. CAMPBELL
Size dependence of the internal energy in Ising and vectos spin glasses
*Phys. Rev. B **68**, 180402 (4 pages) (2003)*

H.G. KATZGRABER, F. PAZMANDI, C.R. PIKE, K. LIU, R.T. SCALETTAR, K.L. VEROSUB, G.T. ZIMANYI
Reversal field memory in magnetic hysteresis
*J. App. Phys. **93**, 6617-6620 (2003)*

H.G. KATZGRABER, A.P. YOUNG
Geometry of large-scale low-energy excitations in the one-dimensional Ising spin glass with power-law interactions
*Phys. Rev. B **68**, 224408 (6 pages) (2003)*

J. A. G. KOOPMANN, V.B. GESHKENBEIN, G. BLATTER
Impact of long-range interactions on the disordered vortex lattice
*Phys. Rev. B **68**, 014515 (9 pages) (2003)*

J. A. G. KOOPMANN, V.B. GESHKENBEIN, G. BLATTER
Peak effect at the weak-to strong pinning crossover
Physica C in press (2004)

L. KRUSIN-ELBAUM, G. BLATTER, T. SHIBAUCHI
Separated Spin and Charge Degrees of Freedom in High-T_c Superconductors
In preparation

A.V. LEBEDEV, G. BLATTER, C.W.J. BEENAKKER, G.B. LESOVIK
Entanglement in Mesoscopic Structures: Role of Projection
Phys. Rev. B submitted, cond-mat/0311649 (2003)

A.V. LEBEDEV, G.B. LESOVIK, G. BLATTER
Entanglement in a Noninteracting Mesoscopic Structure
Phys. Rev. Lett. submitted, cond-mat/0311423 (2003)

G.B. LESOVIK, A.V. LEBEDEV, G. BLATTER
Wave Function Collapse in a Mesoscopic Device
Phys. Rev. Lett. submitted, cond-mat/0310020 (2003)

G.B. LESOVIK, T. MARTIN, G. BLATTER
Electronic Entanglement in the Vicinity of a Superconductor,
*Eur. Phys. J. B **24,** 287-290 (2002)*

F. MOHAMED, M. TROYER, G. BLATTER, I. LUK'YANCHUK
Interaction of vortices in superconductors with κ close to $2^{-1/2}$
*Phys. Rev. B **65**, 224504 (6 pages) (2002)*

J.J. MORENO, H.G. KATZGRABER, A.K. HARTMANN
Finding the low temperature state with parallel tempering, simulated annealing, and simple Monte Carlo
*Int. J. Mod. Phys. C **14**, 285-302 (2003)*

F. NIEDERER, A.L. FAUCHERE, G. BLATTER
Spontaneous magnetic moments in clean normal-metal-superconductor proximity layers
*Phys. Rev. B **65**, 132515 (4 pages) (2002)*

S. ROTHER, Y. KOVAL, P. MÜLLER, R. KLEINER, D.A. RYNDYK, J. KELLER, CH. HELM
Charge-imbalance effects in intrinsic Josephson systems
Phys. Rev. B, cond-mat/0207634, accepted

S. ROTHER, Y. KOVAL, P. MÜLLER, R. KLEINER, D.A. RYNDYK, J. KELLER, CH. HELM
Charge-imbalance effects in intrinsic Josephson systems
*Phys. Rev. B **67**, 024510 (2003)*

D.A. RYNDYK, J. KELLER, C. HELM
Nonequilibrium effects due to charge fluctuations in intrinsic Josephson systems
*J. Phys. Cond. Mat. **14**, 815-826 (2002)*

T. SHIBAUCHI, L. KRUSIN-ELBAUM, G. BLATTER, C.H. MIELKE
Uncovering large quantum dissipative gapped regime in overdoped BiSrCaCuO
submitted to Nature

T. SHIBAUCHI, L. KRUSIN-ELBAUM, G. BLATTER, C.H. MIELKE
Uncovering large quantum fluctuations in overdoped $Bi_2Sr_2CaCu_2O_{8+y}$
*Phys. Rev. B **67**, 064514-1/6 (2003)*

M.A. SKVORTSOV, D.A. IVANOV, G. BLATTER
Vortex viscosity in the moderately clean limit of layered superconductors
Phys. Rev. B **67**, 014521 (11 pages) (2003)

V.K. THORSMØLLE, R.D. AVERITT, M.P. MALEY, L.N. BULAEVSKII, C. HELM, A.J. TAYLOR
Josephson plasma resonance in $Tl_2Ba_2CaCu_2O_8$ in a magnetic field measured using THz spectroscopy
*Physica B **312**, 84-85 (2002)*

S. WEHRLI, C. HELM
Interface Steps in field effect devices
J.Appl.Phys. submitted, cond-mat/0312441 (2004)
In collaboration with project 9 T.M. Rice & M. Sigrist, ETHZ

Project 7, R. Nesper, ETH Zurich

F. BIERI, F. KRUMEICH, H.J. MUHR, R. NESPER
The first Vanadium Oxide Nanotube containing an Aromatic Amine as Template
Preprint

T.J. GELDBACH, C. J DEN REIJER, M. WÖRLE, P. PREGOSIN
Protonation and NMR studies on C-13-acetate enriched Ru $(OAc)_2$ (Binap) Acetate as a source of water in P-C bond splitting
*Inorg. Chim. Acta, **330**, 155-160 (2002)*

J. HABERECHT, F. KRUMEICH, R. NESPER
High yield molecular borazine-precursors for Si-B-N-C ceramics
*Chem. Mater. **16**, **3**, 418-423 (2003)*

J. HABERECHT, A. KRUMMLAND, F. BREHER, B. GEBHARDT, H. RÜEGGER, R. NESPER, H. GRÜTZMACHER
Functionalized Borazines as Precursors for New Silica-Gels
*Dalton Trans. **11**, 2126-2132 (2003)*

K. HEGETSCHWEILER, R. C. FINN, R.S. RARIG, J. SANDER, S. STEINHAUSER , M. WÖRLE, R. ZUBIETA
1,3,5-triamono-1,3,5-trideoxy-cis-inositol, a ligand with a remarkable versatility for metal ions
*Inorg. Chim. Acta **337**, 39 (2002)*

L. KAVAN, M. KALBAC, M. ZUKALOVA, R. NESPER ET AL.
Lithium Storage in Nanostructures TiO_2 made by hydrothermal growth
*Chem. Mater. **16**, **3**, 477-485 (2004)*

F. KRUMEICH, K.S. PILLAI, M. NIEDERBERGER, R. NESPER
Neuartige Vanadiumoxid-Nanoröhren mit ungewöhnlicher Wandstruktur
*Z. Kristallogr. Supp **I8**, S.62 (2001)*

E. LEONTIDIS, M. ORFANOU, T. KYPRIANIDOU-LEODIDOU, F. KRUMEICH , W. CASERI
Composite Nanotubes Formed by Self-Assembly of PbS Nanoparticles
*Nanoletters **3**, 569-572 (2003)*

A. MICHAILOVSKY, F. KRUMEICH, G. PATZKE
Solvothermal Morphology Studies: Alkali/Alkaline Earth Molybdates
Helv .Chim. Acta (accepted) (2003)

A. MICHAILOVSKI, F. KRUMEICH, G. PATZKE
Hierarchical growth of mixed ammonium molybdenum/ tungsten bronze nanorods
Chem. Mater. (in print) (2004)

R. NESPER, G. PATZKE
Nanotubes – Functional particles of the 21st century?
*Nachrichten aus der Chemie **49**, 886 (2001)*

M. NIEDERBERGER, F. KRUMEICH, H.-J. MUHR, M. MÜLLER, R. NESPER
Synthesis and Characterization of Novel Nanoscopic Molybdenum Oxide Fibres
*J.Mater.Chem. **11**, 1941-1945 (2001)*

M. NIEDERBERGER, F. KRUMEICH, K. HEGETSCHWEILER, R. NESPER
An iron polyolate complex as a precursor for the controlled synthesis of monodispersed iron oxide colloids
*Chemistry of Materials **14**, 78-82 (2002)*

G.R. PATZKE, F. KRUMEICH, R. NESPER
Oxidic Nanotubes and Nanorods – Anisotropic Modules for a Future Nanotechnology
*Angew. Chem. Int .Ed. **41**, 2446-2461 (2002)*

K.S. PILLAI, F. KRUMEICH, H.-J. MUHR, M. NIEDERBERGER, R. NESPER,
The first oxide nanotubes with alternating inter-layer distances
*Solid State Ionics **141**, 185-190 (2001)*

V. SEPELAK, M. MENZEL, K. BECKE, F. KRUMEICH
Mechanochemical Reduction of Magnesium Ferrite
*J. Phys. Chem. B **106**, 6672-6678 (2002)*

M. WÖRLE, F. KRUMEICH, F. BIERI, H.-J. MUH, R. NESPER
Flexible V_7O_{16} Layers as the Common Structural Element of Vanadium Oxide Nanotubes and a New Crystalline Vanadate
*Z. Anorg. Allg. Chemie **628**, 2778-2784 (2002)*

***** F. XU, R. CZERW, S. WEBSTER, D. L. CARROLL, J. BALLATO, R. NESPER
Nonlinear optical transmission in VOx nanotubes and VOx nanotube composites
*Appl. Phys. Lett. **81**, 1711-1713 (2002)*

F. ZÜRCHER, R. NESPER
Cationic Channels with Partial Anion Occupation in the Zintl Phases $Ba_2Mg_{12}Ge_{7.33}$ and $Ba_6Mg_{17.4}Li_{2.6}Ge_{12}O_{0.64}$
*Z. Anorg. Allg. Chemie **628**, 1581-1589 (2002)*

J. ZYGMUNT, F. KRUMEICH, R. NESPER
Novel Silica Nanotubes with a High Aspect Ratio - Synthesis and Structural Characterization
*Adv. Mater. **15**, 18, 1538-1541 (2003)*

Project 8, H. R. Ott, ETH Zurich

E. ANNESE, J.-P. RUEFF, M. GRIONI, G. VANKO, L. DEGIORGI, L. BRAICOVICH, R. GUSMEROLI, C. DALLERA
Valence changes in YbS under pressure: a resonant x-ray emission study
Submitted
In collaboration with project 12 G. Margaritondo, EPFL

M. ANGST, D. DI CASTRO, R. PUZNIAK, A. WISNIEWSKI, J. JUN, S.M. KAZAKOV, J. KARPINSKI, S. KOHOUT, H. KELLER
Anisotropic properties of MgB_2 by torque magnetometry
Physica C in print
In collaboration with project 13 H. Keller, UniZh

M. ANGST, R. PUZNIAK, A. WISNIEWSKI, J. JUN, S. M. KAZAKOV, J. KARPINSKI
Disorder-induced phase transition of vortex matter in MgB_2
*Phys. Rev. B **67**, 012502 (2003)*

M. ANGST, R. PUZNIAK, A. WISNIEWSKI, J. JUN, S.M. KAZAKOV, J. KARPINSKI, J. ROOS, H. KELLER
Comments on Superconducting anisotropy and evidence for intrinsic pinning in single crystalline MgB_2
submitted to Phys.Rev.B., cond-mat/0206407
In collaboration with project 13 H. Keller, UniZh

M. ANGST, R. PUZNIAK, A. WISNIEWSKI, J. ROOS, H. KELLER, P. MIRANOVIC, J. JUN, S.M. KAZAKOV, J. KARPINSKI
Anisotropy of the superconducting state properties and phase diagram of MgB_2 by torque magnetometry on single crystals
*Physica C **385**, 143-154 (2003)*
In collaboration with project 13 H. Keller, UniZh

S. BRODERICK, L. DEGIORGI, H.R. OTT, J.L. SARRAO, Z. FISK
Giant magneto-optical response of erromagnetic EuB_6
*Eur. Phys. J. B **27** (6 pages) (2002)*

S. BRODERICK, L. DEGIORGI, H.R. OTT, J.L. SARRAO, Z. FISK
Polar Kerr rotation of the ferromagnet EuB_6
*Eur. Phys. J.B. **33**, 47-54 (2003)*

M. BRÜHWILER, B. BATLOGG, S.M. KAZAKOV, J. KARPINSKI
Evidence for two electronic components in Na_xCoO_2 (x = 0.7-0.75)
submitted to Phys. Rev. Lett. cond-mat/0309311

YU BUKHANTSEV, B. KUNDYS, A. NABIALEK, S. VASILIEV, A. WISNIEWSKI, J. JUN, S.M. KAZAKOV, J. KARPINSKI, H. SZYMCZAK
The correlation between the transverse and longitudinal magnetostriction in a polycrystalline MgB_2 superconductor
Supercond. Sci. Technol. ***16****, 707 (2003)*

YU BUKHANTSEV, A. NABIALEK, B. KUNDYS, S. VASILIEV, A. WISNIEWSKI, J. JUN, S.M. KAZAKOV, J. KARPINSKI, A. SZEWCZYK, H. SZYMCZAK
Pinning induced magnetostriction in superconducting MgB_2 ceramics
*Phys. Stat. Sol. (a) No.****1****, 82 (2003)*

G. CAIMI, S. BRODERICK, H.R. OTT, L. DEGIORGI, A.D. BIANCHI, Z. FISK
Magneto-optical Kerr effect in $Eu_{1-x}Ca_xB_6$
Phys. Rev. B ***69****, 012406 (2004)*

A. CARRINGTON, P.J. MEESON, J.R. COOPER, L. BALICAS, N.E. HUSSEY, E.A. YELLAND, S. LEE, A. YAMAMOTO, S. TAJIMA, S.M. KAZAKOV, J. KARPINSKI
Determination of the Fermi Surface of MgB_2 by the de Haas--van Alphen Effect
Phys. Rev. Lett. ***91****, 037003 (2003)*

A. CARRINGTON, P.J. MEESON, J.R. COOPER, L. BALICAS, N.E. HUSSEY, E.A. YELLAND, S. LEE, A. YAMAMOTO, S. TAJIMA, S.M. KAZAKOV, J. KARPINSKI
Determination of the Fermi surface of MgB_2 by the de Haas-van Alphen effect
Physica C, in print

V. CHABANENKO, R. PUZNIAK, A. NABIALEK, S. VASILIEV, V. RUSAKOV, L. HUANQUIAN, R. SZYMCZAK, H. SZYMCZAK, J. JUN, J. KARPINSKI, V. FINLEL
Flux jumps and H-T diagram of instability for MgB_2
Journal of Low Temp. ***3-4****, 175-191 (2003)*

M.A. CHERNIKOV, C. BEELI, E. FELDER, S. BÜCHI, H.R. OTT
Spin freezing in the decagonal phase of the A1-Mn-Pd alloy system
Physical Review B ***68****, 094202 (2003)*

M. CHIAO, G. WIGGER, CH. BERGEMANN, H.R. OTT, S.S. SAXENA, A.D. BIANCHI
Tuning of Magnetic Moment in $Eu_{(1-x)}Ca_xB_6$
Acta Physics Pol., B ***34****, 1441 (2003)*

J.R. COOPER, A. CARRINGTON, P.J. MEESON, E.A. YELLAND, N.E. HUSSEY, L. BALICAS, S. TAJIMA, S. LEE, S.M. KAZAKOV, J. KARPINSKI
de Haas-van Alphen effect in MgB_2 crystals
Physica C ***385****, 75-85 (2003)*

R. CUBITT, M. R. ESKILDSEN, C. D. DEWHURST, J. JUN, S. M. KAZAKOV, J. KARPINSKI
Effects of Two-Band Superconductivity on the Flux Line Lattice in Magnesium Diboride
Phys. Rev. Lett. ***91****, 047002 (2003)*
In collaboration with project 2 Ø. Fischer, UniGe

D. DAGHERO, R.S. GONNELLI, G.A. UMMARINO, V.A. STEPANOV, J. JUN, S.M. KAZAKOV, J. KARPINSKI
Point-contact spectroscopy in MgB_2 single crystals in magnetic field
Physica C ***385****, 255-264 (2003)*

L. DEGIORGI, S. BRODERICK, H.R. OTT, J.L. SARRAO, Z. FISK
The ferromagnetic phase transition in EuB_6: optical evidence for quasiparticle undressing
Physica B ***312****, 327-328 (2002)*

L. DEGIORGI, S. BRODERICK, B. RUZICKA, H.R. OTT, J.L. SARRAO, Z. FISK
Scaling between magnetization and Drude weight in EuB_6
Phys. Rev. B (Rapid Commun.), in press.

D. DI CASTRO, R. KHASANOV, D.G. ESHCHENKO, J. ROOS, I.M. SAVIC, A. SHENGELAYA, L. BUD'KO, P.C. CANFIELD, K. CONDER, J. KARPINSKI, S. M. KAZAKOV, R.A. RIBEIRO, H. KELLER
Absence of a boron isotope effect on the magnetic penetration depth in MgB_2
submitted to Phys. Rev. Lett.
In collaboration with project 13 H. Keller, UniZh

S.V. DORDEVI, D.N. BASO, R.C. DYNE, B. RUZICKA, V. VESCOLI, L. DEGIORGI, H. BERGER, R. GAAL, L. FORRÓ, E. BUCHER
Optical properties of the quasi-two-dimensional dichalcogenides 2H-$TaSe_2$ and 2H-$NbSe_2$
Eur. Phys. J. B ***33****, 15 (2003)*
In collaboration with project 11 L. Forró, EPFL and project 12 G. Margaritondo, EPFL

T.B. DOYLE, A. WISNIEWSKI, M. ZEHATMAYER, H.W. WEBER, J. KARPINSKI
Equilibrium behaviour and vortex pinning in MgB_2 single crystals
Physica C in print

M. R. ESKILDSEN, C. D. DEWHURST, B. W. HOOGENBOOM, C. PETROVIC AND P. C. CANFIELD
Hexagonal and Square Flux Line Lattices in $CeCoIn_5$
Submitted to Phys. Rev. Lett. (cond-mat/0211585)
In collaboration with project 2 Ø. Fischer, UniGe

M.R. ESKILDSEN, N. JENKINS, G. LEVY, M. KUGLER, Ø. FISCHER, J. JUN, S.M. KAZAKOV, J. KARPINSKI
Vortex Imaging in Magnesium Diboride with H_c
Physical Rev.B ***68****, 100508 (2003)*
In collaboration with project 2 Ø. Fischer, UniGe

***** M. R. ESKILDSEN, M. KUGLER, S. TANAKA, J. JUN, S. M. KAZAKOV, J. KARPINSKI, Ø. FISCHER
Vortex Imaging in the π-Band of Magnesium Diboride
Phys. Rev. Lett. ***89****, 187003 (4pages) (2002)*
In collaboration with project 2 Ø. Fischer, UniGe

M. R. ESKILDSEN, M. KUGLER, G. LEVY, S. TANAKA, J. JUN, S. M. KAZAKOV, J. KARPINSKI, Ø. FISCHER
Scanning Tunneling Spectroscopy on Single Crystal MgB_2
*Physica C **385**, 169-177 (2003)*
In collaboration with project 2 Ø. Fischer, UniGe

M. R. ESKILDSEN, M. KUGLER, G. LEVI, S. TANAKA, J. JUN, S. M. KAZAKOV, J. KARPINSKI, O . FISCHER
Vortex lattice imaging in single crystal MgB_2 by scanning tunneling spectroscopy
*Physica C **388-389**, 143-144 (2003)*
In collaboration with project 2 Ø. Fischer, UniGe

Z. FISK, H.R. OTT, V. BARZYKIN, L.P. GOR'KOV
The emerging picture of ferromagnetism in the divalent hexaborides
*Physica B **312** 808-810 (2002)*

J.L. GAVILANO, S. MUSHKOLAJ, D. RAU, H.R. OTT, A. BIANCHI, D.P. YOUNG, Z. FISK
^{11}B-NMR in CaB_6
*Physica B **312,** 813-814 (2002)*

J.L. GAVILANO, S. MUSHKOLAJ, D. RAU, H.R. OTT, A. BIANCHI, D.P. YOUNG, Z. FISK
NMR studies of YbB_6
*Physica B **326-333**, 570-571 (2003)*

J.L. GAVILANO, D. RAU, S. MUSHKOLAJ, H.R. OTT, P. MILLET, F. MILA
DC-susceptibility and NMR response of a low-dimensional quantum magnet: $Na_2V_3O_7$
*Physica B **312**, 622-623 (2002)*
In collaboration with project 9 T.M. Rice & M. Sigrist, ETHZ

J.L. GAVILANO, D. RAU, S. MUSHKOLAJ, H.R. OTT, P. MILLET, F. MILA
A low-dimensional spin S=1/2 system at the quantum critical limit: $Na_2V_3O_7$
*Physical Review Letters, Vol. **90**, 167202 (2003)*
In collaboration with project 9 T.M. Rice & M. Sigrist, ETHZ

J.L. GAVILANO, D. RAU, SH. MUSHKOLAJ, H.R. OTT, F. MILA, P. MILLET
Low-temperature NMR studies of $Na_2V_3O_7$
*Physica B **329-333**, 703-704 (2003)*
In collaboration with project 9 T.M. Rice & M. Sigrist, ETHZ

J.L. GAVILANO, D. RAU, B. PEDRINI, J. HINDERER, H.R. OTT, S. KAZAKOV AND J. KARPINSKI
Charge Ordering in $Na_{0.7}Co0_2$ below 300 K
Phys. Rev. B, Rapid. Comm., submitted

K. GIANNÒ, A.V. SOLOGUBENKO, H.R. OTT, A.D. BIANCHI, Z. FISK
Low-temperature thermal conductivity of CaB_6 and EuB_6
*J. Phys.: Condens. Matter **15**, 6739-6748 (2003)*

R.S. GONNELLI, D. DAGHERO, A. CALZOLARI, G.A. UMMARINO, VALERIA DELLAROCCA, V.A. STEPANOV, J. JUN, S.M. KAZAKOV, J. KARPINSKI
The Magnetic-field Dependence of the Gaps in a Two-band Superconductor: A Point-contact Study of MgB_2 Single Crystals
submitted to Phys. Rev. Lett., cond-mat/0308152

R.S. GONNELLI, D. DAGHERO, A. CALZOLARI, G.A. UMMARINO, V. DELLAROCCA, V.A. STEPANOV, S.M. KAZAKOV, J. KARPINSKI, C. PORTESI, E. MONTICONE, V. FERRANDO, C. FERDEGHINI
Point-Contact Spectroscopy in MgB_2: from Fundamental Physics to Thin-Film Characterization
*Supercond. Sci. Technol. **17**, S1-S8 (2004)*

R.S. GONNELLI, D. DAGHERO, G.A. UMMARINO, V. DELLAROCCA, A. CALZOLARI, V.A. STEPANOV, J. JUN, S.M. KAZAKOV, J. KARPINSKI
Directional point-contact spectroscopy of MgB_2 single crystals in magnetic field: two-band superconductivity and critical fields
Physics C in print

R.S. GONNELLI, D. DAGHERO, G.A. UMMARINO, V.A. STEPANOV, J. JUN, S.M. KAZAKOV, J. KARPINSKI
Independent determination of the two gaps by directional point-contact spectroscopy in MgB_2 single crystals
*Sup.Sci.Techn. **16**, 171-175 (2003)*

N. JENKINS, M.R. ESKILDSEN, M. KUGLER, Ø. FISCHER, J. JUN, S.M. KAZAKOV, J. KARPINSKI
Shrinking of the π band in MgB_2 by aluminium doping
submitted to Phys. Rev. Lett.
In collaboration with project 2 Ø. Fischer, UniGe

J. KARPINSKI, M. ANGST, J. JUN, S.M. KAZAKOV, R. PUZNIAK, A. WISNIEWSKI, J. ROOS, H. KELLER, A. PERUCCHI, L. DEGIORGI, M.R. ESKILDSEN, P. BORDET, L. VINNIKOV, A. MIRONOV
MgB_2 single crystals: high pressure growth and physical properties
*Supercond. Sci. Technol. **16**, 221- 230 (2003)*
In collaboration with project 2 Ø. Fischer, UniGe and project 13 Keller, UniZh

J. KARPINSKI, S.M. KAZAKOV, J. JUN, M. ANGST, R. PUZNIAK, A. WISNIEWSKI, P. BORDET
Single crystal growth of MgB_2 and thermodynamics of Mg-B-N system at high pressure
*Physica C **385**, 42-48 (2003)*

J. KARPINSKI, S.M. KAZAKOV, J. JUN, N.D. ZHIGADLO, M. ANGST, R. PUZNIAK, A. WISNIEWSKI
MgB2 and $Mg_{1-x}Al_xB_2$ single crystals: high-pressure growth and physical properties

Physica C in print, cond mat/0304658

S.M. KAZAKOV, J. KARPINSKI, J. JUN, P. GEISER, N.D. ZHIGADLO, R. PUZNIAK, A.V. MIRONOV
Single crystal growth and properties of MgB_2 and $Mg(B_{1-x}C_x)_2$
Physica C in print, cond mat/0304656

S.M .KAZAKOV, R. PUZNIAK, A.V. MIRONOV, J. JUN, N.D. ZHIGADLO, J. KARPINSKI
Impact of carbon substitution on structural and superconducting properties of MgB_2 single crystals
to be submitted to Phys. Rev. B

R. KHASANOV, T. SCHNEIDER, J. KARPINSKI, H. KELLER
Finite size and pressure effects in $YBa_2Cu_4O_8$ probed by the magnetic field penetration depth measurements
Submitted to Phys. Rev. B
In collaboration with project 13 H. Keller, UniZh

I.L. LANDAU, H.R. OTT
Temperature dependence of the upper critical field of type-II superconductors from isothermal magnetization data: Application to high-temperature superconductors
Phys. Rev. B **66,** 144506 (8 pages) (2002)

I.L. LANDAU, H.R. OTT
Model of the mixed state of type-II superconductors in high magnetic fields
*Journal of Physics-Condensed Matter **14**, L313-L318 (2002)*

I.L. LANDAU, H.R. OTT
Some remarks on vortex matter in high-T_c superconductors
*J. Low Temperature Physics, Vol. **130**, 287-310 (2003)*

I.L. LANDAU, H.R. OTT
Temperature dependence of the upper critical field of high-T_c superconductors from isothermal Magnetization data. Application to polycrystalline samples and ceramics
*Physica C **385**, 544-550 (2003)*

I.L. LANDAU, H.R. OTT
Equilibrium magnetization of high-T_c superconductors below the irreversibility line
*Physical Review B **67**, 092505 (2003)*

I.L. LANDAU, H.R. OTT
Temperature dependence of the upper critical field of high-T_c superconductors from isothermal magnetization data: influence of a temperature dependent Ginzburg-Landau parameter
*Physica C **398**, 73-77 (2003)*

I.L. LANDAU, A.V. SOLOGUBENKO, H.R. OTT
Ambivalence of the anisotropy of the vortex lattice in an anisotropic type-II superconductor
*Physical Review B **68**, 132506 (2003)*

S. MITROVIC, L. PERFETTI, C. SONDERGAARD, G. MARGARITONDO, M. GRIONI, N. BARISIC, L. FORRÓ, L. DEGIORGI
Electronic structure of a quasi-one-dimensional insulator : The molybdenum red bronze $K_{0.33}M0O_3$
*Phys. Rev. B **69**, 035102 (2004)*
In collaboration with project 11 L. Forró, EPFL and project 12 G. Margaritondo, EPFL

H.R. OTT
Ferromagnetic metals, an old problem revisited
*Physica B **318**, 77- 81 (2002)*

L. PERFETTI, S. MITROVIC, G. MARGARITONDO, M. GRIONI, L. FORRÓ, L. DEGIORGI, H. HOECHST
Mobile small polarons and the Peierls transition in the quasi-one-dimensional conductor $K_{0.3}MoO_3$
*Phys. Rev. B **66**, 075107 (8 pages) (2002)*
In collaboration with project 11 L. Forró, EPFL and project 12 G. Margaritondo, EPFL

G.K. PERKINS, Y. BUGOSLAVSKY, A.D. CAPLIN, J. MOORE, T.J. TATE, R. GWILLIAM, J. JUN, S.M. KAZAKOV, J. KARPINSKI, L.F. COHEN
Effects of proton irradiation and ageing on the superconducting properties of single crystalline and polycrystalline MgB_2
*Supercond. Science Techn. **17**, 232-235 (2004)*

A. PERUCCHI, L. DEGIORGI, J. JUN , M. ANGST, J. KARPINSKI
Magneto-optical study of the superconducting gap of MgB_2 single crystals
*Phys. Rev. Lett. **89** 097001 (4 pages) (2002)*

A. PERUCCHI, G. CAIMI, H.R. OTT, L. DEGIORGI. A.D. BIANCHI, Z. FISK
Optical Evidence for a Spin-Filter Effect in the Charge Transport of $Eu_{0.6}Ca_{0.4}B_6$
*Phys. Rev. Lett. **92**, 067401 (2004)*

A. PERUCCHI, L. DEGIORGI, J. JUN, M. ANGST, J. KARPINSKI
Far-infrared optical properties of MgB_2 single crystals
*Physica C **385**, 273 (2003)*

T. PLACKOWSKI, C. SULKOWSKI, J. KARPINSKI, J. JUN, S.M. KAZAKOV
Magneto-thermopower for single-crystal MgB_2: An evidence for strong electron-phonon coupling anisotropy
Phys. Rev. B in print
In collaboration with project 4 A. Junod, UniGe

R. PUZNIAK, M. ANGST, A. SZEWCZYK, J. JUN, S.M. KAZAKOV, J. KARPINSKI
Enhanced anisotropic upper critical field and peak effect in $Mg(B_{0.94}C_{0.06})_2$ single crystals
submitted to Phys. Rev. B

D. RAU, J.L. GAVILANO, SH. MUSHKOLAJ, C. BEELI, M.A. CHERNIKOV, H.R. OTT

Anomalous magnetism in decagonal $Al_{69.8}Pd_{12.1}Mn_{18.1}$
*Physical Review B **68**, 13204 (2003)*

D. RAU, J.L. GAVILANO, SH. MUSHKOLAJ, C. BEELI, H.R. OTT
Magnetism of decagonal $Al_{69.8}Pd_{12.1}Mn_{18.1}$
*Physica B **329-333**, 1103-1104 (2003)*

B. RUZICKA, V. VESCOLI, L. DEGIORGI
Charge dynamics in low-dimensional quantum systems
*J. Phys.: Condens. Matter **15**, S2501 (2003)*

A. SHUKLA, M. CALANDRA, M. D'ASTUTO, M. LAZZERI, F. MAURI, CH. BELLIN, M. KRISCH, J. KARPINSKI, S. M. KAZAKOV, J. JUN, D. DAGHERO, K. PARLINSKI
Phonon dispersion and lifetimes in MgB_2
*Phys .Rev. Letters **90**, 095506 (2003)*

A.V. SOLOGUBENKO, J. JUN, S.M. KAZAKOV, J. KARPINSKI, H.R. OTT
Thermal conductivity of single-crystalline MgB_2
*Phys. Rev. B **66**, 014504 (8 pages) (2002)*

A.V. SOLOGUBENKO, J. JUN, S.M. KAZAKOV, J. KARPINSKI , H.R. OTT
Temperature dependence and anisotropy of the bulk upper critical field H_{c2} of MgB_2
*Phys. Rev. B **65**, 180505 (4 pages) (2002)*

V. SOLOGUBENKO, J. JUN, S.M. KAZAKOV, J. KARPINSKI, H.R. OTT
Anomalous low-temperature thermal conductivity of MgB_2
*Physica C **388-389**, 133-134 (2003)*

A.V. SOLOGUBENKO, S.M. KAZAKOV, H.R. OTT
Diffusive energy transport in the S=1 Haldane chain compound $AgVP_2S_6$
*Physical Review B **68**, 094432 (2003)*

A.V. SOLOGUBENKO, I.L. LANDAU, H.R. OTT, A. BILUSIC, A. SMONTARA, H. BERGER
Unusual Magnetic-Field-Induced Phase Transition in the Mixed State of Superconducting $NbSe_2$
*Physical Review Letters, Vol. **91**, 197005 (2003)*
In collaboration with project 12 G. Margaritondo, EPFL

A.V. SOLOGUBENKO, H.R. OTT, G. DHALENNE, A. REVCOLEVSCHI
Universal behaviour of spin-mediated energy transport in S = 1/2 chain cuprates: $BaCu_2Si_2O_7$ as an example
*Europhysics Letters, Vol. **62**, 540-546 (2003)*

L. YA. VINNIKOV, J. KARPINSKI, S. M. KAZAKOV, J. JUN, J. ANDEREGG, S. L. BUD'KO, P. C. CANFIELD
Vortex structure in MgB_2 single crystals by Bitter decoration technique
*Phys. Rev. B **67**, 092512 (2003)*

L. YA. VINNIKOV, J. KARPINSKI, S. M. KAZAKOV, J. JUN, J. ANDEREGG, S. L. BUD'KO, P. C. CANFIELD
Bitter decoration of vortex structure in MgB_2 single crystals
*Physica C **385**, 177-179 (2003)*

P. VONLANTHEN, K.B. TANAKA, A. GOTO, W.G. CLARK, P. MILLET, J.Y. HENRY, J.L. GAVILANO, H.R. OTT, F. MILA, C. BERTHIER, M. HORVATIC, Y. TOKUNAGA, P. KUHNS, A.P. REYES, W.G. MOULTON
High-magnetic-field NMR studies of $LiVGe_2O_6$: A quasi-one-dimensional spin S=1 system
*Phys. Rev.B **65**, 214413 (10 pages) (2002)*
In collaboration with project 9 T.M. Rice & M. Sigrist, ETHZ

Y. WANG, F. BOUQUET, I. SHEIKIN, P. TOULEMONDE, B. REVAZ, M. EISTERER, H.W. WEBER, J. HINDERER, A. JUNOD
Specific heat of MgB_2 after irradiation
*J. Phys.: Cond. Matter **15**, 883-893 (2003)*
Project 3 R. Flükiger, UniGe and project 4 A. Junod, UniGe

G. A. WIGGER, R. MONNIER, H.R. OTT, D.P. YOUNG, Z. FISK
Electronic Transport in EuB_6
Phys. Rev. B, accepted for publication

G.A. WIGGER, CH. WÄLTI, H.R. OTT, A.D. BIANCHI, Z. FISK
Magnetization-dependent electronic transport in Eu-based hexaborides
*Phys. Rev. B **66**, 212410 (4 pages) (2002)*

Y. XU, M. KHAFIZOV, L. SATRAPINSKY, P. KUS, A. PLECENIC, J. KARPINSKI, J. JUN, S.M. KAZAKOV, R. SOBOLEWSKI
Picosecond dynamics of the superconducting state in MgB_2
Physica C in print

D.P. YOUNG, Z. FISK, J.D. THOMPSON, H.R. OTT, S.B. OSEROFF, R.G. GOODRICH
Magnetic properties - Parasitic ferromagnetism in a hexaboride? Reply
*Nature **420**, 144 (2002)*

M. ZEHETMAYER, M. EISTERER, J. JUN, S. M. KAZAKOV, J. KARPINSKI, AND H. W. WEBER
Fishtail effect in neutron irradiated superconducting MgB_2 single crystals
Submitted to Phys. Rev. B

M. ZEHETMAYER, M. EISTERER, J. JUN, S. M. KAZAKOV, J. KARPINSKI, A. WISNIEWSKI, H.W. WEBER
Anisotropy in superconducting MgB_2: A comparison of SQUID and torque measurements
Physica C, in print

M. ZEHETMAYER, M. EISTERER, S.M. KAZAKOV, J. KARPINSKI, A. WISNIEWSKI, R. PUZNIAK, A. DAIGNERE, H.W. WEBER

Effects of neutron and electron irradiation on superconducting $HgBa_2CuO_{4+x}$ single crystals
Physica C in print

M. ZEHETMAYER, M. EISTERER, H.W.WEBER, J.JUN, S.M.KAZAKOV, J. KARPINSKI
Reversible and irreversible properties of superconducting MgB_2
*Physica C **388-389**, 159 (2003)*

M. ZEHETMAYER. F.M. SAUERZOPF, H.W. WEBER, J. KARPINSKI, M. MURAKAMI
Comparative study of sequential neutron irradiation and annealing effects in superconducting $YBa_2Cu_3O_{7-x}$, $Y_2Ba_4Cu_8O_{16}$ and $NdBa_2Cu_3O_{7-x}$ single crystals
*Physica C **383**, 232-240 (2002)*

Project 9, T. M. Rice and M. Sigrist, ETH Zurich

N. AGRAIT, E. BASCONES, C. DE LAS HERAS, F. GUINEA, T.M. RICE, G. RUBIO-BOLLINGER, S. VIEIR
Single-channel transmission in gold one-atom contacts and chains
*Phys. Rev. B **67**, 121407-121410 (2003)*

***** V.I. ANISIMOV, R. HLUBINA, M.A. KOROTIN, V.V. MAZURENKO, T.M. RICE, A.O. SHORIKOV, M. SIGRIST
First-order transition between a small gap semiconductor and a ferromagnetic metal in the Isoelectronic alloy $FeSi_{1-x}Ge_x$
*Phys. Rev. Lett. **89**, 257203 (4 pages) (2002)*

Y. ASANO, Y. TANAKA, M. SIGRIST, S. KASHIWAYA
Josephson current in s-wave superconductor/Sr_2RuO_4 junctions
*Phys. Rev. B **67**, 184505-184511(2003)*

E. BAUER, G. HILSCHER, H. MICHOR, CH. PAUL, E. SCHEIDT, A. GRIBANOV, Y. SEROPEGIN, H. NÖEL, M. SIGRIST, P. ROGL
Heavy Fermion superconductivity and magnetic order in non-centrosymmetric $CePt_3Si$
*Phys. Rev. Lett. **92**, 27003-27006 (2004)*

***** F. BECCA, F. MILA
Peierls-like transition induced by frustration in a two-dimensional antiferromagnet
*Phys. Rev. Lett. **89**, 037204 (4 pages) (2002)*

***** F. BECCA, F. MILA, D. POILBLANC
Tetramerization of a frustrated spin-1/2 chain
*Phys. Rev. Lett. **91**, 067202-067205 (2003)*

L. BENFATTO, C. MORAIS SMITH
Signature of stripe pinning in optical conductivity
*Phys. Rev. B **68**, 184513-184217 (2003)*

L. BENFATTO, C. MORAIS SMITH
Optical response for a discrete stripe
To appear in Physica C (2003)

L. BENFATTO, S.G. SHARAPOV, H. BECK
Effect of orbital currents on the restricted optical sum rule
Submitted to Europhys. Lett. (2003)
In collaboration with project 10 P. Martinoli, UniNe

L. BENFATTO, A. TOSCHI, S. CAPRARA, C. CASTELLANI
Phase-fluctuation contribution to the depletion of the superfluid stiffness in continuum and lattice models for s- and d-wave superconductors
Submitted to Phys. Rev. B, (2003)

B. BINZ, D. BAERISWYL, B. DOUCOT
Wilson's renormalization group applied to 2D lattice electrons in the presence of van Hove singularities
*Eur. Phys. J. B **25**, 69-87 (2002)*

B. BINZ, D. BAERISWYL, B. DOUCOT
Weakly interacting electrons and the renormalization group
*Ann. Phys. (Leipzig) **12**, 704-732 (2003)*

B. BINZ, D. BAERISWYL, B. DOUCOT
Weak-coupling instabilities of two-dimensional lattice electrons
To appear in Physica C

B. BINZ, M. SIGRIST
Metamagnetism of itinerant electrons in multi-layer ruthenates
To be published in Europhys. Lett

S. DOMMANGE, M. MAMBRINI, B. NORMAND, F. MILA
Static impurities in the Kagome lattice: dimer freezing and mutual repulsion
*Phys. Rev. B **68**, 224416-224424 (2003)*

T. DROESE, R. BESSELING, P. KES, C. MORAIS SMITH
Plastic depinning in artificial vortex channels: competition between bulk and boundary nucleation
*Phys. Rev. B **67**, 064508 (2003)*

F. DUC, P. MILLET, S. RAVY, A. THIOLLET, A. GHORAYEB, A. STEPANOV, F. MILA
Low temperature superstructure and charge ordering effect in η-$Na_{1.286}V_2O_5$
To appear in Phys. Rev. B

M. FERRERO, F. BECCA, F. MILA
Freezing and large time scales induced by geometrical frustration
*Phys. Rev. B **68**, 214431-214442 (2003)*

S. FRATINI, B. VALENZUELA, D. BAERISWYL
Variational wave function for generalized Wigner lattices in one dimension
*J. Phys. IV France **12**, p. 9-69 (2002)*

S. FRATINI, B. VALENZUELA, D. BAERISWYL
Incipient quantum melting of the one-dimensional Wigner lattice
To appear in Synth. Met

P. FRIGERI, D.F. AGTERBERG, A. KOGA, M. SIGRIST
Superconductivity without inversion symmetry: MnSi versus $CePt_3Si$
To be published in Phys. Rev. Lett

P.A. FRIGERI, C. HONERKAMP, T.M. RICE
Landau-Fermi liquid analysis of the 2D t-t' Hubbard model
*Eur. Phys. J. B **28**, 61-70 (2002)*

J.L. GAVILANO, D. RAU, S. MUSHKOLAJ, H.R. OTT, P. MILLET, F. MILA
DC-susceptibility and NMR response of a low-dimensional quantum magnet: $Na_2V_3O_7$
*Physica B **312,** 622-623 (2002)*
In collaboration with project 8 H.R. Ott, ETHZ

J.L. GAVILANO, D. RAU, S. MUSHKOLAJ, H.R. OTT, P. MILLET, F. MILA
A low-dimensional spin S=1/2 system at the quantum critical limit: $Na_2V_3O_7$
*Physical Review Letters **90**, 167202-167205 (2003)*
In collaboration with project 8 H.R. Ott, ETHZ

J.L. GAVILANO, D. RAU, SH. MUSHKOLAJ, H.R. OTT, F. MILA, P. MILLET
Low-temperature NMR studies of $Na_2V_3O_7$
*Physica B **329-333**, 703-704 (2003)*
In collaboration with project 8 H.R. Ott, ETHZ

T. GLOOR, F. MILA
Correlation gap in armchair carbon nanotubes
*Europhys. Lett. **61**, 513-519 (2003)*

T. GLOOR, F. MILA
Strain induced correlation gaps in carbon nanotubes
Submitted to Eur. Phys. J. B.

M.O. GOERBIG, P. LEDERER, C. MORAIS SMITH
Microscopic theory of the reentrant IQHE in the first and second excited LLs
*Phys. Rev. B **68**, 241302- 241305 (2003)*

M.O. GOERBIG, P. LEDERER, C. MORAIS SMITH
Competition between quantum-liquid and electron-solid phases in intermediate Landau levels
To appear in Phys. Rev. B (15.3.2004)

M.O. GOERBIG, P. LEDERER, C. MORAIS SMITH
Second generation of composite fermions in the Hamiltonian theory
Submitted to Phys. Rev. B (2004)

M.O. GOERBIG, P. LEDERER, C. MORAIS SMITH
The mathematical foundation of self-similarity in quantum Hall systems
Submitted to Europhys. Lett. (2004)

M.O. GOERBIG, C. MORAIS SMITH
Scaling approach to the phase diagram of quantum Hall systems
*Europhys. Lett. **63**, 736-742 (2003)*

M.O. GOERBIG, C. MORAIS SMITH
Magneto roton instabilities and static susceptibilities in higher Landau levels
*Phys. Rev. B **66**, 241101 (2002)*

J. GORYO, M. SIGRIST
Feedback effect in p-wave pairing state
*J. Phys. Chem. Solids **63**, 1537-1540 (2002)*

V. GRITSEV, D. BAERISWYL
Exactly soluble isotropic spin-1/2 ladder models
*J. Phys. A, Math. Gen. **36**, 12129-12144 (2003)*

V. GRITSEV, B. NORMAND, D. BAERISWYL
Phase diagram of the generalized spin ladder with ring exchange
Submitted to Eur. Phys. J. B

V. GRITSEV, B. NORMAND, D. BAERISWYL
Phase diagram of the Heisenberg spin ladder with ring exchange
To appear in Phys. Rev. B.

N. HASSELMANN, A.H. CASTRO NETO, C. MORAIS SMITH
Coupling of longitudinal and transverse stripe fluctuations
*Journal of Superconductivity: Incorporating Novel Magnetism **16**, 491 (2003)*

N. HASSELMANN, A.H. CASTRO NETO, C. MORAIS SMITH
Spin-glass phase of cuprates
*Phys. Rev. B **69**, 014424-014444 (2004)*

N. HASSELMANN, A.H. CASTRO NETO, C. MORAIS SMITH
Topological defects and the spin glass phase of cuprates
*Europhys. Lett. **56**, 870-876 (2001)*

A. HONECKER, F. MEIER, D. LOSS, B. NORMAND
Spin dynamics and coherent tunnelling in the molecular magnetic rings Fe_6 and Fe_8
*Eur. Phys. J B **27**, 487 (2002)*

C. HONERKAMP, T.M. RICE
Cuprates and ruthenates: Similarities and differences
*J. Low Temp.Phys. **131**, 159-167 (2003)*

C. HONERKAMP, M. SALMHOFER, T.M. RICE
Flow to strong coupling in the two-dimensional Hubbard model
*Eur. Phys. J. B **27**, 127-134 (2002)*

V. JURICIC, L. BENFATTO, A.O. CALDEIRA, C. MORAIS SMITH
Dynamics of topological defects in a spiral: a scenario for the spin-glass phase of cuprates
To appear in Phys. Rev. Lett. (2004)

V. JURICIC, B. SAZDOVIC
Thirring sine-Gordon relationship by the Canonical methods
*Eur. Phys. J. C **32**, 443-452 (2004)*

***** K. KODAMA, M. TAKIGAWA, M. HORVATIC, C. BERTHIER, H. KAGEYAMA, Y. UEDA, S. MIYAHARA, F. BECCA, F. MILA
Magnetic superstructure in the two-dimensional quantum antiferromagnet $SrCu_2(BO_3)_2$
*Science **298**, 395-399 (2002)*

A. KOGA, N. KAWAKAMI,T.M. RICE, M. SIGRIST
Orbital-selective Mott transition in the degenerate Hubbard model
Submitted to Phys. Rev. Lett.

A. KOGA, N. KAWAKAMI, M. SIGRIST
Quantum phase transitions of the S=1 Shastry-Sutherland model
*J. Phys. Soc. Jpn. **72**, 938-942 (2003)*

H. KUSUNOSE, T.M. RICE
Single-particle spectrum in the electron-doped cuprates
*Phys. Rev. Lett. **91**, 186407-106410 (2003)*

H. KUSUNOSE, T.M. RICE, M. SIGRIST
Electronic thermal conductivity of multigap superconductors: Application to MgB_2
*Phys. Rev. B **66**, 214503 (5 pages) (2002)*

H. KUSUNOSE, M. SIGRIST
The penetration depth in Sr_2RuO_4: Evidence for orbital-dependent superconductivity
*Europhys. Lett. **60**, 281-287 (2002)*

***** A. LAUCHLI, D. POILBLANC, T.M. RICE, S.R. WHITE
Li-induced spin and charge excitations in a spin ladder
*Phys. Rev. Lett. **88**, 257201 (4 pages) (2002)*

***** P. LEMMENS, K.-Y. CHOI, E. E. KAUL, CH. GEIBEL, K. BECKER, W. BRENIG, R. VALENTI, C. GROS, M. JOHNSSON, P. MILLET, F. MILA
Evidence for an unconventional magnetic instability in the spin-tetrahedra system $Cu_2Te_2O_5Br_2$
*Phys. Rev. Lett. **87**, 227201 (2001)*

M. MATSUMOTO
Microscopic model for the magnetization plateaus in NH_4CuCl_3
*Phys. Rev. **68**, 18403-18406 (2003)*

M. MATSUMOTO, C. BELARDINELLI, M. SIGRIST
Upper critical field of the 3-Kelvin phase in Sr_2RuO_4
*J. Phys. Soc. Jpn. **72**, 1623-1626 (2003)*

***** M. MATSUMOTO, B. NORMAND, T.M. RICE, M. SIGRIST
Magnon dispersion in the field-induced magnetically ordered phase of $TlCuCl_3$
*Phys. Rev. Lett. **89**, 077203 (4 pages) (2002)*

M. MATSUMOTO, B. NORMAND, T.M. RICE, M. SIGRIST
Field- and pressure-induced magnetic quantum phase transitions in $TlCuCl_3$
To be published in Phys. Rev. B.

M. MATSUMOTO, M. SIGRIST
Ehrenfest relations and magnetoelastic effects in field-induced ordered phases
Submitted to Phys. Rev. B.

F. MILA, D. DEAN
Dynamic spin-glass behavior in disorder-free, two component model of quantum frustrated magnets
Eur. Phys. J. B, in press.
Project 9, Rice

S. MIYAHARA, F. BECCA, F. MILA
Theory of spin density profile in the magnetization plateaus of $SrCu_2(BO_3)_2$
*Phys. Rev. B **68**, 024401-024410 (2003)*

S. MIYAHARA, F. MILA
Effect of Spin-orbit interction in $LaTiO_3$
*Progress of Theoretical Physics Suppl. **145,** p. 266 (2002)*

B. NORMAND, A.P. KAMPF
Suppression of static stripe formation by next-neighbor hopping
*Phys. Rev. B **65**, 020509 (4 pages) (2002)*

B. NORMAND, M. MATSUMOTO, O. NOHADANI, S. WESSEL, S. HAAS, T. M. RICE, M. SIGRIST
Pressure- and field-induced magnetic quantum phase transitions in $TlCuCl_3$
To appear in J. Phys.: Condens. Matter.

B. NORMAND, F. MILA
Absence of effective spins 1/2 induced by nonmagnetic impurities in a class of low-dimensional magnets
*Phys. Rev. B **65**, 104411 (7 pages) (2002)*

B. NORMAND, A. M. OLES
Circulating-current states and ring-exchange interactions in cuprates
To appear in Physica C

K. PENC, M. MAMBRINI, P. FAZEKAS, F. MILA
Quantum phase transition in the SU(4) spin-orbital model on the triangular lattice
*Phys. Rev. B **68**, 012408-012411 (2003)*
In collaboration with project 11 L. Forró, EPFL

M. RACZKOWSKI, B. NORMAND, A.M. OLES
Vertical and diagonal stripes in the extended Hubbard model
*Phys. Stat. Sol. (b) **236**, 376-379 (2003)*

*****T.M. RICE
To condense or not to condense
*Science **298**, 760-761(2002)*

T.M. RICE

Some open issues in correlated electron systems
J. Phys. Chem. Solids ***63****, 1319-1323 (2002)*

T.M. RICE
Computations and the future of materials physics
Physica B ***318****, 82-86 (2002)*

M. SIGRIST
Ehrenfest relations for ultrasound absorption in Sr_2RuO_4
Prog. Theor. Phys. ***107****, 917-925 (2002)*

M. SIGRIST, M. TROYER
Orbital and spin correlations in $Ca_{2-x}Sr_xRuO_4$: a mean field study
Submitted to Eur Phys. J. B.

T. SILLER, M. TROYER, T.M. RICE, S.R. WHITE
Transition between hole pairs and four-hole clusters in four-leg t-J ladders
Phys. Rev. B ***65****, 205109 (10 pages) (2002)*

M. TERNES, C. WEBER, M. PUIVETTA, F. PATTHEY, J. P. PELZ, T. GIAMARCHI, F. MILA, W-D. SCHNEIDER
Electronic bandstructure of a two-dimensional dilute "solid": Ce superlattice on Ag(111)
Submitted to Phys. Rev. Lett.
In collaboration with project 18 T. Giamarchi, UniGe

R. VALENTI, T. SAHA-DASGUPTA, F. MILA
Ab initio investigation of $VOSeO_3$, a spin gap system with coupled spin dimers
Phys. Rev. B ***68****, 244111-244114 (2003)*

B. VALENZUELA, S. FRATINI, D. BAERISWYL
Charge and spin order in one-dimensional electron systems with long-range Coulomb interactions
Phys. Rev. B ***68****, 045112-045122 (2003)*

F. VERNAY, K. PENC, P. FAZEKAS, F. MILA
Orbital degeneracy as a source of frustration in $LiNiO_2$
Submitted to Phys. Rev. B.
In collaboration with project 11 L. Forró, EPFL

K. VOELKER, M.SIGRIST
Unconventional superconductivity in $MgCNi_3$
Submitted to Phys. Rev. Lett.

P. VONLANTHEN, K.B. TANAKA, A. GOTO, W.G. CLARK, P. MILLET, J.Y. HENRY, J.L. GAVILANO, H.R. OTT, F. MILA, C. BERTHIER, M. HORVATIC, Y. TOKUNAGA, P. KUHNS, A.P. REYES, W.G. MOULTON
High-magnetic-field NMR studies of $LiVGe_2O_6$: A quasi-one-dimensional spin S=1 system
Phys. Rev.B ***65****, 214413 (10 pages) (2002)*
In collaboration with project 8 H.R. Ott, ETHZ

C. WEBER, L. CAPRIOTTI, G. MISGUICH, F. BECCA, M. ELHAJAL, F. MILA
Ising transition driven by frustration in a 2D classical model with continuous symmetry
Phys. Rev. Lett. ***91****, 177202-177205 (2003)*

S. WEHRLI, C. HELM
Interface Steps in field effect devices
J.Appl.Phys. submitted, cond-mat/0312441 (2004)
In collaboration with project 6 G. Blatter, ETHZ

S. WEHRLI, E. KOCH, M. SIGRIST
Field-doping of C60 crystals: Polarization and Stark splitting
Phys. Rev. B ***68****, 115412-115425 (2003)*

S. WESSEL, M. INDERGAND, A.LAUCHLI, U. LEDERMANN, M. SIGRIST
Inhomogeneously doped two-leg ladder systems
Phys. Rev. B ***67****, 184517-7 (2003)*

S. WESSEL, A. JAGANNATHAN, S. HAAS
Quantum Antiferromagnetism in Quasicrystals
Phys. Rev. Lett. ***90****, 177205-177208 (2003)*

V. ZLATIC, I. MILAT, B. HORVATIC, B. COQBLIN, G. CZYCHOLL, C. GRENEBACH
Thermoelectric power of derium and ytterbium intermetallics
Phys. Rev. ***68****, 104432-104442 (2003)*

Project 10, P. Martinoli, University of Neuchâtel

D.F. AGTERBERG, M.J.W.DODGSON,
Reply to comment on London theory for superconducting phase transitions in external magnetic fields: Applications to UPt_3
Phys. Rev. Lett. ***91****, 079702 (2003)*

N. ANDRENACCI, G.G.N. ANGILELLA, H. BECK, R. PUCCI
Linear response around a local impurity in the pseudogap regime of an anisotropic superconductor : precursor pairing vs the d-density-wave scenario
submitted to Phys. Rev. B

N. ANDRENACCI, H.BECK
The internal structure of preformed pairs in underdoped high temperature superconductors
to be submitted to Phys. Rev. B

N. ANDRENACCI, H.BECK
Internal structure of preformed Cooper pairs
Submitted to Physica C Proceedings

N. ANDRENACCI, H.BECK
Internal structure of fluctuating Cooper pairs
Submitted to European Physical Journal B

J. AFFOLTER, M. TESEI, H. PASTORIZA, CH. LEEMANN, P. MARTINOLI,
Observation of Ising-like critical fluctuations in frustrated Josephson junction arrays with modulated coupling energies
Physica C ***369****, 313-316 (2002)*

H. BECK, PH. CURTY, A. SEWER, N. ANDRENACCI, S. SHARAPOV
Pairing fluctuations in high temperature superconductors
*Ukrainian Journal of Physics **48**, 829-836 (2003)*

L. BENFATTO, S.G. SHARAPOV, H. BECK,
Effect of orbital currents on the restricted optical sum rule
submitted to Phys. Rev. B
In collaboration with project 9 T.M. Rice & M. Sigrist, ETHZ

***** M. CALAME, S.E. KORSHUNOV, CH. LEEMANN, P. MARTINOLI
Collective Pinning of a Frozen Vortex Liquid in Ultrathin Superconducting $Yba_2Cu_3O_7$ Films
*Phys. Rev. Lett. **86**, 3630-3633 (2001)*

S. CANDIA, CH. LEEMANN, S. MOUAZIZ, P. MARTINOLI,
Investigation of vortex dynamics in Josephson junction arrays with magnetic flux noise measurements
*Physica C **369**, 309-312 (2002)*

PH. CURTY , H.BECK
Anomalous behaviour of high temperature superconductors arising from amplitude fluctuations
to be submitted to Phys. Rev. B

PH. CURTY, H. BECK
The separate role of pairing amplitude and phase in high temperature superconductors
Phys. Rev. Lett. **91**, 257002 (2003)

M.J.W. DODGSON
Phase transitions in isolated vortex chains
Phys. Rev. B **66,** 014509 (9 pages) (2002)

H. FANGOHR, A.E. KOSHELEV, AND M.J.W. DODGSON
Vortex matter in layered superconductors without Josephson coupling: Numerical simulations within a mean-field approach
*Phys. Rev. B **67**, 174508 (2003)*

S.E. KORSHUNOV
Fluctuation-dissipation theorem and flux noise in overdamped Josephson- junction arrays
*Phys. Rev. B **66**, 104513 (8 pages) (2002)*

S.E. KORSHUNOV
Kinks pairs unbinding on domain walls and the sequence of phase transitions in fully frustrated XY models
*Phys. Rev. Lett. **88**, 167007 (4 pages) (2002)*

S.E. KORSHUNOV
Magnetoinductance of Josephson junction arrays with frozen vortex diffusion
*Phys. Rev. B **68**, 094512 (2003)*

S.E. KORSHUNOV
Phase transitions in antiferromagnetic XY model with a Kagomé lattice
*Phys. Rev. B **65**, 054416 (2002)*

T. MAITRA, H. BECK, A. TARAPHDER
Antiferromagnetism and superconductivity in a model with extended pairing interactions
*European Physical Journal B **21**, 527–533 (2001)*

***** R. MEYER, S.E. KORSHUNOV, CH. LEEMANN, P. MARTINOLI
Dimensional crossover and hidden incommensurability in Josephson junction arrays of periodically repeated Sierpinski gaskets
*Phys. Rev. B **66**, 104503 (12 pages) (2002)*

A. RÜFENACHT, P. CHAPPATTE, S. GARIGLIO, C. LEEMANN, J. FOMPEYRINE, J.-P. LOCQUET, P. MARTINOLI
Growth of single unit-cell superconducting $La_{2-x}Sr_xCuO_4$ films
*Solid State Electronics **47**, 2167 (2003)*
In collaboration with project 5 J.M. Triscone, UniGe

A. SEWER, H. BECK
Fluctuating diamagnetism in underdoped high-temperature superconductors
*Phys. Rev. B **64**, 014510, 8 pages (2001)*

A. SEWER, H. BECK
Thermodynamic properties of the attractive Hubbard model
*Phys. Rev. B **64**, 224524 (15 pages) (2001)*

S.G. SHARAPOV, H. BECK
Effective action approach and Carlson-Goldman mode in d-wave superconductors
*Phys. Rev. B **65**, 134516 (17 pages) (2002)*

S.G. SHARAPOV, H. BECK, V.M. LOKTEV
Ginzburg-Landau theory for the time-dependent phase field in a two-dimensional d-wave superconductor
*Physica C, **364-365**, 437- 440 (2001)*

S.G. SHARAPOV, H. BECK, V.M. LOKTEV
Finite-temperature time-dependent effective theory for the phase field in two-dimensional d-wave neutral superconductors
*Phys. Rev. B **64**, 134519 (18 pages) (2001)*

S.G. SHARAPOV, V.P .GUSYNIN, H. BECK
Low-temperature superfluid stiffness of a d-wave superconductor in a magnetic field
*Phys. Rev. B **66**, 012515 (4 pages) (2002)*

S.G. SHARAPOV, V.P. GUSYNIN, H .BECK
Effective action approach to the Leggett's mode in two-band superconductors
*European Physical Journal B **30**, 45-51 (2002)*

***** S.G. SHARAPOV, V.P. GUSYNIN, H. BECK
Transport properties in the d-density-wave state in an external magnetic field: The Wiedemann-Franz law
*Phys. Rev. B, **67**, 144509 (2003)*

S.G. SHARAPOV, V.P. GUSYNIN, H. BECK
Low termperature superfluid density of d-wave superconductor in an applied magnetic field
*Ukrainean Journal of Physics **48**, 863-868 (2003)*

S.G. SHARAPOV, V.P. GUSYNIN, H. BECK
Magnetic oscillations in planar systems with the Dirac-like spectrum of quasiparticle excitations
*To appear in Phys. Rev. B **69**, cond-mat/ 0308216 (2004)*

S.G. SHARAPOV, V.P. GUSYNIN, H. BECK
d-density wave state in an external magnetic field
Submitted to Physica C Proceedings (cond-mat/0304574)

Project 11, L. Forró, EPF Lausanne

N. BARISIC, L. FORRÓ, D. MANDRUS, R. JIN, J. HE, P. FAZEKAS
The electrical properties of $Cd_2Re_2O_7$ under pressure
*Physical Review B **67**, 245112 (2003)*

N. BARISIC, R. GAAL, I. KEZSMARKI, G. MIHALY, L. FORRÓ
Pressure dependence of the thermoelectric power of single-walled carbon nanotubes
Submitted to Phys. Rev. B, Rapid Communications

H. BERGER, S. F. LEE, S. H. HUANG, H. W. CHANG, T. M. CHUANG, Y. LIOU, Y. D. YAO, Y. HWU, D. ARIOSA, R. GAAL, A. SALEH, G. MARGARITONDO, L. V. GASPAROV, D. B. TANNER
Coexistence of ferromagnetism and high-temperature superconductivity in Dy-doped BiPbSrCaCuO
*Surf. Rev. Lett. **9**, 1109 (2002)*
In collaboration with project 12 G. Margaritondo, EPFL

M. BOVET, S. VAN SMAALEN, H. BERGER, R. GAÁL, L. FORRÓ, L. SCHLAPBACH, P. AEBI
Interplane coupling in the quasi-two-dimensional 1T-TaS_2
*Phys. Rev. B **67**, 125105 (2003)*
In collaboration with project 12 G. Margaritondo, EPFL, project 14 P. Aebi, UniNe and project 15 L. Schlapbach, UniFr & EMPA

J. DEMSAR, L. FORRÓ, H. BERGER, D. MIHAILOVIC
Femtosecond "snapshots" of gap-forming charge-density-wave correlations in quasi-two-dimensional dichalcogenides 1T-TaS_2 and 2H-$TaSe_2$
*Phys. Rev. B **66**, 041101 (2002)*
In collaboration with project 12 G. Margaritondo, EPFL

S.V. DORDEVI, D.N. BASO, R.C. DYNE, B. RUZICKA, V. VESCOLI, L. DEGIORGI, H. BERGER, R. GAÁL, L. FORRÓ, E. BUCHER
Optical properties of the quasi-two-dimensional dichalcogenides 2H-$TaSe_2$ and 2H-$NbSe_2$
*Eur. Phys. J. B **33**, 15 (2003)*
In collaboration with project 8 H.R. Ott, ETHZ and project 12 G. Margaritondo, EPFL

P. FAZEKAS, K. PENC, H. BERGER, L. FORRÓ, S. CSONKA, I. KEZSMARKI, G. MIHALI
$BaVS_3$: from spin gap insulator to non-Fermi-liquid
*Physica B **312**, 694 (2002)*
In collaboration with project 12 G. Margaritondo, EPFL

R. GAÁL, G. MIHALY, H. BERGER, F. RULLIER-ALBENQUE, L. FORRÓ
Tunneling spectroscopy of $Bi_2Sr_2CaCu_2O_7$ High T_c superconductor with disorder
Submitted

L. V. GASPAROV, K. G. BROWN, A. C. WINT, D. B. TANNER, H. BERGER, G. MARGARITONDO, R. GAÁL, L. FORRÓ
Phonon anomaly at the charge ordering transition in 1T-TaS_2
*Phys. Rev. B **66**, 094301 (2002)*
In collaboration with project 12 G. Margaritondo, EPFL

S. GARAJ, T. KAMBE, L. FORRÓ, A. SIENKIEWICZ, M. FUJIWARA, K. OSHIMA
Polymer phase of the tetrakis(dimethylamino)ethylene-C60 organic ferromagnet
*Physical Review B **68**, 144430 (2003)*

L.V. GASPAROV, K.G. BROWN, A.C. WINT, D.B. TANNER, H. BERGER, G. MARGARITONDO, R. GAÁL, L. FORRÓ
Phonon anomaly at the charge ordering transition in 1T-TaS_2
*Physical Review B **66**, 094301 (2002)*

***** A. JÁNOSSY, T. FEHÉR, A. ERB
Diagonal Antiferromagnetic Easy Axis in Lightly Hole Doped $Y_{1-x}Ca_xBa_2Cu_3O_6$
*Physical Review Letters **91**, 177001(2003)*

A.A. KORDYUK, S. V. BORISENKO, M. S. GOLDEN, S. LEGNER, K. A. NENKOV, M. KNUPFER, J. FINK, H. BERGER, L. FORRÓ, R. FOLLATH
Doping dependence of the Fermi surface in $(Pb,Bi)_2Sr_2CaCu_2O_{8+\delta}$
*Phys. Rev. B **66**, 014502 (2002)*
In collaboration with project 12 G. Margaritondo, EPFL

D. MIHAILOVIC, D. DVORSEK, V.V. KABANOV, J. DEMSAR, J. STEFAN, L. FORRÓ, H. BERGER
Femtosecond data storage, processing and search using collective excitations of a macroscopic quantum state
*Appl. Phys. Lett. **80**, 871 (2002)*

In collaboration with project 12 G. Margaritondo, EPFL

S. MITROVIC, L. PERFETTI, C. SONDERGAARD, G. MARGARITONDO, M. GRIONI, N. BARISIC, L. FORRÓ, L. DEGIORGI
Electronic structure of a quasi-one-dimensional insulator : The molybdenum red bronze $K_{0.33}MoO_3$
*Phys. Rev. B **69**, 035102 (2004)*
In collaboration with project 8 H.R. Ott, ETHZ and project 12 G. Margaritondo, EPFL

K. PENC, M. MAMBRINI, P. FAZEKAS, F. MILA
Quantum phase transition in the SU(4) spin-orbital model on the triangular lattice
*Phys. Rev. B **68**, 012408-012411 (2003)*
In collaboration with project 9 T.M. Rice & M. Sigrist, ETHZ

L. PERFETTI, S. MITROVIC, G. MARGARITONDO, M. GRIONI, L. FORRÓ, L. DEGIORGI, H. HOECHST
Mobile small polarons and the Peierls transition in the quasi-one-dimensional conductor $K_{0.3}MoO_3$
*Phys. Rev. B **66**, 075107 (8 pages) (2002)*
In collaboration with project 8 H.R. Ott, ETHZ and project 12 G. Margaritondo, EPFL

Z. V. POPOVIC, G. MIHÁLI, I. KEZSMÁRKI, H. BERGER, L. FORRÓ, V. V. MOSHCHALKOV
Phonon and spin dynamics in $BaVS_3$ single crystal
*Phys. Rev. B **65**, 132301 (2002)*
In collaboration with project 12 G. Margaritondo, EPFL

***** F. SIMON, V.A. ATSARKIN, V.V. DEMIDOV, R. GAÁL, Y. MORITOMO, M. MILJAK, A. JÁNOSSY, L. FORRÓ
Electron spin resonance and relaxation studies of double-layered manganites
*Physical Review B **67**, 224433 (2003)*

F. VENTURINI, M. OPEL, H. BERGER, L. FORRÓ, B. REVAZ
Doping dependence of the electronic Raman spectra in cuprates
*J. Phys. Chem. Solids **63**, 2345 (2002)*
In collaboration with project 3 R. Flükiger, UniGe and project 12 G. Margaritondo, EPFL

F. VENTURINI, M. OPEL, T. P. DEVEREAUX, J. K. FREERICKS, I. TÜTTO, B. REVAZ, E. WALKER, H. BERGER, L. FORRÓ, R. HACKL
Observation of an unconventional metal-insulator transition in overdoped CuO_2 compounds
*Phys. Rev. Lett. **89**, 107003 (2002)*
In collaboration with project 3 R. Flükiger, UniGe and project 12 G. Margaritondo, EPFL

F. VERNAY, K. PENC, P. FAZEKAS, F. MILA
Orbital degeneracy as a source of frustration in $LiNiO_2$
Submitted to Phys. Rev. B.

In collaboration with project 9 T.M. Rice & M. Sigrist, ETHZ

Project 12 G. Margaritondo, EPF Lausanne

***** M. ABRECHT, D. ARIOSA, D. CLOETTA, S. MITROVIC, M. ONELLION, X. X. XI, G. MARGARITONDO, D. PAVUNA
Strain and High Temperature Superconductivity: Unexpected Results from Direct Electronic Structure Measurements in Thin Films
*Phys. Rev. Letters **91**, 057002 (2003)*

M. ABRECHT, D. ARIOSA, D. CLOETTA, D. PAVUNA, L. PERFETTI, M. GRIONI, G. MARGARITONDO
Photoemission, Correlation And Superconductivity: New Avenues
*Intern. J. Modern Phys. B **17**, 3449 (2003)*

M. ABRECHT, D. ARIOSA, M. ONELLION, G. MARGARITONDO, D. PAVUNA
Structural phase transition in early growth of BSCCO-2212 films on STO substrates
*J. of Appl Phys. **91**, 1187- 1189 (2002)*

E. ANNESE, J.-P. RUEFF, M. GRIONI, G. VANKO, L. DEGIORGI, L. BRAICOVICH, R. GUSMEROLI, C. DALLERA
Valence changes in YbS under pressure: a resonant x-ray emission study
Submitted
In collaboration with project 8 H.R. Ott, ETHZ

R. BEL, K. BEHNIA, H. BERGER
Ambipolar Nernst effect in $NbSe_2$
*Phys. Rev. Lett. **91**, 066602 (2003)*

H. BERGER, S. F. LEE, S. H. HUANG, H. W. CHANG, T. M. CHUANG, Y. LIOU, Y. D. YAO, Y. HWU, D. ARIOSA, R. GAAL, A. SALEH, G. MARGARITONDO, L. V. GASPAROV, D. B. TANNER
Coexistence of ferromagnetism and high-temperature superconductivity in Dy-doped BiPbSrCaCuO
*Surf. Rev. Lett. **9**, 1109 (2002)*
In collaboration with project 11 L. Forró, EPFL

K. BILJAKOVIC, M. MILJAK, D. STARESINIC, J.C. LASJAUNIAS, P. MONCEAU, H. BERGER, F. LEVY
Fractional power law susceptibility and specific heat in low-temperature insulating state of TaS_3
*Europhys. Lett. **62**,(4) 554-560 (2003)*

S.V. BORISENKO, A.A. KORDYUK, T.K. KIM, S. LEGNER, K.A. NENKOV, M.KNUPFER, M.S. GOLDEN, J. FINK, H. BERGER, R. FOLLATH
Superconducting gap in the presence of bilayer splitting in underdoped $(Pb,Bi)_2Sr_2CaCu_2O_{8+\delta}$
*Phys. Rev. B **66**, 140509 (2002)*

S. V. BORISENKO, A. A. KORDYUK, T. K. KIM, A. KOITZSCH, M. KNUPFER, M. S. GOLDEN, J. FINK M. ESCHRIG, H. BERGER, R. FOLLATH
Anomalous enhancement of the coupling to the magnetic resonance mode of underdoped Pb-Bi2212
Phys. Rev. Lett. ***90****, 207001 (2003)*

M. BOVET, D. POPOVIC, F. CLERC, C. KOITZSCH, U. PROBST, E. BUCHER, H. BERGER, D. NAUMOVIC, P. AEBI
Pseudogapped Fermi surfaces of 1T-TaS_2 and 1T-$TaSe_2$: A charge density wave effect
Phys. Rev. B accepted, (15 Mar 2004)
In collaboration with project 14 P. Aebi, UniNe

M. BOVET, S. VAN SMAALEN, H. BERGER, R. GAAL, L. FORRÓ, L. SCHLAPBACH, P. AEBI
Interplane coupling in the quasi-two-dimensional 1T-TaS_2
Phys. Rev. B ***67****, 125105 (2003)*
In collaboration with project 11 L. Forró, EPFL, project 14 P. Aebi, UniNe and project 15 L. Schlapbach, UniFr & EMPA

F. CLERC, M. BOVET, H. BERGER, L. DESPONT, C. KOITZSCH, M.G. GARNIER, P. AEBI
Charge density waves in 1T-TaS_2: An angle-resolved photoemission study
Physica C, submitted
In collaboration with project 14 P. Aebi, UniNe

F. CLERC, M. BOVET, H. BERGER, L. DESPONT, C. KOITZSCH, O. GALLUS, L. PATTHEY, M. SHI, J. KREMPASKI, M. G. GARNIER, P. AEBI
Spin-orbit splitting in the valence bands of 1T-TaS_2 and 1T-$TaSe_2$
J. of Physics C, submitted
In collaboration with project 14 P. Aebi, UniNe

C. DALLERA, E. ANNESE, J.-P. RUEFF, A. PALENZONA, G. VANKO, L. BRAICOVICH, A. SHUKLA, M. GRIONI
Determination of pressure-induced valence changes in $YbAl_2$ by resonant inelastic x-ray emission
Phys. Rev. B ***68****, 245114 (2003)*

C. DALLERA, M. GRIONI, A. PALENZONA, M. TAGUCHI, E. ANNESE, G. GHIRINGHELLI, A. TAGLIAFERRI, N.B. BROOKES, TH. NEISIUS, L. BRAICOVICH
The α–γ transition in metallic Ce revisited with resonant spectroscopies
Submitted

C.DALLERA, M. GRIONI
Resonant scattering of x-rays as a probe of valence and hybridization in solids
Structural Chemistry ***14****, 57-67 (2002)*

C. DALLERA, M. GRIONI, A. SHUKLA, G. VANKO, J. SARRAO, J.P. RUEFF, D.L. COX
New spectroscopy solves an old puzzle: the Kondo scale in heavy fermions
Phys. Rev. Lett. ***88****, 196403 (4 pages) (2002)*

C.DALLERA, M. GRIONI, A. SHUKLA, G. VANKO, J. SARRAO
Truly bulk-sensitive spectroscopic measurements of valence in heavy fermion materials
J. Synchrotron Rad. ***9****, 242-245 (2002)*

J. DEMSAR, L. FORRÓ, H. BERGER, D. MIHAILOVIC
Femtosecond "snapshots" of gap-forming charge-density-wave correlations in quasi-two-dimensional dichalcogenides 1T-TaS_2 and 2H-$TaSe_2$
Phys. Rev. B ***66****, 041101 (2002)*
In collaboration with project 11 L. Forró, EPFL

S.V. DORDEVI, D.N. BASO, R.C. DYNE, B. RUZICKA, V. VESCOLI, L. DEGIORGI, H. BERGER, R. GAAL, L. FORRÓ, E. BUCHER
Optical properties of the quasi-two-dimensional dichalcogenides 2H-$TaSe_2$ and 2H-$NbSe_2$
Eur. Phys. J. B ***33****, 15 (2003)*
In collaboration with project 8 H.R. Ott, ETHZ and project 12 G. Margaritondo, EPFL

S. FAGOT, P. FOURY-LEYLEKIAN, S. RAVY, J-P. POUGET, H. BERGER
One-dimensional instability in $BaVS_3$
Phys. Rev. Lett. ***90****, 196401 (2003)*

***** V. FAVRE-NICOLIN, S. BOS, J. E. LORENZO, J. L. HODEAU, J. F. BERAR, P. MONCEAU, R. CURRAT, F. LEVY H. BERGER
Structural Evidence for Ta-Tetramerization Displacements in the Charge-Density-Wave Compound $(TaSe_4)_2I$ from X-Ray Anomalous Diffraction
Phys. Rev. Letters ***87****, 015502 (2001)*

P. FAZEKAS, K. PENC, H. BERGER, L. FORRÓ, S. CSONKA, I. KEZSMARKI, G. MIHALI
$BaVS_3$: from spin gap insulator to non-Fermi-liquid
Physica B ***312****, 694 (2002)*
In collaboration with project 11 L. Forró, EPFL

L. V. GASPAROV, K. G. BROWN, A. C. WINT, D. B. TANNER, H. BERGER, G. MARGARITONDO, R. GAAL, L. FORRÓ
Phonon anomaly at the charge ordering transition in 1T-TaS_2
Phys. Rev. B ***66****, 094301 (2002)*
In collaboration with project 11 L. Forró, EPFL

G. GHIRINGHELLI, N.B. BROOKES, E. ANNESE, H. BERGER, C. DALLERA, M. GRIONI, L. PERFETTI, A. TAGLIAFERRI, L. BRAICOVICH
Low-energy electronic excitations in layered cuprates by copper L3 resonant inelastic x-ray scattering
Submitted

M. GRIONI, L. PERFETTI, H. BERGER, J. VOIT, H. HOECHST
Evidence for strong correlations in a 1D Peierls system
Physica B ***312-313****, 559-561 (2002)*

Y. HIRAI, I. ZIVKOVIC, B.H. FRAZER, A. REGINELLI, L. PERFETTI , D. ARIOSA, G. MARGARITONDO, M. PRESTER, D. DROBAC, D.T. JIANG,Y. HU, T.K. SHAM, I. FELNER, M. PEDERSON, M. ONELLION
Magnetic interactions and electronic states in superconducting and nonsuperconducting ruthenocuprates
*Phys. Rev. B **65**, 054417 (6 pages) (2002)*

T.K. KIM, A.A. KORDYUK, S.V. BORISENKO, A. KOITZSCH, M. KNUPFER, H. BERGER, J. FINK
Doping dependence of the mass enhancement in (Pb,Bi) Sr_2 $CaCa_2Cu_2O_8$ at the antinodal point in the superconducting and normal state
*Phys. Rev. Lett. **91**, 167002 (2003)*

A.A. KORDYUK, S. V. BORISENKO, M. S. GOLDEN, S. LEGNER, K. A. NENKOV, M. KNUPFER, J. FINK, H. BERGER, L. FORRÓ, R. FOLLATH
Doping dependence of the Fermi surface in $(Pb,Bi)_2Sr_2CaCu_2O_{8+\delta}$
*Phys. Rev. B **66**, 014502 (2002)*
In collaboration with project 11 L. Forró, EPFL

A. A. KORDYUK, S. V. BORISENKO, T. K. KIM, K. A. NENKOV, M. KNUPFER, J. FINK, M. S. GOLDEN, H. BERGER, R. FOLLATH
Origin of the peak-dip-hump line shape in the superconducting-state photoemission spectra of $Bi_2Sr_2CaCu_2O_{8+x}$
*Phys. Rev. Lett. **89**, 077003 (2002)*

C. KUNTSCHER, S. SCHUPPLER, P. HAAS, B. GORSHUNOV, M. DRESSEL, M. GRIONI, F. LICHTENBERG, A. HERRNBERGER, F. MAYR, J. MANNHART
Extremely small energy gap in the quasi-one-dimensional conducting chain compound $SrNbO_{3.41}$
*Phys. Rev. Lett. **89**, 236403 (4 pages) (2002)*

D. MIHAILOVIC, D. DVORSEK, V.V. KABANOV, J. DEMSAR, J. STEFAN, L. FORRÓ, H. BERGER
Femtosecond data storage, processing and search using collective excitations of a macroscopic quantum state
*Appl. Phys. Lett. **80**, 871 (2002)*
In collaboration with project 11 L. Forró, EPFL

S. MITROVIC, L. PERFETTI, C. SONDERGAARD, G. MARGARITONDO, M. GRIONI, N. BARISIC, L. FORRÓ, L. DEGIORGI
Electronic structure of a quasi-one-dimensional insulator : The molybdenum red bronze $K_{0.33}MoO_3$
*Phys. Rev. B **69**, 035102 (2004)*
In collaboration with project 8 H.R. Ott, ETHZ and project 12 G. Margaritondo, EPFL

D. PAVUNA
Phase Diagram and Electronic Properties of High-T_c Superconducting Cuprates
*Modern Physics Letters B **17**, 393 (2003)*

L. PERFETTI, H. BERGER, A. REGINELLI, L. DEGIORGI, H. HOECHST, J. VOIT, G. MARGARITONDO, M. GRIONI
Spectroscopic indications of polaronic carriers in the quasi-one-dimensional conductor $(TaSe_4)_2I$
*Phys. Rev. Lett. **87**, 216404 (4 pages) (2001)*

***** L. PERFETTI, A. GEORGES, S. FLORENS, S. BIERMANN, S. MITROVIC, H. BERGER, Y. TOMM, H. HOECHST, M. GRIONI
Spectroscopic signatures of a bandwidth-controlled Mott transition at the surface of 1T-$TaSe_2$
*Phys. Rev. Lett. **90**, 166401 (2003)*

L. PERFETTI, S. MITROVIC, G. MARGARITONDO, M. GRIONI, L. FORRO, L. DEGIORGI, H. HOECHST
Mobile small polarons and the Peierls transition in the quasi-one-dimensional conductor $K_{0.3}MoO_3$
*Phys. Rev. B **66**, 075107 (8 pages) (2002)*
In collaboration with project 11 L. Forró, EPFL and project 8 H.R. Ott, ETHZ

L. PERFETTI, S. MITROVIC, M. GRIONI
Fermi liquid and non-Fermi liquid spectral lineshapes in low-dimensional solids
*J. Electron Spectr. Rel. Phenom. **127**, 77- 84 (2002)*
Project 12 G. Margaritondo, EPFL

L. PERFETTI, C. ROJAS, A. REGINELLI, L. GAVIOLI, H. BERGER, G. MARGARITONDO, M. GRIONI
Quasi particle Scattering Processes in a Model Fermi Liquid:1T-$TiTe_2$
*Surf. Rev. and Lett. **9**, 1117 (2002)*
Project 12 G. Margaritondo, EPFL

Z. V. POPOVIC, G. MIHÁLI, I. KEZSMÁRKI, H. BERGER, L. FORRÓ, V. V. MOSHCHALKOV
Phonon and spin dynamics in $BaVS_3$ single crystal
*Phys. Rev. B **65**, 132301 (2002)*
In collaboration with project 11 L. Forró, EPFL

M.L. SCHNEIDER, S. RAST, M. ONELLION, J. DEMSAR, A.J. TAYLOR, Y. GLINKA, N.H. TOLK, Y.H. REN, G. LÜPKE, A. KLIMO, Y. XU, R. SOBOLEWSKI, W. SI, X.H. ZENG, A. SOUKIASSIAN, X.X. XI, M. ABRECHT, D. ARIOSA, D. PAVUNA, A. KRAPF, R. MANZKE, J.O. PRINTZ, M.S. WILLIAMSEN, K.E. DOWNUM, P. GUPTASARMA, I. BOZOVIC
Carrier relaxation time divergence in single and double layer cuprates,
*Eur. Phys. J. B **36**, 327 (2003)*

A. SMONTARA, I TKALCEC, A. BILUSIC, M. BUDIMIR, H. BERGER
Anisotropy of the thermal conductivity in $(TaSe_4)_2I$
*Physica B **316-317**, 279 (2002)*

* A.V.SOLOGUBENKO, I.L.LANDAU, H.R.OTT, A.BILUSIC, A.SMONTARA AND H.BERGER
Unusual magnétique-field-induced phase transition in the mixed state of superconducting $NbSe_2$
Phys. Rev. Lett. ***91****, 197005 (2003)*
In collaboration with project 8 H.R. Ott, ETHZ

D. STARESINIC , K. BILJAKOVIC, W. BRUTTING, K. HOSSEINI, P. MONCEAU, H. BERGER, F. LEVY
Wide-temperature-range dielectric response of the charge-density-wave system TaS_3
Phys. Rev. B ***65****, 165109 (2002)*

D. STARESINIC, A. KIS, K. BILJAKOVIC, B. EMERLING, J. W. BRILL, J. SOULETIE, H. BERGER, F .LEVY
Specific heats of the charge density wave compounds o-TaS_3 and $(TaSe_4)_2I$
Eur. Phys. J. B ***29****, 71 (2002)*

F. VENTURINI, M. OPEL, H. BERGER, L. FORRÓ, B. REVAZ
Doping dependence of the electronic Raman spectra in cuprates
J. Phys. Chem. Solids ***63****, 2345 (2002)*
In collaboration with project 3 R. Flükiger, UniGe and project 11 L. Forró, EPFL

F. VENTURINI, M. OPEL, T. P. DEVEREAUX, J. K. FREERICKS, I. TÜTTO, B. REVAZ, E. WALKER, H. BERGER, L. FORRÓ, R. HACKL
Observation of an unconventional metal-insulator transition in overdoped CuO_2 compounds
Phys. Rev. Lett. ***89****, 107003 (2002)*
In collaboration with project 3 R. Flükiger, UniGe and project 11 L. Forró, EPFL

I. ZIVKOVIC, Y. HIRAI, B.H. FRAZER, M. PRESTER, DJ. DROBAC, D. ARIOSA, H. BERGER, D. PAVUNA , G. MARGARITONDO, I. FELNER, M. ONELLION
Ruthenocuprates $RuSr_2(Eu,Ce)_2Cu_2O_{10-y}$: Intrinsic magnetic multilayers
Phys. Rev. B ***65****, 144420 (8 pages) (2002)*

I. ZIVKOVIC, D. DROBAC, D. ARIOSA, H. BERGER, D. PAVUNA, M. PRESTER
Superconducting transition in ruthenocuprate viewed from the studies of imaginary part of ac-susceptibility
Europhys. Lett. ***60****, 917 (2002)*

Project 13, H. Keller, University of Zurich

M. ANGST, D. DI CASTRO, R. PUZNIAK, A. WISNIEWSKI, J. JUN, S.M. KAZAKOV, J. KARPINSKI, S. KOHOUT, H. KELLER
Anisotropic properties of MgB_2 by torque magnetometry
Physica C in print
In collaboration with project 8 H.R. Ott, ETHZ

M. ANGST, R. PUZNIAK, A. WISNIEWSKI, J. JUN, S.M. KAZAKOV, J. KARPINSKI, J. ROOS, H. KELLER
Comments on Superconducting anisotropy and evidence for intrinsic pinning in single crystalline MgB_2
submitted to Phys.Rev.B., cond-mat/0206407
In collaboration with project 8 H.R. Ott, ETHZ

M. ANGST, R. PUZNIAK, A. WISNIEWSKI, J. ROOS, H. KELLER, P. MIRANOVIC, J. JUN, S.M. KAZAKOV, J. KARPINSKI
Anisotropy of the superconducting state properties and phase diagram of MgB_2 by torque magnetometry on single crystals
Physica C ***385****, 143-154 (2003)*
In collaboration with project 8 H.R. Ott, ETHZ

* D. CHARALAMBOUS, P. G. KEALEY, E. M. FORGAN, T. M. RISEMAN, M. W. LONG, C. GOUPIL, R. KHASANOV, D. FORT, P. J. C. KING, S. L. LEE, F. OGRIN
Vortex motion in type-II superconductors probed by muon spin rotation and small-angle neutron scattering
Phys. Rev. B ***66****, 054506 (4 pages) (2002)*

D. DI CASTRO, R. KHASANOV, D.G. ESHCHENKO, J. ROOS, I.M. SAVIC, A. SHENGELAYA, L. BUD'KO, P.C. CANFIELD, K. CONDER, J. KARPINSKI, S. M. KAZAKOV, R.A. RIBEIRO, H. KELLER
Absence of a boron isotope effect on the magnetic penetration depth in MgB_2
submitted to Phys. Rev. Lett.
In collaboration with project 8 H.R. Ott, ETHZ

J. KARPINSKI, M. ANGST, J. JUN, S. M. KAZAKOV, R. PUZNIAK, A.WISNIEWSKI, J. ROOS, H. KELLER, A. PERUCCHI, L. DEGIORGI, M. R. ESKILDSEN, P. BORDET, L. VINNIKOV, A. MIRONOV
MgB_2 single crystals: high pressure growth and physical properties
Supercond. Sci. Technol. ***16****, 221-230 (2003)*
In collaboration with Project 2 Ø. Fischer, UniGe and project 8 H.R. Ott, ETHZ

* H. KELLER
Unconventional isotope effects in cuprate high-temperature superconductors
Physica B ***326****, 283-288 (2003)*

* R. KHASANOV, D. G. ESHCHENKO, H. LUETKENS, E. MORENZONI, T. PROKSCHA, A. SUTER, N. GARIFIANOV, M. MALI, J. ROOS, K. CONDER, H. KELLER
Direct Observation of the Oxygen Isotope Effect on the In-Plane Magnetic Field Penetration Depth in Optimally Doped $YBa_2Cu_3O_{7-d}$
Physical Review Letters ***92****, 057602-1 - 057602-4 (2004)*

R. KHASANOV, T. SCHNEIDER, J. KARPINSKI, H. KELLER
Finite size and pressure effects in $YBa_2Cu_4O_8$ probed by the magnetic field penetration depth measurements
Submitted to Phys. Rev. B
In collaboration with Project 8 H.R. Ott, ETHZ

***** R. KHASANOV, A. SHENGELAYA, K. CONDER, E. MORENZONI, I.M. SAVIC, H. KELLER
The oxygen-isotope effect on the in-plane penetration depth in underdoped $Y_{1-x}Pr_xBa_2Cu_3O_{7-\delta}$ as revealed by muon-spin rotation
Journal of Physics: Condensed Matter ***15****, L17-L23 (2003)*

R. KHASANOV, A. SHENGELAYA, E. MORENZONI, M. ANGST, K. CONDER, I. M. SAVIC, D. LAMPAKIS, E. LIAROKAPIS, A. TATSI, H. KELLER
Site-selective oxygen isotope effect on the magnetic-field penetration depth in under doped $Y_{0.6}Pr_{0.4}Ba_2Cu_3O_{7-d}$
Physical Review B ***68****, 220506 (2003)*

E. MORENZONI, H. GLÜCKLER, T. PROKSCHA, R. KHASANOV, H. LUETKENS, M. BIRKE, E. M. FORGAN, CH. NIEDERMAYER, M. PLEINES
Implantation studies of keV positive muons in thin metallic films
Nuclear Instruments and Methods in Physics Research B ***192****, 254-266 (2002)*

E. MORENZONI, R. KHASANOV, H. LUETKENS, T. PROKSCHA, A. SUTER, N. GARIFIANOV, H. GLÜCKLER, M. BIRKE, E. FORGAN, H. KELLER, J. LITTERST, CH. NIEDERMAYER, G. NIEUWENHUYS
Low energy muons as probes of thin films and near surface regions
Physica B ***326****, 196-204 (2003)*

T. SCHNEIDER, R. KHASANOV, K. CONDER, H. KELLER
Relevance of electron–lattice coupling in cuprate superconductors
J. Phys.: Condens. Matter ***15****, L763–L769 (2003)*

***** A. SHENGELAYA, R. KHASANOV, D. G. ESHCHENKO, I. FELNER, U. ASAF, I. M. SAVIC, H. KELLER, K. A. MÜLLER
Coexistence of magnetism and superconductivity in $Eu_{1.4}Ce_{0.6}RuSr_2Cu_2O_{10}$: A muon spin rotation and magnetization study
Physical Review B ***69****, 024517-1 - 024517-6 (2004)*

Project 14, P. Aebi, University of Neuchâtel

M. BOVET, D. POPOVIC, F. CLERC, C. KOITZSCH, U. PROBST, E. BUCHER, H. BERGER, D. NAUMOVIC, P. AEBI
Pseudogapped Fermi surfaces of 1T-TaS_2 and 1T-$TaSe_2$: A charge density wave effect
Phys. Rev. B accepted, (15 Mar 2004)
In collaboration with project 12 G. Margaritondo, EPFL

M. BOVET, V. N. STROCOV, F. CLERC, C. KOITZSCH, D. NAUMOVIC, P. AEBI
Excited states mapping by secondary photoemission
Phys. Rev. Lett., submitted.

M. BOVET, S. VAN SMAALEN, H. BERGER, R. GAAL, L. FORRÓ, L. SCHLAPBACH, P. AEBI
Interplane coupling in the quasi-two-dimensional 1T-TaS_2
Phys. Rev. B ***67****, 125105 (2003)*
In collaboration with project 11 L. Forró, EPFL, project 12 G. Margaritondo, EPFL and project 15 L. Schlapbach, UniFr & EMPA

F. CLERC, M. BOVET, H. BERGER, L. DESPONT, C. KOITZSCH, M.G. GARNIER, P. AEBI
Charge density waves in 1T-TaS_2: An angle-resolved photoemission study
Physica C, submitted
In collaboration with project 14 P. Aebi, UniNe and project 12 G. Margaritondo, EPFL

F. CLERC, M. BOVET, H. BERGER, L. DESPONT, C. KOITZSCH, O. GALLUS, L. PATTHEY, M. SHI, J. KREMPASKI, M. G. GARNIER, P. AEBI
Spin-orbit splitting in the valence bands of 1T-TaS_2 and 1T-$TaSe_2$
J. of Physics C, submitted
In collaboration with project 12 G. Margaritondo, EPFL

L. DESPONT, C. LICHTENSTEIGER, F. CLERC, C. KOITZSCH, D. NAUMOVIC, M.G. GARNIER, F.J. GARCIA DE ABAJO, M.A. VAN HOVE, J.-M. TRISCONE, P. AEBI
Study of the ferroelectric polarization of ultra-thin films of $PbTiO_3$ by X-ray photoelectron diffractio,
Phys. Rev. B, submitted
In collaboration with project 5 J.M. Triscone, UniGe

R. FASEL, P. AEBI
X-ray photoelectron diffraction: probing atom positions and molecular orientation at surfaces
Chimia, ***56****, 566-572 (2002)*

J. HAYOZ, C. KOITZSCH, M. BOVET, D. NAUMOVIC, L. SCHLAPBACH, P. AEBI
Electronic Structure of the YH_3 phase from Angle-Resolved Photoemission Spectroscopy
Phys. Rev. Lett. ***90****, 196804 (2003)*
In collaboration with project 15 L. Schlapbach, UniFr & EMPA

J. HAYOZ, C. KOITZSCH, D. POPOVIC, M. BOVET, D. NAUMOVIC, P. AEBI
Angle-scanned photoemission on YbHx : relevance for switchable mirrors
Surf. Rev. Lett., accepted

* D. NAUMOVIC, P. AEBI, L. SCHLAPBACH, C. BEELI, K. KUNZE, T.A. LOGRASSO, D.W. DELANEY
Formation of a stable Decagonal Quasicrystalline Al-Pd-Mn Surface Layer
Phys. Rev. Lett. ***87****, 195506-1 – 195506-4 (2001)*
In collaboration with project 15 L. Schlapbach, UniFr & EMPA

P. STAROWICZ, O. GALLUS, TH. PILLO, Y. BAER
Size Effects in Photoemission of One-Dimensional Metals
Phys. Rev. Lett. ***89****, 256402 (4 pages) (2002)*

Project 15, L. Schlapbach, University of Fribourg and EMPA

M. BOVET, S. VAN SMAALEN, H. BERGER, R. GAAL, L. FORRÓ, L. SCHLAPBACH, P. AEBI
Interplane coupling in the quasi-two-dimensional 1T-TaS_2
Phys. Rev. B ***67****, 125105 (2003)*
In collaboration with project 11 L. Forró, EPFL, project 12 G. Margaritondo, EPFL and project 14 P. Aebi, UniNe

O. GRÖNING, R. CLERGERAUX, L. NILSSON, P. RUFFIEUX, P. GRÖNING, L. SCHLAPBACH
Prospects and limitations of carbon nanotube field emission electron sources
Chimia ***56****, 553-561(2002)*

O. GRÖNING, L-O. NILSSON, P. GRÖNING, L. SCHLAPBACH
Properties and characterization of chemical vapor deposition diamond field emitters
Solid-State Electronics ***45****, 929 (2001)*

P. GRÖNING, P. RUFFIEUX, L. SCHLAPBACH, O. GRÖNING
Carbon Nanotubes for Cold Electron Emission
Advanced Engineering Materials ***5,*** *541-550 (2003)*

J. HAYOZ, C. KOITZSCH, M. BOVET, D. NAUMOVIC, L. SCHLAPBACH, P. AEBI
Electronic Structure of the YH_3 Phase from Angle-Resolved Photoemission Spectroscopy
Submitted to Phys. Rev. Lett.
In collaboration with project 14 P. Aebi, UniNe

W.I. MILNE, K.B.K. TEO, G.A.J. AMARATUNGA, P. LEGAGNEUX, L. GANGLOFF, J.-P. SCHNELL, V. SEMET, V.T. BINH, O. GRÖNING
Carbon nanotubes as field emission sources
Journal of Materials Chemistry, accepted for publication (2004)

W.I. MILNE, K.B.K. TEO, M. CHHOWALLA, G.A.J. AMARATUNGA, S.B. LEE, D.G. HASKO, H. AHMED, O. GRÖNING, P. LEGAGNEUX, L. GANGLOFF, J.P. SCHNELL, G. PIRIO, D. PRIBAT, M. CASTIGNOLLES, A. LOISEAU, V. SEMET, V.T. BINH
Electrical and Field Emission Investigation of Individual Carbon Nanotubes from Plasma Enhanced Chemical Vapour Deposition
Diamond and Related Materials ***12****, 422-428 (2003)*

* D. NAUMOVIC, P. AEBI, L. SCHLAPBACH, C. BEELI, K. KUNZE, T.A. LOGRASSO, D.W. DELANEY
Formation of a stable Decagonal Quasicrystalline Al-Pd-Mn Surface Layer
Phys. Rev. Lett. ***87****, 195506-1 – 195506-4 (2001)*
In collaboration with project 14 P. Aebi, UniNe

* P. RUFFIEUX, O. GRÖNING, M. BIELMANN, L. SCHLAPBACH, C. SIMPSON, K. MÜLLEN, P. GRÖNING
Supramolecular columns of hexabenzocoronenes on copper and gold (111) surfaces
Physical Review B ***66****, 073409 (4 pages) (2002)*

P. RUFFIEUX, O. GRÖNING, M. BIELMANN, P. GRÖNING
Hydrogen chemisorption on sp^2-bonded carbon: Influence of the local curvature and local electronic effects
Appl. Physics A, acc. for publ. (2004)

* P. RUFFIEUX, O. GRÖNING, M. BIELMANN. P. MAURON, L. SCHLAPBACH, P. GRÖNING
Hydrogen adsorption on sp^2-bonded carbon: Influence of the local curvature
Phys. Rev. B ***66****, 245416 (8 pages) (2002)*

P. RUFFIEUX, P. GRÖNING, O. GRÖNING, M. BIELMANN, M. MELLE-FRANCO, F. ZERBETTO
Charge-density oscillation on graphite induced by the interference of electron waves
Submitted to the Phys. Rev. Lett. (2004)

K.B.K. TEO, S.–B. LEE, M. CHHOWALLA, V. SEMET, V.T. BINH, O. GRÖNING, M. CASTIGNOLLES, A. LOISEAU, G. PIRIO, P. LEGAGNEUX, D. PRIBAT, D.G. HASKO, H. AHMED, G.A.J. AMARATUNGA, W.I. MILNE
Plasma enhanced chemical vapour deposition carbon nanotubes/nanofibers – how uniform do they grow?
Nanotechnology ***14****, 204-211 (2003)*

A. VAN ZUUK, C. TH. H. HEERKENS, A. H. V. VAN VEEN, T. F. TEEPEN, M. J. WIELAND, O. GRÖNING, P. KRUIT
Fabrication and characterization of silicon carbide field emitter array
Microelectronic Engineering, accepted for publication (2004)

Project 16, A. Furrer, ETH Zurich and PSI Villigen

N. CAVADINI, D. ANDREICA, F.N. GYGAX, A. SCHENCK, K. KRÄMER, H.-U. GÜDEL, H. MUTKA, A. WILDES
Local spin susceptibility in $KCuCl_3$
*Physica B **335**, 37-40 (2003)*

N. CAVADINI, CH. RÜEGG, A. FURRER, H.-U. GÜDEL, K. KRÄMER, H. MUTKA, P. VORDERWISCH
Triplet excitations in low-H_c spin-gap systems $KCuCl_3$ and $TlCuCl_3$: An inelastic neutron scattering study
*Phys. Rev. B **65**, 132415/1-4 (2002)*

N. CAVADINI, CH. RÜEGG, A. FURRER, H.-U. GÜDEL, K. KRÄMER, H. MUTKA, A. WILDES, K. HABICHT, P. VORDERWISCH
Triplet modes in a quantum spin liquid across the critical field
*Int. J. Mod. Phys. B **16**, 3302-3305 (2002)*

***** U. DIVAKAR, A.J. DREW, S.L. LEE, R. GILARDI, J. MESOT, F.Y. OGRIN, D. CHARALAMBOUS, E.M. FORGAN, G.I. MENON, N. MOMONO, M. ODA, C. DEWHURST
Direct observation of the flux-line vortex glass phase in a type-II superconductor
Phys. Rev. Lett., submitted

A. FURRER, K. CONDER, P. HÄFLIGER, A. PODLESNYAK
Isotope, pressure and doping effects on the pseudogap in the LSCO-type compounds studied by neutron spectroscopy
Physica C, in print

***** A. FURRER, D. RUBIO TEMPRANO, J. MESOT, K. CONDER, K.A. MÜLLER
On the Pseudogap State in Y- and La-Type High-Temperature Superconductors: Doping Dependence, Isotope Effects, and Electronic Properties Studied by Neutron Spectroscopy
*J. Supercond. **15**, 361-365 (2002)*

R. GILARDI, A. HIESS, N. MOMONO, M. ODA, M. IDO, J. MESOT
Unusual interplay between copper-spin and vortex dynamics in slightly overdoped $La_{1.83}Sr_{0.17}CuO_4$
Europhys. Lett., submitted

***** R. GILARDI, J. MESOT, A. DREW, U. DIVAKAR, S.L. LEE, E.M. FORGAN, O. ZAHARKO, K. CONDER, V.K. ASWAL, C.D. DEWHURST, R. CUBITT, N. MOMONO, M. ODA
Direct Evidence for an Intrinsic Square Vortex Lattice in the Overdoped High-T_c Superconductor $La_{1.83}Sr_{0.17}CuO_{4+\delta}$
*Phys. Rev. Lett. **88**, 217003 (4 pages) (2002)*

***** R. GILARDI, J. STAHN, F. ALTORFER, N. MOMONO, M. ODA, J. MESOT
Doping dependence of the tetragonal-orthorhombic phase transition in the superconducting compound $La_{2-x}Sr_xCuO_{4\pm d}$
*Appl. Phys. A **74**, S1624-S1626 (2002)*

R. GILARDI, J. MESOT, A.J. DREW, U. DIVAKAR, S.L. LEE, N.H. ANDERSEN, J. KOHLBRECHER, N. MOMONO, M. ODA
Field-induced hexagonal to sqare transition of the vortex lattice in overdoped $La_{1.8}Sr0.2CuO_4$
Physica C, in print

R. GILARDI, S. STREULE, J. MESOT, A.J. DREW, U. DIVAKAR, S.L. LEE, S.P. BROWN, E.M. FORGAN, N. MOMONO, M.ODA
A Small angle neutron scattering study of the vortex matter in $La_{2-x}Sr_xCuO_4$ (x=0.17)
*Int. J. Mod. Phys. B **17**, 3411-3414 (2003)*

R. GILARDI, S. STREULE, A. HIESS, H.M. RONNOW, M. ODA, N. MOMONO, M. IDO, J. MESOT
Spin dynamics in the mixed phase of $La_{2-x}Sr_xCuO_4$ (z=0.10, x=0.17)
Physica B, in print

***** P.S. HÄFLIGER, A. PODLESNYAK, K. CONDER, A. FURRER
Pressure effect on the pseudogap in the optimally doped high-temperature superconductor $La_{1.81}Sr_{0.15}Ho_{0.04}Cu_{16}O_4$
Phys. Rev. Lett., submitted

P.S. HÄFLIGER, A. PODLESNYAK, K. CONDER, E. POMJAKUSHINA, A. FURRER
Observation of the pseudogap in the overdoped high-temperature superconductor $La_{1.71}Sr_{0.25}Ho_{0.04}CuO_4$
Europhys. Lett., to be submitted

M. MÜLLER, H.-J. MIKESKA, N. CAVADINI
Dynamical structure factors for dimerized spin systems
*J. Phys.: Condens. Matter **15**, 8513-8526 (2003)*

***** D. RUBIO TEMPRANO, K. CONDER, A. FURRER, H. MUTKA, V. TROUNOV, K.A. MÜLLER
Copper and Oxygen Isotope effects on the pseudogap in the high-temperature superconductor $La_{1.81}Ho_{0.04}Sr_{0.15}CuO_4$ studied by neutron crystal-field spectroscopy
*Phys. Rev. B **66**, 184506 (4 pages) (2002)*

***** D. RUBIO TEMPRANO, J. MESOT, S. JANSSEN, K. CONDER, A. FURRER, A. SOKOLOV, V. TROUNOV, S.M. KAZAKOV, J. KARPINSKI, H. MUTKA, K.A. MÜLLER
Isotope effects on the pseudogap in high-temperature superconductors
*Appl. Phys. A **74**, S1630-S1634 (2002)*

* CH. RÜEGG, N. CAVADINI, A. FURRER, K. KRÄMER, H.U. GÜDEL, P. VORDERWISCHE, H. MUTKA
Spin dynamics in the high- field phase of quantum-critical S=1/2 $TlCuCl_3$
*Appl. Phys. A **74**, S840-S842 (2002)*

* CH. RÜEGG, N. CAVADINI, A. FURRER, H.U. GÜDEL, K. KRÄMER, H. MUTKA, A. WILDES, K. HABICHT, P. VORDERWISCH
Bose-Einstein condensation of the triplet states in $TlCuCl_3$
*Nature **423**, 62-65 (2003)*

Project 17, D. van der Marel, University of Geneva

A. B. KUZMENKO, N. TOMBROS, H. J. A. MOLEGRAAF, M. GRÜNINGER, D. VAN DER MAREL, S. UCHIDA
c-Axis Optical Sum Rule and a Possible New Collective Mode in $La_{2-x}Sr_xCuO_4$
*Phys. Rev. Lett. **91**, 037004 (2003)*

C. A. KUNTSCHER, D. VAN DER MAREL, M. DRESSEL, F. LICHTENBERG, J. MANNHART
Signatures of polaronic excitations in quasi-one-dimensional $LaTiO_{3.41}$
*Phys. Rev. B **67**, 035105 (2003)*

C. PRESURA, M. POPINCIUC, P. H. M. VAN LOOSDRECHT, D. VAN DER MAREL, G. MARIS, T. T. M. PALSTRA, H. YAMADA, Y. UEDA
Charge ordering signatures in the optical properties of β-$Na_{0.33}V_2O_5$
*Phys. Rev. Lett. **90**, 026402 (2003)*

S. TAJIMA, S. UCHIDA, D. VAN DER MAREL, D. N. BASOV
Comment on "Phase Diagram of $La_{2-x}Sr_xCuO_4$ Probed in the Infrared: Imprints of Charge Stripe Excitations"
*Phys. Rev. Lett **91**, 129701 (2003)*

A. A. TSVETKOV, F. P. MENA, P. H. M. VAN LOOSDRECHT, D. VAN DER MAREL,Y. REN, A. A. NUGROHO, A. A. MENOVSKY, I. S. ELFIMOV, G. A. SAWATZKY
Structural, electronic, and magneto-optical properties of YVO_3
*Physical Review B **69**, 075110 (2004)*

F. P. MENA, D. VAN DER MAREL, M. FÄTH, A. A. MENOVSKY, J. A. MYDOSH
Heavy Carriers and Non-Drude Optical Conductivity in MnSi
*Phys. Rev. B **67**, R241101 (2003)*

D. VAN DER MAREL
Short-range spin- and pair-correlations: a variational wave-function
Michael J. Rice memorial issue of "Synthetic Metals", in press (2004)

*D. VAN DER MAREL, H. J. A. MOLEGRAAF, J. ZAANEN, Z. NUSSINOV, F. CARBONE, A. DAMASCELLI, H. EISAKI, M. GREVEN, P. H. KES, M. LI
Quantum critical behaviour in a high-T_c superconductor
*Nature **425**, 271-274 (2003)*

Project 18, T. Giamarchi, University of Geneva

C. BOLECH, T. GIAMARCHI
Point-contact tunneling involving spin-triplet superconductors
To appear in Phys. Rev. Lett. (2004)

A.F. HO, M.A. CAZALILLA, T. GIAMARCHI
Deconfinement in a 2D optical lattice of coupled 1D boson systems
Submitted to PRL, cond-mat/0310382.

T. GIAMARCHI, E. ORIGNAC, D. POILBLANC
Les échelles quantiques
*Pour la science **305**, 58 – 65 (2003)*

T. NATTERMANN, T. GIAMARCHI, P. LE DOUSSAL
Quantum creep in one dimensional charge density waves and Luttinger liquids
Submitted to PRL (March 2003)

T. NATTERMANN, T. GIAMARCHI, P. LE DOUSSAL
Variable-range hopping and quantum creep in one dimension
*Phys. Rev. Lett. **91**, 056603 (2003)*

E. OLIVE, JC. SORET, P. LE DOUSSAL, T. GIAMARCHI
Numerical simulation evidence of dynamical transverse Meissner effect and moving Bose glass phase *Phys. Rev. Lett. **91**, 037005 (2003)*

P. PARUCH, T. GIAMARCHI, J.-M. TRISCONE
Domain wall creep in mixed c-a axis $Pb(Zr0_{.2}Ti0_{.8})O_3$ thin films
*Annalen der Physik **13**, 95 (2004)*
In collaboration with project 5 J.M. Triscone, UniGe

A. ROSSO, T. GIAMARCHI
X-ray diffraction of a disordered charge density wave
*Phys. Rev. B **68**, 140201(R) (2003)*

G. SCHEHR, T. GIAMARCHI, P. LE DOUSSAL
Specific heat of the quantum Bragg glass
Submitted to PRL (Dec 2002)

G. SCHEHR, T. GIAMARCHI, P. LE DOUSSAL
Specific heat of classical disordered elastic systems
*Phys. Rev. Lett. **91**,11700. (2003)*

G. SCHEHR, T. GIAMARCHI, P. LE DOUSSAL

Specific heat of the quantum Bragg Glass
To appear in Europhys. Lett. (2004)

M. TERNES, C. WEBER, M. PIVETTA, F. PATTHEY, J. P. PELZ, T. GIAMARCHI,F. MILA, W.-D. SCHNEIDER
Electronic bandstructure of a two-dimensional dilute "solid": Ce superlattice on Ag(111)
Submitted to PRL.(Jan 2004)
In collaboration with project 9, Rice

***** T. TYBELL, P. PARUCH, T. GIAMARCHI, J.-M. TRISCONE
Domain wall creep in epitaxial ferroelectric $Pb(Zr0_{.2}Ti_{0.8})O_3$ thin films
Phys. Rev. Lett. ***89****, 097601 (4 pages) (2002)*
In collaboration with project 5 J.M. Triscone, UniGe

5.2 Scientific articles in journals without peer review

Project 3 R. Flükiger, University of Geneva

A. BRUNIGER, R. FLÜKIGER
Internationale Zusammenarbeit bei der Hochtemperatur supraleitung im Energiebereich
SEV/VSE Bulletin 02.011.01

R. FLUKIGER, E. GIANNINI
Bi, Pb(2223) tapes: present and future
Scenet Newsletter, No. ***3****, 7-10 (2003)*

Project 6 G. Blatter, ETH Zurich

C. HELM, L.N. BULAEVSKII
Optics with Spatial Dispersion Josephson Plasma Resonance, Online Proceedings of "Future Perspectives of Superconducting Josephson Devices"
Online Proceeding, Pommersfelden 29.6.-4.7.2002, http://www.physik.uni-erlangen.de/PI3/intrinsic/.

H.G. KATZGRABER, G. FRIEDMAN, G.T. ZIMANYI
Fingerprinting hysteresis
Cond-mat/0307178

H.G. KATZGRABER,I. CAMPBELL
Critical properties of the three- and four-dimensional gauge glass
Cond-mat/0310100

L. KRUSIN-ELBAUM, T. SHIBAUCHI, G. BLATTER, C.H. MIELKE, M. LI, M.P. MALEY, P.H. KES
Pseudogap state in overdoped $Bi_2Sr_2CaCu_2O_{8+y}$
Proceedings of the US-Polish Workshop, Ladek Zdroj, Poland, July 14-16 (2002), eds. P.W. Klamut and G.W. Crabtree, Physica C ***387****, 169-174 (2003)*

Project 7 R. Nesper, ETH Zurich

C. KUBATA, A. KRÄNZLIN, M. WÖRLE, R. NESPER
$Eu_5Mg_{18}Si_{13}$ - a new phase in the Eu/Mg/Si-system
Chimia ***56****, 395 (2002)*

C. KUBATA, F. KRUMEICH, M. WÖRLE, R. NESPER
A New Phase in the Yb/Si-System

Chimia ***56****, 395 (2002)*

IVANTCHENKO, F. KRUMEICH, R. NESPER
New Reactions of Sodium Acetylide
Chimia **56**, 393 (2002)

G. R. PATZKE, A. MICHAILOVSKI, F. KRUMEICH,R. NESPER
Oxidic Nanotubes and Nanorods
International Conferenceon High Pressure – Science and Technology, Bordeaux, 2003

G. R. PATZKE, A. MICHAILOVSKI, F. KRUMEICH,R. NESPER
Solvothermal Morphology Design of Transition Metal Oxides
6th International Conference on Materials Chemistry: Frontiers and Interfaces, Sheffield, 2003

G. R. PATZKE, A. MICHAILOVSKI, F. KRUMEICH,R. NESPER
Solvothermal Morphology Design: Nanoscale Tungsten Oxides
Euromat 2003, Lausanne, 2003

S. PIOTTO PIOTTO, A. ZÜRN, R. NESPER
CURVIS – A Computer program to analyze phase transition
Chimia **349**, 2056 (2002)

X. QINGXING, M. WÖRLE, R. NESPER
A New Zintl Phase synthesized via Thermal Decomposition
Chimia **56**, 405 (2002)

J. WILLEMS, R. NESPER
Zintl Phase Double Salts: An Overview (Poster)
Chimia ***56****,* 405 (2002)

A. ZÜRN, S. PIOTTO PIOTTO, C. MENSING, B. RÜTTIMANN, R. NESPER, W. UHLIG
New media for teaching inorganic chemistry
Chimia ***56****,* 406 (2002)

Project 9 T.M. Rice, ETH Zurich

Y. ASANO, T. HIRAI, Y. TANAKA, J. INOUE, M. SIGRIST, S. KASHIWAYA
Effects of spin-orbit scattering on Josephson current between s-wave superconductor and Sr_2ruO_4,
Physica C ***388****, 505-506 (2003)*

L. BENFATTO, A. TOSCHI, S. CAPRARA, C. CASTELLANI
Coherence length in superconductors from weak to strong coupling
cond-mat/0109486
S. FRATINI, B. VALENZUELA AND D. BAERISWYL
Variational wave function for generalized Wigner lattices in one dimension
Proc. Int. Workshop on Electronic Crystals, J. Phys. (France) IV 12, Pr9-69 (2002)

N. HASSELMANN, A.H. CASTRO NETO AND C. MORAIS SMITH
Charge density wave formation in the low-temperature- tetragonal phase of cuprates
Cond-mat/0112029

C. HONERKAMP, T.M. RICE
Single band model for the unconventional superconductivity in both cuprates and ruthenates
*Physica C **388**, 11-14 (2003)*

H. KUSUNOSE, M. SIGRIST
Penetration Depth in Sr_2RuO_4 : Nonlocal Effects in a Multi Orbital Superconductor
ETH preprint

S. MIYAHARA, F. MILA
Effect of spin-orbit interation in $LaTiO_3$
Prog. Theor. Phys. Suppl. 145 (2002) 266-271

M. RACZKOWSKI, B. NORMAND AND A. M. OLES
Vertical and Diagonal Stripes in the Extended Hubbard Model
To appear in Phys. Stat. Sol. (cond-mat/0205437)

M. SIGRIST
The complex interplay of spin and orbital degrees of freedom
Proceedings: Magnetism, Lecture Notes of the 1st Summer School on Condensed Matter Research

M. SIGRIST
Ruthenates: unconventional superconductivity and magnetic properties
Proceedings: Hvar workshop on Strongly correlated electrons

Project 12 G. Margaritondo, EPF Lausanne

M. ABRECHT, D. ARIOSA, D. CLOETTA, G. MARGARITONDO, D. PAVUNA
Electronic Properties of High Temperature Superconducting Thin Films Grown by Pulsed Laser Deposition, published in Oxide Physics and NanoEngineering V
In proceedings of SPIE volume 4811: "Superconducting and Nano-engineering IV", I. Bozovic, D. Pavuna (eds) p.102 (2002)

C. DALLERA, M. GRIONI, A. SHUKLA, G. VANKO, J.L. SARRAO, J.-P. RUEFF, D.L. COX
Intermediate valence and Kondo energy-scale probed by resonant inelastic x-ray scattering
ESRF Highlights 2002, p. 51-52

M. GRIONI, H. BERGER, L. PERFETTI, S. MITROVIC, A. REGINELLI, H. HOECHST
Band features and strong correlations in 1D Peierls systems
*J. Phys. IV France **12**, p. 9-33 (2002)*

D. PAVUNA, M. ABRECHT, D. CLOETTA, X. X. XI, G. MARGARITONDO, D. ARIOSA
Systematic studies of (magneto)transport, structural and electronic properties of ultra-thin films of high-T_c cuprates and related layered oxides
*Current Appl. Phys. **2** (4) 345-348 (2002)*

M.L. SCHNEIDER, S. RAST, M. ONELLION, J. DEMSAR, A.J. TAYLOR, Y. GLINKA, N.H. TOLK, Y.H. REN, G. LÜPKE, A. KLIMOV, Y. XU, R. SOBOLEWSKI, WEIDONG SI, X.H. ZENG, A. SOUKIASSIAN, X.X. XI, M. ABRECHT, D. ARIOSA, D. PAVUNA, R. MANZKE, J.O. PRINTZ, D.K. PARKHURST, K.E. DOWNUM, P. GUPTASARMA, I. BOZOVIC
Femtosecond optical studies of cuprates
In proceedings of SPIE volume 4811: "Superconducting and Nano-engineering IV", I. Bozovic, D. Pavuna (eds) p.174 (2002)

G. MARGARITONDO
A historically correct didactic first step in the quantum world: stressing the interplay of relativity, thermodynamics and quantum physics
*European J. Phys **24**, 15 (2003)*

G. MARGARITONDO
The Future of X-ray Sources: New Ideas and New Plans
*Synchrotron Rad. in Natural Sci. **2**. 10 (2003)*

Project 15 L. Schlapbach University of Fribourg and EMPA

O. GRÖNING, L. NILSSON, P. GRÖNING, L. SCHLAPBACH
From Diamond to Carbon Nanotube Field Emitter
*Mat. Res. Soc. Symp. Proc. **675**, W6.1.1-12 (2001)*

O. GRÖNING, R. CLERGERAUX, L. NILSSON, P. RUFFIEUX, L. SCHLAPBACH, P. GRÖNING
Carbon Nanotubes for Future Field Electron Emission Devices
Proceeding of the Electrochemical Society 2002-18 "Cold Cathodes II", p. 45 (2002)

Project 18 T. Giamarchi, University of Geneva

T. GIAMARCHI, R. CHITRA, P. LE DOUSSAL
Disordered elastic systems and electronic crystals
*J. Phys IV (France) **12**, 277-282 (2002)*

T. NATTERMANN, T. GIAMARCHI, P. LE DOUSSAL
Variable range hopping and quantum creep in one dimension
Cond-mat/0303233 (5 pages) (2003)

5.3 Books and scientific articles in anthologies

MaNEP Management, University of Geneva

* M. KUGLER, O. KUFFER (EDITORS)
MaNEP Facilities
Editor MaNEP, 110 pages, April 2003
700 copies.

O. KUFFER, M. KUGLER, A.A. MANUEL, I. MAGGIO-APRILE, R. CARTONI (EDITORS)
MaNEP Newsletter
Bi-annual edition (2001-2003), 6 issues of 8 pages, 1500 copies per issue.

Project 2 Ø. Fischer, University of Geneva

B. W. HOOGENBOOM, CH. RENNER, I. MAGGIO-APRILE, Ø. FISCHER
Scanning tunneling spectroscopy on vortex cores in high-T_c superconductors
In: Vortices in unconventional superconductors and superfluids, R. P. Huebener, N. Schophohl and G. E. Volovik (eds.), Springer series in solid-state science ***132*** *(2002) 269-282*

Project 3 R. Flükiger, University of Geneva

E. BELLINGERI, R. FLÜKIGER
The compound TIBCCO
(Chapter C3) *of "Handbook of Superconducting Materials", Volume 1, Superconductivity, Materials and Processes, edited by D. Cardwell and D. Ginley, IOP Publishing Ltd, Bristol and Philadelphia*

R. FLÜKIGER, W. KLOSE
Superconductors, transition temperature and characterisation of elements, alloys and components
In: Subvolume ***21*** *E: Tl…Zr, Landolt-Bornstein, New Series, Springer-Verlag, (eds.) (2002)*

R. FLÜKIGER
Growth of A15 type single crystals and polycrystals and their physical properties
(Chapter B2.5) of "Handbook of Superconducting Materials", Volume 1, Superconductivity, Materials and Processes, edited by D. Cardwell and D. Ginley, IOP Publishing Ltd, Bristol and Philadelphia, 391-406 (2003)

R. FLÜKIGER
Overview of low T_c materials for conductor applications
(Chapter B3.3.1) of "Handbook of Superconducting Materials", Volume 1, Superconductivity, Materials and Processes, edited by D. Cardwell and D. Ginley, IOP Publishing Ltd, Bristol and Philadelphia, 585-602 (2003)

B. SEEBER
Processing of low T_c conductors: the compounds $PbMo_6S_8$ and $SnMo_6S_8$
(Chapter B3.3.5) of "Handbook of Superconducting Materials", Volume 1, Superconductivity, Materials and Processes, edited by D. Cardwell and D. Ginley, IOP Publishing Ltd, Bristol and Philadelphia, 685-706 (2003)

C. SENATORE, M. POLICHETTI, N. CLAYTON, R. FLÜKIGER, S. PACE
Detection of the Vortex Dynamic Regimes in MgB_2 by Third Harmonic AG susceptibility Measurements
In: "Horizons in Superconductivity", to be published in 2004

H. SUO, P.TOULEMONDE, R. FLÜKIGER
Processing of low T_c conductors: the compound MgB_2
(Chapter B3.3.6) of "Handbook of Superconducting Materials", Volume 1, Superconductivity, Materials and Processes, edited by D. Cardwell and D. Ginley, IOP Publishing Ltd, Bristol and Philadelphia, 707-719 (2003)

Project 4, A. Junod, University of Geneva

A. JUNOD, Y. WANG, F. BOUQUET, P. TOULEMONDE
Specific heat of the 38-K superconductor MgB_2 in the normal and superconducting state: bulk evidence for a double gap
In: Studies of High Temperature Superconductors, Ed. A. Narlikar, Nova Publishers, Commack (N.Y.) ***38****, 179, cond-mat/0106394 (2002)*

Project 6 G. Blatter ETH Zurich

* G. BLATTER, V.B. GESHKENBEIN
Vortex Matter
In: The Physics of Superconductors, Vol. 1, Conventional and High-T_c superconductors, eds. K.H. Bennemann and Ketterson (Springer, Berlin, 2003) 726 - 936

Project 8 H.R. Ott, ETH Zurich

D. BAERYSWIL, L. DEGIORGI (EDITORS)
Strong interactions in low dimensions
In: Kluwer Acad. Pub. (2003)
In collaboration with project 9 T.M.Rice & M. Sgrist, ETHZ

L. DEGIORGI
Optical properties of correlated systems
In "Concepts in Electron Correlation", Proceedings of the ARW NATO Workshop Hvar, Croatia, page 363, October 2002,
Eds. A.C. Hewson and V. Zlatic, Kluwer Academic Publishers (2003)

H.R. OTT
High-T_c Superconductivity
In: The Physics of Superconductors Vol. I,
eds. K.H. Bennemann and J.B. Ketterson (Springer, Berlin, 385-494 (2003)

Project 9 T.M. Rice – M. Sigrist, ETZ Zurich

D. BAERYSWIL, L. DEGIORGI (EDITORS)
Strong interactions in low dimensions
In: Kluwer Acad. Pub. (2003)
In collaboration with project 8 H.R. Ott, ETHZ

A.H. CASTRO NETO, C. MORAIS SMITH
Charge inhomogeneities in strongly correlated systems
In: "Strong interactions in low dimensions", ed. By D. Baeriswyl and L. Degiorgi, Kluwer Acad. Pub. in print (2003)

A.H. CASTRO NETO, C. MORAIS SMITH
Charge inhomogeneities in strongly correlated systems
In: " Strong Interactions in Low Dimensions", ed. By D. Baeriswyl and L. Degiorgi, Kluwer Acad. Pub. (2003)

M.O. GOERBIG, P. LEDERER, C. MORAIS SMITH
Comment faire fondre un cristal d'électrons bidimensionnels sous champ magnétique
Spécial recherche, Journal of the University Paris-Sud (2004)

M.O. GOERBIG, P. LEDERER, C. MORAIS SMITH
La réentrance de l'effet Hall quantique entier,
Images de la physique, magazine of CNRS (2004)

M. SIGRIST
Ruthenates: unconventional superconductivity and magnetism, Concepts of Electron Correlations
by A.C. Hewson and V. Zlatic, Kluver Academic Publishers (2003)

Project 12 G. Margaritondo EPF Lausanne

I.BOZOVIC, D. PAVUNA (EDITORS)
Oxide Physics and Nano-engineering V
In: Proceedings of SPIE - vol. 4811 Int. Society for Optical Engineering - Bellingham, USA (2002)

M. GRIONI
Photoemission in quasi-one-dimensional systems and atomic chains
In: Strong interactions in low dimensions, Eds. D. Baeriswyl and L. Degiorgi (Kluwer, 2003)

L. PERFETTI, M. GRIONI, G. MARGARITONDO
In: Photo-excited processes, Diagnostics and Applications, A. Peled ed., (Kluwer, 2003)

G. MARGARITONDO
Elements of Synchrotron Light for Biology Chemistry, and Medical Research
(Oxford, New York, 2002)

G. MARGARITONDO, Y. HWU, G. TROMBA
Synchrotron Light: from Basics to Coherence and Coherence-related Applications
In: Synchrotron Radiation: Fundamentals, Methodologies and Applications, S. Mobilio and G. Vlaic Eds. (Società Italiana di Fisica, Bologna 2003), p. 25.

Project 15 L. Schlapbach, University of Fribourg and EMPA

P. GRÖNING
Cold Plasma Processes in Surface Science and Technology
In: "Handbook of Thin Films Material" edited by H.S. Nalwa, Vol. 1, Chapter 4, 219–257, (2002) IAcademic Press, New York (2002)

***** P. GRÖNING, L. NILSSON, P. RUFFIEUX, R. CLERGEREAUX, O. GRÖNING
Carbon Nanostructures for Cold Electron Sources
In: Encyclopedia of Nanoscience and Nanotechnology, edited by H.S. Nalwa, Academic Press, New York, in press (2003)

P. GRÖNING, L. NILSSON, P. RUFFIEUX, R. CLERGEREAUX, O. GRÖNING
Carbon Nanostructures for Cold Electron Sources
In: Encyclopedia of Nanoscience and Nanotechnology, Edited by H.S. Nalwa, American Scientific Publishers, ISBN 1-58883-001-2, (January 2004)

Project 16 A. Furrer ETH Zurich and PSI Villigen

***** N. CAVADINI, CH. RÜEGG, A. FURRER, H.U. GÜDEL, K. KRÄMER, H. MUTKA, A. WILDES, K. HABICHT, P. VORDERWISCH
Triplet Modes in a Quantum Spin Liquid Across the Critical Field
In: Physical Phenomena in High Magnetic Fields – IV, ed. by G. Boebinger, Z. Fisk, L.P. Gor'kov, A. Lacerda, J.R. Schrieffer, World Scientific, Singapore, 410-413 (2002)

A. FURRER
Neutron scattering investigations of charge inhomogeneities and the pseudogap state in high-temperature superconductors
Structure and Bonding
Volume: Superconductivity in Complex Systems, eds. A. Bussmann-Holder and K.A. Müller (Springer, Heidelberg), in print

J. MESOT, D. RUBIO TEMPRANO, A. FURRER
Neutron Crystal-field spectroscopy in rare-earth based high-temperature superconductors
In: Trends in Applied Spectroscopy (to be published)

J. MESOT, D. RUBIO TEMPRANO, A. FURRER
Neutron Crystal-Field Spectroscopy in Rare-Earth Based High-Temperature Superconductors
In: Trends in Applied Spectroscopy (Research Trends, Trivandrum, p. 75-100 (2002)

Project 18 T. Giamarchi, University of Geneva

S. BIERMANN, A. GEORGES, T. GIAMARCHI, A. LICHTENSTEIN
Quasi-one-dimensional organic conductors: dimensional crossover and some puzzles
In: "Strongly correlated fermions and bosons in low dimensional disordered systems" Ed. IV. Lerner et al., Kluwer (Dordrecht), (2002)
T. GIAMARCHI
Disordered Wigner crystals
In: "Strongly correlated fermions and bosons in low dimensional disordered systems", Ed. IV. Lerner et al., Kluwer (Dordrecht), (2002)

T. GIAMARCHI
Quantum Physics in one Dimension
International Series of Monographs on Physics 121, Oxford University Press (2004)

T. GIAMARCHI
Electronic Glasses
Enrico. Fermi school on "Quantum Phenomena in Mesoscopic Systems", Varenna 2002, published in "Quantum phenomena in mesoscopic systems" (Proceedings of the International School of Physics "Enrico Fermi" course CLI) IOS Press (2003)

T. GIAMARCHI, T. NATTERMANN, P. LE DOUSSAL
Transport in Luttinger Liquids
In: the Proceedings of the EURESCO conference "Fundamental Problems in Mesoscopic Physics", Granada.
To be published by Kluwer (Nato Science series).

T. GIAMARCHI, E. ORIGNAC
Disordered Quantum Solids
In "Theoretical Methods for Strongly Correlated Electrons", D. Senechal et al. ed, Springer (2004)

5.4 Reports

Project 3 R. Flükiger, University of Geneva

CTI Topnano report, project ARIANA 3, Sept. 2002

CTI Topnano report, project EDM 2, Sept. 2002

Final GROWTH project ("BIG POWA") report, after 36 + 3 months.
"High current Bi,Pb(2223) conductors with innovative geometry for power applications"

R. FLÜKIGER
Assessing the Impact of High Temperature Superconductivity on the Electric Power Sector
IEA Report, Nov. 2001

R. FLÜKIGER
High current Bi(2223) conductors with innovative wire geometry for power applications
5th Frame Program: GROWTH Projects: BIG POWA, Mid-Term Report, January 2002

***IEA** report, Nov. 2002*

Project 7 R. Nesper, ETH Zurich

Design, Synthesis, and Selforganization of Supramolecular Nano Particles
NRP 47, wischenbericht 2002

Synthesis, structure, and properties of solids
NF-project no 20-56841.99, continuation proposal 2002

The Synthesis, Structure and Properties of New Materials Based on Inorganic Clathrate Systems
IHP-EU project no IHP-RTN-99-1project, proposal (granted 2002)

Synthesis and Characterization of Advanced Electroactive Materials for Electrodes of Rechargeable Lithium-Ion Batteries
NF-project no 21-59216.99, Zwischenbericht 2002
Project 7, Nesper

Project 9 T.M. Rice – M. Sigrist ETH Zurich

B. BINZ
Strong electron correlations caused by weak interactions
Unpublished (December 2002), 10 pages

Project 15 L. Schlapbach

O. GRÖNING
Carbon Nanotubes for Future Electron Emission Devices
Empa-Activities, ISSN 1660 – 1394 (2002)

O. GRÖNING
Carbon Nanotubes for Electron Sources
Empa-Annual Report (2003)

P. RUFFIEUX
Interaction of Hydrogen with sp^2-bonded carbon: Effects on the localelectronic structure
Empa-Activities (2003)

Project 16 A. Furrer ETH Zrich and PSI Villigen

R. GILARDI, J. MESOT , A.J. DREW, U. DIVAKAR, S.L. LEE, E.M. FORGAN, C.D. DEWHURST, R. CUBITT
Field-induced transition from hexagonal to square vortex lattice in $La_{1.83}Sr_{0.17}CuO_4$
ILL Annual RepEort 2002, 52-53. (ILL Grenoble, April 2003)

R. GILARDI, S. STREULE, A. HIESS, H.M. RONNOW, M. ODA, N. MOMONO, J. MESOT
Spin dynamics in the mixed phase of $La_{2-x}Sr_xCuO_4$ (x=0.10, x=0.17)
Proceedings of the SCNS Workshop 2002, http://whisky.ill.fr/Events/ONSITE/SCNS/

J. MESOT
Superconductivity and magnetism
Proceedings of the Introductory Course of the ECNS 2003 Conference (1st-2nd September 2003) http://www-llb.cea.fr/ecns2003/lectures/lectures.html

J. PADIYATH, CH. RÜEGG, N. CAVADINI, J. MESOT, A. FURRER, K. KRÄMER, H.-U. GÜDEL, T. PERRING, C. FROST, H. MUTKA, J. STRIDE
Triplet modes in S=1/2 $TlCuCl_3$ studied by time-of-flight neutron scattering on single crystals
Proceedings of the SCNS Workshop 2002, http://whisky.ill.fr/Events/ONSITE/SCNS/

PSI • Scientific Report 2002 / Volume II
see: http://num.web.psi.ch/reports/2002/reports-2002.htm (numerours reports about the topics of the present project)

PSI • Scientific Report 2003 / Volume III
see: http://num.web.psi.ch/reports/2003/reports-2003.htm
(numerous reports about the topics of the NCCR project MaNEP)

* ***SINQ Experimental Reports***
see: http://sinq.web.psi.ch/sinq/exp_reports.html
(numerous reports on neutron scattering experiments related the present project)

6 Diplomas, theses and awards

6.1 Diploma

Project 2 Ø. Fischer, University of Geneva

Cédric Goetchmann
Etude par microscopie à effet tunnel de films minces de C60 déposés sur différents substrats
O. Kuffer, diploma supervisor
Date of the award: 26.09.2003
University of Geneva

Project 4 A. Junod, University of Geneva

Violeta Guritanu
Etude de la chaleur spécifique du Nb_3Sn: possibilité de supraconductivité à deux gaps
A. Junod, diploma supervisor
Date of the award: 26.09.2003
University of Geneva

Project 5 J.-M. Triscone, University of Geneva

Céline Lichtensteiger
Croissance et propriétés de structures artificielles
J.-M. Triscone, diploma supervisor
Date of the award: December 2001
University of Geneva

Nicolas Stucki
Réseaux artificiels de domaines ferroélectriques: recherche d'une interaction domaine-domaine et haute densité
Date of the award: 30.06.2003
University of Geneva

Project 6 G. Blatter, ETH Zurich

Paulo Corti
Vortex Dynamics in high-T_c superconductors: motion on small scales
G. Blatter, diploma supervisor
Date of the award: Fall 2001
ETHZ

Roland Schmucki
Neue ansatze für die seitenketten-resonanz-zuordnung in der NMR-strukturermittlung von proteinen
G. Blatter and K. Wuthrich, diploma supervisors
Date of the award: 01.07.2003
ETH Zürich

Urs Stocker
Quantum Cryptography: Error correction and privacy amplification
G. Blatter and N. Gisin, diploma supervisors
Date of the award: 01.12.2003
ETH Zürich

Ivo Kaelin
Optics of media with spatial dispersion
C. Helm and G. Blatter, diploma supervisors
ETH Zürich

Project 7 R. Nesper, ETH Zurich

Daniel Widmer
Phase transitions of borides and borides carbides under high pressure for the synthesis of carbon clathrate structures
R. Nesper, diploma supervisor
ETH Zürich

Project 8 H.R. Ott, ETH Zurich

Raffaele Dell Amore
Energietransport in I-D Spinsystemen
Date of the award: 01.01.2004
ETH Zürich

Project 9 T.M. Rice – M. Sigrist, ETH Zurich

Urs Aeberhard
The fate of zero-conductance resonance in nano-wires with spin-orbit coupling
M. Sigrist, diploma supervisor
Date of the award: 15.03.2004
ETH Zürich

Julien Dorier
Orbital ordering in the quantum compass model
Date of the award: 31.03.2004
ETH Zürich

David Eichenberger
Correlations and phase separation in carbon nanotubes
Date of the award: 31.03.2004
ETH Zürich

Andreas Lüscher
Spin gap and thermal properties of $Na_2V_3O_7$
F. Mila, V. Kotov, diploma supervisors
Date of the award: 31.03.2003
ETH Zürich

Bernhard Metzger
Vortex charging in a chiral superconductor
M. Sigrist, diploma supervisor
Date of the award: 15.10.2003
ETH Zürich

Cedric Weber
Study of the classical antiferromagnetic Heisenberg model on a square lattice with nearest and next-nearest neighbour coupling
F. Mila, F. Becca, diploma supervisor
Date of the award: 31.03.2003
EPFL

Cyril Belardinelli
Nucleation of unconventional superconductivity at interfaces
M. Sigrist, diploma supervisor
ETH Zürich

Michel Ferrero
Dynamical properties of the Heisenberg antiferromagnet on a trimerized kagome lattice: a classical Monte Carlo study
F. Mila, F. Becca, diploma supervisor
EPFL

Jenssen Page
Etude numérique du modèle T-U-J unidimensionnel dans la limite du couplage fort
D. Baeriswyl, X. Zotos, diploma supervisor
Université de Fribourg

Project 10 P. Martinoli, University of Neuchâtel

Aloïs Jaber
La structure de paires de Cooper préformées en-dessus de T_c
H. Beck, S. Sharapov, diploma supervisors
Date of the award: Feb. 2002
University of Neuchâtel

Pierre Chappatte
Etude du comportement en température et en champ magnétique de films supraconducteurs ultra minces de $la_{2-x}Sr_xCuO_4$
Date of the award: 15.10.2003
University of Neuchâtel

Project 13 H. Keller, University of Zurich

Maria Bruun
Beobachtung einer metallischen phase in schwach dotiertem $La_{2-x}Sr_xCuO_4$ anhand von elektronenparamagnetischer resonanz
A. Schengelaya, H. Keller, K.A. Müller, diploma supervisors
Date of the award: 15.09.2003
University of Zürich

Project 14 P. Aebi, University of Neuchâtel

Florian Clerc
Multicouches de C60 déposées sur Cu(111)
P. Aebi, diploma supervisor
Date of the award: Feb. 2002
University of Fribourg

Laurent Despond
Photodiffraction sur films minces de $PBTIO_3$
P. Aebi, diploma supervisor
Université de Fribourg

Project 16 A. Furrer, ETH Zurich and PSI Villigen

Michael Oettli
Neutron scattering investigations of the quantum spin dimmer compound NH_4CuCl_3
A. Furrer, Ch. Rüegg, diploma supervisor
Date of the award: 29.12.2004
PSI

Sabine Streule
Magnetic phase diagram of the high-T_c superconductor $La_{2-x}Sr_xCuO_4$ studied with small angle neutron scattering and magnetisation measurements
R. Gilardi, J. Mesot, diploma supervisors
ETH Zürich and PSI Villigen

6.2 Theses

Project 2 Ø. Fischer, University of Geneva

Olivier Kuffer
Scanning Tunnelling Microscopy Study of Polarization Phenomena in Ferroelectric Heterostructures
Ø. Fischer, thesis supervisor
Date of the award: 01.07.2001
University of Geneva

Bart Hoogenboom
Scanning tunnelling spectroscopy on vortex cores in $BI_2SR_2CACu_2O_{8+\delta}$
Ø. Fischer, B. Giovannini and J. Aarts, thesis supervisors
Date of the award: 16.08.2002
University of Geneva

Project 3, R. Flükiger, University of Geneva

Enrico Giannini
Phase formation and texture development in Ag-sheated $(Bi,Pb)_2Sr_2Ca_2Cu_3O_{10+\delta}$ superconducting tapes
F. Flükiger, thesis supervisor
Date of the award: 01.07.2001
University of Geneva

Reynald Passerini
Formation, caractérisation et propriétés mécaniques sous contrainte uniaxiale du Bi, Pb(2223) dans les rubans à gaine d'argent
F. Flükiger, thesis supervisor
Date of the award: 30.11.2001
University of Geneva

Francesco Grilli
Numerical modelling of high temperature superconducting tapes and cables
M. Hasler, thesis supervisor
Date of the award: 01.03.2004
EPF Lausanne

Grégoire Witz
Préparation et caractérisation de conducteurs à base de Bi, Pb(2223) ayant des pertes AC réduites
R. Flükiger, thesis supervisor
Date of the award: 15.12.2003
University of Geneva

Project 4 A. Junod, University of Geneva

Yuxin Wang
Specific heat study of unconventional anisotropic superconductors: MgB_2, $Yba_2Cu_3O_7$, $NdBa_2Cu_3O_x$
A. Junod, thesis supervisor
Date of the award: 16.01.2004
University of Geneva

Project 5

Stefano Gariglio
Transport properties of latio$_{3+\delta}$ and RE-B$A_2Cu_3O_{7-\delta}$ thin films: a study of correlation effects
J.-M. Triscone, thesis supervisor
Date of the award: 31.01.2003
University of Geneva

Project 6 G. Blatter, ETH Zurich

Hanspeter Buchler
Phase transitions in quantum condensed matter
G. Blatter, W. Zwerger, thesis supervisors
Date of the award: 01.04 2003
ETH Zürich

Project 7 R. Nesper, ETH Zurich

Fabian Bieri
Sol-Gel synthese von vanadiumoxid-nanoröhren und Eisenoxidnanopartikeln sowie deren charakterisierung und mikrostrukturierung
R. Nesper, thesis supervisor
Date of the award: 31.12.2003
ETH Zürich

Project 8 H.R. Ott, ETH Zurich

Giannò Konrad
Electrical and thermal transport of hexaborides and icosahedral quasicrystals
H.R. Ott and G. Blatter, thesis supervisors
Date of the award: 18.10.2002
ETH Zürich

Dominic Rau
Magnetism and structure of quasicrystals
M. Erbudak, H.R. Ott and J. Gavilano, thesis supervisors
Date of the award: 28.01.2003
ETH Zürich

Project 9, T.M. Rice – M. Sigrist, ETH Zurich

Christophe Aebischer
Dielectric catastrophe at the mott transition
D. Baeriswyl, thesis supervisor
Date of the award: 23.01.2002
University of Fribourg

Benedict Binz
Weak-coupling instabilities of two-dimensional lattice electrons
D. Baeriswyl, thesis supervisor
Date of the award: 15.04.2002
University of Fribourg

Andrea Läuchli
Quantum magnetism and strongly correlated electrons in low dimensions
T.M. Rice, thesis supervisor
Date of the award: 01.12.2002
ETH Zürich

Project 10 P. Martinoli, University of Neuchâtel

Jérôme Affolter
Influence of anisotropy and disorder on the dynamic response of Josephson junction arrays
P. Martinoli, thesis supervisor
Date of the award: 01.07.2001
University of Neuchâtel

Alain Sewer
Model study of anomalous properties of short coherence length superconductors
H. Beck and X. Zotos, IRRMA, thesis supervisors
Date of the award: 01.11.2001
University of Neuchâtel

Phililppe Curty
Amplitude and phase fluctuations in high temperature superconductors
H. Beck, thesis supervisor
Date of the award: 15.12.2003
University of Neuchâtel

Project 12 G. Margaritondo, EPF Lausanne

Luca Perfetti
Angle-resolved photoelectron spectroscopy on strongly correlated electron-phonon systems
G. Margaritondo, thesis supervisor
Date of the award: 20.09.2002
EPFL

Mike Abrecht
Photoemission studies on thin films grown by pulsed laser deposition; epitaxial strain effects on the electronic structure of high temperature superconductors
D. Pavuna and G. Margaritondo, thesis supervisors
Date of the award: 15.06.2003
EPFL

Project 13 H. Keller, University of Zurich

Rustem Khasanov
Studies of the oxygen-isotope effect on the magnetic field penetration depth in cuprate superconductors
H. Keller, E. Morenzoni and T. Schneider, thesis supervisors
Date of the award: 31.10.2003
University of Zürich

Project 14 P. Aebi, University of Neuchâtel

Marc Bovet
Realistic band structure calculation augmented photoemission
P. Aebi, thesis supervisor
Date of the award: 15.09.2003
Université de Neuchâtel

Olivier Gallus
Photoemission study of one-dimensional metal-chains
Y. Baer, thesis supervisor
Date of the award: 15.09.2003
Université de Neuchâtel

Project 15 L Schlapbach, University of Fribourg and EMPA

Pascal Ruffieux
Interaction of hydrogen with SP_2-bonded carbon: effects on the local electronic structure
P. Groening, thesis supervisor
Date of the award: 31.08.2002
EMPA

Project 16 A. Furrer, ETH Zurich and PSI Villigen

Daniel Rubio Temprano
Pseudogap in high-temperature superconductors studied by neutron crystal-filed spectroscopy: doping dependence and isotope effects
A. Furrer, thesis supervisor
Date of the award: 01.02.2002
ETH Zürich

Project 17 D. van der Marel, University of Geneva

Presura Cristian Nicolea
Energetics and ordering in strongly correlated oxides as seen in optics
D. van der Marel, thesis supervisor
Date of the award: 23.05.2003
University of Geneva

6.3 Awards

Project 3 R. Flükiger, University of Geneva

Francesco Grilli
Award for best poster, IEEE conference on electromagnetic field computation, Perugia, Italy
Date: 16.06.2002

Hong-Li Suo, Concetta Beneduce, Marc Dhallé, Nicolas Musolino, Xiao-Dong Su, René Flükiger
Best material paper at ICMC conference, Madison, USA
Date: 15-17 July 2001

Hong-Li Suo
Chinese National Award: best PhD work on materials
Date: 01.12.2003

Project 4 A. Junod, University of Geneva

Frederic Bouquet and Yuxing Wang
2003 Swiss Physical Society Award for Condensed Matter Physics sponsored by IBM: T*hermodynamics of a new superconductor: MgB_2, the "double-barrelled oldtimer"*
Date: 01.03.2003

Frederic Bouquet
Charles Haenny price of the "Association Vaudoise des Chercheurs en Physique" for his popular science paper *Le supraconducteur qui dormait sur les étagères*
Date: 20.06.2003

Project 6 G. Blatter, ETH Zurich

Hanspeter Buchler
Silver medal of the ETHZ for his thesis on *Phase transitions in quantum condensed matter*
Date: 01.01.2004

Vadim Geshkenbein
ETH Zürich: Latsis Award
Date 21.09.2001

Project 7 R. Nesper, ETH Zurich

Reinhard Nesper
Guest professorship for Nanoscience, university of Oslo
Date: 01.09.2003

Project 9 T.M. Rice – M. Sigrist, ETH Zurich

Andreas Läuchli
Silver medal of ETH Zurich for doctor thesis entitled: *Quantum magnetism and strongly correlated electrons in low-dimensional systems*
Date: 01.04.2003

T. Maurice Rice
Fellow of the Royal Society
Date: 01.07.2002

Project 10 P. Martinoli, University of Neuchâtel

Mauro Tesei
Poster award at the 3rd European Conference on Vortex Matter in Superconductors, Crete, for the poster entitled: *Magnetic localization effect and dynamic response of a Josephson junction array on a dice lattice*.
Date: 20-28 09 2003.

Project 12 G. Margaritondo, EPF Lausanne

Giorgio Margaritondo
2003 SKORE-A (Swiss-Korean Outstanding Research Effort Award)

Luca Perfetti
Best EPFL thesis 2002

Project 14 H. Keller, University of Zurich

Christian Koitzsch
ECOSS prize 2003, European conference on surface science, Praha, Czech Republic: best poster
Date: 01.09.2003

Project 15 L. Schlapbach, University of Fribourg and EMPA

Pascal Ruffieux
Charmey prize 2003 for his excellent PhD Thesis

Pascal Ruffieux
Young scientist award of the Groupe Suisse de Travail Surfaces et Interfaces GSSI

Project 16 A. Furrer, University of Zurch and PSI Villigen

Nordal Cavadini
Silver medal of the ETH Zürich for PhD work entitled: *Investigation of magnetic correlations in quantum spin systems by neutron scattering experiments*
Date: 31.12.2002

Raffaele Gilardi
Poster prize at the 19th general conference of the EPS condensed matter division, Brighton, U.K.
Date: 11.04.2002

Raffaele Gilardi
Young scientists award, 3rd European conference on neutron scattering, Montpellier, France
Date: 06.09.2003

Joël Mesot
ETH Zürich: Latsis prize
Date: 31.12.2002

Christian Rüegg
Poster prize at the 1st summer school on condensed matter research, Zuoz, Switzerland
Date: 17.08.2002